

Subsurface architecture of fluvial-deltaic deposits
in high- and low-accommodation settings

Jennifer Yvonne Stuart

Submitted in accordance with the requirements for the degree of
Doctor of Philosophy

University of Leeds
School of Earth and Environment
May 2015

Intellectual Property and Publication Statements

The candidate confirms that the work submitted is her own and that appropriate credit has been given where reference has been made to the work of others. This copy has been supplied on the understanding that it is copyright material and that no quotation from the thesis may be published without proper acknowledgement.

The work in Chapter 2 of the thesis has appeared in publication as follows:

Stuart, J.Y., Mountney, N.P., McCaffrey, W.D., Lang, S.C., Collinson, J.D., 2014. Prediction of channel connectivity and fluvial style in the flood-basin successions of the Upper Permian Rangal coal measures (Queensland). AAPG Bull. 98, 191-212.

As the primary author, I was responsible for carrying out the research, running the models, drafting figures and writing the paper. The contribution of the other authors was minor editorial suggestions.

© 2015 The University of Leeds and Jennifer Y. Stuart.

The right of Jennifer Y. Stuart to be identified as Author of this work has been asserted by her in accordance with the Copyright, Designs and Patents Act 1988.

Acknowledgements

Firstly I would like to thank my supervisors Dr Nigel Mountney and Prof. Bill McCaffrey for giving me the opportunity to do this PhD, and for their support and guidance throughout my PhD. I would like to give Nige extra thanks for the hours spent proofreading my work over the last four years.

I would like to thank the sponsors of the Fluvial Research Group (Areva, BHP Billiton, ConocoPhillips, Nexen, Saudi Aramco, Shell & Woodside) for providing me with funding to carry out this research. I would like to thank Woodside for providing seismic and well data for my research, and in particular Simon Lang, Keith Adamson and Ed Hooper for invaluable support, assistance and guidance throughout the project. I also thank Woodside and Shell, for my internships and giving me a fantastic ten months in Perth and Den Haag. Thank you to Mads Huuse and the University of Manchester for the free use of computer facilities to carry out frequency decomposition.

I am grateful for all the experiences and opportunities I have received during my PhD, especially demonstrating on fieldtrips and for the wonderful times and discussions I had attending conferences, particularly AAPG.

Thank you to my fellow members of FRG and the Gin Wednesday club for the support and occasional distraction. I would like also to give thanks to my friends, in particular, to Lucy Gold, for being my oldest friend so having seen me through 17 years of study-based 'existential crises'; to Laura Nuttall and Rose Rae, for all the PhD pick-me-up talks; to all my other friends from home, uni, Shell and Woodside who have helped and supported me along the way, not least, Steven Banham, Hayley Cox, Phoebe Fox-Bekerman, Megan Jenkins, Kat and Rob Lowther, Sarah Nelson, Viki O'Connor and Jo Venus.

I would like to thank The Royal Society and Prof. James Jackson, for the 1995 Royal Society Christmas Lecture, "Planet Earth, an explorer's guide", for getting me interested in geology.

I would like to thank my family for the years of support, hugs, encouragement and occasional kicks up the backside: thank you to Graham, Sheryl, Scarlett the Wonder Dog, Grandma and Grandad. Finally to my wonderful parents: I will never be able to thank you enough for all of the help, love and support you have given me; the food-parcels, walks and cups of tea that magically appeared while I was typing – Thank you.

Preface

Several chapters within this thesis (Chapters 2, 4 and 6) were written as papers which were submitted to various geoscience journals for publication, and thus they are stand-alone pieces of work. The literature review and background sections within these chapters are focused at a particular aspect relating to the study (e.g. sedimentology, seismic geomorphology), and as a result of the common theme of the papers, do overlap. This should assist the reader by presenting the most relevant information pertaining to the subject to be discussed.

Publications at time of submission

In print:

Stuart, J.Y., Mountney, N.P., McCaffrey, W.D., Lang, S.C., Collinson, J.D., 2014. Prediction of channel connectivity and fluvial style in the flood-basin successions of the Upper Permian Rangal coal measures (Queensland). AAPG Bull. 98, 191-212.

Under review:

Stuart, J. Y., Mountney, N. P. McCaffrey, W. D., Adamson, K. R., Hooper, E. C. (UNDER REVIEW) Seismic geomorphology and sedimentology of fluvial environments in the subsurface: fluvio-deltaic Triassic Mungaroo Formation, North West Shelf, Australia. Marine and Petroleum Geology.

Stuart, J. Y., Mountney, N. P. McCaffrey, W. D., Adamson, K. R., Hooper, E. C. (UNDER REVIEW) Architectural styles of a fluvio-deltaic succession investigated with seismic attributes and spectral decomposition: Late Triassic Mungaroo Formation, offshore Western Australia. Marine and Petroleum Geology

.

Abstract

Combined seismic and well interpretation methods can be used to elucidate detail of the subsurface architecture of fluvial and fluvio-deltaic deposits. Observations made from wireline and core logs, including facies and analysing the relative proportions of architectural elements and facies associations indicative of depositional sub-environments, can be used to interpret patterns of cyclicity, changes in local accommodation conditions, and periods of increased seasonal, tidal and marine influence.

Horizon slices, taken from 3D seismic volumes aid in the visualisation of laterally discontinuous, often thinly-bedded, fluvial deposits. Seismic facies, when combined with core and wireline log facies, can be interpreted as a series of 'seismic elements'. The relative proportions of seismic elements mapped out on horizon slices allows the interpretation of depositional environments and accommodation setting; allowing the distinction between fluvial and deltaic settings. A number of data conditioning and seismic interpretation techniques can be used to enhance the visualisation of channelized and non-channelized fluvio-deltaic deposits in the subsurface. Frequency decomposition (and the making of colour-blended volumes) allows the visualisation of the detail of channel belt deposits such as channel belt migration and lateral accretion deposits.

Allogenic processes, particularly base-level (buttress) rise and fall have been shown to exert a control on the overall stacking pattern of the studied fluvio-deltaic deposits, whereas autogenic processes are interpreted as the major control on the local arrangement and architecture of channel belt and overbank deposits.

The first study in this thesis uses the Upper Permian Rangal Coal Measures, a large-scale fluvial system, which accumulated in a foreland basin setting in the Bowen Basin, Queensland, Australia. The study investigates the architecture and connectivity of splay and distributary channels. The second study uses the Late Triassic Mungaroo Formation, a Mississippi-scale fluvio-deltaic system with a fluvially-dominated, tidally-influenced delta, which accumulated in the Northern Carnarvon Basin, Northwest Shelf, Australia. The study investigates different seismic interpretation techniques and investigates the relative control on fluvio-deltaic deposition of allogenic and autogenic processes.

Contents

1	Introduction.....	1
1.1	Project rationale.....	1
1.2	Key research questions (aims and objectives).....	4
1.3	Methods.....	5
1.4	Thesis overview.....	7
1.4.1	<i>Chapter 1: Introduction.....</i>	7
1.4.2	<i>Chapter 2: Prediction of fluvial style and connectivity of minor channels in the flood basin successions of the Upper Permian Rangal Coal Measures (Queensland).....</i>	7
1.4.3	<i>Chapter 3: Sedimentology of fluvial system within a delta-plain setting: a case study from the Triassic Mungaroo Formation.....</i>	8
1.4.4	<i>Chapter 4: Seismic geomorphology and sedimentology of fluvial environments in the subsurface: fluvio-deltaic Triassic Mungaroo Formation, North West Shelf, Australia.....</i>	9
1.4.5	<i>Chapter 5: Well log and seismic interpretation techniques useful in the subsurface interpretation of fluvial deposits....</i>	10
1.4.6	<i>Chapter 6: Subsurface geomorphology of a fluvio-deltaic succession investigated with seismic attribute analysis and spectral decomposition: Late Triassic Mungaroo Formation, offshore Western Australia.....</i>	11
1.4.7	<i>Chapter 7: Discussion: the application of subsurface interpretation techniques to the investigation of controls on styles of fluvio-deltaic sedimentation.....</i>	12
1.4.8	<i>Chapter 8: Conclusions.....</i>	12
2	Prediction of channel connectivity and fluvial style flood basin successions using wireline logs and stochastic modeling: Case study of the Upper Permian Rangal Coal Measures (Queensland).....	15
2.1	Chapter Overview.....	15
2.2	Introduction.....	16
2.3	Geological Setting.....	23
2.4	Data and Methods.....	24
2.5	Architectural Elements.....	25

2.5.1	<i>Correlation</i>	34
2.5.2	<i>Element Proportions</i>	34
2.5.3	<i>Channel Element Thicknesses and Widths</i>	34
2.6	Interpretation.....	40
2.6.1	<i>Analogue Measurements</i>	40
2.6.2	<i>Modeling</i>	41
2.7	Discussion.....	51
2.7.1	<i>Depositional Models</i>	51
2.7.2	<i>Limitations of data</i>	54
2.8	Conclusions.....	57
2.9	Future work.....	58
3	Sedimentology of a fluvial system within a delta-plain setting: a case study from the Triassic Mungaroo Formation	59
3.1	Chapter overview.....	59
3.2	Dataset.....	62
3.3	Regional stratigraphy.....	62
3.3.1	<i>Paleogeography</i>	62
3.3.2	<i>Chronostratigraphy</i>	62
3.3.3	<i>Tectonostratigraphic evolution</i>	67
3.3.4	<i>Mungaroo Formation Sediment Provenance</i>	75
3.4	Summary of previous work.....	78
3.5	Lithofacies of the Mungaroo Formation.....	82
3.5.1	<i>Overview</i>	82
3.5.2	<i>Lithofacies in detail</i>	82
3.6	Lithofacies associations.....	100
3.7	Depositional environment.....	111
3.7.1	<i>Tidal indicators</i>	111

3.7.2	<i>Trace fossils and bioturbation</i>	118
3.7.3	<i>Interpreted logs</i>	119
3.7.4	<i>Facies association proportions within the logged section of the Mungaroo Formation</i>	125
3.7.5	<i>Depositional setting</i>	125
3.8	Palaeocurrent analysis.....	129
3.8.1	<i>Channel complex paleocurrent readings</i>	129
3.8.2	<i>Fluvial style summary</i>	134
3.9	Chapter summary.....	134
4	Seismic geomorphology and sedimentology of fluvial environments in the subsurface: fluvio-deltaic Triassic Mungaroo Formation, North West Shelf, Australia	137
4.1	Chapter Overview.....	137
4.2	Introduction.....	138
4.2.1	<i>Project background</i>	138
4.3	Study area and data.....	142
4.3.1	<i>Geologic setting</i>	146
4.4	Methods.....	150
4.4.1	<i>Well-log interpretation</i>	150
4.4.2	<i>Seismic Interpretation & Attribute Analysis</i>	150
4.5	Mungaroo Fm Lithofacies associations.....	153
4.6	Seismic element mapping.....	155
4.6.1	<i>Seismic element scheme</i>	155
4.6.2	<i>S1</i>	157
4.6.3	<i>S3</i>	159
4.6.4	<i>S6</i>	162
4.7	Statistical Analysis.....	165
4.7.1	<i>Element proportions</i>	165
4.7.2	<i>Channel and valley orientations – palaeodrainage</i>	169

4.8	Depositional environment.....	171
4.8.1	S1-S2.....	171
4.8.2	S2-S3.....	171
4.8.3	S5-S6.....	172
4.9	Ambiguity in interpretations.....	172
4.10	Conclusions.....	173
5	Seismic interpretation techniques useful in the interpretation of subsurface fluvial deposits.....	177
5.1	Introduction.....	177
5.2	Well-log correlation.....	180
5.3	Seismic methods.....	182
5.3.1	<i>Data conditioning.....</i>	<i>182</i>
5.3.2	<i>Horizon slicing (PetrelTM).....</i>	<i>184</i>
5.3.3	<i>Proportional slicing and amplitude extraction (PetrelTM)....</i>	<i>187</i>
5.4	Spectral (frequency) decomposition (GeotericTM).....	190
5.4.1	<i>RGB blending.....</i>	<i>190</i>
5.4.2	<i>HD frequency decomposition (HDFD).....</i>	<i>194</i>
5.5	Additional seismic methods: attributes.....	196
5.6	Chapter summary.....	201
6	Architecture of a fluvio-deltaic succession investigated with seismic attribute analysis and spectral decomposition: Late Triassic Mungaroo Formation, offshore Western Australia.....	203
6.1	Chapter Overview.....	203
6.2	Introduction.....	204
6.2.1	<i>Context.....</i>	<i>204</i>
6.2.2	<i>Aim and objectives.....</i>	<i>206</i>
6.2.1	<i>Study area & data</i>	<i>207</i>
6.2.2	<i>Geological setting.....</i>	<i>208</i>

6.2.3	<i>Stratigraphy</i>	212
6.3	Methods.....	212
6.4	Results.....	218
6.4.1	<i>Comparison of seismic reflection to frequency decomposition data</i>	218
6.5	Fluvio-deltaic architectural elements.....	223
6.5.1	<i>Meander belts (S1-S2)</i>	223
6.5.2	<i>Amalgamated channel belts (S5-S6)</i>	232
6.5.3	<i>Lateral migration (S6-S7)</i>	233
6.6	Discussion.....	240
6.6.1	<i>Sequence stratigraphic setting</i>	240
6.6.2	<i>Buffers and buttresses model</i>	241
6.7	Conclusions.....	246
7	Discussion: Controls on depositional style of fluvio-deltaic deposits: case study of the Mungaroo Formation..	249
7.1	Chapter overview.....	249
7.2	Introduction.....	249
7.3	Allogenic controls.....	251
7.3.1	<i>Introduction</i>	251
7.3.2	<i>Climate</i>	254
7.3.3	<i>Tectonic controls</i>	258
7.3.4	<i>Base-level rise and fall</i>	261
7.4	Autogenic controls.....	277
7.4.1	<i>Introduction</i>	277
7.4.2	<i>Avulsion</i>	277
7.4.3	<i>Local floodplain effects</i>	280
7.4.4	<i>Channel-body clustering (discussion of avulsion rate v floodplain aggradation)</i>	282
7.5	Discussion.....	284

7.5.1	<i>Accommodation vs. Sediment supply</i>	284
7.6	Mungaroo Fm Depositional model.....	289
7.6.1	<i>Modern analogues</i>	289
7.6.2	<i>Generic observations of response to allogenic and autogenic controls</i>	294
7.7	Conclusions.....	297
8	Conclusions and future work	299
8.1	Chapter overview.....	299
8.2	Research questions.....	299
8.2.1	<i>To what extent do minor (secondary and tertiary crevasse splay and distributary) channels contribute to fluvial overbank successions, and how likely are they to form connected reservoir bodies?</i>	299
8.2.2	<i>What is the nature of the stratigraphy and sedimentology of the Triassic Mungaroo Formation in block WA-404-P, Exmouth Plateau, Australia?</i>	301
8.2.3	<i>What are the broad variations in depositional environment at key intervals of the Mungaroo Formation? Can seismic facies be used to distinguish between fluvial and fluvio-deltaic deposits?</i>	302
8.2.4	<i>What techniques can be employed to identify channelized deposits at a range of scales, and also non-channelized floodplain deposits? Can any seismic interpretation techniques be used to bring out more detailed interpretations?</i>	303
8.2.5	<i>How can a range of seismic interpretation techniques, including spectral decomposition, be used to resolve the internal architecture of channel belt deposits within the Mungaroo Formation? Can these techniques provide further insight into fluvial styles, distinguishing between entrenched valleys and amalgamated channel belts?</i>	304
8.2.6	<i>What are the possible autogenic and allogenic controls on the variations in depositional style identified in the Mungaroo Formation? What can this tell us about fluvio-deltaic systems more generally?</i>	305
8.3	Concluding remarks.....	307
8.4	Recommendations for future work.....	308
8.4.1	<i>Three-dimensional modelling of the Mungaroo Formation..</i>	308

8.4.2	<i>Seismic QI.....</i>	309
8.4.3	<i>Comparison with modern and ancient analogues.....</i>	309
	References.....	311
	Appendices	325

List of figures

Figure 1.1: Location of study areas used in the Rangal Coal Measures and Mungaroo Formation studies as part of this thesis.	6
Figure 2.1: Fluvial sequence stratigraphy (Shanley & McCabe, 1994)	18
Figure 2.2: Schematic diagram- Low net:gross fluvial overbank environment	19
Figure 2.3: Location of the South Blackwater Mine	22
Figure 2.4: Rangal Coal Measures wireline log architectural element scheme	27
Figure 2.5: Correlation panels	29
Figure 2.6: Fence diagram	35
Figure 2.7: Element proportions	36
Figure 2.8: Channel element thickness	37
Figure 2.9: Ob river modern analog	39
Figure 2.10: A-B interseam Reconnect output	44
Figure 2.11: B-C interseam Reconnect output, modeled as a splay	45
Figure 2.12: B-C interseam Reconnect output, modeled as a distributary network	46
Figure 2.13: A-B interseam architectural model	53
Figure 2.14: B-C interseam architectural model, splay geometry	55
Figure 2.15: B-C interseam architectural model, distributary geometry	56
Figure 3.1: Study location map	61
Figure 3.2: Well locations	63
Figure 3.3: Late Triassic paleogeography	64
Figure 3.4: Regional play intervals and sea level curve for the NW Shelf	65
Figure 3.5: NW Shelf Triassic chronostratigraphic chart	64
Figure 3.6: Regional stratigraphic cross-section	69
Figure 3.7: Seismic-to-well-tie	70
Figure 3.8: Well correlation panel featuring stratigraphic surfaces and seismic units used in this study	71

Figure 3.9: W-E seismic section highlighting interpreted horizons, pre-, syn- and post-rift tectonostratigraphic packages	74
Figure 3.10: Isochron thickness maps demonstrating fault movement	77
Figure 3.101: Core photographs and sketches of Mungaroo Formation lithofacies	93
Figure 3.12: Facies associations of the Mungaroo Formation interpreted from core and wireline data	101
Figure 3.13: Tidal indicator core photographs	115
Figure 3.14: Sedimentary core logs from the S2-S3 interval of the Mungaroo Formation (Well-11)	120
Figure 3.15: Facies association proportions calculated from logged thickness	126
Figure 3.16: Proportions of the Mungaroo Formation interpreted as fluvial, upper delta plain and lower delta plain settings	126
Figure 3.17: Facies association proportions by depositional setting	128
Figure 3.18: Features of the tidal-fluvial transition zone	130
Figure 3.19: Fluvial channel style interpreted from channel complexes 1-6 in the core logs of Well-11	133
Figure 4.1: Location map	143
Figure 4.2: Well locations	144
Figure 4.3: Tectonostratigraphic column	145
Figure 4.4: Late Triassic paleogeographic map	148
Figure 4.5: Core and wireline log example	149
Figure 4.6: Flattening (horizon slicing) workflow	154
Figure 4.7: Seismic element scheme	156
Figure 4.8: S1 Seismic element map	158
Figure 4.9: S3 Seismic element map	160
Figure 4.10: S6 Seismic element map	161
Figure 4.11: Seismic profile view of Mungaroo Fm deposits	163
Figure 4.12: Element proportions	166
Figure 4.13: Paleodrainage orientations	170

Figure 4.14: Horizon slice limitations	174
Figure 5.1: Fluvial depositional Styles	179
Figure 5.2: Laterally discontinuous fluvial deposits as expressed in seismic and well data	181
Figure 5.3: Noise reduction	183
Figure 5.4: Spectral enhancement	185
Figure 5.5: Comparison of shallow and deep seismic expression of fluvial deposits	186
Figure 5.6: Flattening (horizon slicing) workflow	188
Figure 5.7: Comparison of time, horizon and stratal slices	189
Figure 5.8: Comparison of proportional slice to amplitude extraction over a 50 ms window	189
Figure 5.9: Creating an RGB blended volume	191
Figure 5.10: HD Frequency Decomposition	195
Figure 5.11: RDR Edge Detection surface attribute	197
Figure 5.12: Dip angle attribute	197
Figure 5.13: Dip azimuth surface attribute	199
Figure 5.14: Relative acoustic impedance attribute	199
Figure 5.15: Bedform attribute	200
Figure 5.16: Terrace thickness attribute	200
Figure 6.1: Location map	210
Figure 6.2. Well Locations	211
Figure 6.3: Stratigraphy of the Northern Carnarvon Basin	213
Figure 6.4: Seismic interpretation workflow	216
Figure 6.5: Reflectivity and spectral decomposition stratal slices from the S1-S2, S5-S6 and S6-S7 intervals	220
Figure 6.6: Interpretation of S1-S2 fluvial features	224
Figure 6.7: Method for determining the rugosity of an interpreted channel belt	229
Figure 6.8: Core log from Well-09 demonstrating the typical sedimentology of the S1-S2 interval channel deposits	231

Figure 6.9: Interpretation of the S5-S6 deposits using reflectivity, RGB blending, HDFD and wireline log data	235
Figure 6.10: S6-S7 lateral accretion deposits interpreted from horizon slices from seismic reflectivity RGB blended and HDFD volumes.	236
Figure 6.11: Peace river, modern analogue to the S6-S7 interval deposits.	238
Figure 6.12: Interpreted sedimentary log and supplementary core photographs from Well-09, S6-S7 interval	239
Figure 6.13: Sequence stratigraphic model of the S1-S2, S5-S6 and S6-S7 intervals	243
Figure 6.14: Buffers and Buttresses model	245
Figure 7.1: Upstream and downstream relative influence of allogenic controls on fluvial architecture (after Shanley & McCabe, 1994).	252
Figure 7.2: Upstream and downstream influence of allogenic processes (After Ethridge et al., 1998)	252
Figure 7.3: Relationship between sediment transport and climate	256
Figure 7.4: Sedimentary response to climate cycles	256
Figure 7.5: Dampier Sub-basin subsidence and sedimentation rates	260
Figure 7.6: Buffers and Buttresses model general	265
Figure 7.7: Effect of buttress rise on a fluvio-deltaic succession	267
Figure 7.8: Effect of buttress fall	268
Figure 7.9: Composite surface development in a, thin preservation space, in association with a channel sheet, and b, in thicker preservation space in association with a multivalley complex (after Holbrook, 2009)	270
Figure 7.10: High accommodation conditions may not result in the formation of an erosive 'composite surface	271
Figure 7.11: S1-S2 buffer and buttress model	275
Figure 7.12: S2-S3 buffer and buttress model	276
Figure 7.13: S5-S6 buffer and buttress model	278
Figure 7.14: S6-S7 buffer and buttress model	279
Figure 7.15: Local and regional avulsion events identified in the S2-S3 interval	281
Figure 7.16: Alluvial stratigraphy produced by a) increased aggradation rates and b) non-random avulsive clustering	283

Figure 7.17: Barrell diagrams	288
Figure 7.18: Generalised fluvio-deltaic depositional model	290
Figure 7.19: S1-S2, modern analog: Madagascar	291
Figure 7.20: S2-S3 modern analogue: Cumberland Marshes	293
Figure 7.21: S5-S6 modern analogue: Kobuk River	295
Figure 7.22: S6-S7 modern analog, Peace River	296

List of tables

Table 2.1: Summary of tertiary channel dimensions from the Ob River, Siberia	41
Table 2.2: A-B interseam modeling results, modeled with a splay geometry	47
Table 2.3: B-C interseam modeling results, modeled with a splay geometry	48
Table 2.4: B-C interseam modeling results, modeled with a distributary geometry	49
Table 3.1: Seismic horizons and related stratal surfaces used in the study	67
Table 3.2: Overview of previous lithofacies studies of the Mungaroo Formation	79
Table 3.3: Characteristic lithofacies of the Mungaroo Formation	96
Table 3.4: Lithofacies and facies associations of the Mungaroo Formation	107
Table 3.5: Bioturbation index (BI) describing the proportion of deformation and reworking of a sedimentary package by bioturbation. From Taylor and Goldring (1993)	118
Table 4.1: Dimensions of seismic elements for the S1-S2 interval	167
Table 4.2: Dimensions of seismic elements for the S2-S3 interval	167
Table 4.3: Dimensions of seismic elements for the S5-S6 interval	168
Table 6.1: Stratigraphic surfaces used in the study	214
Table 6.2: Rugosity measurements for meander belts of the S1-S2 interval	230
Table 7.1: Parameters indicating a change in A/S ratio (after Martinius et al., 2014)	285
Table 7.2: Response of fluvio-deltaic systems to allogenic and autogenic controls, as observed in the Mungaroo Formation	297

Chapter 1 Introduction

This chapter provides an overview of the thesis and its structure. The key research questions are described at the outset and the rationale behind the research is explained. Each subsequent chapter is outlined in turn to summarise the thesis. The case studies for this research were conducted from two principal study areas: part of the Upper Permian Rangal Coal Measures, explored using a well-based dataset from mining companies, Queensland, Australia; part of the Late Triassic Mungaroo Formation, explored with seismic and well data from the Exmouth Plateau, Northern Carnarvon Basin, offshore Western Australia.

1.1 Project rationale

Fluvio-deltaic systems are increasingly recognised for their importance as hydrocarbon reservoirs, yet the wide-ranging styles of deposits associated with such systems, including those associated with overbank regions, crevasse splay deltas, distributary channels, tidal and seasonally-influenced channels, channel belts and the fill of incised valleys, introduces a level of complexity that can make analysis and prediction of subsurface facies and architecture problematic. The stratigraphic architecture of fluvio-deltaic systems records the complex interplay of a range of allogenic and autogenic processes, which collectively exert a variety of controls on palaeoenvironmental development in both up-dip and down-dip settings; such controls are expressed in the sedimentary architecture and morphology of the preserved sedimentary succession.

Numerous studies into the subsurface architecture of large-scale fluvial and fluvio-deltaic systems have been conducted in recent years (e.g. Miall, 1983; Fielding, 1984, 1985; Miall 1985, 1988; Schumm, 1993; Miall. 1994; Hampson et al., 1999; Miall 2002, Cohen et al., 2005; Gibling, 2006; Postma, 2008). However, many of these studies have relied on analysis of combined datasets that utilise both outcrop and well data (e.g. Hampson et al., 2005) because the scale of fluvial deposits being investigated are commonly at or below the scale necessary for seismic resolution of the details of fluvial stratigraphy (Bridge & Tye, 2000). Many past studies of fluvial architecture that utilise 3D seismic data rely on the examination of deposits from the relatively shallow subsurface, for which seismic resolution is greater, such as those of the Gulf of Thailand, Malay Basin or McMurray Formation, Alberta (cf. Miall, 2002; Posamentier, 2005; Hubbard et al., 2011; Reijenstein et al., 2011; Hagstrom et al., 2014).

In recent years, seismic interpretation techniques have evolved from the seismic stratigraphy methods developed by the likes of Vail & Mitchum (1997), through the application of seismic attributes (e.g. Chopra & Marfut, 2005, 2007, 2008; Posamentier, 2005; Sarkar et al., 2010), stratal slicing (e.g. Zeng et al., 1998a, 1998b; Hardage, 1999; Posamentier, 2005; Rabelo et al., 2007; Wood, 2007; de Groot et al., 2010; Zeng, 2010, 2013; Dorn, 2011, 2013) and spectral decomposition (e.g. Henderson et al., 2008; Van Dyke, 2010; McArdle & Ackers, 2012; Lowell et al, 2014; McArdle et al., 2014), which have greatly improved the detail of observable depositional features in the subsurface.

There remains some debate as to the relative importance of extrinsic (allogenic or boundary condition) controls and intrinsic (autogenic) controls on the stratigraphy and architecture of fluvio-deltaic deposits, particularly in regard to the applicability of some long-established sequence-stratigraphic models to

non-marine strata (Allen & Posamentier, 1993; Shanley & McCabe, 1994; Ethridge et al., 1998; Weissmann et al., 2000; Plint et al., 2001; Holbrook, 2006). Specifically, it is uncertain how the relative interplay of allogenic and autogenic controls is expressed in fluvial and fluvio-deltaic successions.

There remains, therefore, a need to develop a method for more accurately constraining the subsurface architecture of more deeply-buried fluvial and fluvio-deltaic deposits, at depths more typical of conventional hydrocarbon reservoirs. Such a method is important because it provides the opportunity to relate preserved sedimentary architecture and morphology of such successions to the extrinsic and intrinsic controls that govern the accumulation of such deposits.

This study addresses these shortcomings in two ways: firstly, by undertaking a detailed architectural study of a fluvial overbank succession (Rangal Coal Measures) in order to assess the impact of changing accommodation conditions on the development of fluvial depositional sequences; secondly, by undertaking a joint investigation of the sedimentological, architectural and seismic geomorphological complexity of an ancient fluvio-deltaic system (the Triassic Mungaroo Formation). Different seismic interpretation techniques are explored and an idealised workflow is presented for the interpretation of stratigraphically complex, (seismically) small-scale fluvial deposits, incorporating sedimentology, stratigraphy and seismic geomorphology analysis. This research focuses primarily on the channelized deposits of fluvio-deltaic successions, relating them to their corresponding overbank setting in order to assess their depositional sub-environments, and the nature of the governing controls.

The Rangal Coal Measures has been interpreted as a large-scale, high-accommodation, low net:gross fluvial system (Fielding et al., 2003) and as such provides an opportunity to study high-net:gross channel and overbank successions that may be analogous to those of the non-marine-influenced portion of the Mungaroo Formation. The dense network of wireline log data from the South Blackwater Mine allows the examination of such deposits at a sub-seismic scale, albeit within a restricted spatial extent (2 km²).

The seismic and well dataset used in the study of the Mungaroo Formation was provided by Woodside Energy Ltd. The high quality seismic dataset (augmented by wireline logs and over 300 m of core) was chosen in order to study fluvial architecture on a wider scale (approx. 3000 km²).

The locations of the study areas for both case studies are shown in Figure 1.1.

1.2 Key research questions (aims and objectives)

The aim of this research is to investigate the sub-surface architecture of fluvio-deltaic settings, at a variety of scales, using a combination of seismic wireline log and core data. Specific aims include: (i) to assess to what extent minor (secondary and tertiary crevasse splay and distributary) channels contribute to fluvial overbank successions, in order to determine the possible allogenic and autogenic controls that influence the spatial variability of such deposits; (ii) to investigate the sedimentary architecture and geomorphology of depositional sub-environments of deeply buried fluvio-deltaic deposits; (iii) to assess variations in the boundary conditions of fluvio-deltaic systems, and their influence upon the sedimentology, stratigraphy and geomorphology of such systems; thereby discuss the relative importance of extrinsic (allogenic) and intrinsic (autogenic) processes as controls of the development of fluvio-deltaic

depositional sequences, and the detailed architecture of depositional (channel and overbank) assemblages within the sequences.

The key research objectives of this study are as follows: (i) to develop and employ a wireline log facies scheme for identifying fluvial channel and overbank facies associations, and use this scheme to aid in the distinction between high and low net:gross fluvial successions; to use simple stochastic modelling to assess the potential for connectivity between small scale channelised deposits; (iii) to establish a repeatable methodology for the assessment of the sedimentary architecture and geomorphology of depositional sub-environments of deeply buried fluvio-deltaic deposits, using a combination of well-log and 3D seismic data.

1.3 Methods

The chapters of this thesis are intended to be read as stand-alone pieces of work that collectively build upon an overarching research theme. Therefore, the methods used in each chapter are specific to that chapter and as such are detailed therein and described in brief below.

The study of the Rangal Coal Measures was conducted using wireline log and core data, in order to create a wireline log-architectural element scheme. Fluvial architectural elements (ranging from primary and secondary channels to crevasse splay channels and overbank fines, for example lacustrine mudrocks and coal) identified using the wireline log scheme were correlated and used to create fence panels illustrative of interseam packages. Possible assemblages and connectivity of crevasse splay and distributary channels were modelled using a stochastic modelling package. A detailed description of methods used can be found in Chapter 2.

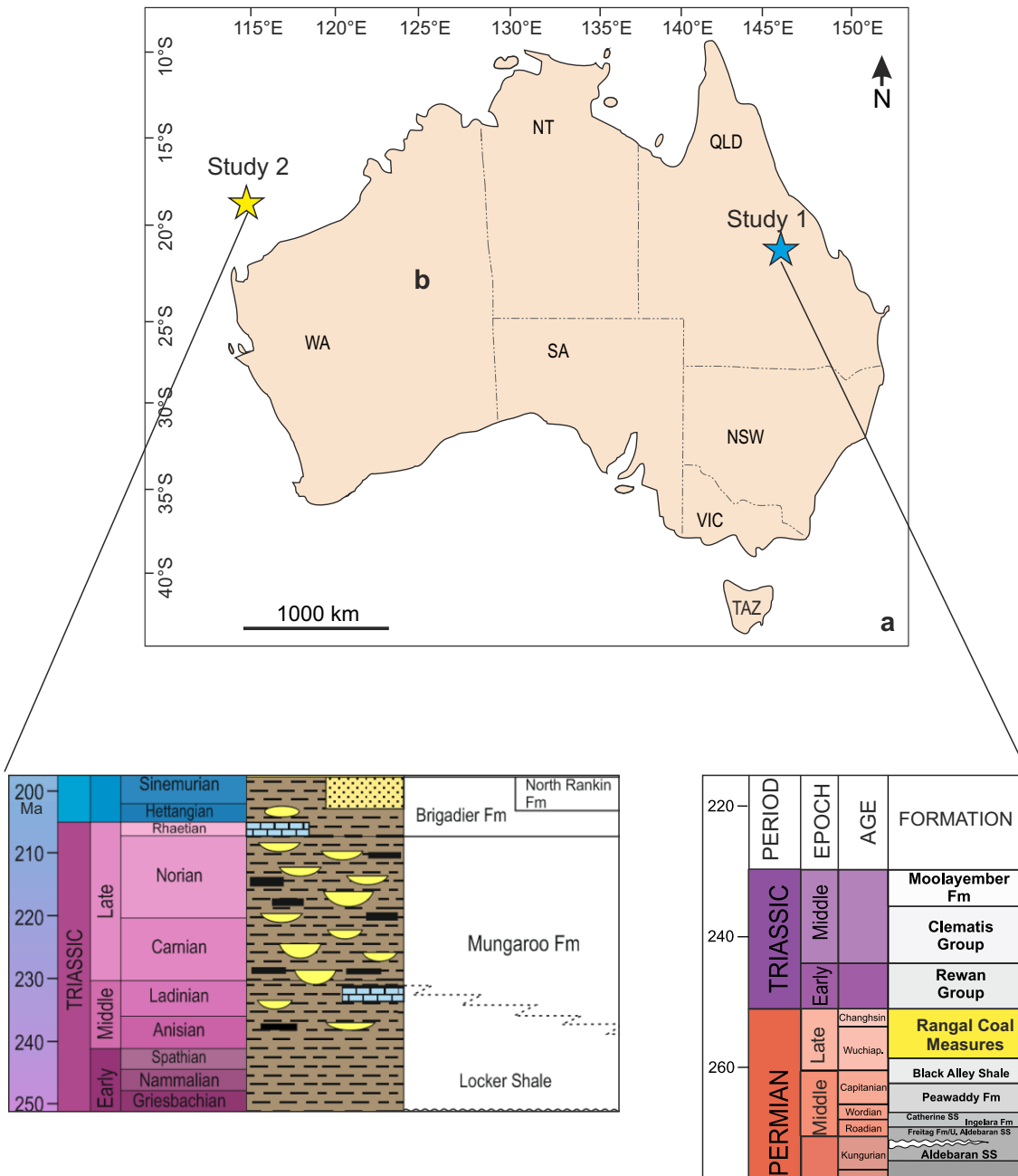


Figure 1.1: Location and simplified stratigraphy of the two study areas used in this thesis.

The study of the Mungaroo Formation was conducted as several sub-studies, employing a range of well and seismic interpretation methods: Well log interpretation techniques were correlation, sedimentary core logging, and facies analysis. Seismic interpretation techniques included horizon slicing, creating a 'seismic element' scheme, linking sedimentology to seismic geomorphology, attribute analysis and frequency decomposition. A detailed description of the seismic methods used can be found in Chapters 4 and 5.

1.4 Thesis overview

1.4.1 Chapter 1: Introduction

Chapter 1 is an introduction to the thesis; setting the scene in terms of project rationale and detailing the overall project aim and objectives. The chapter sets out, the key research questions, and outlines the structure of the thesis.

1.4.2 Chapter 2: Prediction of fluvial style and connectivity of minor channels in the flood basin successions of the Upper Permian Rangal Coal Measures (Queensland)

Research question: To what extent do minor (secondary and tertiary crevasse splay and distributary) channels contribute to fluvial overbank successions and how likely are they to form connected reservoir bodies?

Chapter 2 describes the architecture of two overbank (interseam) intervals from the Upper Permian Rangal Coal Measures from the South Blackwater Mine, Queensland, Australia. The Rangal Coal Measures and equivalents of the Bowen Basin have been used to study fluvial processes and architecture (c.f. Flood & Brady, 1985; Fielding et al., 1993) as the density of data available from mining noreholes and sidewalls allows the study of such deposits in great detail.

The large-scale floodbasin deposits of the Rangal Coal Measures and equivalents have been interpreted as analogous to those of the Mississippi (Flood & Brady, 1985), with similar, large-scale crevasse delta deposits being preserved. The lithofacies of the Rangal Coal Measures identified by Fielding et al. (1993) are deemed typical of coal-bearing fluvial successions, and therefore may be analogous to the coal-bearing intervals of the Mungaroo Formation.

Wireline log character is assessed with reference to literature encompassing fluvial systems, the occurrence of coal interseam deposits and previous studies of the Rangal Coal Measures, in order to create an architectural element scheme describing channelized and non-channelized overbank deposits. The relative infill proportions of each architectural element are calculated and likely channel assemblages and connectivity are measured using Reconnect™, a fluvial stochastic modelling software package designed to run multiple iterations of simple models in a short time period. The resultant channel distributions are used as input for 3D architectural models of the two interseams, and likely accommodation settings are distinguishing for the two interseams discussed.

1.4.3 Chapter 3: Sedimentology of fluvial system within a delta-plain setting: a case study from the Triassic Mungaroo Formation

Research question: What is the range of styles of deposition within the cored interval of the Mungaroo Formation; what insight into the varied channel styles of fluvio-deltaic depositional systems can be inferred from these observations?

Chapter 3 discusses the sedimentology and stratigraphy of the Late Triassic Mungaroo Formation, primarily using core log data from block WA-404-P, Exmouth Plateau, Northern Carnarvon Basin, Australia. This chapter serves as

grounding in terms of study location and stratigraphy of the Mungaroo Formation, which is referred to throughout the subsequent chapters of the thesis. Within this study, the Mungaroo Formation is divided into 6 seismic-stratigraphic intervals bounded by flooding surfaces (S1-S2, S2-S3, S3-S4, S5-S6, and S6-S7). The sedimentology of the Mungaroo Formation is described in terms of lithofacies, facies associations, and the occurrence and distribution of tidal indicators. The interpretation is based largely upon the S2-S3 interval, which has a near-complete cored section. The relative proportions of the facies associations are used to split the formation into packages of increased or decreased marine influence, which are associated with lower delta plain, upper delta plain and alluvial floodplain. The style of channel deposits is interpreted from lithofacies assemblages, stacking characteristics and interpreted barform migration styles in order to assess the evolution of channel style through time.

1.4.4 Chapter 4: Seismic geomorphology and sedimentology of fluvial environments in the subsurface: fluvio-deltaic Triassic Mungaroo Formation, North West Shelf, Australia

Research question: What are the broad variations in depositional environment at key intervals of the Mungaroo Formation? Can seismic facies be used to distinguish between fluvial and fluvio-deltaic deposits?

Chapter 4 establishes a link between sedimentology and seismic expression of the Mungaroo Formation through the development of a 'seismic element scheme' that links the facies associations established in Chapter 3 to seismic facies and seismic geomorphology. The element scheme encompasses channel and channel belt deposits, crevasse belt deposits, overbank fines and organic-rich deposits such as gleysols and mud-prone accumulations indicative

of poorly-drained floodplains. Seismic techniques key to the visualisation of fluvial deposits, such as stratal and horizon slicing, are introduced. The bulk of this chapter focusses on the generation of 'seismic element' maps using the aforementioned scheme and their use in the interpretation of the depositional sub-environments of three of the intervals of the Mungaroo Formation (S1-S2, S2-S3, S5-S6), horizon slices of which show contrasting channel and overbank morphologies.

1.4.5 Chapter 5: Well log and seismic interpretation techniques useful in the subsurface interpretation of fluvial deposits

Research question: What techniques can be employed to identify channelized deposits and non-channelized floodplain deposits at a range of scales? How can seismic interpretation techniques be used to enable more detailed interpretations?

Chapter 5 builds upon the work of Chapter 4 by exploring different seismic and supporting well-log interpretation techniques that are useful in the identification of fluvial and fluvio-deltaic deposits in the subsurface. Such techniques encompass well correlation, noise reduction, frequency enhancement, stratal slicing and flattening of seismic cubes, spectral decomposition and colour blending of seismic cubes. The chapter also outlines several further seismic attributes, adjustment in the values of which may be beneficial in the identification and analysis of fluvial and thinly-bedded deposits in the subsurface.

1.4.6 Chapter 6: Subsurface geomorphology of a fluvio-deltaic succession investigated with seismic attribute analysis and spectral decomposition: Late Triassic Mungaroo Formation, offshore Western Australia

Research question: How can a range of seismic interpretation techniques, including spectral decomposition, be used to resolve the internal architecture of channel-belt deposits? Can these techniques provide further insight into fluvial styles, distinguishing between entrenched valleys and amalgamated channel belts?

Chapter 6 presents the most successful of the techniques outlined in Chapter 5 as a workflow that has been successfully employed in the interpretation of the deposits of the Mungaroo Formation, and may be employed in other, analogous depositional settings. The chapter principally demonstrates the improved observations and interpretations that may be made from horizon slices taken from spectrally decomposed and colour blended volumes, compared with equivalent slices from seismic reflection data. The chapter demonstrates how, in cases where only the larger-scale features of fluvial and fluvio-deltaic systems may be identified using horizon slices, the equivalent slice taken from a colour-blended volume may reveal substantially greater detail, including the style of internal fill of channel belts within valley deposits, the ability to distinguish between amalgamated channel belt sands and incised multi-valley complexes, and even the presence of scroll bar surfaces within individual point-bar elements. The chapter also places several of the intervals of the Mungaroo Formation (S1-S2, S5-S6 and S6-S7) in a sequence-stratigraphic context, and explains the overall stacking patterns of the Mungaroo Formation depositional sequences in terms of base level changes.

1.4.7 Chapter 7: Discussion: the application of subsurface interpretation techniques to the investigation of controls on styles of fluvio-deltaic sedimentation

Research question: What are the possible allogenic and autogenic controls on fluvio-deltaic successions? Which combination of allogenic and autogenic controls best explain the variations in depositional style seen in the Mungaroo Formation? What can this tell us about fluvio-deltaic depositional systems in general?

Chapter 7 draws together the findings and conclusions from chapters 2, 3, 4 and 6, the aim being to present a discussion of allogenic and autogenic controls on fluvio-deltaic successions, with which to consider the development of the Mungaroo Formation fluvio-deltaic system (and with reference to the Rangal Coal Measures) in terms of temporal evolution, and the interplay of allogenic and autogenic processes in controlling both the overall stacking pattern and architecture of the Mungaroo Formation, and more detailed, local geomorphological variations. This discussion is augmented by the presentation of a series of ‘buffers and buttresses’ models (*sensu* Holbrook, 2006), explaining the boundary condition variations at the time of deposition of several of the Mungaroo Formation intervals (S1-S2, S2-S3, S5-S6 and S6-S7), as well as a discussion of the interplay of accommodation and sediment supply. The findings from the studies of the Mungaroo Formation and Rangal Coal Measures are summarised as a series of predicted generic responses of fluvio-deltaic systems to changes in allogenic and autogenic controls.

1.4.8 Chapter 8: Conclusions

Chapter 8 provides a concise overview to the thesis and outlines the following summary points: (i) the main controls on the deposition of the Mungaroo

Formation, and (ii) the techniques useful in the interpretation of fluvio-deltaic deposits. Additionally, the chapter discusses each of the research questions posed in Chapters 2 to 6, providing summary answers to each of the stated research questions in turn. The chapter considers the overall implications of the action of spatially and temporally variable allogenic and autogenic processes during the deposition of fluvio-deltaic successions. The chapter concludes with suggestions for future work that build upon the research carried out for this thesis

Chapter 2 Prediction of channel connectivity and fluvial style flood basin successions using wireline logs and stochastic modeling: Case study of the Upper Permian Rangel Coal Measures (Queensland)

The work presented in this chapter has been published in AAPG Bulletin as the following paper:

Stuart, J. Y., Mountney, N. P., McCaffrey, W. D., Lang, S. C., & Collinson, J. D. (2014). Prediction of channel connectivity and fluvial style in the flood-basin successions of the Upper Permian Rangel coal measures (Queensland). AAPG bulletin, 98(2), 191-212.

Research question: To what extent do minor (Secondary and tertiary crevasse splay and distributary channels) contribute to fluvial overbank successions; and how likely are they to form connected reservoir bodies?

2.1 Chapter Overview

Predicting the presence and connectivity of reservoir-quality facies in otherwise mud-prone fluvial overbank successions is important as such sandbodies can potentially provide connectivity between larger neighboring sandbodies. This paper addresses minor channelized fluvial elements (crevasse splay and distributary channels), and attempts to predict connectivity between such sandbodies in 2 interseam packages of the Upper Permian Rangel Coal Measures of northeastern Australia. Channel body percent as measured in well logs were 2% in the upper (Aries-Castor) interseam, and 17% in the lower (Castor-Pollux) interseam. Well spacing was too great to allow accurate

correlation of channel bodies. The Ob River, Siberia, was used as modern analogue to supply planform geometric measurements of splay and distributary channels, so that stochastic modeling of channel bodies was possible. The resulting models demonstrated that (i) channel-body connectivity is more uniform between minor distributary channels than between crevasse splay channels; (ii) relatively good connectivity is seen in proximal positions in splays, but decreases distally from the source as channel elements diverge; (iii) connectivity tends to be greater down the axis of splays, with more isolated channel bodies occurring at the margins.

2.2 Introduction

The distribution of sand bodies in fluvial overbank settings is strongly controlled by processes that dictate the style and frequency of overbank flooding (Benedetti 2003) via the breaching of levees, the generation of crevasse splays (Morozova & Smith 2000), and the development of minor distributary channels (Smith *et al.* 1989). In particular, size, longevity, spatial distribution and style of connection of splays to primary channels governs the distribution of sand-prone elements in overbank successions. The presence of reservoir-quality facies, such as secondary and tertiary splay and distributary channel deposits, in otherwise mud-prone fluvial overbank successions may provide significant connectivity between neighboring major channel elements in avulsion-prone channel belts, as in the Westphalian Coal Measures, Durham, UK (Fielding, 1986).

Although determination of three-dimensional sedimentary architecture and overbank connectivity is crucial for reservoir prediction in low net:gross floodplain settings, the typical km-scale well spacing in some hydrocarbon fields is too great and the total number of wells too few for the development of the

appropriate predictive models. Likewise tertiary splay and minor distributary channel elements (≤ 3 m thickness – Avenell 1998) are typically below the vertical resolution of seismic data (Bridge & Tye 2000; Ethridge & Schumm 2007), and their presence cannot be ascertained, nor their impact on connectivity inferred, from such data.

In low-accommodation fluvial settings, sand-prone channel elements are preferentially preserved as stacked and overlapping multi-story and multi-lateral bodies, whereas in higher accommodation settings, mud-prone overbank elements have greater preservation potential and neighboring channel bodies tend to be spatially isolated (Bristow & Best 1993). Figure 2.1 shows the classic fluvial sequence stratigraphic model of Shanley & McCabe (1994), illustrating the effect of changing accommodation (driven by base level change) on fluvial systems. An increased rate of accommodation creation is commonly attributed to one or both of the following driving mechanisms: (1) high rates of basin subsidence such as encountered in many foreland basin settings (e.g. Marenessi *et al.* 2005); (2) base-level rise (Bristow *et al.* 1999; Bourquin *et al.* 2006). Most systems are governed by a combination of these factors, although one may be dominant (Ethridge *et al.* 1998).

Facies associations routinely identified in low net:gross, relatively high-accommodation fluvial overbank settings include those associated with mires, levees, secondary and tertiary distributary channels, and splays and splay complexes, including those composed of multiple tertiary splay channels, as well as finer-grained units: floodplain-lake fills and floodplain fines, including palaeosols (Smith & Pérez-Arlucea 1994; Jorgensen & Fielding 1996; Cazanacli & Smith 1998; Farrell 2001). Figure 2.2 illustrates the typical architecture and internal facies make-up of these depositional elements.

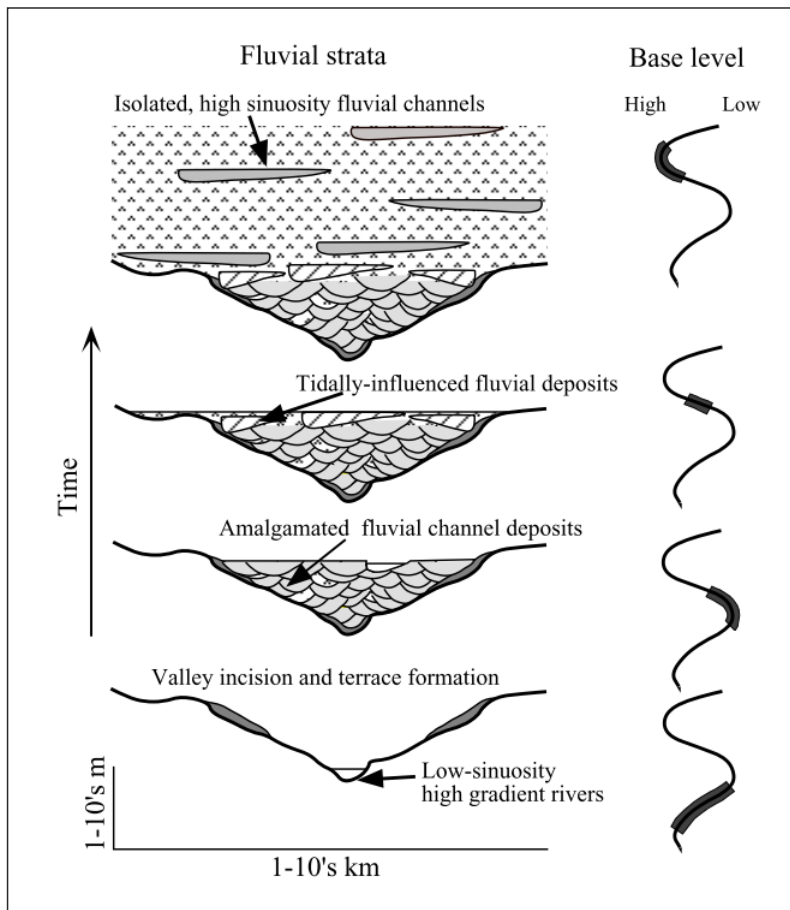


Figure 2.1: Fluvial sequence stratigraphic model (reproduced from Shanley & McCabe, 1994), demonstrating the effect of changing base level on fluvial stratigraphy.

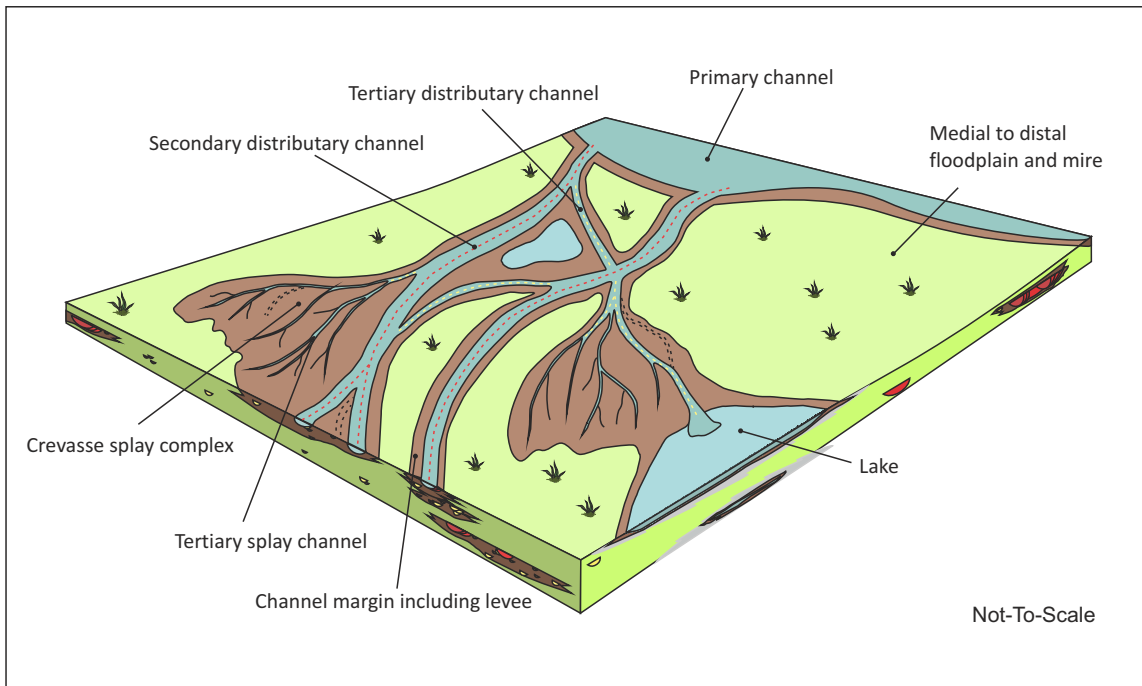


Figure 2.2: Schematic diagram illustrating the typical facies associations and architectural elements encountered in a low net:gross fluvial overbank environment.

Reservoir-quality sandstones are most likely to be present in the overbank setting as networks of secondary and tertiary channel elements, the accumulated deposits of which typically attain thicknesses of up to a few meters, and which may form laterally extensive splay bodies over distances of several kilometers. It is, however, typically difficult to distinguish between deposits of some of the smaller-scale overbank elements, particularly when relying on core or well-logs alone for interpretation (Brierley *et al.* 1997).

The aim of this study is to demonstrate the architecture and connectivity of secondary (distributary) and tertiary (distributary and splay) channelized sand bodies in a low net:gross fluvial setting, to assess the potential for communication between reservoir-quality (sandy) elements in overbank settings. Specific objectives of this study are (i) to document criteria by which minor channelized elements can be identified on wireline logs, (ii) to quantify infill proportions and dimensions of tertiary channels, (iii) to present quantitative data on plan-view geometries of modern tertiary channel elements, and (iv) to stochastically model the predicted lateral and vertical connectivity of tertiary channels. The connectivity of such sand bodies is investigated for two interseam intervals at the South Blackwater Mine, Queensland (location shown on Figure 2.3), a Permian coal-bearing flood basin succession.

This work is significant for the following reasons: (i) current models that predict sand-body occurrence in flood basin settings are overly simplistic and largely qualitative in nature (Bridge & Tye 2000); (ii) current approaches to estimating hydrocarbon reserves in fluvial reservoirs routinely only assess the geometry of major (primary) fluvial sand bodies (e.g. multi-storey channel complexes), and this potentially underestimates the true volume by ignoring the additional significant volume associated with minor secondary and tertiary channel and

splay elements; (iii) few models currently exist with which to assess the role of minor secondary and tertiary channel and splay elements in terms of their role in aiding communication and connectivity between primary channel bodies.

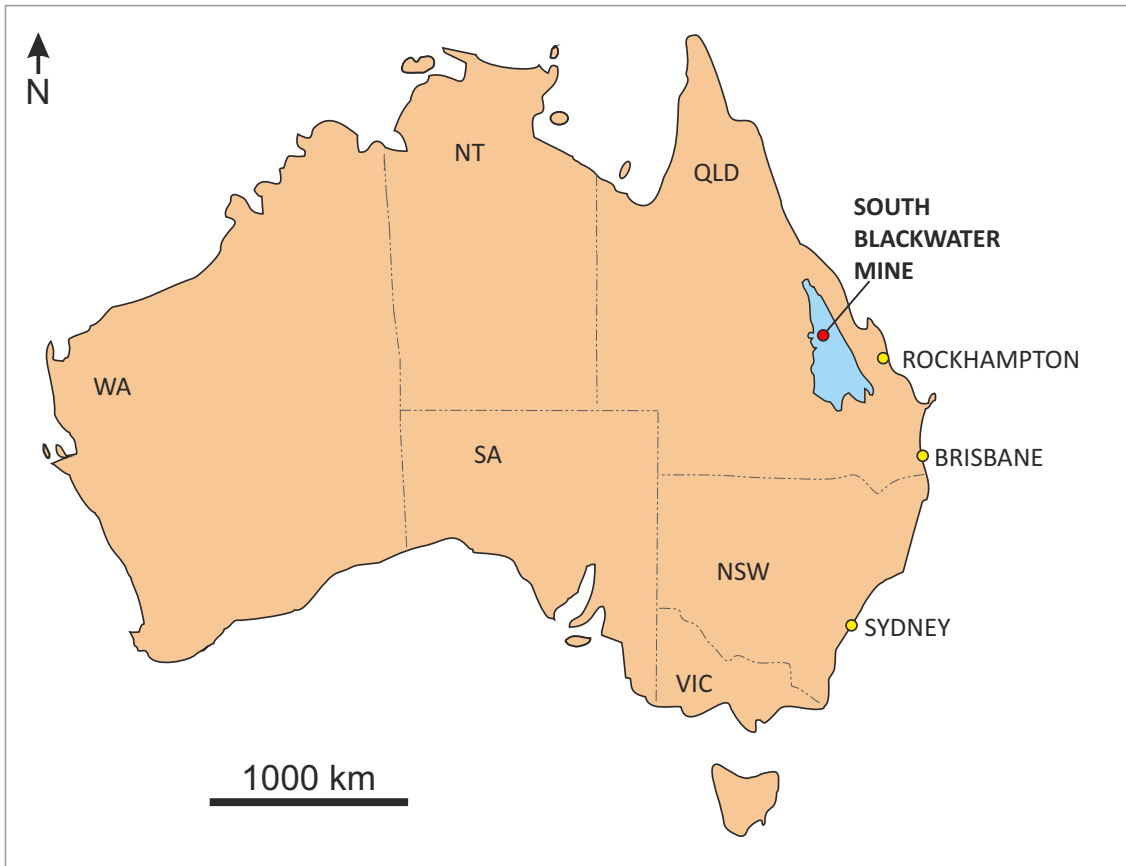


Figure 2.3: Location of the Bowen Basin and South Blackwater Mine. Location of basins from Allen & Fielding (2007) and Fielding et al. (1993).

2.3 Geological Setting

The Permian Rangal Coal Measures at the South Blackwater Mine, Bowen Basin, Queensland (Figure 2.3) are exposed in a series of open cast workings and have been penetrated by a series of shallow boreholes for which well-log and core data are available. The coal measures are widespread throughout the basin and they have been exploited through intensive open-cut mining since the 1970s (Mutton 2003). The Rangal Coal Measures form part of the fill of the Bowen Basin, which evolved – along with several other Eastern Australian Gondwanan basins – as part of the Middle-Late Palaeozoic Tasman Orogen (Fielding *et al.* 1993; Fielding 2001). Three pulses of sedimentation directed southwards along the basin axis occurred during the Late Permian, the last of which was responsible for the accumulation of the Wuchiapingian-Changhsingian age Rangal Coal Measures and equivalents, which represent the preserved deposits of a large scale fluvial system (Fielding *et al.* 1993; Allen & Fielding 2007). The sheet-like nature of primary channel deposits formed in the Rangal Coal measures is indicative of a low-sinuosity system and the Rangal Coal Measures are considered to have formed in a broad alluvial plain setting (Fielding *et al.* 1993).

At the South Blackwater Mine, the Rangal Coal Measures preserve three mineable coal seams within the study area: Aries (A), Castor (B) and Pollux (C). Within the Rangal Coal Measures, several facies associations have been recognized by previous research. Fielding *et al.* (1993) identified the following: Sheet-like sandstone channel bodies; laterally accreted, heterolithic channel bodies; proximal overbank; crevasse channel fill; floodplain; lake floor; mire. Avenell (1998) interpreted wireline and core data as recording: sheet-like channel sandstone bodies (primary channel elements); heterolithic distributary

channel bodies (secondary channel elements); minor crevasse channel bodies (tertiary channel elements); levee; floodplain; lacustrine and mire. Michaelsen *et al.* (2000) interpreted the interseam deposits as: trunk river channels and crevasse feeder channels; levee bank–proximal crevasse splay; distal splay–overbank; marsh; peat mire and floodplain lake.

2.4 Data and Methods

The study covers a 2km² area of the South Blackwater Mine, Queensland. Detailed correlation of a subsurface part of the Rangal Coal Measures succession was undertaken using a high-density subsurface dataset of wireline logs from 63 coal exploration wells. Available well logs included, including gamma-ray (GR), density, caliper and sonic logs were utilized.

High-resolution lithologic logs were made for each well in the dataset using Oilfield Data Manager (ODM) software, primarily via the interpretation of GR and density log responses. For the purpose of lithology interpretation, GR cut-offs were defined as follows: clay and mudstone, >110 API GR; siltstone and silty sandstone, 110-90 API GR; 'clean' sandstone (>60% sand), <90 API GR (Avenell, 1998). Coal was easily identified by its distinctive signature characterized by very low GR values coincident with low density values.

After assigning lithologies to each well, architectural elements (Miall, 1985) were assigned to packages of deposits deemed to have been formed by the same processes. To help achieve this, an extended and refined lithology and facies scheme for the Rangal Coal Measures was developed from a previous core-based study at the South Blackwater Mine (Avenell 1998) and this was used as the basis for the architectural-element scheme developed in this study. Patterns in well-log curves and lithologic cycles were identified and assigned

to fluvial and overbank architectural elements. Architectural elements were then correlated between subsurface wells in an attempt to characterize two-dimensional facies changes and, where possible, the likely three-dimensional sedimentary architecture and style of connectivity of secondary and tertiary fluvial channel elements considered to have arisen as a product of crevassing in a distributary system.

Where it was not possible to predict architectural-element type and extent from groups of neighboring well logs, measurements and estimates of likely plan-form geometry were made via the adoption and implementation of geometries of similar elements from analogous modern systems. Study of these modern fluvial systems involved the measurement of channel widths, lengths and sinuosities using Google Earth® imagery. These analogue data were integrated into reservoir models of the study area using Reckconnect®, a fluvial stochastic modeling software package. Reckconnect was chosen due to its ability to run multiple iterations of models in a short time period, in order to test the effect on reservoir connectivity of changing the dimensions and other parameters of the channel-element sand bodies.

Interpretations of the depositional sub-environments of the Rangal Coal Measures interseam intervals were then made based on the proportions and distributions of architectural elements observed in each of the two interseam intervals, one between the Aries (A) and Castor (B) seams, and the other between the Castor (B) and Pollux (C) seams.

2.5 Architectural Elements

Seven principal architectural elements have been identified in the study area between the Aries (A) and Pollux (C) seams (Figure 2.4) using defined GR cut-

offs for sand (<90), silty sand (90-110) and mud (>110), together with correlation of wireline log signatures between neighboring well-logs. The architectural element scheme is based on that of Avenell (1998).

Secondary channel elements. The wireline log character of these elements shows a sharp, erosional base, with a fining-up, blocky or bell-shaped gamma response. These deposits are <90 API GR. These elements are greater than 3 m thick and are interpreted as heterolithic distributary channel-fill deposits (Fielding et al. 1993). Distributary channels are typically bounded by levees, are subject to some lateral accretion, and grade laterally into finer-grained floodplain deposits (Avenell, 1998), in places causing local 'washouts' of the Castor (B) seam.

Tertiary channel elements. These elements have a GR of <110 API GR, in a succession of <3 m-thickness sandstone. They are typically sharp-based, fining-up to clayey, silty sandstones. The overall log signature is blocky or bell-shaped. Laterally more extensive tertiary channel elements are interpreted as those of mature crevasse channels, analogous to the stage 3 splay channels of Smith et al. (1989). Less extensive, poorly developed tertiary channel elements are interpreted as immature or abruptly abandoned splay channels of a stage 1 or stage 2 crevasse splay (Smith et al. 1989).

Channel-margin (including levee) and lake-margin elements. Channel-margin deposits form the finer-grained equivalent to adjoining channelized deposits. They typically exhibit fine-grained (alternating high and low GR) log patterns,

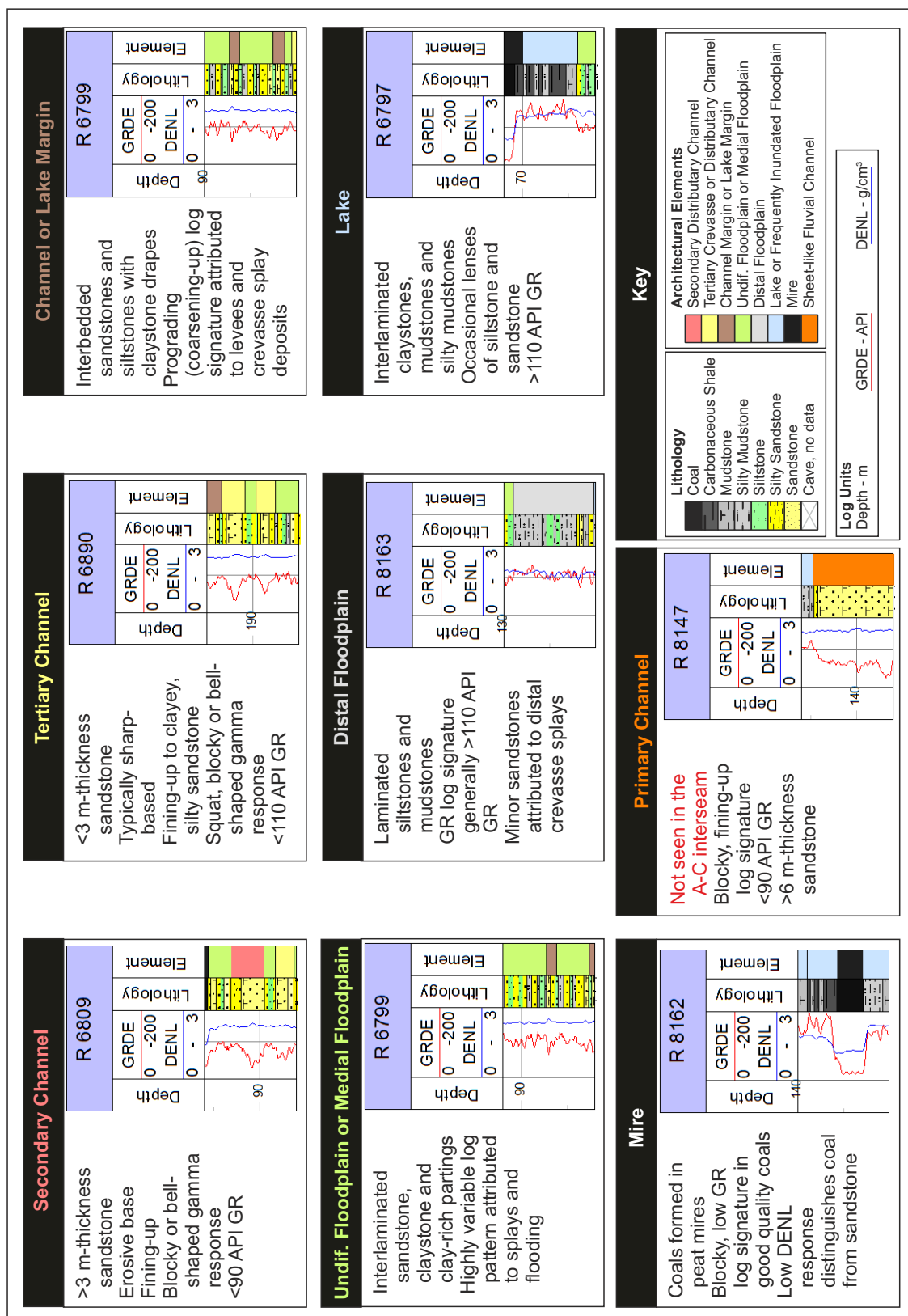


Figure 2.4: Architectural element scheme of the fluvial and overbank deposits of the Rangal Coal Measures present in the interseam packages of the South Blackwater Mine, Queensland (Adapted in part from Avenell 1998). Lithologies and architectural elements assigned using gamma-ray (GRDE) and density (DENL) logs.

corresponding to interbedded sandstones, siltstones and clay drapes. Lake-margin deposits routinely exhibit coarsening-up, progradational log patterns, but are difficult to distinguish from levee channel-margin deposits where observed in wireline borehole logs alone.

Proximal to medial floodplain elements. Deposits of these elements consist of interlaminated sandstone, siltstone and clay-rich partings, with a highly variable log pattern attributed to splays and flooding.

Distal floodplain elements. Deposits of these elements are characterized by laminated siltstones and mudstones, with a GR log signatures generally >110 API GR. Minor sandstone intervals identified in these packages likely represent the distal deposits of crevasse splays.

Floodplain lake and frequently inundated floodplain elements. These deposits of interlaminated claystones, mudstones and silty-mudstones, with rare lenses of siltstone and sandstone, have GR log readings generally >110 GR API. They are indicative of a system subject to seasonal flooding.

Mire elements. Within these deposits, a blocky, low GR-log signature is indicative of coals. This 'blocky' GR response, together with a low DENL response distinguishes coal from sandstone. These deposits constitute coal seams and carbonaceous shales formed in peat mires.

Thick and sheet-like primary channel-fill elements are not encountered in the interseam deposits of the study area, though such bodies are identified from some wells beneath the C seam. Most wells stopped at or just beneath the C seam, so correlation of these extensive sand-prone elements has not been possible.

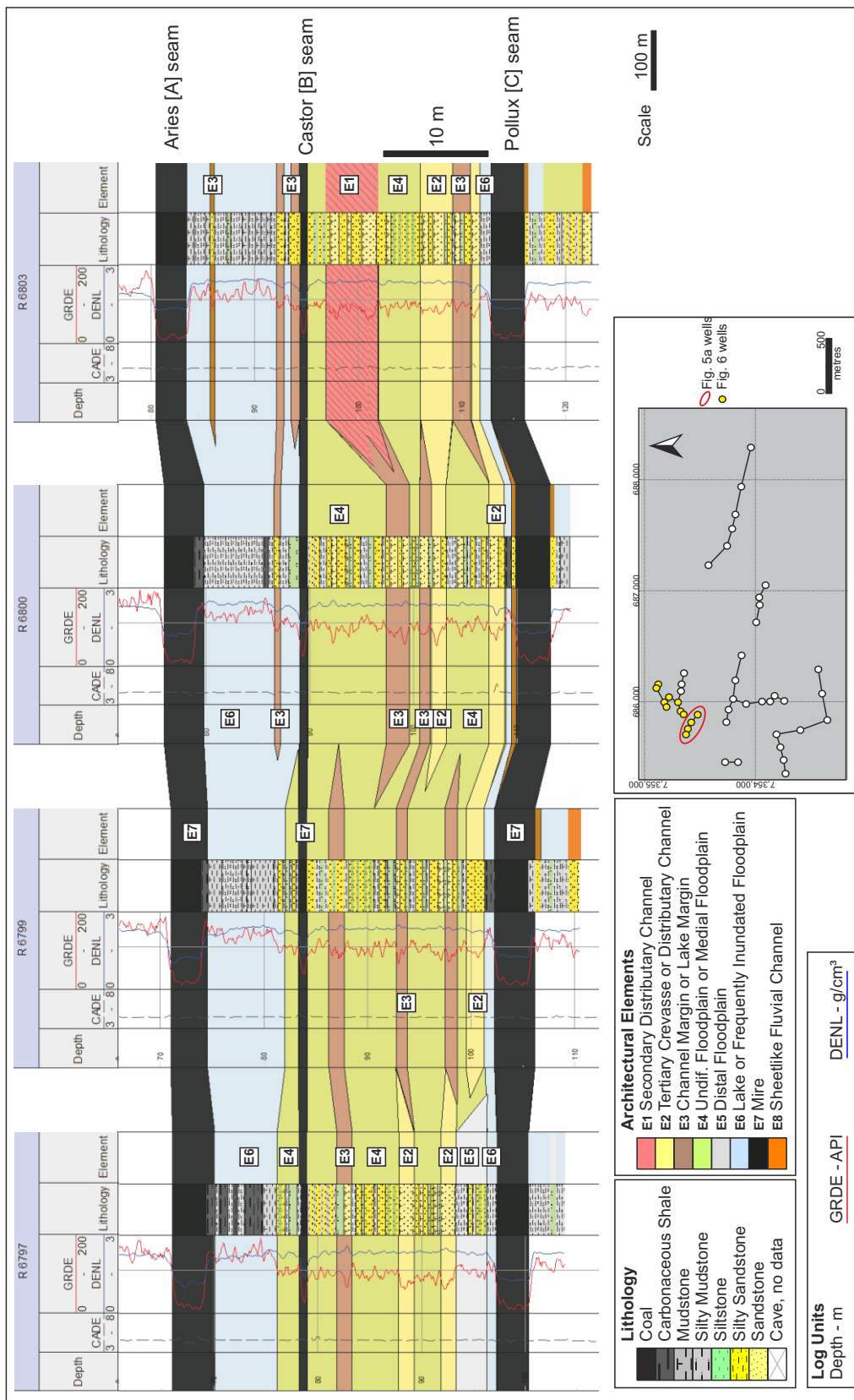
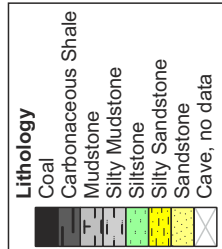
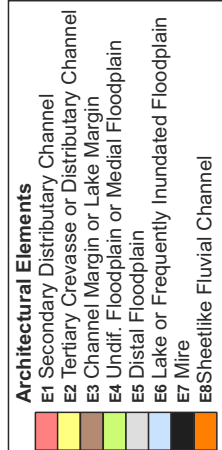
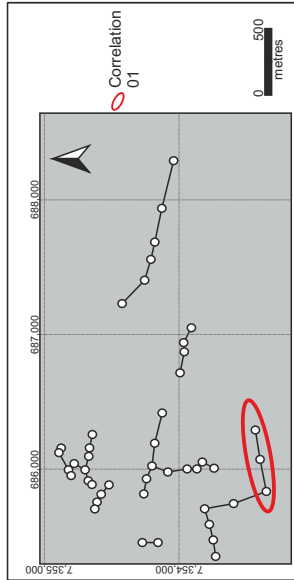
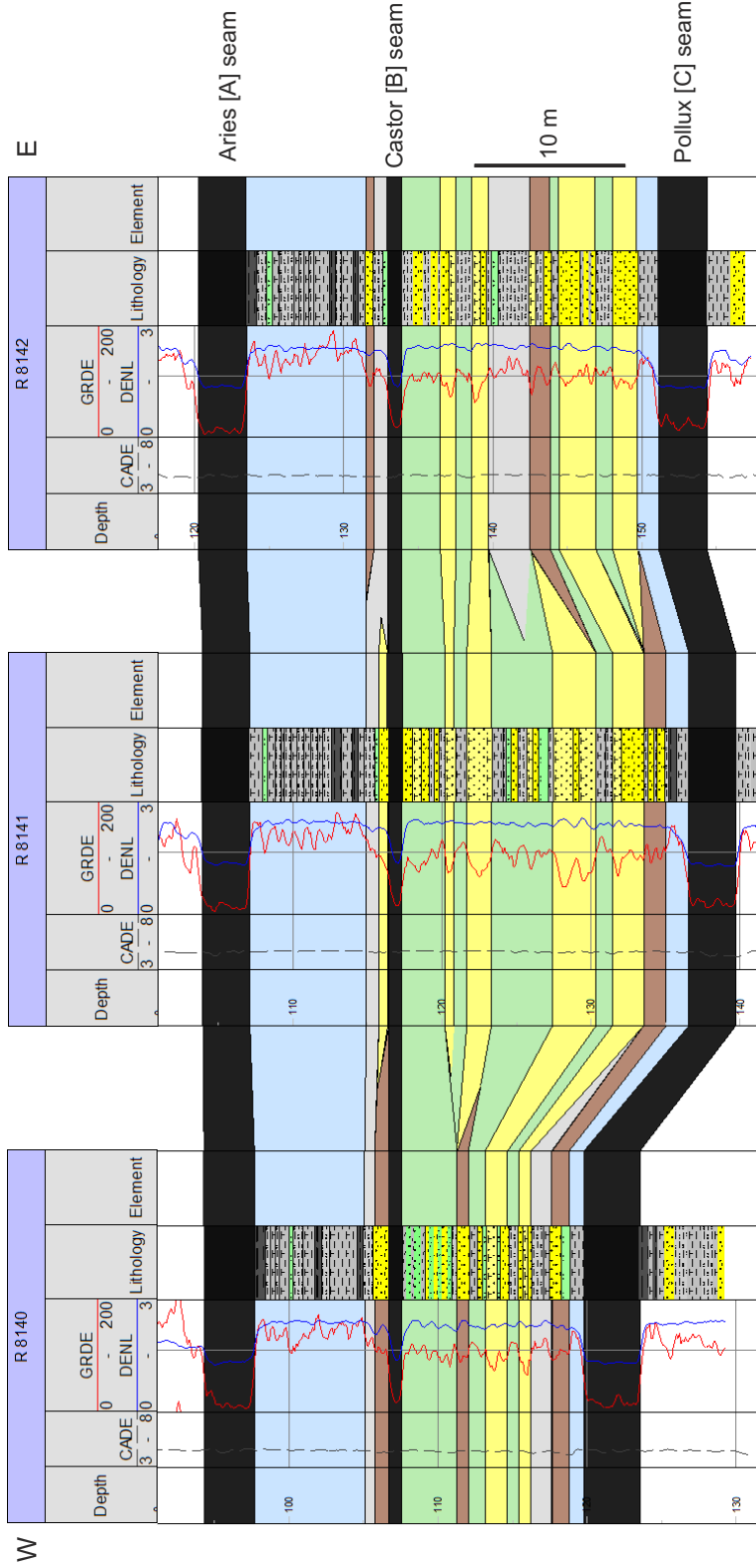


Figure 2.5a: Correlation panels illustrating the interseam deposits of the Rangal Coal Measures. **a.** Correlation panel from the NE of the study area (location circled on the inset map), demonstrating negligible net:gross A-B interseam and low-to-moderate net:gross B-C interseam, where both tertiary and secondary channels are present. Location of the correlation is shown in the inset map, as is the location of the fence diagram (Figure 2.6). Wireline log abbreviations: GRDE (gamma ray, API units), DENL (density), CADE (caliper).

Correlation 01



Scale 100 m

Fig. 2.5b. Correlation panel 01, demonstrating negligible net:gross A-B interseam and low net:gross B-C interseam

Correlation 11

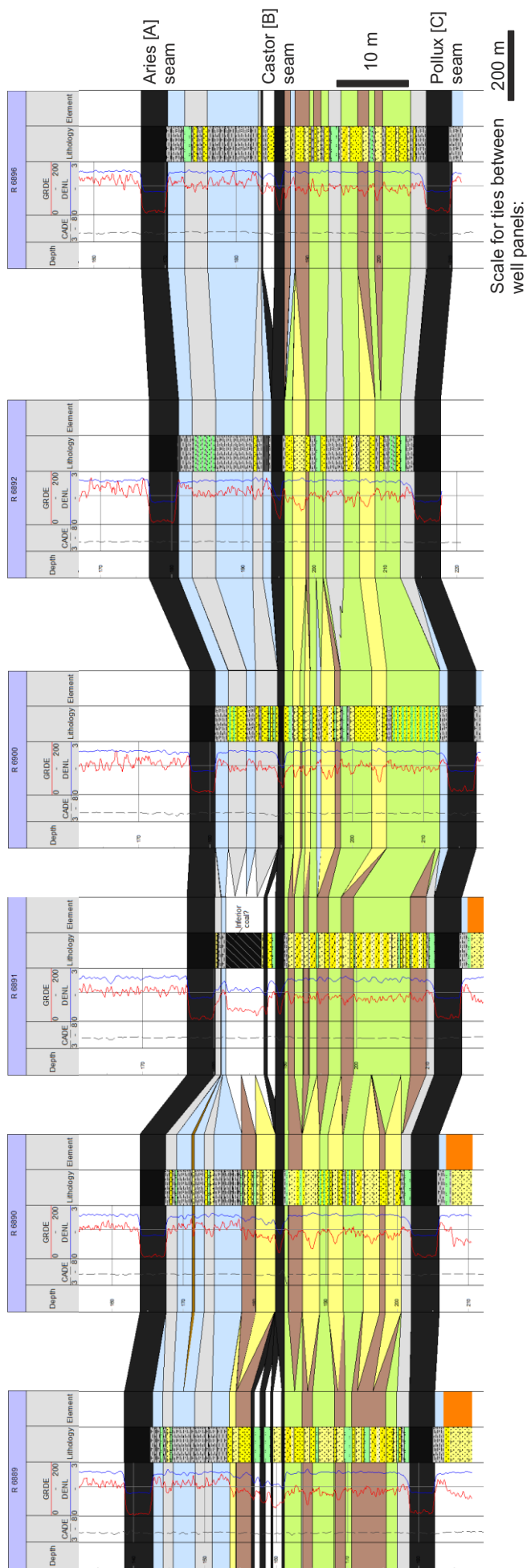
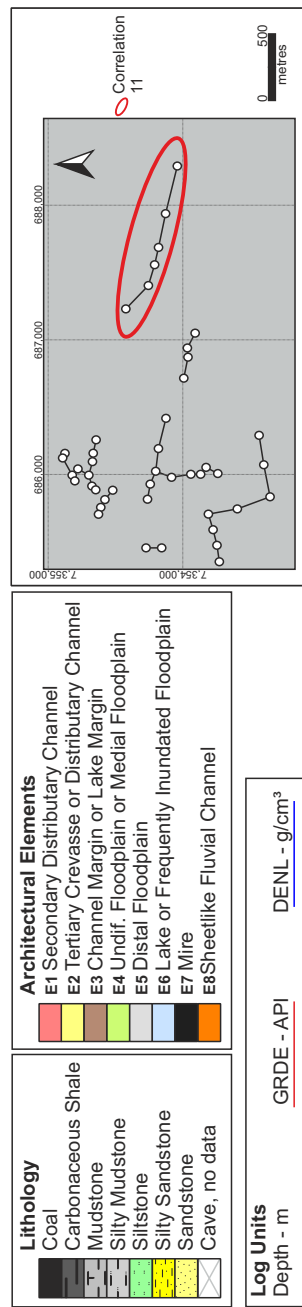
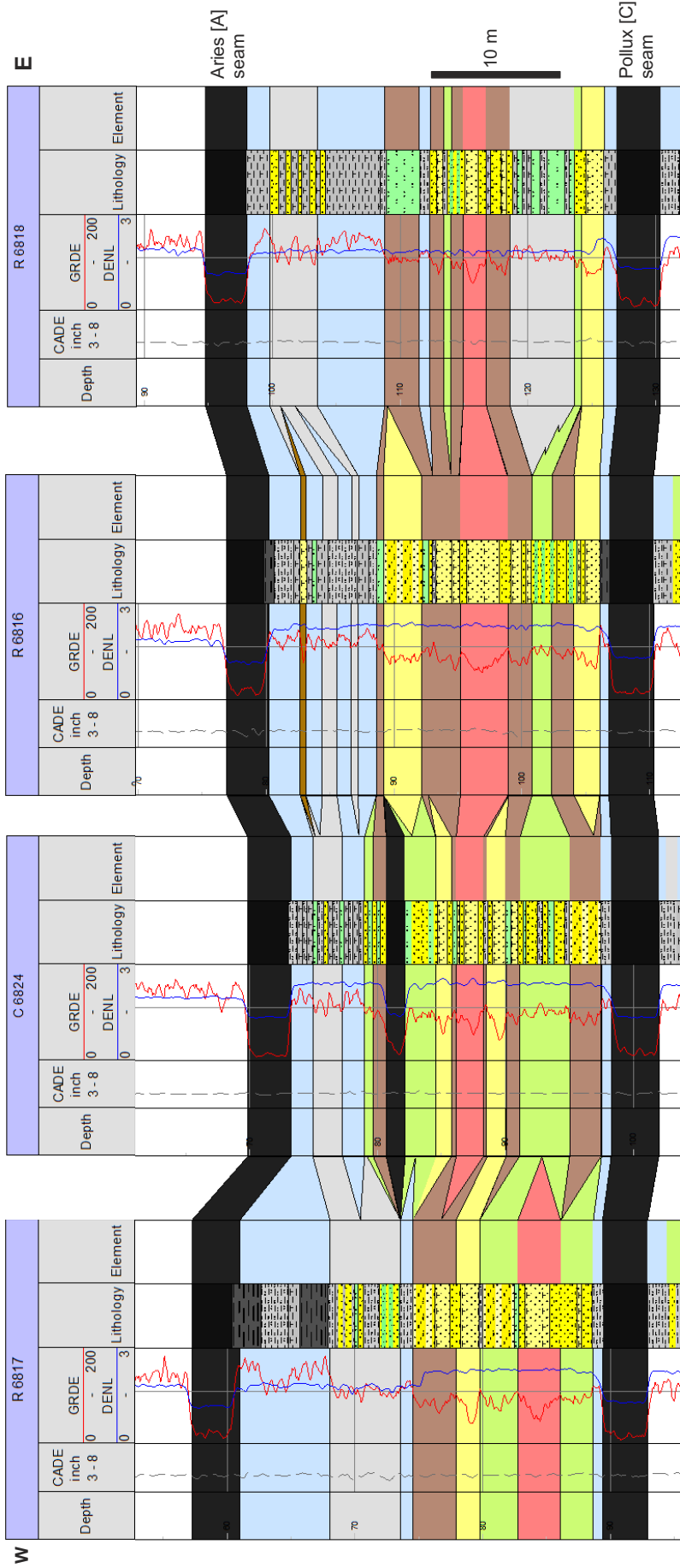


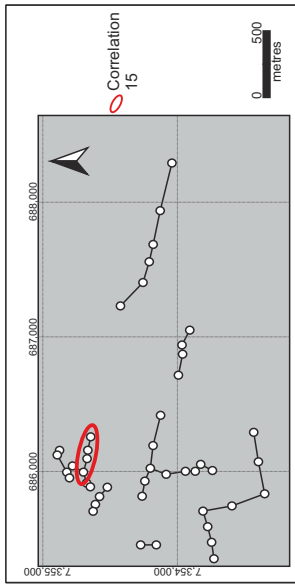
Fig. 2.5c. Correlation panel 11, demonstrating negligible net:gross A-B interseam and low-moderate net:gross B-C interseam



Correlation 15



Scale for ties between well panels: 100 m



- Architectural Elements**
- E1 Secondary Distributary Channel
 - E2 Tertiary Crevasse or Distributary Channel
 - E3 Channel Margin or Lake Margin
 - E4 Undif. Floodplain or Medial Floodplain
 - E5 Distal Floodplain
 - E6 Lake or Frequently Inundated Floodplain
 - E7 Mire
 - E8 Sheetlike Fluvial Channel

- Lithology**
- Coal
 - Carbonaceous Shale
 - Mudstone
 - Silty Mudstone
 - Siltstone
 - Silty Sandstone
 - Sandstone
 - Cave, no data

Log Units

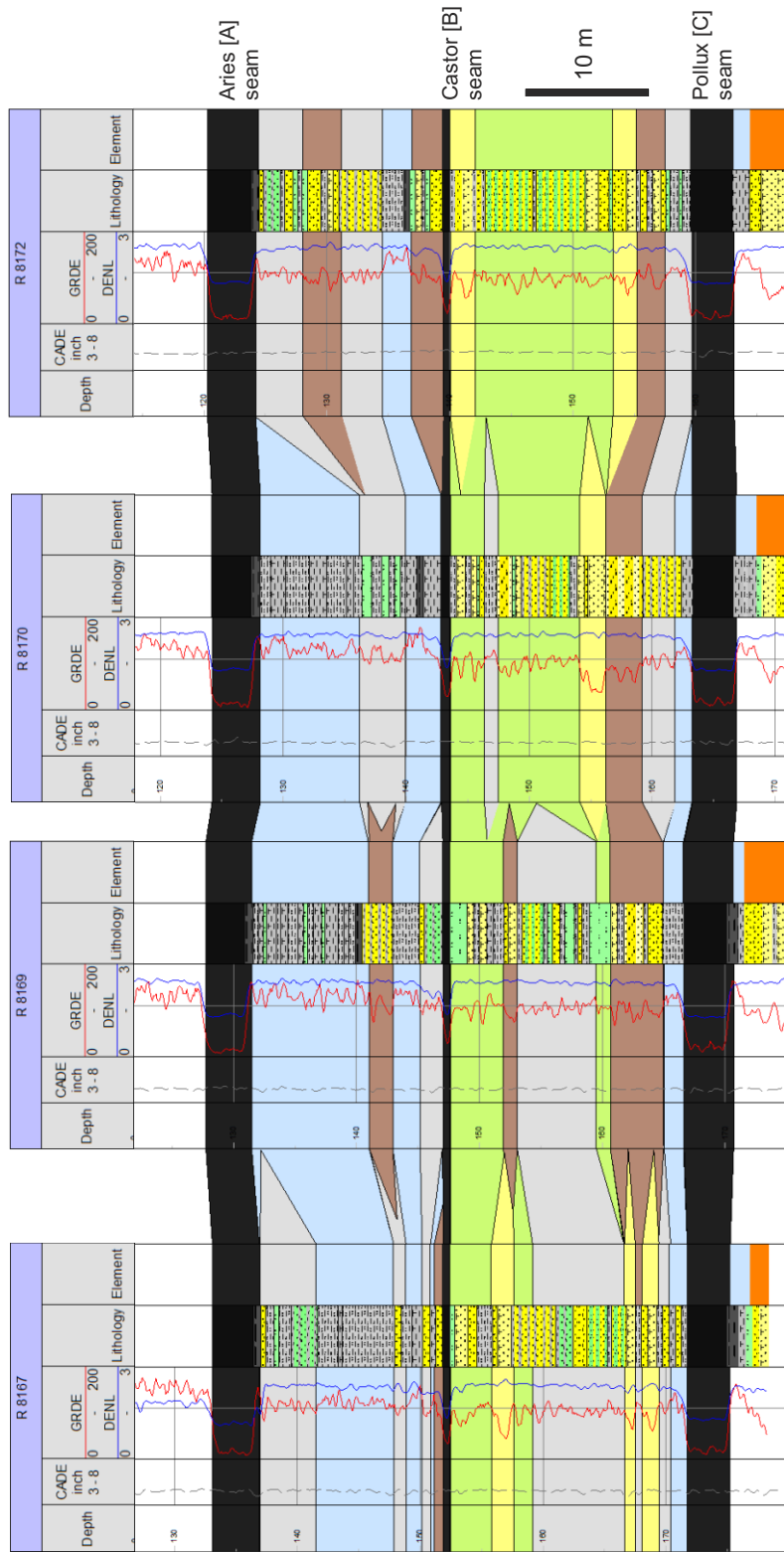
Depth - m

GRDE - API

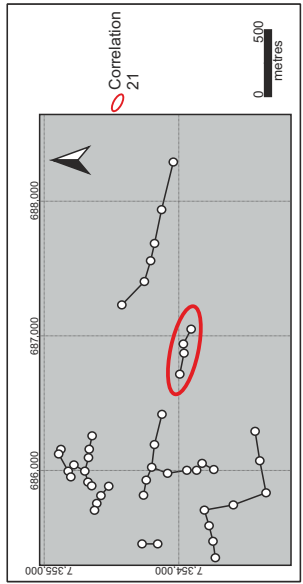
DENL - g/cm³

Fig. 2.5d. Correlation panel 15, demonstrating negligible net: gross A-B interseam and moderate net: gross B-C interseam

Correlation 21



Lithology	Architectural Elements
<ul style="list-style-type: none"> Coal Carbonaceous Shale Mudstone Silty Mudstone Siltstone Silty Sandstone Sandstone Cave, no data 	<ul style="list-style-type: none"> E1 Secondary Distributary Channel E2 Tertiary Crevasse or Distributary Channel E3 Channel Margin or Lake Margin E4 Undif. Floodplain or Medial Floodplain E5 Distal Floodplain E6 Lake or Frequently Inundated Floodplain E7 Mire E8 Sheetlike Fluvial Channel



Scale for ties between well panels: 100 m

Fig. 2.5e. Correlation panel 21, demonstrating negligible net: gross A-B interseam and low-moderate net: gross B-C interseam

Log Units
 Depth - m GRDE - API DENL - g/cm³

2.5.1 Correlation

Figure 2.5a details a typical subsurface well correlation, taken from the northeast of the study area (see inset map for location), demonstrating both secondary and tertiary channels. The correlation utilizes caliper, gamma-ray and density wireline logs to identify the three major coal seams present in the studied interval, to interpret the interseam lithology, and to interpret the architectural elements present in the interseams. Further correlation panels are demonstrated in Figures 2.5b-2.5e. Fence diagrams collating key correlation panels were constructed to demonstrate the three-dimensional architecture of the interseam deposits (Figure 2.6) and to identify key areas of secondary and tertiary fluvial channel deposition.

2.5.2 Element Proportions

Proportions of the A-B, and B-C interseam intervals infilled by each architectural element were measured from their thicknesses in each interpreted well log (Figure 2.7). Net:gross was calculated for each interval (A-C, A-B, B-C), taking only 'clean' (GR <90 API) sandstone as net. The correlation panel and fence diagram (Figs. 2.5 & 2.6) demonstrate that the B-C interseam has a greater proportion of channel elements and therefore a higher net:gross than the A-B interseam.

2.5.3 Channel Element Thicknesses and Widths

Channel-element thicknesses were determined from well logs. A frequency plot reveals the distribution of the range of channel thicknesses (Figure 2.8), where frequency refers to the number of appearances in well logs. It was not possible to measure channel-element widths using the well correlation data alone because well spacing was greater than the width of the channel elements in most cases, such that estimated widths measured from correlation panels

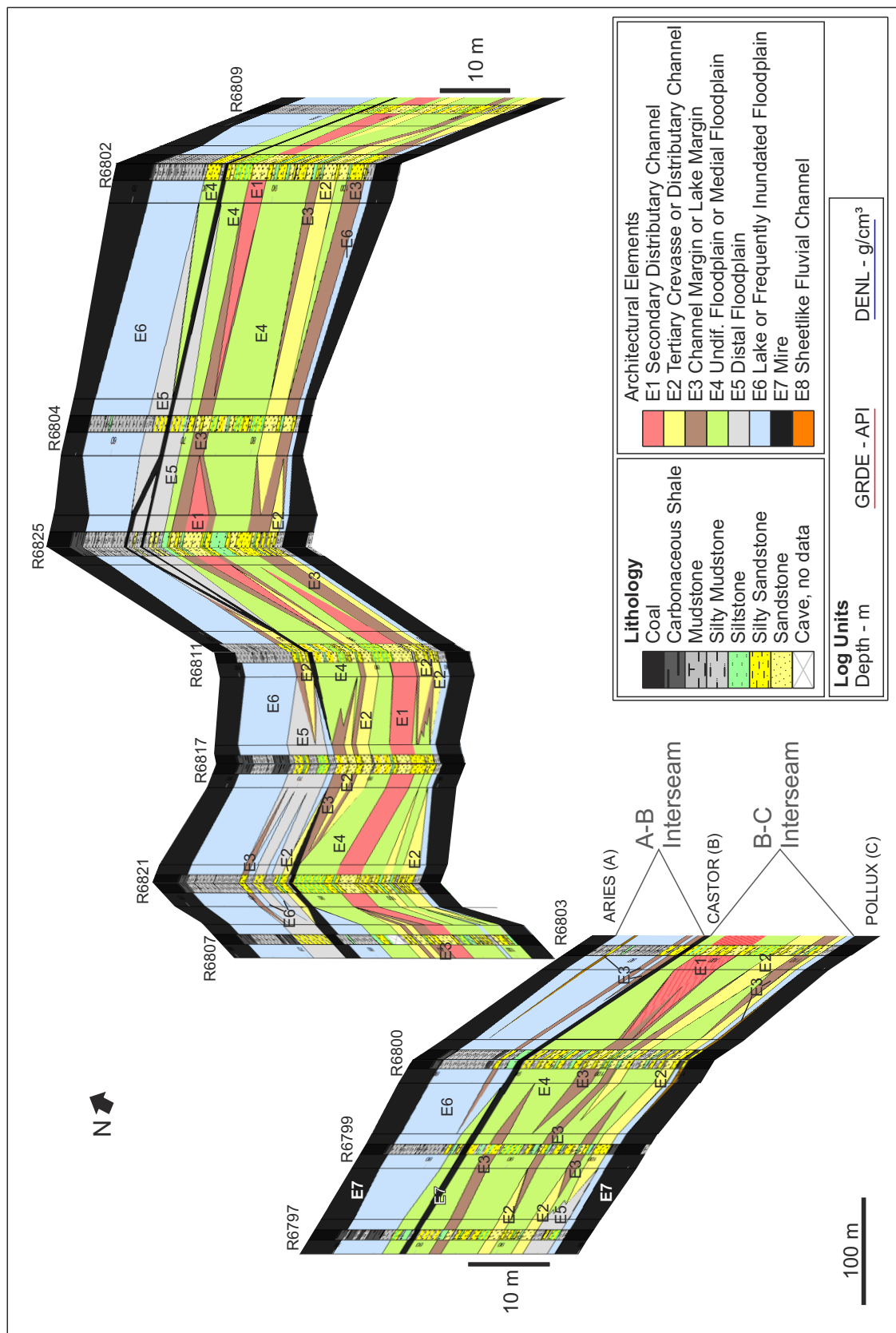


Figure 2.6: Fence diagram demonstrating presumed 3D spatial geometry of elements. Laterally continuous fine-grained floodplain deposits are accurately correlated. Well spacing was too wide (50 m to 250 m) to accurately correlate tertiary channels, which globally are typically less than 250m width (Gibling 2006). Attempts to correlate individual channel bodies has led to some unrealistic correlations. Negligible net: gross in A-B interseam, 20% net:gross in B-C interseam.

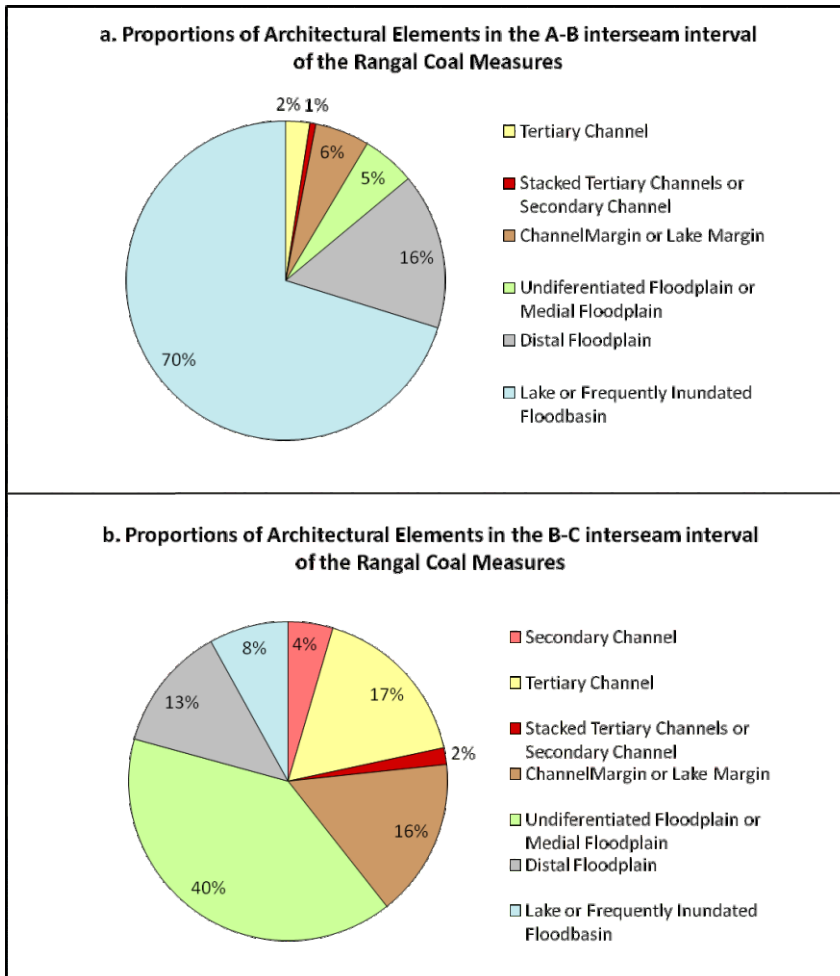


Figure 2.7: Well logs provided proportions of infill by each architectural element in both (a) the Aries-Castor (A-B) interseam and (b) the Castor-Pollux (B-C) interseam. Proportions measured by thickness of occurrence in studied well logs. The A-B interseam is dominated by distal deposits, with only 2% tertiary channel infill, whereas the B-C interseam is dominated by medial deposits, with 17% tertiary channel infill.

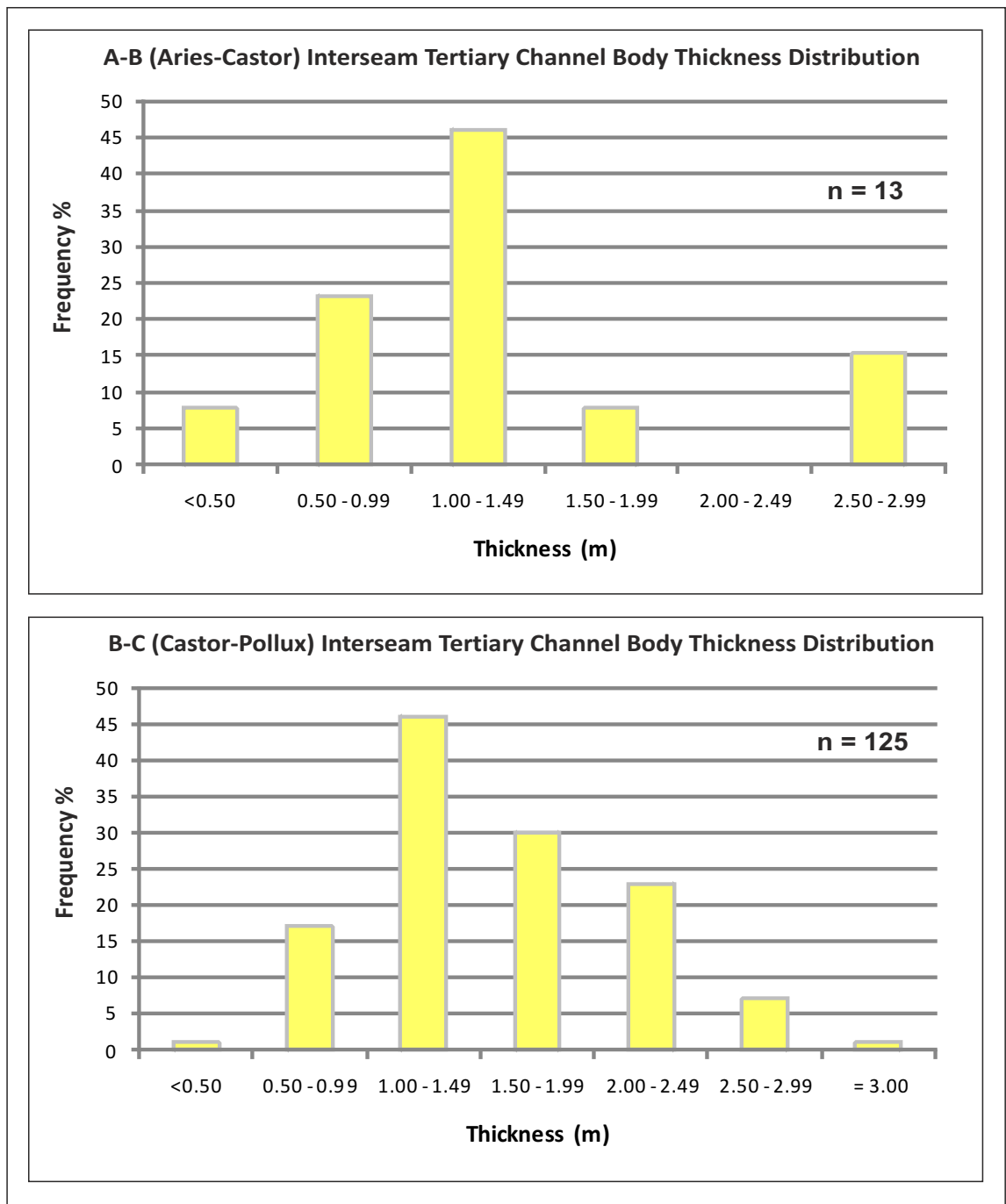
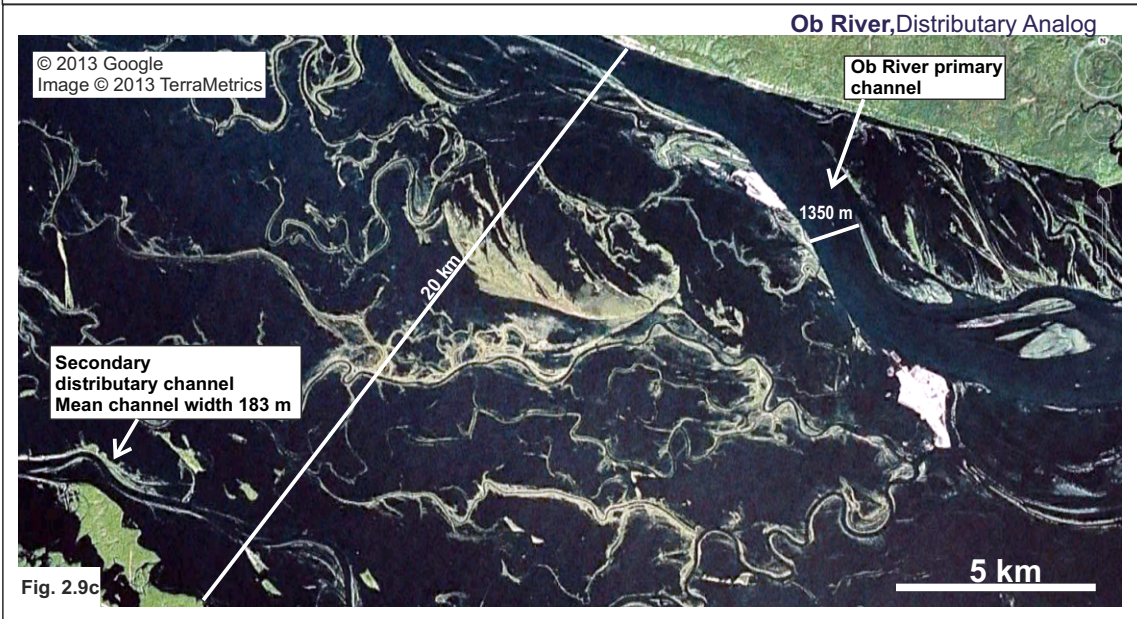
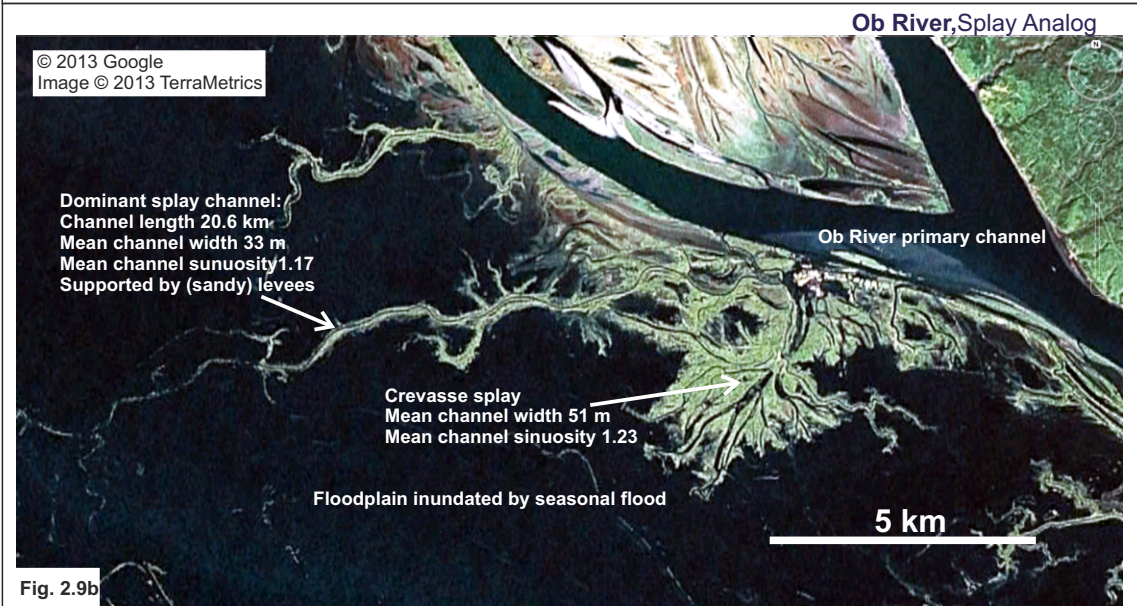
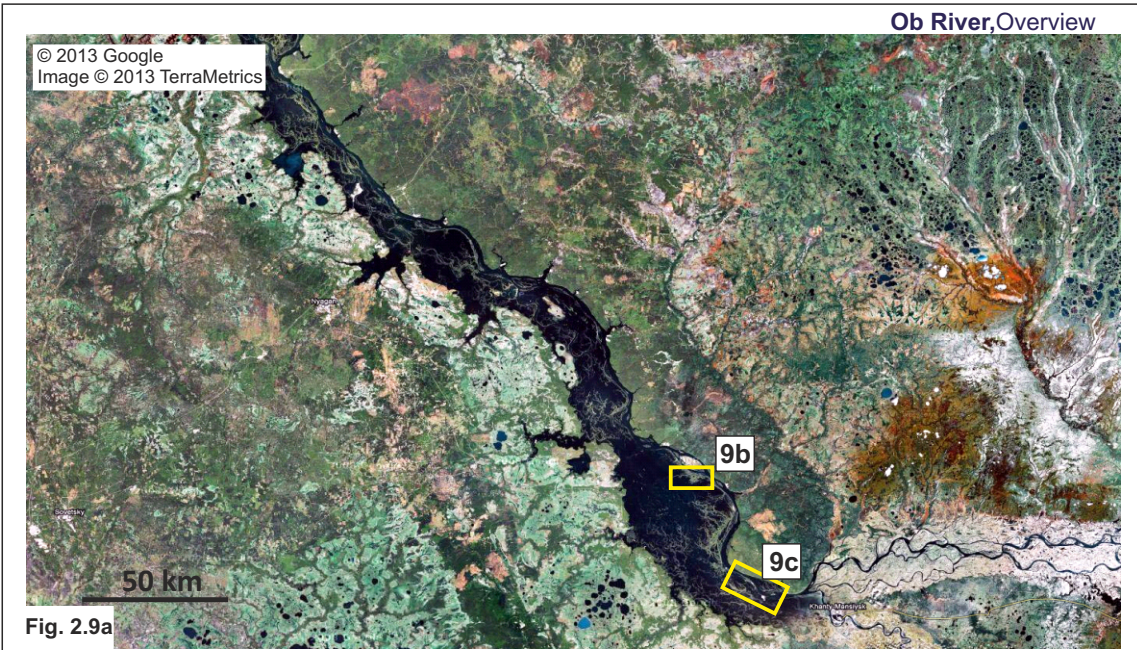


Figure 2.8: Tertiary channel element thickness data taken from well logs in both the A-B and B-C interseams.

Figure 2.9: (a) Overview image of the Ob River, Siberia. This large-scale, distributary system has a up to 40 km-wide floodplain. The primary channel is low sinuosity, over 1 km wide, and numerous secondary distributary and tertiary (distributary and crevasse) channels are present. (b) A typical crevasse splay from the Ob River, Siberia, measuring 5 km in length. Green areas represent the raised crevasse complex, and tertiary channel levees. Dark areas of the floodplain are inundated by spring flood waters. (c) Secondary and tertiary distributary channels in the Ob River, Siberia. Channels exhibit a range of sinuosities and bifurcations are common. Splay complexes exhibit a fractal nature, with mini 'splays' often originating from larger splay complexes and tertiary channels.



effectively became a function of the well spacing rather than a true indicator of channel-body width.

2.6 Interpretation

2.6.1 Analogue Measurements

In cases where it is not possible to directly derive all the information necessary to build accurate reservoir models from available datasets, analogue data may be used to approximate the missing parameters (e.g. plan-form geometry) that cannot be determined from the primary subsurface dataset alone (Alexander, 1993; Lang *et al.* 2002). For overbank depositional systems whose constituent architectural elements (e.g. floodplain and splay) are readily preserved, such as those of the Rangal Coal Measures, modern analogues must be chosen from relatively high-accommodation fluvial and fluvio-deltaic settings in which extensive peat-forming processes are acting and for which frequent flooding, crevassing and deposition occurs on the floodplain.

One modern example is the Ob River, Siberia. The Ob River was selected as a suitable analog as it is set within the large-scale, continental, non-tropical peat-forming depositional system in the West Siberian Plain (Lang *et al.* 2002). The Ob River has a very large primary channel (Figure 2.9). However it is the numerous secondary and tertiary channels, running roughly perpendicular to the primary channel, that have been identified as likely modern equivalents of the distributary and splay channels present at the time of deposition of the Rangal Coal Measures at the location of the South Blackwater Mine (Lang *et al.* 2002). This analogue is used to link surface geomorphology to subsurface sedimentology in the South Blackwater Mine dataset. The Ob River system floods seasonally (Figure 2.9a), with floods emanating from breaches in levees

that result in widespread crevassing, the generation and maintenance of secondary and tertiary distributary channels (Figure 2.9b) during spring floods. As the floods dry during summer months, the receding water leaves abundant floodplain lakes across the floodplain (Lang *et al.* 2002). Figure 2.9c illustrates a typical crevasse splay complex of the Ob River, and this is considered to be similar in both scale and morphology to those envisaged for the South Blackwater study succession, based on the similarity in scale of the various architectural elements known from the two systems.

Measurement of the dimensions of the planform geometries of tertiary channels of the Ob River (both splay and distributary), including width, length and sinuosity, were taken from Google Earth aerial photographs (Table 2.1). Sinuosity is calculated as the channel length divided by the down-valley length of the channel. Mean sinuosity (1.16) and width (41.60 m) of splay channels (N = 43) was less than that of the distributary tertiary channels (sinuosity = 1.27; width = 59.75 m, N = 24).

Table 2.1: Summary of tertiary channel dimensions from the Ob River, Siberia

Channel Type	Mean Width (m)	Mean Length A (km)	Mean Sinuosity
Distributary Tertiary	59.75	11.12	1.27
Splay 1 Tertiary	50.95	5.85	1.23
Splay 2 Tertiary	41.14	1.83	1.06
Splay 3 Tertiary	34.40	3.92	1.18
Splay 4 Tertiary	34.38	2.22	1.21
Splay 5 Tertiary	32.57	1.81	1.12
All Splay Tertiary	41.60	3.13	1.16

2.6.2 Modeling

The tertiary channels in the Ob River record little evidence for significant lateral migration via the accretion of point-bar deposits, so preserved sediment

geometries are assumed to be similar to those on the surface. Measurements of the widths and sinuosities of active channels from the Ob River analogue were therefore used in combination with the subsurface data, to derive estimates of likely infill proportions and channel thickness:width relationships for the Rangal Coal Measures. These were in turn used to define input ranges for stochastic models of the interseams made using Reckconnect (fluvial stochastic modeling software).

Reckconnect is a stochastic, object-based model that quickly models channel bodies to assess the effect of changing channel body dimensions and distributions on connectivity (Collinson & Preater, 2009). Models are created using channel body thickness and channel percentage data from wells, and geometric data (e.g. channel body width and sinuosity). Modelled output is simple, treating all channel bodies as reservoir, and all other deposits (model background) as non-reservoir. The models allow quantification of channel body connectivity, as well as connectivity to pseudo-wells.

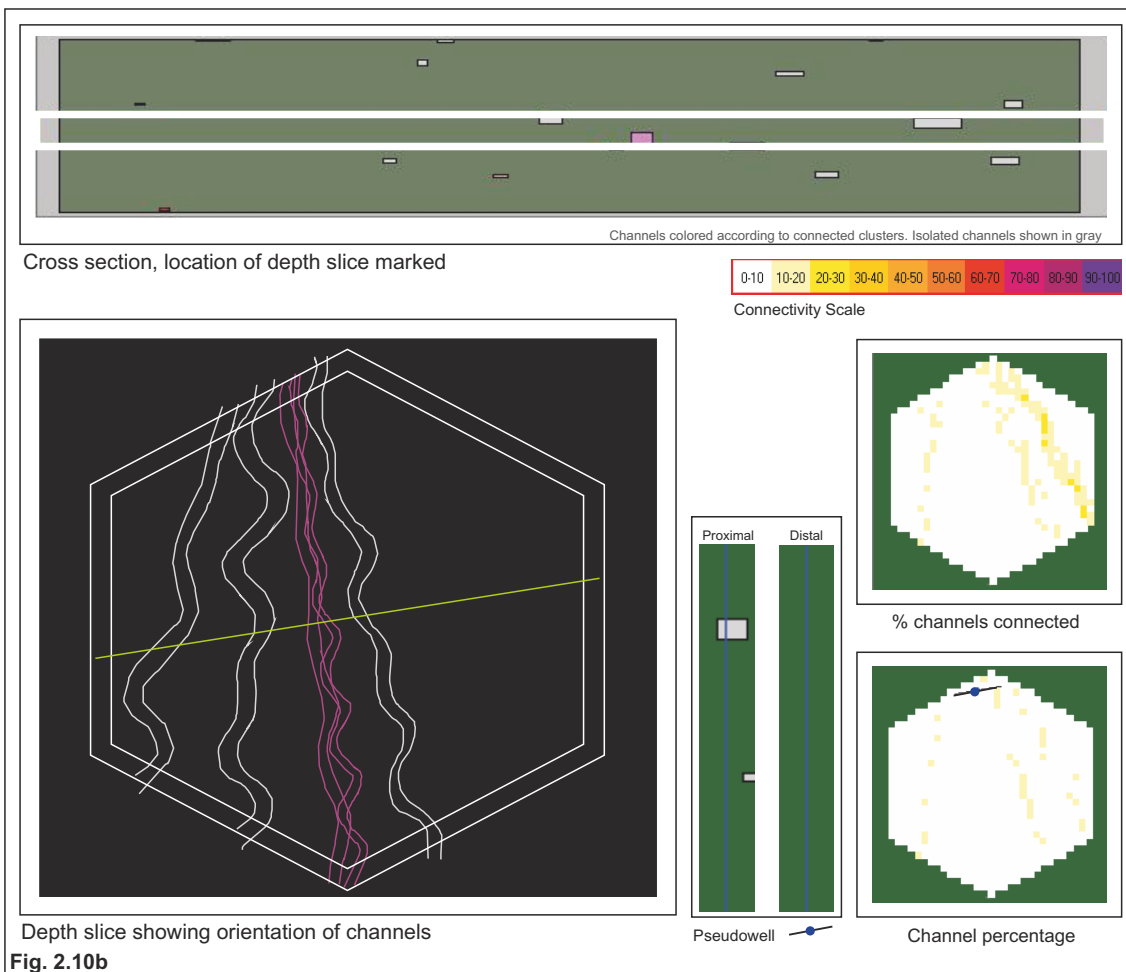
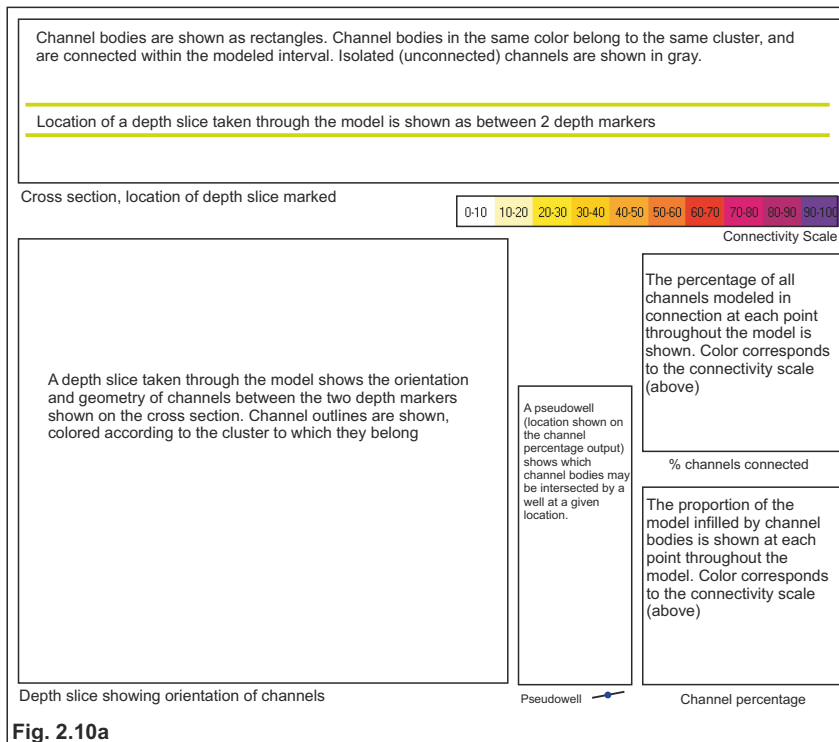
For each model run, graphic output from a randomly selected run was generated to illustrate the form of modeled channel geometries, and predicted style of clustering, channel connectivity (where channel connectivity by volume is defined as the mean percentage of sand connected to a random sandy point), and channel-body percentages observed in pseudo-wells. Results demonstrate potential well connectivity to sand bodies in the model, where well connectivity is defined as the probability (%) that pseudo-wells are connected by a continuous sandy path (Figure 2.10a).

Reckconnect is not suitable for modeling two types of channel simultaneously (i.e. secondary and tertiary channels), and therefore models were built to

represent the distribution of tertiary channels, which make up a greater proportion of interseam infill. In the A-B (Aries-Castor) interseam, infill by minor channels is 2% by tertiary channels and <1% by secondary channels. In the B-C (Castor-Pollux) interseam, the bias towards tertiary channels is greater with 17% infill by tertiary channels and 2% by secondary channels.

As both splay and distributary channels are identified in the South Blackwater Mine (Avenell, 1998) and in the Ob River (Figure 2.10), both of these fluvial styles were modeled for the interseam deposits.

Figure 2.10 (Over Page): (a) Schematic diagram explaining the graphic outputs of Reckconnect modeling runs used in Figs. 10b-12. The graphic output represents one random replication out of 100 iterations made in each modeling run. (b) Graphic output of a random replication from a Reckconnect modeling run, representing the A-B interseam, with a splay geometry. With only 2% channel infill in the interval, the cross-section shows very few channels, the majority of which are isolated (shown in grey). The depth slice demonstrates channel orientations and geometries (depth slice location shown in light green on the cross-section). The connectivity scale can be used to interpret the channel connectivity and channel percentage outputs: Channel connectivity is negligible across most of the model. Mean channel connectivity is 11%; i.e. 11% of the 2% of the model infilled by channel bodies is connected. In this scenario, only 0.02% of the modeled interval is represented by reservoir-quality sand bodies that are in some way connected. The pseudo wells demonstrate that in both proximal and distal locations, the well is likely only to intersect isolated channels, if any. Table 2c shows the statistical output from this replication.



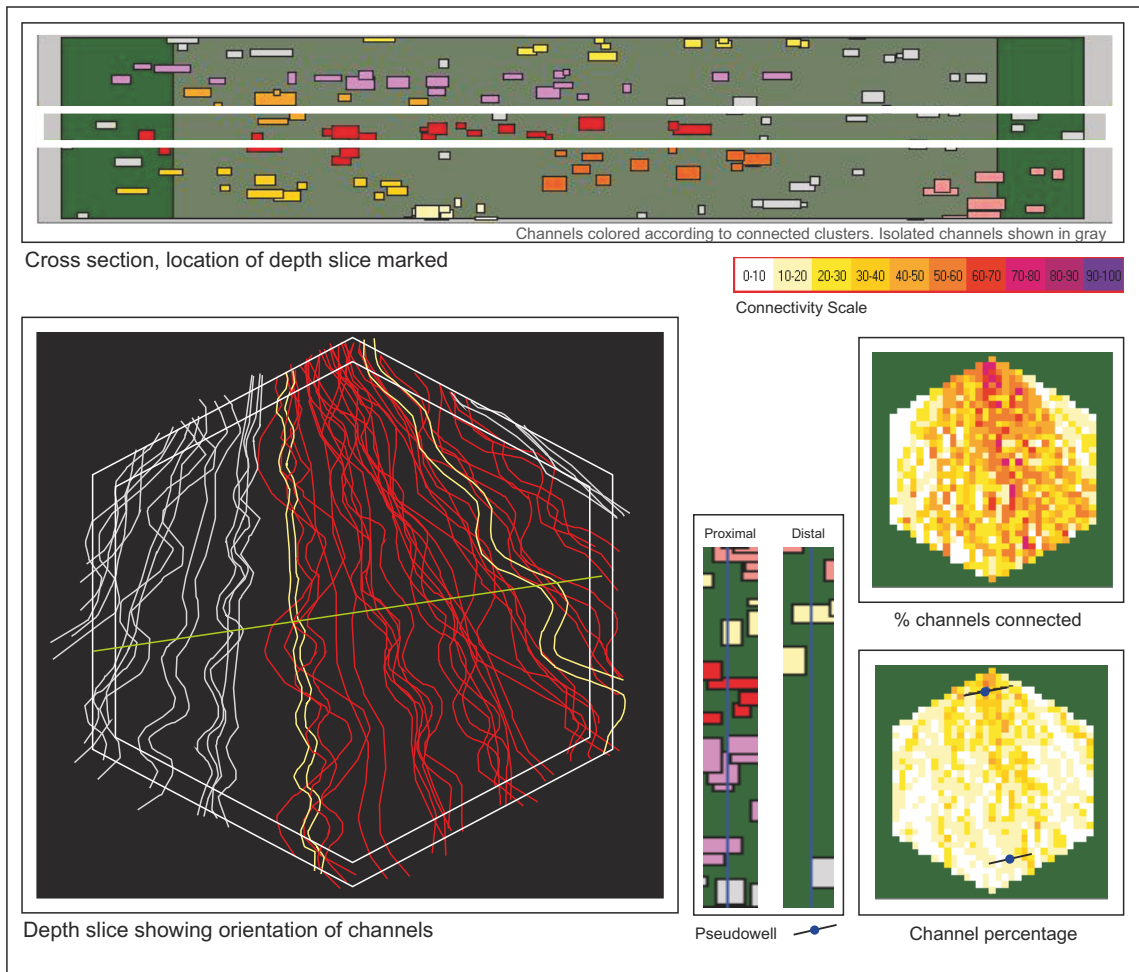


Figure 2.11: Graphic output of a random replication from a Reconnect modeling run, representing the B-C interval, with a splay geometry. The cross-section shows five main channel clusters. As expected in a crevasse splay setting, isolated (grey) channels occur most commonly towards the margins of the modeled splay complex. The depth slice demonstrates channel orientations and geometries (depth slice location shown in light green on the cross-section). The connectivity scale can be used to interpret the channel connectivity, and channel percentage outputs: Channel connectivity is highest in a proximal location and as it decreases distally, is greater along the axis of the splay than towards the outer margins. Mean channel connectivity is 20%, but is as high as 80% near the source of the splay. The pseudo-wells demonstrate that in a proximal location, it is possible to intersect almost all of the channel clusters. In a distal location, however, the well intersects fewer channels, and is likely to intersect isolated channels. Table 3c shows the statistical output from this replication.

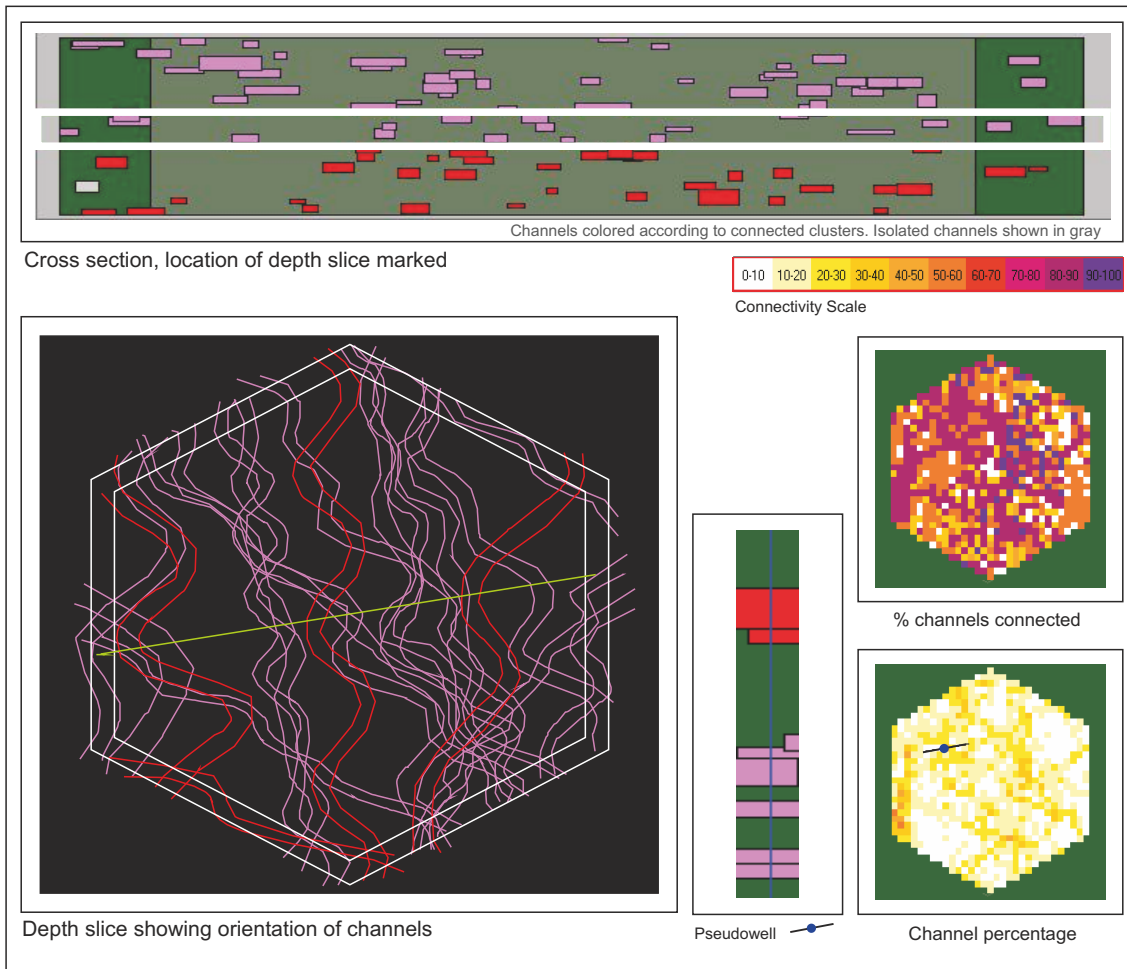


Figure 2.12: Graphic output of a random replication from a Reconnect modeling run, representing the B-C interval, with a distributary geometry (i.e. the channels do not have a fixed point of origin). The cross-section shows three main channel clusters. Only a few isolated (grey) channels are present. The depth slice demonstrates channel orientations and geometries (depth slice location shown in light green on the cross-section). The connectivity scale can be used to interpret the channel connectivity, and channel percentage outputs: The more random orientation of channels allows greater connectivity between channel bodies (45% of channel bodies are connected). There is also a more random spread of connectivities and channel percentages in the model. Mean channel connectivity is 45%, but is as high as 90-100% in some areas. The pseudo-well demonstrates that it is possible to intersect the two largest channel clusters, so that the pseudo well is in communication with 77% of the channel bodies. Table 4c shows the statistical output from this replication.

Figures 2.10-2.12 show random replications from modeling runs conducted with 100 replications in each run. As well as the graphic output, Reckconnect also generates statistics covering channel proportion, channel connectivity and sand connectivity to pseudo-wells for each modeling run, summaries of which are given in tables 2.2-2.44. Model inputs are listed in Tables 2.2a, 2.3a and 2.4a.

Table 2.2. A-B interseam modeling results, modeled with a splay geometry

Table 2.2a. Reckconnect model parameters for the A-B (splay) interseam

Reservoir Thickness m	Mean Azimuth deg.	Channel %	Mode Thickness m	Thickness Variation %	Mode Width m	Width Variation %	Sinuosity Sinuosity	Sinuosity Variation %
30	170	2	1.26	53	41.6	50	1.16	28

Table 2.2b. Output statistics for the A-B (splay) interseam

Run	No. Channels	Channel %	% Single Story	Channel Connectivity No.	Channel Connectivity %	Well Connectivity
1	13	1	100	9	13	2
2	14	2	100	9	13	1
3	14	2	100	9	12	4
4	14	1	40	9	14	2
5	12	1	50	10	16	2
6	14	1	50	10	13	1
7	14	2	60	9	13	1
8	13	2	95	12	17	1
9	14	1	69	9	13	3
10	13	2	100	10	13	2
Mean	13.5	1.5	76.4	9.6	13.7	1.9

Table 2.2c. Output statistics for the A-B (splay) random replication (Fig. 2.11b)

Run	No. Channels	Channel %	Channel Connectivity No.	Channel Connectivity %	Well Connectivity
3	18	2	7	11	1

Table 2.3. B-C interseam modeling results, modeled with a splay geometry**Table 2.3a.** Reconnect model parameters for the B-C (splay) interseam

Reservoir Thickness m	Mean Azimuth deg.	Channel %	Mode Thickness m	Thickness Variation %	Mode Width m	Width Variation %	Sinuosity	Sinuosity Variation %
30	170	17	1.59	40	41.6	50	1.2	28

Table 3b. Output statistics for the B-C (splay) interseam

Run	No. Channels	Channel %	% Single Story	Channel Connectivity No.	Channel Connectivity %	Well Connectivity
1	130	14	14	14	20	44
2	131	16	85	14	20	47
3	130	14	87	14	19	42
4	136	15	84	15	22	51
5	128	14	84	12	20	45
6	132	15	85	18	26	59
7	134	17	82	20	29	47
8	130	15	82	16	24	44
9	123	15	85	14	20	40
10	128	15	83	15	21	42
Mean	130.2	15	77.1	15.2	22.1	46.1

Table 2.3c. Output statistics for the B-C (splay) random replication (Fig.2. 12)

Run	No. Channels	Channel %	Channel Connectivity No.	Channel Connectivity %	Well Connectivity
2	141	15	15	20	53

Table 2.4. B-C interseam modeling results, modeled with a distributary geometry**Table 2.4a.** Reconnect model parameters for the B-C (distributary) interseam

Reservoir Thickness m	Mean Azimuth deg.	Channel %	Mode Thickness m	Thickness Variation %	Mode Width m	Width Variation %	Sinuosity Sinuosity	Sinuosity Variation %
30	170	17	1.59	40	59.8	50	1.3	28

Table 2.4b. Output statistics for the B-C (distributary) interseam

Run	No. Channels	Channel %	% Single Story	Channel Connectivity No.	Channel Connectivity %	Well Connectivity
1	90	15	86	38	43	83
2	94	17	84	63	68	88
3	89	15	84	51	57	80
4	89	14	90	42	48	74
5	96	17	83	51	54	83
6	90	16	86	43	45	71
7	87	16	85	43	47	80
8	98	17	79	64	70	85
9	94	15	83	45	52	77
10	93	16	82	52	59	77
Mean	92	15.8	84.2	49.2	54.3	79.8

Table 2.4c. Output statistics for the B-C (distributary) random replication (Fig. 13)

Run	No. Channels	Channel %	Channel Connectivity No.	Channel Connectivity %	Well Connectivity
1	92	12	39	45	77

The sand-poor A-B interseam was modeled with a splay (fan-like) geometry (Figure 2.10b), whereby all modeled channels were forced to originate from a single point; this is the most likely arrangement to account for the low proportion of channel-infill and interpreted poor channel network development within the modeled interseam volume. The B-C interseam was modeled with both splay and distributary geometries, the latter type being characterized by channels that have no fixed point of origin within the model.

Due to the low proportion (2%) of channel-body infill in the A-B interval, very few channel bodies are modeled, and the majority (on average 87%) of those that are present are isolated (i.e. are not in communication with another channel body within the modeled interval) (Figure 2.10b). Channel-body connectivity was low across most of the model (mean channel-body connectivity = 13%). The pseudo-wells demonstrate that, in both proximal and distal locations, wells are likely only to intersect isolated (i.e. non-clustered) channel bodies, if any, with the mean well connectivity being only 1.9%.

The B-C interseam, when modeled as a crevasse splay complex (Figure 2.11), displayed the following features compared to the model for the A-B interseam: greater overall channel-body percentage (17%), greater mean channel-body thickness (1.59 m), which resulted in higher mean connectivity of channel bodies (22%) such that they formed multiple clusters of connected channel bodies. As expected in a splay, channel-body connectivity decreased distally and away from the axis of the splay, with isolated channel bodies more commonly occurring towards the splay margins. Figure 2.11 demonstrates a representative output from the B-C (splay) modeling runs: pseudo-wells demonstrate that, for a proximal location, it is possible for wells to intersect almost all of the channel clusters, whereas for distal locations, a well will

intersect fewer channel bodies, the majority of which are likely to be isolated. Mean well connectivity is 46%: i.e. by intersecting channel clusters, a single well would be predicted, on average, to be in communication with 46% of the channel bodies modeled.

When modeled with distributary tertiary channels – i.e. where channels have no fixed point of origin (Figure 2.12) – the B-C interseam displayed the following features: distributary tertiary channels were modeled with greater widths and sinuosities than crevasse-splay channels, using width and sinuosity measurements provided from the Ob River (Table 2.1). This resulted in greater amalgamation and stacking of channel bodies and generated fewer but larger channel-body clusters, yielding an average channel-body connectivity of 54% by volume. Channel-body connectivity was distributed more randomly across the modeled interval compared to that predicted by models of the interval that used a splay-type geometry (Figure 11, '% channels connected' inset Figure). As a result, pseudo-wells were, on average, likely to intersect all of the channel clusters, yielding a mean well connectivity of 79.8%.

2.7 Discussion

2.7.1 Depositional Models

Typical plan-form geometries of tertiary channel-body assemblages – i.e. elements generated in splay complexes and distributary channel settings – from the Ob River have been combined with channel body distributions resulting from the random replications of stochastic modeling runs in order to propose three-dimensional architectural models of the A-B (Aries-Castor) and B-C (Castor-Pollux) interseam deposits of the Rangal Coal Measures succession.

Upper (A-B interseam) interval: The A-B interseam is a poorly developed crevasse splay complex, with few, poorly connected channel bodies in a very low net:gross, distal floodplain setting (Figure 2.13). Negligible connectivity is predicted for this interval. Channel bodies are mostly immature, being poorly developed, thin and isolated. The inset well-logs taken from the South Blackwater Mine dataset demonstrate typical successions from the interval (Figure 2.13). Channel bodies present are interpreted as small scale-tertiary channels that abruptly grade laterally into channel-margin levee and lake-margin deposits.

Lower (B-C interseam) interval: The B-C (Castor-Pollux) interseam can be interpreted as large, well-developed crevasse splay complex (Figure 2.14), which evolved over time to preserve a network of interconnected splay-channel elements in a medial floodplain setting (similar to those seen in the Ob River). Connectivity likely exhibits a large spatial variation, being significantly greater in proximal positions, where channels are more closely clustered adjacent to the source of the splay. The inset wireline well logs demonstrate typical medial and distal successions from the interval (Figure 2.14).

The B-C interseam can alternatively be interpreted as a complex assemblage of bifurcating, meandering distributary channel bodies (Figure 2.15). Distributary channel bodies interpreted from this part of the succession are considered to be of low sinuosity (Fielding et al. 1993). A network of distributary-channel elements will have a higher overall connectivity, and a more random distribution of connectivity than channel elements modeled as a crevasse-splay morphology.

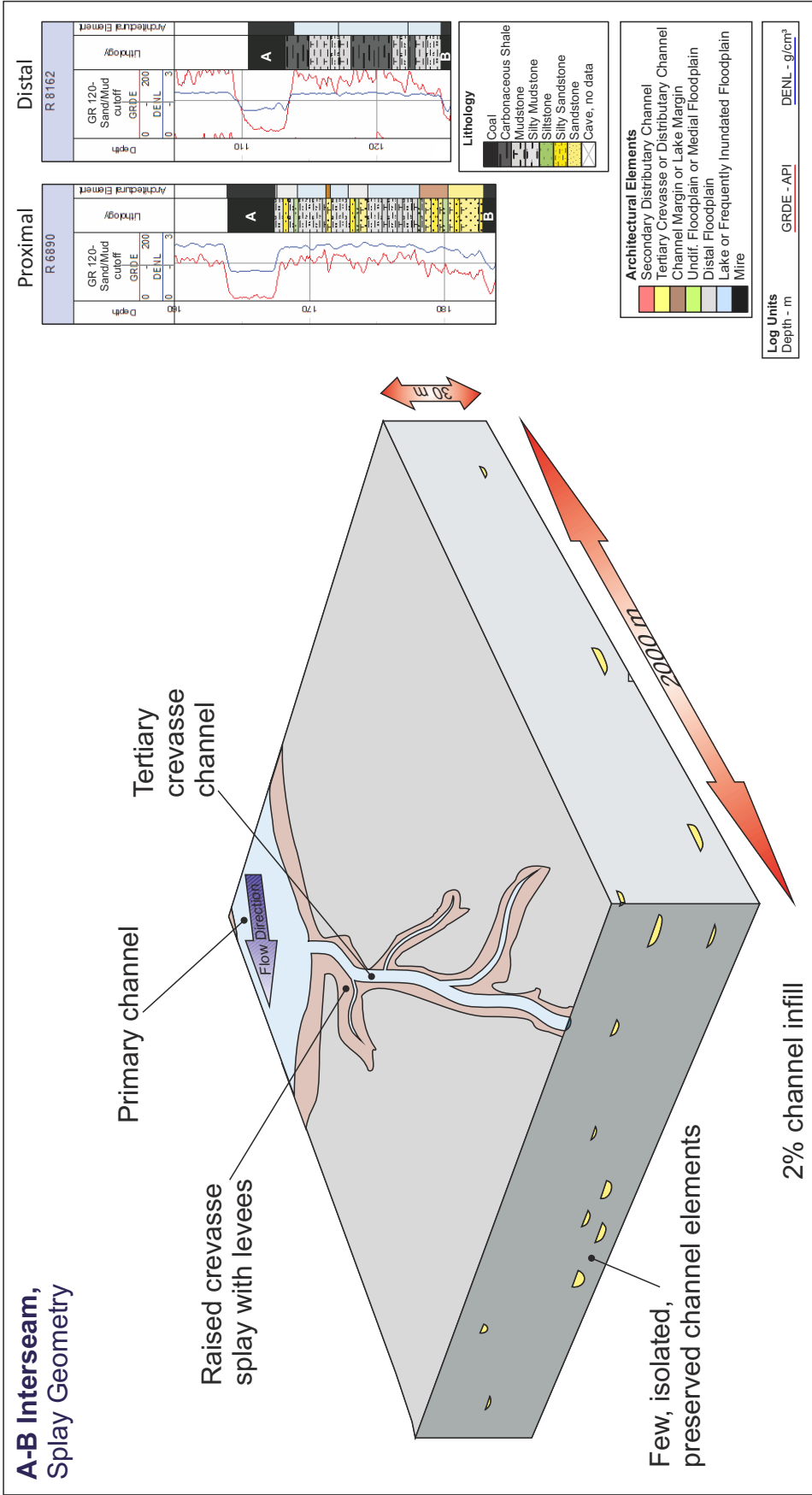


Figure 2.13: Simplified 3D architectural model of the Aries [A] - Castor [B] seam interval, incorporating planform geometries from modern analogues, and channel element dimensions and distributions from Reconnect modeling. Analysis of wireline-log data indicates that silty mudstones, mudstones and claystones dominate the interval; typical of distal floodplain and lacustrine deposits. The inset logs are examples of proximal and distal logs from the A-B interseam. Tertiary channel elements present in the interval tend to be isolated, and are interpreted as small-scale, crevasse splay channels, bordered by leveed channel-margin deposits. Channelised elements are attributed to the distributary fluvial system that was responsible for drowning out the B seam peat mire environment.

A network of distributary channels originating at various points along a reach of the larger primary channel might explain the large number of channel bodies observed in the subsurface succession, in contrast to the relatively channel-poor overlying A-B interseam. The inset well-logs demonstrate successions predicted at various locations in such a system. Deposits in the South Blackwater Mine dataset generally grade laterally from channel element, to channel-margin element, to medial floodplain element, and locally to distal floodplain element (Avenell 1998). The B-C interseam is considered to be closely analogous to the floodplain morphology of the modern Ob River.

The difference in fluvial style between A-B interseam deposits and the lower B-C interseam deposits may be attributed to a number of factors. The deposits could have formed during an episode of increased rate of accommodation creation, resulting in drowning of mires, splays and more medial floodplain deposits, thereby preferentially preserving distal floodplain deposits, rather than primary channel deposits.

2.7.2 Limitations of data

The principal limitation for this study is the limited lateral extent of the data, leading to uncertainty as to where the data is situated in the overall depositional system, and how representative of that system it is. A single splay in the Ob River (Figure 2.9c) is 4000 m by 5000 m, yet the entire study area at South Blackwater Mine measures only 1000 m by 2000 m. Thus, the predictions of subsurface fluvial architecture arising from this study could represent only a small portion of a much larger system, so care must be taken when extrapolating interpretations made from such small sub-sections of what

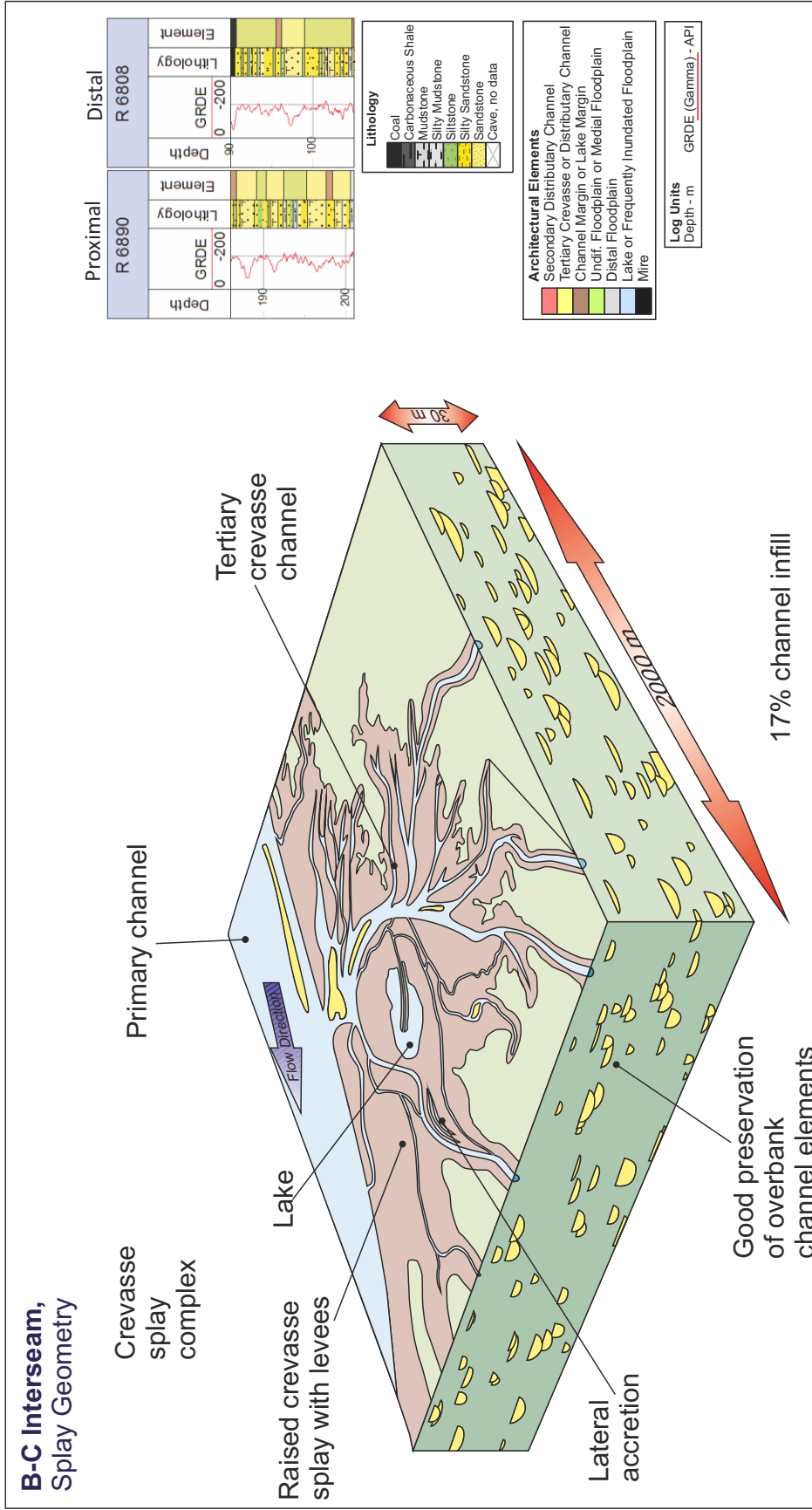


Figure 2.14: Simplified 3D architectural diagram for the B-C interseam, with tertiary channels present as leveed crevasse splay channels. The diagram incorporates platform geometries of the Ob River modern analogue with channel distributions inline with model outputs from Reckonnect. Medial floodplain deposits are dominantly preserved. Isolated channels tend towards the margins of the splay, with connectivity decreasing distally from the splay source. There is overlapping of channels (as demonstrated by the BC-1 modeling run, Figure 11). The connectivity between channel bodies may be further enhanced by potential connectivity through fine sand or silty-sand splay stacks. The inset well log sections illustrate anticipated proximal and distal well logs for such a splay-based system.

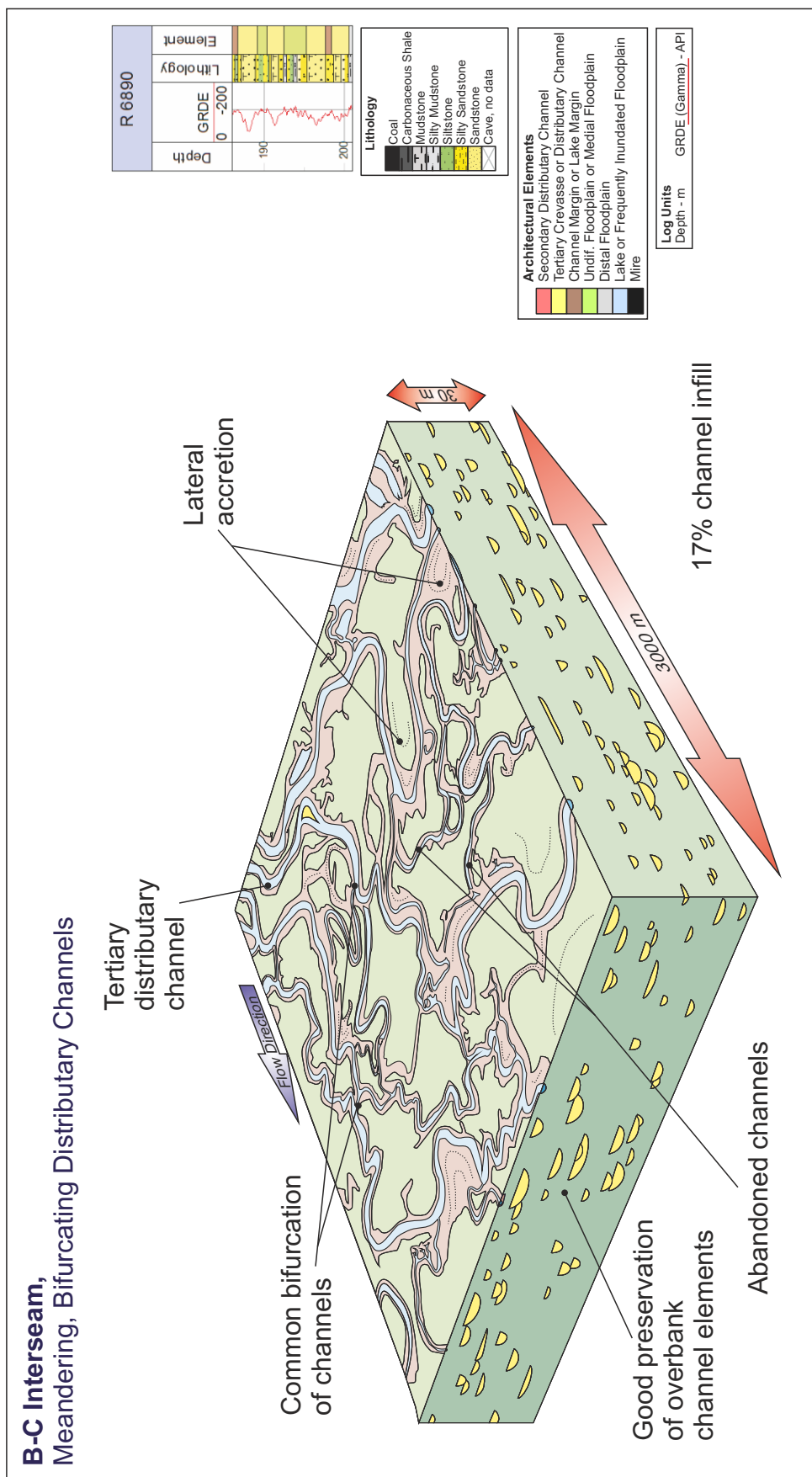


Figure 2.15: Simplified 3D architectural diagram for the B-C interseam, with tertiary channels present as leveed, meandering, bifurcating distributary channels. The diagram incorporates planform geometries of the Ob River modern analogue with channel distributions inline with model outputs from Reconnect. Medial floodplain deposits are dominantly preserved. Some channels are isolated, however connectivity is good where channels overlap. The inset well log sections illustrates relatively high net:gross areas anticipated within the system.

is overall a much larger fluvial system. This may explain the contrasting styles of deposition interpreted in the A-B and B-C interseams, including the observed differences in the proportions of overall channel bodies – 2% versus 17%, respectively.

Although apparently an extremely low net:gross interval, with negligible reservoir potential, the A-B interseam examined in the study area might represent a low net:gross fluvio-lacustrine environment located in a floodplain setting, at a stratigraphic level which overall has a greater reservoir potential elsewhere within the larger system. Analysis of a larger dataset from a wider spatial area could provide additional insight into the regional variability of such systems.

2.8 Conclusions

Subsurface datasets, even those of relatively high resolution such as the closely spaced coal mine wells of the South Blackwater Mine, may still not provide data of sufficient density of coverage to accurately resolve small-scale (tertiary) channel-element dimensions in flood basin settings. Where the spacing of subsurface wells is greater than the mean width of any channel elements present, modern analogues can be a useful tool in supplementing the primary dataset to yield information regarding likely analogous plan-form geometries. All sand-prone elements interpreted with confidence in the wireline logs were channelized deposits; thinner, sheet-like deposits being too thin to reliably interpret or correlate.

Simple models created using Reckconnect reservoir modeling software demonstrate some characteristic features of channel connectivity in small-scale distributive fluvial systems developed in flood basin settings, such as those of

the Rangal Coal Measures succession: (i) channel-body connectivity is more uniform where levee breaches result in distributary channels rather than in splay complexes; (ii) relatively good connectivity is seen in proximal positions in splays, but decreases distally from the source as channel elements diverge; (iii) connectivity tends to be greater down the axis of splays, with more isolated channel bodies occurring at the margins.

Good connectivity between channel bodies is expected in some cases (e.g. in the B-C interseam, which has a 17% channel proportion). However, where channel percentage is very low, as in the A-B interseam, connectivity between channel bodies is negligible. It is therefore vital to accurately constrain the proportions of infill by each architectural element in the system, in order to produce models with realistic channel-body distributions and connectivities.

Care must be taken when extrapolating findings from small datasets to a larger scale, as a small dataset may provide a biased, non-representative representation of the subsurface at a regional scale. This may be of particular relevance in petroleum exploration, where seismic datasets typically cannot resolve small-scale channel elements, and where well data are sparse, potentially leading to biased estimations of architectural-element proportions, especially where inappropriate analogues have been used to provide supplementary data.

2.9 Future work

This work has investigated small-scale channel deposits, at a sub-seismic scale, and illustrates the importance of channelized deposits as inter-connected reservoir deposits. The remainder of this thesis will investigate larger, seismic-scale channel deposits from the fluvio-deltaic, Triassic Mungaroo Formation.

Chapter 3 Sedimentology of a fluvial system within a delta-plain setting: a case study from the Triassic Mungaroo Formation

Research question: What is the nature of the stratigraphy and sedimentology of the Triassic Mungaroo Formation in block WA-404-P, Exmouth Plateau, Australia?

3.1 Chapter overview

This Chapter aims to describe the sedimentology of a fluvial-dominated succession that accumulated in a large delta-plain system. This will be achieved through detailed examination of a case example from the Triassic Mungaroo Formation of the Northwest Shelf of Australia to describe and interpret the lithofacies, and facies associations present in the succession as revealed from wireline and core logs from a specific study area (WA-404-P). Specific objectives of this chapter are as follows: (i) to identify and describe the lithofacies present in cored sections of the Mungaroo Formation; (ii) to group lithofacies into facies associations relating to assemblages that accumulated in response to sets of genetically related depositional processes; (iii) to explore the possible depositional settings relating to architectural elements composed of facies associations; (iv) to gain insight into the in-channel and overbank style represented by cored sections of the Mungaroo Formation.

The description and interpretation of lithofacies, facies associations and associated information from subsurface well-log and core data is important for characterising the processes that operate in sedimentary successions known only from subsurface settings, and for assessing the relative dominance of fluvial and deltaic processes in relation to the various sub-environments that have given rise to the preserved succession. The lithological observations made

and discussed in this chapter form the basis for the interpretation of seismic architectural elements and the recognition of larger-scale components of depositional environments recognised from seismic data (valley, channel belt and channel network assemblages), as discussed in chapters 5-6. Sedimentological observations discussed in this chapter are specific to the detailed study location: block WA-404-P, an approximately 3000 km² exploration block situated on the Exmouth Plateau, one of the more distal regions of the Northern Carnarvon Basin (Figure 3.1). Given the relatively outboard setting of this block, the deposits described are not necessarily representative of the sedimentology of more inboard locations on the Exmouth Plateau.

The core examined is of high quality and is well-preserved; the studied core sections are particularly useful for reconstructing the gross-scale sedimentology of the system because they penetrate both reservoir (channel-dominated) and non-reservoir (overbank dominated) intervals, thereby providing a relatively complete overview of the sedimentology of cored sections of the depositional system. However, the cored sections examined represent only a small portion of the Mungaroo Formation overall and are limited to the S2-S3 (TR21.1 – TR22.1) interval, which itself is not necessarily representative of other stratigraphic intervals of the formation. The majority of previous studies and much of the past exploration and reservoir development of the Triassic Mungaroo Formation has concentrated on more proximal areas of the system, focussing on inboard sub-basins of the Northern Carnarvon Basin, including, for example, the Dampier Sub-basin, where channel bodies tend to be large and amalgamated than similar bodies present in more distal settings (Seggie et al., 2007). This study provides insight into the less widely investigated distal expression of the Mungaroo Formation.

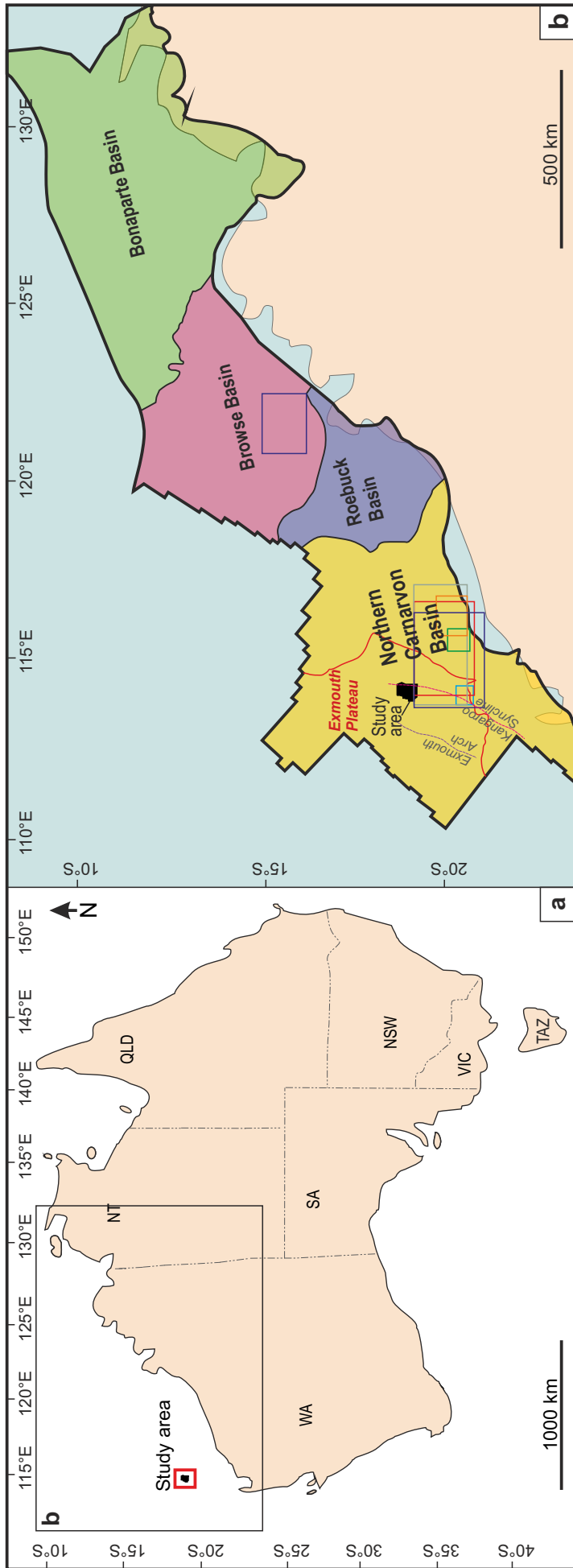


Figure 3.1a: Location of the study, offshore northwest Australia. **b:** Map (locations annotated on Fig. 1a), showing the Northwest Shelf of Australia (thick black outline), and its constituent sedimentary basins: Northern Carnarvon Basin, Roebuck Basin, Browse Basin and Bonaparte Basin (adapted from Marshall & Lang, 2013). The study area is located on the Exmouth Plateau, an outboard province of the Northern Carnarvon Basin. Coloured boxes indicate the study areas of other Mungaroo Formation studies: Bal et al., 2002 (orange); Seggie et al, 2007 (orange); Stoner, 2010 (green); Adamson et al., 2013 (grey); Heldreich et al., 2013 (lt blue); Marshall & Lang, 2013 (dk blue); Payenberg et al., 2013 (red).

3.2 Dataset

This study utilizes data provided by Woodside Energy Ltd., primarily an open-file 3D seismic survey (Colmbard 3D), with an area of approximately 3000 km², located in block WA-404-P, on the Exmouth Plateau, a province of the Northern Carnarvon Basin, on the Northwest Shelf of Australia (Figure 1). The study also utilized data from 12 wells with wireline log suites, 2 of which additionally had core available; the locations of these well are shown in Figure 3.2.

3.3 Regional stratigraphy

3.3.1 Paleogeography

During the Late Triassic, the Northwest Shelf of Australia occupied a palaeolatitude of approximately 30°S (Jablonski, 1997), in southeast Pangea, on the southern margin of the Tethys Sea (Figure 3.3). At this time, the Northern Carnarvon Basin formed an active margin megasequence (Jablonski, 1997) where accommodation space was created by subsidence associated with post-rift cooling of the lithosphere following Paleozoic rifting. The active margin megasequence comprised fluvio-deltaic sequences that were deposited overlying the marine deposits of the Locker Shale, as the rate of subsidence in the basin slowed (Jablonski, 1997; Westphal & Aigner, 1997).

3.3.2 Chronostratigraphy

The Mungaroo Formation records the overall transgression of a fluvio-deltaic system by an advancing shoreline (Payenberg et al., 2013). Within this overall trend, several high-frequency transgressive-regressive cycles are recorded and the preserved sedimentary evidence for these has been identified using seismic and well data, which forms the basis for a sequence stratigraphic correlation

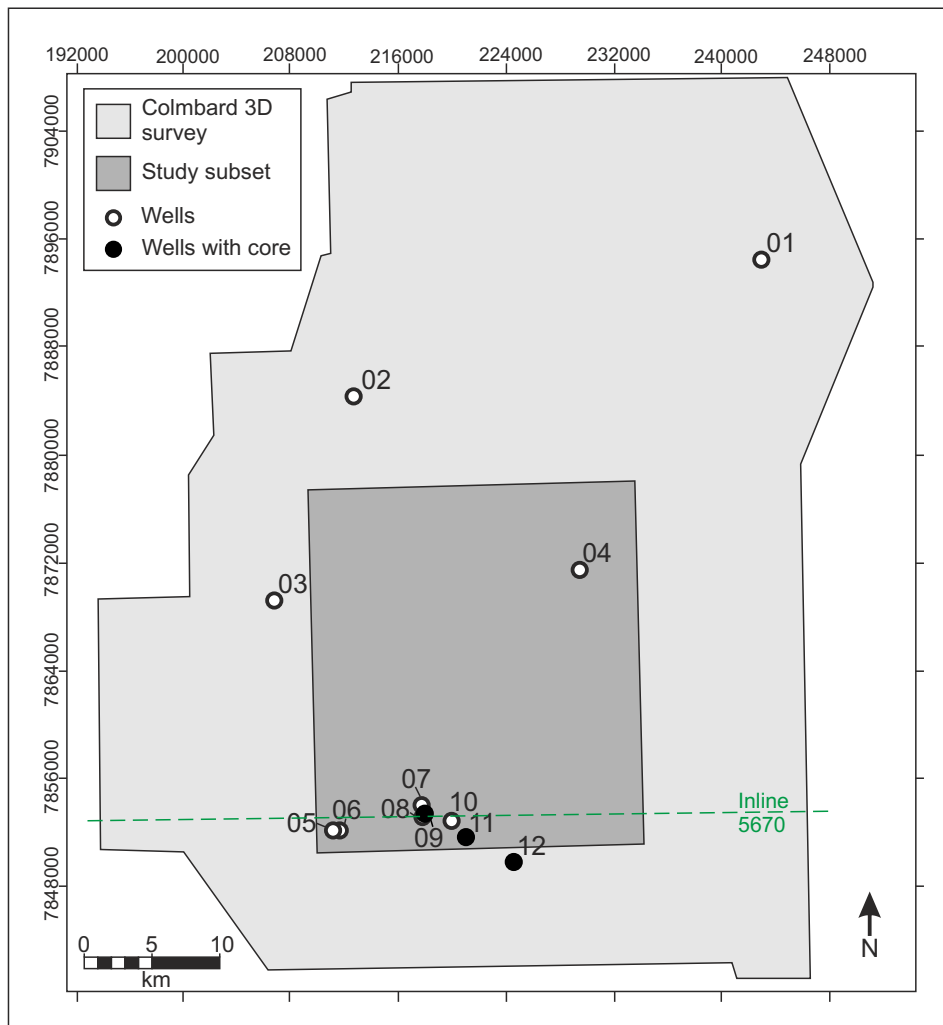


Figure 3.2: Location of wells and study subset (explored in Chapter 6) within the area covered by the Colmbard 3D seismic survey. Location of inline 5670 (c.f. Figure 3.7) is shown by hashed line. Grid measurements are given in m (UTM zone GDA94_50S).

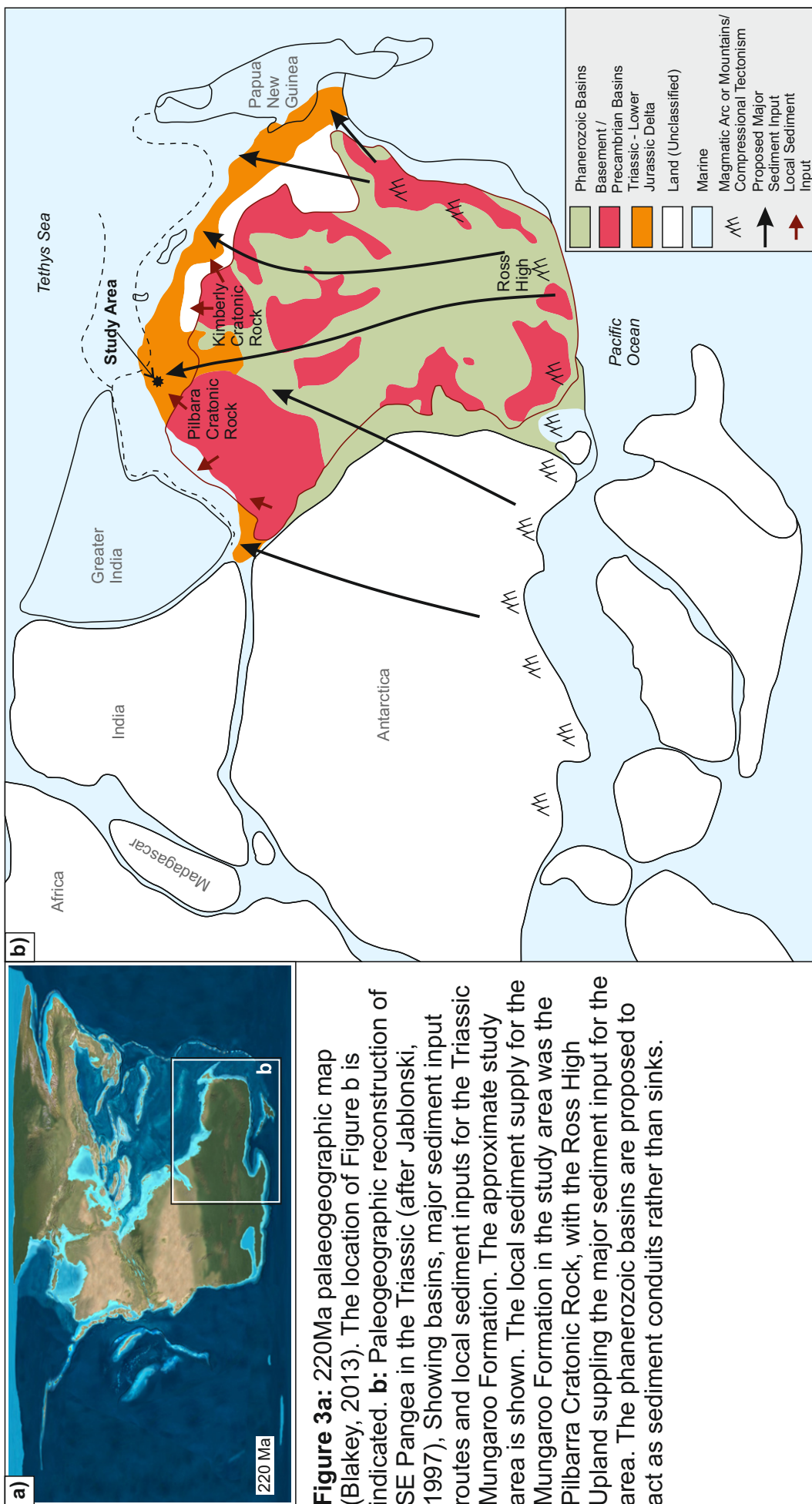


Figure 3a: 220Ma palaeogeographic map (Blakey, 2013). The location of Figure b is indicated. **b:** Paleogeographic reconstruction of SE Pangea in the Triassic (after Jablonski, 1997), showing basins, major sediment input routes and local sediment inputs for the Triassic Mungaroo Formation. The approximate study area is shown. The local sediment supply for the Mungaroo Formation in the study area was the Pilbara Cratonic Rock, with the Ross High Upland supplying the major sediment input for the area. The phanerozoic basins are proposed to act as sediment conduits rather than sinks.

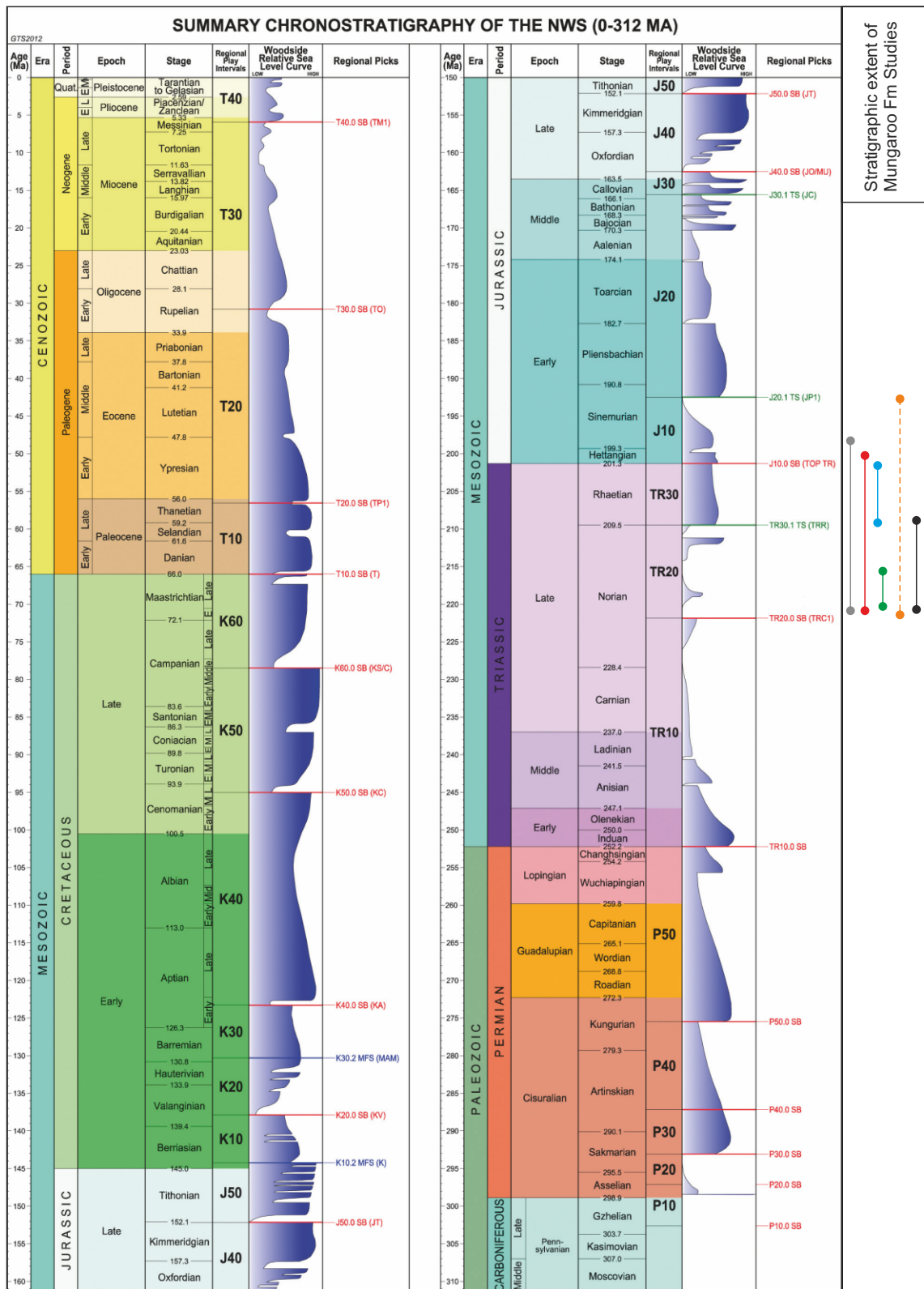


Figure 3.4: Reproduced from Marshall & Lang (2013). Regional play intervals and relative sea level curve for the North West Shelf of Australia, from 0-312 Ma. Key stratigraphic surfaces (SB = sequence boundary, TS = transgressive surface, MFS = maximum flooding surface) are also shown. Stratigraphic extent of Mungaroo Fm studies is shown: Seggie et al, 2007 (orange); Stoner, 2010 (green); Adamson et al., 2013 (grey); Heldreich et al., 2013 (lt blue); Marshall & Lang, 2013 (dk blue); Payenberg et al., 2013 (red); this study (black).

framework (Adamson et al., 2013; Marshall & Lang, 2013). The stratigraphy of the Northwest Shelf has been established using a combination of seismic, sedimentological and palynological and dinocyst data (Marshall & Lang, 2013). Figure 3.4 shows the 0-312 Ma play intervals identified by Marshall and Lang (2013), for which the Triassic is divided into three regional play intervals, TR10 (252.2-237.0 Ma), TR20 (237.0-209.9 Ma) and TR30 (209.5-201.3 Ma) that are themselves split into sub-plays. Within the sub-plays, third-order stratal surfaces (c.f. Vail et al., 1977) were identified. Figure 3.5 shows the chronostratigraphic chart devised by Marshall & Lang (2013), focusing on the Triassic, and showing the regional plays, sub-plays, and significant stratigraphic surfaces and systems tracts. Figure 3.6 presents a SE-NW regional stratigraphic section by Marshall & Lang (2013) across the Northern Carnarvon Basin, through the Dampier Sub-Basin and Exmouth Plateau, and highlights major stratigraphic packages and fault arrangements.

Of 12 seismic horizons mapped in the dataset for this study, seven relate to Triassic stratigraphic surfaces identified by Marshall & Lang (2013). Table 3.1 lists the horizons and related stratal surfaces used in the study. Figure 3.7 shows a synthetic seismogram used to tie well tops to their corresponding seismic events.

Figure 3.8 shows a west-east correlation panel between Well05 and Well11, showing identified stratigraphic surfaces (following Woodside chronostratigraphic nomenclature), and seismic units. Time-structure maps and elevation statistics for the horizons are presented in Appendix 1. This study examines the TR20 play interval, investigating the Norian deposits of the Mungaroo Formation.

Table 3.1: Seismic horizons and related stratal surfaces used in the study.

Seismic horizon	Mean Elevation (-ms TWT)	Stratigraphic surface	Bounding surface type	Stage
Water Bottom	1876	-	-	-
S12	2191	T40.0	Sequence boundary	Messinian
S11	2842	K60.0	Sequence boundary	Campanian
S10	2934	K50.0	Sequence boundary	Cenomanian
S9	3041	K40.0	Sequence boundary	Aptian
S8	3244	J40.0	Sequence boundary	Oxfordian
S7	3335	TR30.1	Transgressive surface	Norian
S6	3517	TR27.2	Maximum flooding surface	Norian
S5	3592	TR26.5	Maximum flooding surface	Norian
S4	3713	TR26.1	Transgressive surface	Norian
S3	3955	TR22.1	Transgressive surface	Norian
S2	4175	TR21.1	Transgressive surface	Norian
S1	4510	TR20.3	Sequence boundary	Norian

Figure 3.9 shows an east-west seismic section through the Colmbard 3D dataset used in the study; this highlights the seismic horizons used, the major faults present, and pre-, syn, and post-rift megasequences. The location of the seismic line is shown on Figure 3.3.

3.3.3 Tectonostratigraphic evolution

The geologic evolution of the Northern Carnarvon Basin broadly comprises four phases: (i) a Palaeozoic to Mesozoic pre-rift phase; (ii) a relatively short-lived,

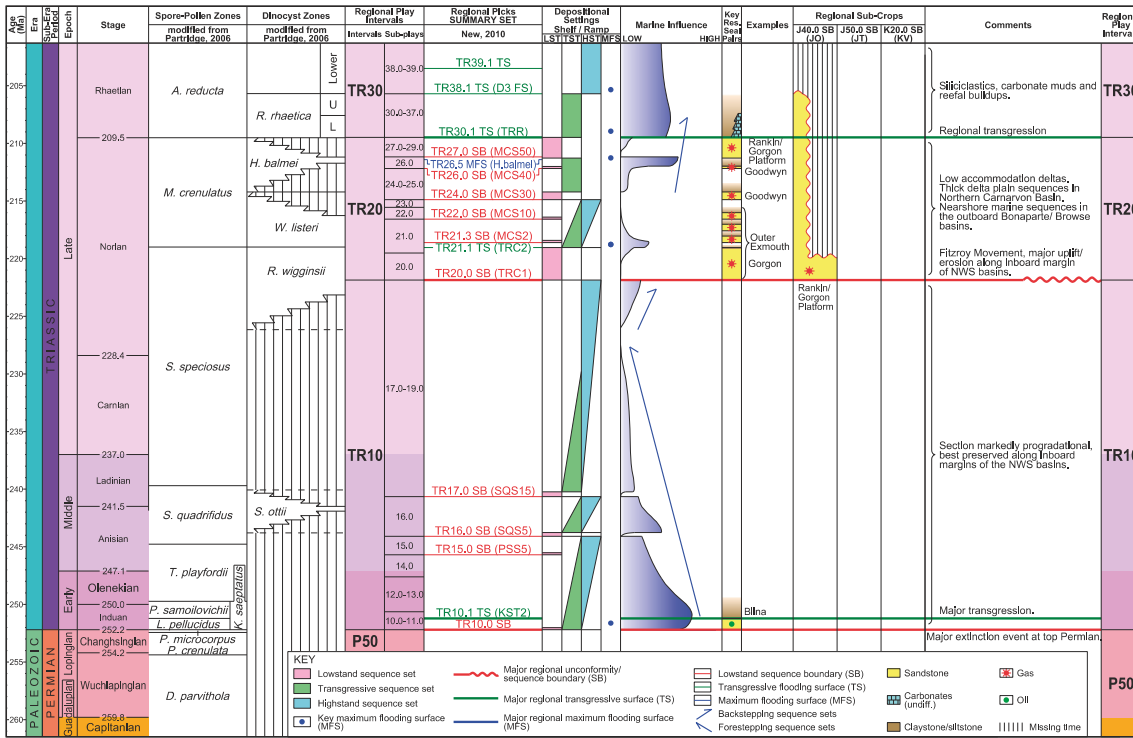


Figure 3.5: Chronostratigraphic chart (reproduced from Marshall & Lang, 2013), for the NW Shelf of Australia, focussing on the three Triassic play intervals identified by Marshall & Lang (2013). Key stratigraphic surfaces, palynological and dinocyst data are shown, as well as interpreted degree of marine influence, hydrocarbon discoveries and tectono-stratigraphic events.

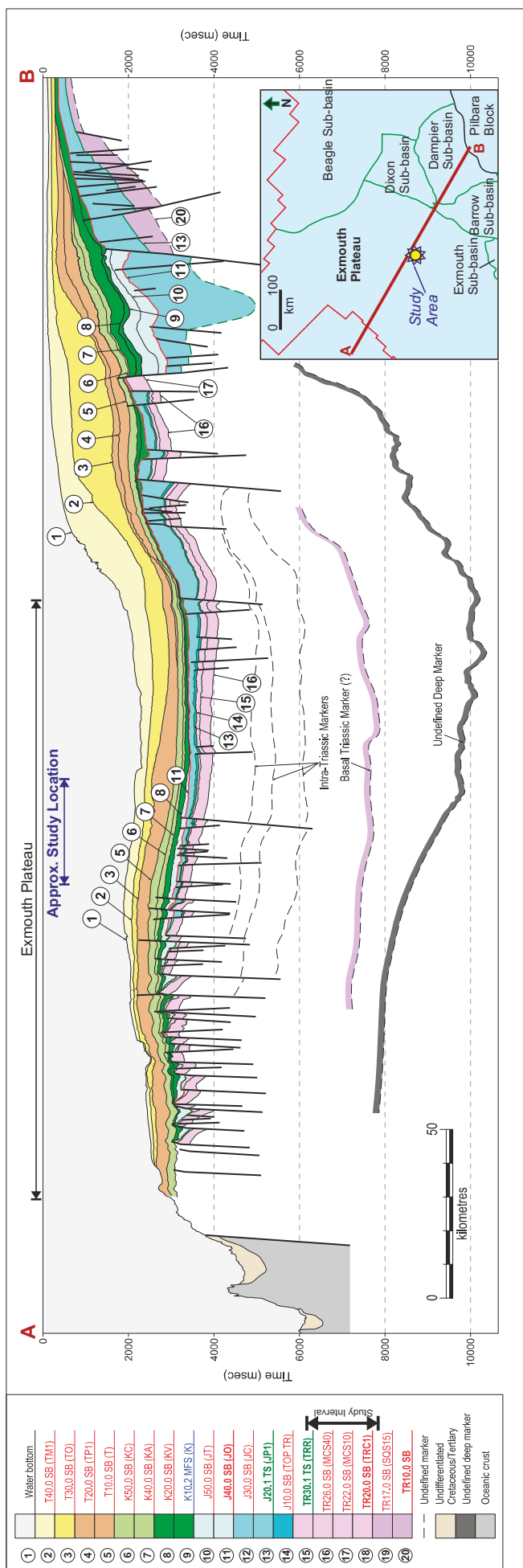
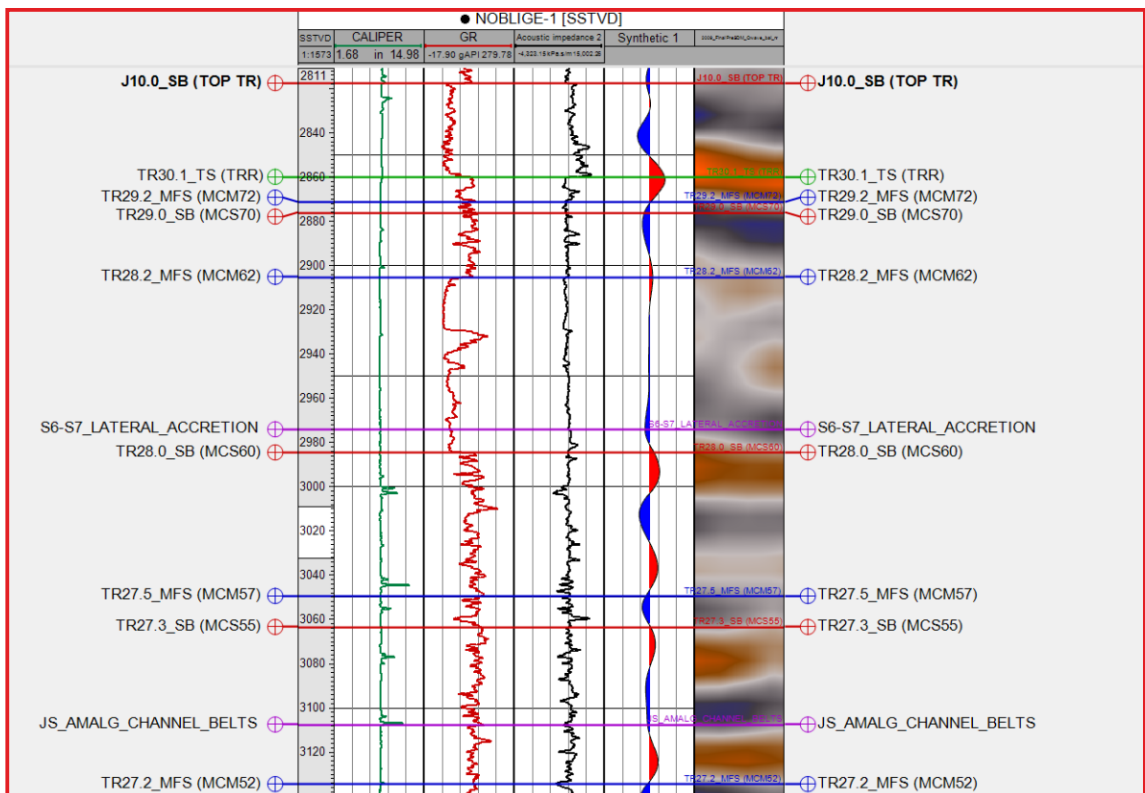
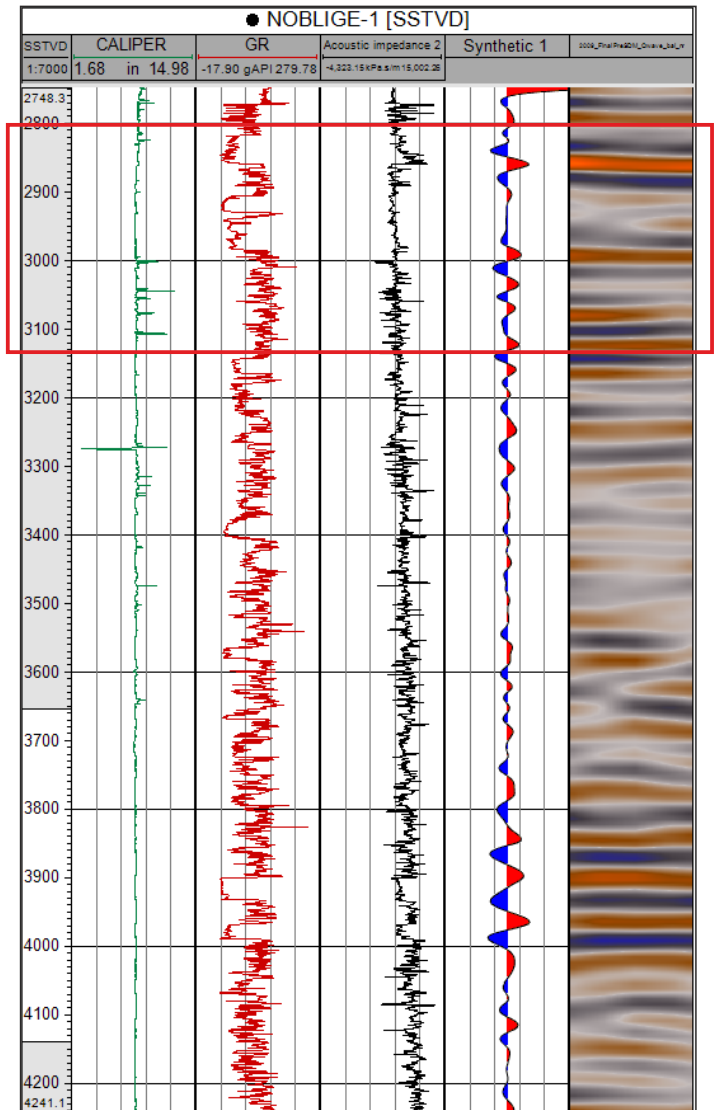


Figure 3.6: Regional cross section across the Northern Carnarvon Basin from the inboard Dampier Sub-basin to the outboard Exmouth Plateau, reproduced from Marshall & Lang (2013). The approximate location of the study area is marked on the cross section and inset location map. Key stratigraphic markers and faults are shown.

Figure 3.7: Right: example synthetic seismogram created in order to facilitate well-to-seismic tie. Below: detailed view of highlighted section, illustrating that stratigraphic markers (interpreted using biostratigraphy and lithostratigraphy by Woodside Energy Ltd) and key fluvial deposits identified in this study, are correctly tied to their corresponding events in the Colmbard 3D seismic dataset (Near Stack data).



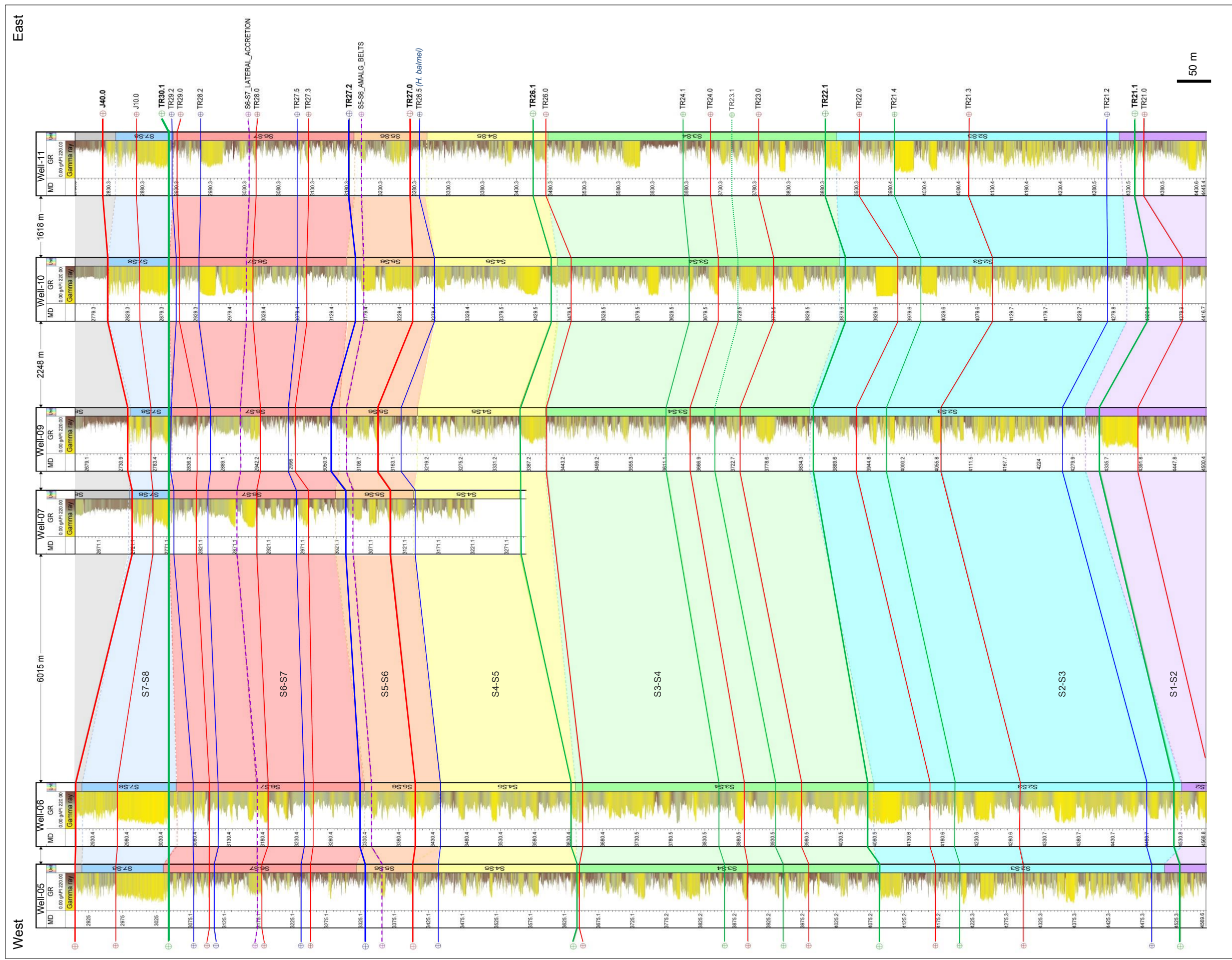


Figure 3.8: West-East correlation panel from Well-05 to Well-11. Stratigraphic surfaces are labelled, and assigned as SB (red), TS (green) or MFS (blue). The panel is also split according to seismic units that fall within the interval penetrated by wells (S1-S2 (incomplete), S2-S3, S3-S4, S5-S6, S6-S7, S7-S8, S8-S9). The J10.0 stratal surface marks the top of the Triassic, TR30.1 (approximate seismic surface S7) marks the top of the Mungaroo Formation.

Pliensbachian to Callovian rift phase; (iii) a post-rift, passive margin phase that lasted until the end of the Cretaceous; (iv) a convergence phase that is currently still in progress (Westphal & Aigner, 1997).

Palaeozoic to Mesozoic pre-rift phase: Western and northwestern Australia formed part of Gondwana during the Palaeozoic (Westphal & Aigner, 1997). Basin subsidence, which commenced in the Permian, resulted in the development of the Westralian Superbasin (Yeats et al., 1986). The Northern Carnarvon Basin forms part of the relic Westralian Superbasin. Rifting in the Late Permian gave rise to an unconformity of regional lateral extent at the Permian-Triassic boundary (Westphal & Aigner, 1997; Jablonski, 1997). During the Triassic, the Northern Carnarvon Basin formed a continental sag basin (Boote & Kirk, 1989), with a sedimentary wedge overlying the Permian-Triassic unconformity that accumulated throughout the Mesozoic (Boote & Kirk, 1989; Jablonski, 1997); the Mungaroo Formation forms part of this wedge.. The onset of fault movement associated with the breakup of Gondwana is evident in the preserved succession dating from latest Triassic time (Westphal & Aigner, 1997), at which time grabens and half-grabens developed.

The Mungaroo Formation is generally considered a high-accommodation fluvio-deltaic system. Evidence for this is found not only in the sedimentary style but also in the subsidence and sedimentation rates for the Northern Carnarvon Basin. High rates of subsidence and sedimentation have been interpreted in the Northern Carnarvon Basin throughout the Triassic (Kaiko & Tait, 2001), with a peak subsidence rate of 0.3 mm//yr at the time of deposition of the Mungaroo Formation.

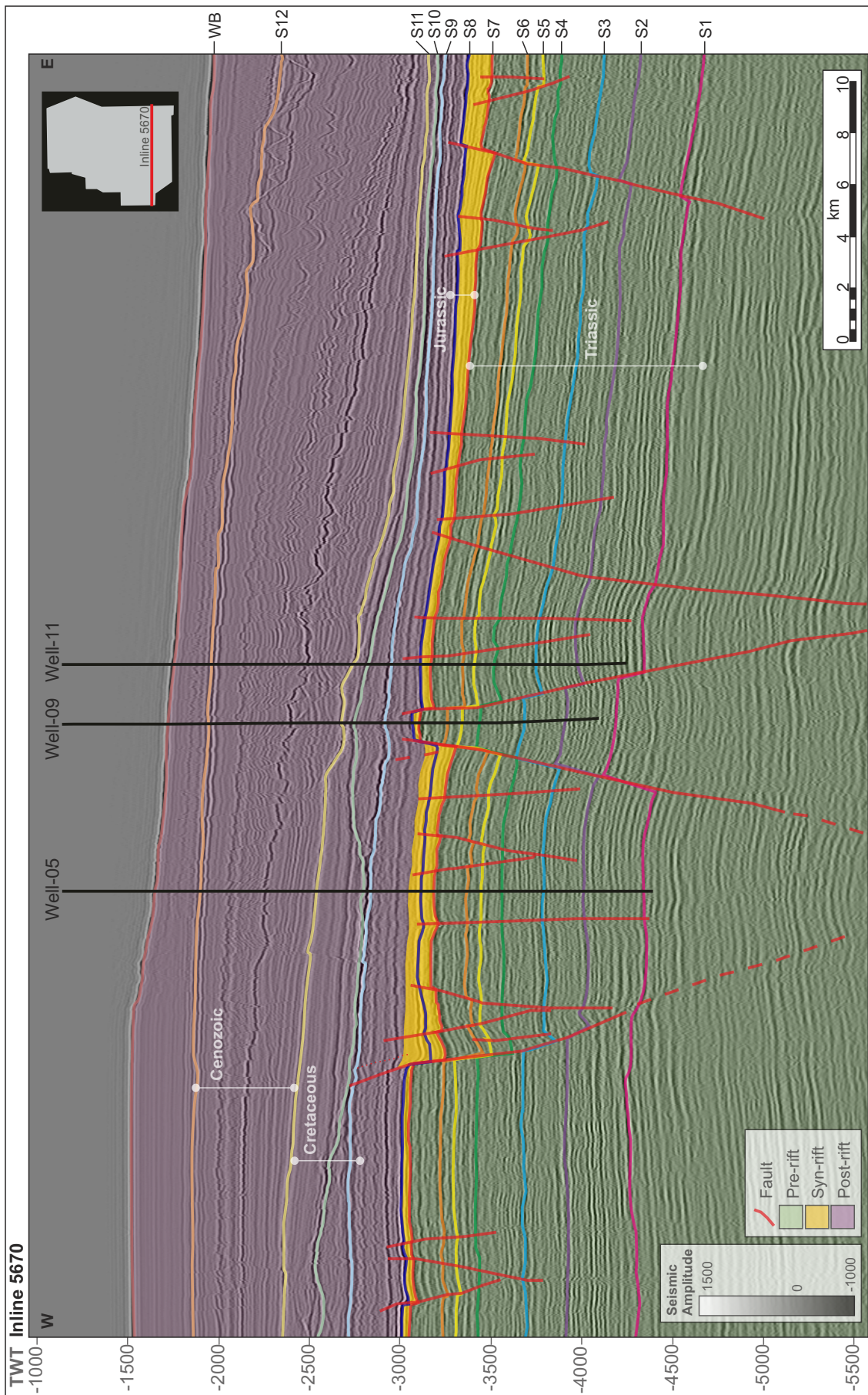


Figure 3.9: An E-W seismic section through the Colmbar 3D dataset, highlighting major faults, and pre-, syn- and post-rift tectonostratigraphic packages. Location of the section is shown on inset map of the Colmbar 3D survey area.

Rift phase: An early syn-rift megasequence is recognized, bounded by transgressive surfaces of Pliensbachian and Callovian age (Westphal & Aigner, 1997). The main phase of rifting on the Exmouth Plateau took place later (Exon et al., 1982). The main syn-rift megasequence was deposited throughout the Late Jurassic and is bounded by transgressive surfaces of Callovian and top Tithonian age (Jablonski, 1997). The rifting resulted in the development of a series of horsts and grabens controlled primarily by northeasterly trending faults. These fault blocks form the main exploration targets for Triassic and Jurassic reservoirs in the area (Wilcox, 1981; Westphal & Aigner, 1997).

Post-rift phase: A passive margin phase persisted in the region until the beginning of the Cenozoic, when convergence between the Australian and Asian plates resulted in northern Australia undergoing a phase of flexural subsidence (Westphal & Aigner, 1997).

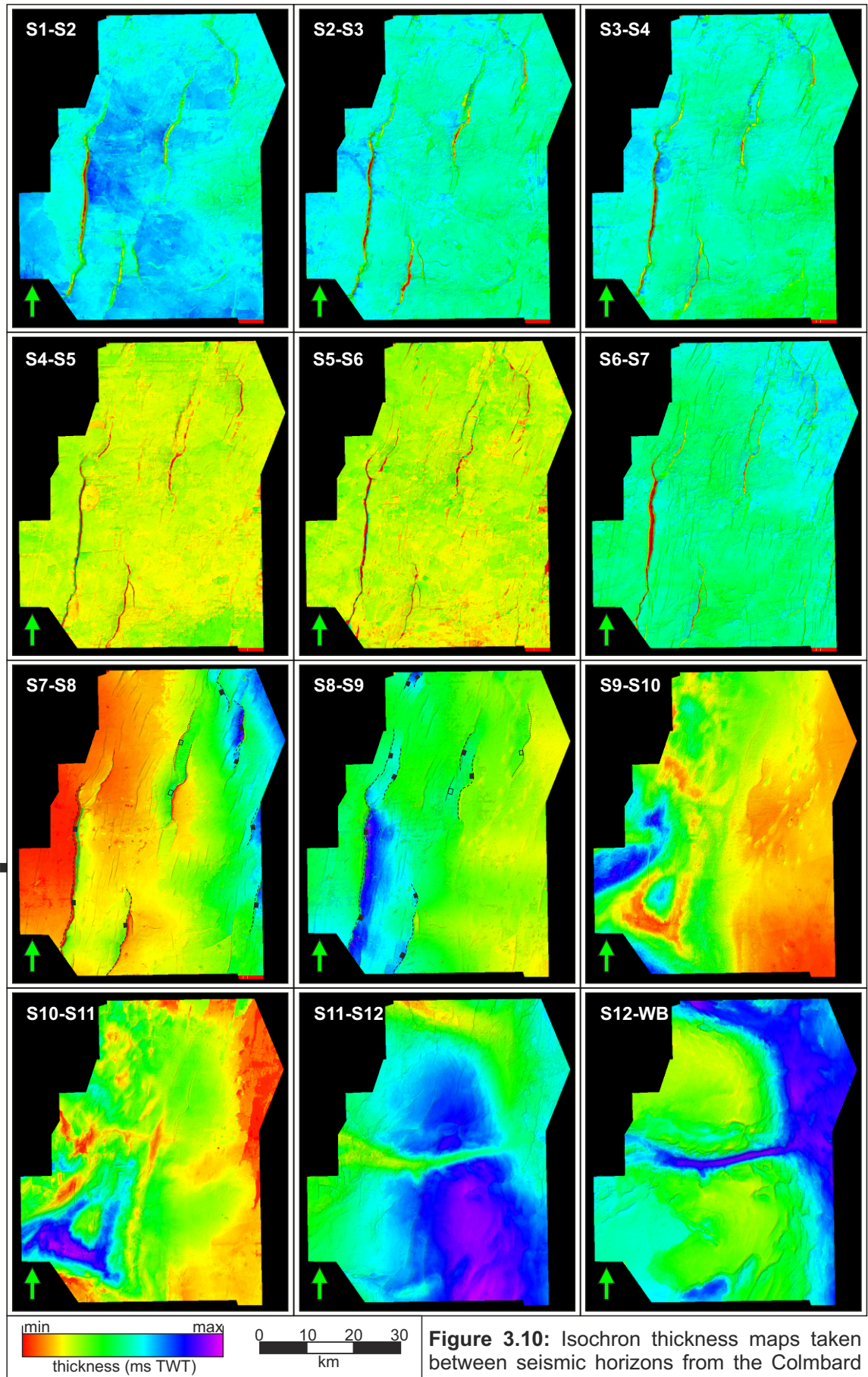
The timing of fault movement can be inferred by changes in sediment thickness on the downthrown side of the faults, as demonstrated by isochron thickness maps taken between the seismic horizons used in this project (Figure 3.10). The differential thickness of sediment accumulations adjacent to faults can be seen in the S7-S8 and S8-S9 isochron maps. These are interpreted as relating to syn-rift sediment packages, resulting from the early and main syn-rift megasequences, respectively. Figure 3.9 highlights major faults and syn-rift packages on an E-W section from the Colmbard 3D survey.

3.3.4 Mungaroo Formation Sediment Provenance and climate

The main source of sediment during the Mesozoic active margin megasequence is attributed to the Ross High Upland (location shown on

Figure 3.3) where a foreland basin developed, creating an extensive fluvial outwash plain. A major drainage system formed from the east to the west, which transported sediments from the Ross High to the North West Shelf (Jablonski, 1997), where they accumulated as the deposits of a large fluvio-deltaic system (Westphal & Aigner, 1997). Triassic sediments are up to 4 km thick in inboard areas such as the Dampier Sub-basin, and up to 6 km thick on more outboard parts of the Exmouth Plateau (Adamson et al., 2013). It is thought that the onshore Phanerozoic basins themselves had little unfilled accommodation space at this time, and so acted as conduits for the bypass of a large volume of sediment to the North West Shelf, rather than as significant depocentres in their own right (Jablonski, 1997). Lewis & Sircombe (2013) carried out heavy mineral analysis and dating of detrital zircons, the results of which support the presence of continental-scale fluvial drainage systems. Lewis and Sircombe (2013) also propose a major sediment input from the south; however this is largely disputed by other regional studies (Adamson et al, 2013; Payenberg et al., 2013) and is at odds both with the data from the Colmbard 3D survey, which shows major channel body trends to aligned E-W, and only minor trends from S-N, and with well data used in the study, where dip readings favour E-W palaeocurrents. A secondary, local sediment source in the Triassic for the Northern Carnarvon Basin is thought to have been the Pilbara Block (Jablonski, 1997), though this likely only acted as a minor source of additional sediment input.

The climate in the Triassic is interpreted to have been temperate to warm, humid and monsoonal with wet and dry periods (Dickens, 1985; Bradshaw et al., 1994)



3.3.5 Summary of previous work

Numerous studies have investigated the regional-scale palaeogeography of the Mungaroo fluvio-deltaic system (e.g., Bradshaw et al., 1994; Jablonski, 1997; Longley et al., 2002), and these studies have shown that the main controls on reservoir distribution are the palaeogeography and structure of the Northwest Shelf.

Previous studies of the sedimentology of the Mungaroo Formation (Adamson et al., 2013; Hocking et al., 1987; Payenberg et al., 2013) have benefited from access to region-wide datasets with wells sited in several sub-basins of the Northern Carnarvon Basin, with core penetrations of the TR20 and TR30 play intervals. However, the majority of the previous studies that have considered the sedimentology and reservoir characteristics of the Mungaroo Formation have been undertaken in relatively inboard locations of the Exmouth Plateau (Adamson et al., 2013; Bal et al., 2002; Heldreich et al., 2013; Jablonski, 1997; Stoner, 2010) and hence tend to describe a more proximal expression of the sedimentology of the palaeoenvironments represented by the Mungaroo Formation than that encountered in this study. Several related studies (e.g., Seggie et al., 2007; Adamson et al., 2013; Payenberg et al., 2013) also describe the stratigraphically younger and more marine influenced Brigadier Formation (TR30 play interval) that directly overlies the Mungaroo Formation. The facies associations described in these studies, including shoreface sands and marine mudstones, reflect the generally more marine-influenced setting at the time of deposition of the Brigadier Formation. Table 3.2 provides a summary overview of previous published research studies that have investigated the lithology of the Mungaroo Formation.

Table 3.2: Overview of previous lithofacies studies of the Mungaroo Formation.

Author	Facies scheme	Facies associations & architectural elements	Observations/trends
Hocking et al., 1987	Medium-coarse-grained sandstone; fine-grained, planar and ripple laminated sandstones, siltstones and claystones; laminated black shale; coal.	Channel belt and isolated channels; floodplain fines; crevasse splays; floodplain lakes; swamps, restricted embayments; marginal marine mudstones.	Predominantly fluvio-deltaic setting.
Bal et al., 2002	Based on Miall, 1978,	Investigating an inboard section of the Mungaroo Formation on the Rankin Trend. Alluvial and estuarine deposits: inter-bedded, massive sandstone and mudstone lithofacies, including within-channel bars, macroforms, channels channel complexes and palaeosol horizons.	Lithofacies are described from core, and calibrated with image and gamma-ray logs. Paleocurrents estimated from dip and image logs. Indicate downstream migrating bedforms.
Seggie et al., 2007	Based on Hocking et al., (1987), using wireline, core logs and petrology.	Split into: channel belt deposits; fluvial channel fills; crevasse splay deposits; overbank floodplain fines; floodplain lakes, swamps and embayments.	Wireline log pattern is also used to interpret log response to core.

Author	Facies scheme	Facies associations & architectural elements	Observations/trends
Stoner, 2010		Channel deposits: Thalweg fill; unit bars; abandonment phase. Floodplain deposits: floodplain mudflat; crevasse splay; splay delta; open lake; swamp.	Identified more deltaic and more fluvial-dominated intervals.
Adamson et al., 2013	Based on Miall, 1978.	Reflects the wide-spread dataset, covering a greater proportion of the Mungaroo Formation: Pro-delta to distal delta front; distal mouth bar; proximal mouth bar; distributary channel; abandoned channel; interdistributary bay; in-filled/vegetated interdistributary bay; transgressive lag; sandy strand-plain, shoreface; tidal inlet/barrier sands; tidal delta; lagoon; swamp; fluvial channel; splay; soil.	Most common identifiable facies associations are: fluvial channel; crevasse splay; soil, swamp and coal; lake; distributary channel; mouth-bar; interdistributary bay; pro-delta; tidal inlet/barrier.
Heldreich et al., 2013	Described in the following categories: medium and coarse-grained sandstones, with parallel laminations and basal lags; parallel laminated or massive mudstones; bioturbated silt and mudstones; nodular and coaly intervals.	Multi-storey fluvial channel sandstones; isolated fluvial channel fill sandstones; sheet-like crevasse splay sandstones; floodplain mudstone and heterolithics.	Trace fossils within bioturbated horizons are indicative of marginal marine/embayment environments.

Author	Facies scheme	Facies associations & architectural elements	Observations/trends
Payenberg et al., 2013	Based on criteria of grain size and sedimentary structures /fabrics using core and wireline log data.	Cross-bedded fluvial sandstones; ripple laminated fluvial sandstones; heterolithic, rooted crevasse splay sandstones; crevasse delta and delta front sandstones; inter-distributary bay mudstones; tidal heterolithics; cross-bedded, bioclastic, upper shoreface sandstones; bioturbated lower shoreface sandstones; laminated mouth-bar deposits.	Depositional environments split into non-marine fluvial and floodplain successions, marginal marine deltaic and inter-distributary bay-fill successions, and marine delta front to shelf successions. Also present a biostratigraphic framework, based on palynomorph taxonomy to identify 'wet' and 'dry' cycles.

3.5 Lithofacies of the Mungaroo Formation

3.5.1 Overview

Sixteen distinct lithofacies are recognised within the Mungaroo Formation examined as part of this study and these are described through adoption of a modified and extended version of Miall's (1978) widely used facies classification scheme. Seven lithofacies are associated with channelized deposits, three are present in both channelized and non-channelized deposits, and nine are associated solely with non-channelized deposits.

The lithofacies identified are as follows: Matrix-supported conglomerate (Gm); Low-angle trough cross-bedded sandstone (St); Planar cross-bedded sandstone (Sp); Planar laminated sandstone (Sh); Massive sandstone (Sm); Ripple-laminated sandstone (Sr); De-watered and convoluted sandstone (Sdc); Laminated mudstone (Fl); Discontinuous laminated siltstone (Flr); De-watered mud and silt (Fdc); Sand-prone heterolithics (Hs); Mud-prone heterolithics (Hf); Massive mud and silt (Fm); Mud, silt and very fine sand with root traces (Fro); Gleysol (Pg); Coal and carbonaceous mud (C). These lithofacies are discussed in detail in section 4.4.2 and key characteristic features are listed in Table 3.3. Assemblages of genetically related lithofacies, forming facies associations, are discussed in Section 4.4.3.

3.5.2 Lithofacies in detail

Each of the recognised lithofacies possesses a distinctive set of sedimentological characteristics that enable identification in core. Core photograph examples and sketches of each lithofacies are shown in Figure 3.11. These specific examples are from Well-11 (Noblige-2).

Matrix-supported conglomerate (Gm): This lithofacies is characterized by dm-thick, light-brown, pebble-bearing sandstone with rare cross-bedding (Figure 3.11a). Clasts are very coarse sand to pebble grade, poorly sorted, angular to sub-rounded, lenticular in shape and are composed of mudstone, siltstone, sandstone, quartz and carbonaceous material. Some examples contain abundant plant material as leaf debris. Matrix is characterised by light-brown to grey, fine- to medium-grained sandstone.

This lithofacies commonly occurs at the base of channel elements. It is interpreted as basal lags of channel fill. The largely intra-formational clasts indicate the re-working of fluvial overbank and previously deposited channel sediments by erosive, high-energy flows. Mud-rich clasts may represent bank-collapse events (Plint, 1986).

Low-angle trough cross-bedded sandstone (St): This lithofacies is a fine- to medium-grained, pale-brown to grey sandstone (Figure 3.11b). Cross-sets are typically inclined at angles $<15^\circ$. Sets of facies St vary in thickness from 0.3 m to 1.0 m. Most commonly, fining-up, erosive-based sets stack to form compound cosets of strata that are themselves several metres thick, and have coarser-grained, erosive-based lags at their base.

Facies St is a common constituent of channel complex deposits (Miall, 1985, 2006) and examples identified in this study most commonly represent deposits of high-energy channel complexes. These deposits are interpreted as in-channel bars deposited as 3-D dunes, in the lower flow regime (Miall, 1988) via moderate to high-energy traction currents (Adamson et al., 2013).

Planar cross-bedded sandstone (Sp): This lithofacies is a very fine-grained to medium-grained, often silty, pale-brown or grey sandstone (Figure 3.11c).

Cross-sets dips are inclined at angles that vary from 15° to 25°. Relatively uncommon changes in orientation have associated reactivation surfaces, typically with mud drapes. Mud (occasionally carbonaceous) drapes are common on cross bed surfaces. Rare bioturbation (unlined traces of an unspecified ichnofacies) are recognised. Predominantly fining-up, approximately 0.3 to 1.0 m-thick sets, commonly with erosive bases, occur stacked as compound cosets that are themselves each tens of metres thick.

Facies Sp is prevalent in channel complexes (Miall, 1985), and is commonly interpreted as having been deposited during the downstream migration or lateral accretion of barforms (Miall, 1985; 1988). Sp is interpreted as the deposits of 2-D dunes, and is generally interpreted as deposited by flows that experienced lower-energy conditions than those responsible for the generation of 3-D, dunes represented by lithofacies St (Miall, 2006). Cleaner, coarser grained sandstones are interpreted as high-energy deposits (Fisher & McGowen, 1963; Davies & Ethridge, 1975); finer-grained, silty sandstones that are commonly present are likely representative of relatively low-energy channel deposits (cf. Davies & Ethridge, 1975; Donselaar & Schmidt, 2010). Lithofacies Sp also occurs as the upper part of higher energy channel deposits relating to channel abandonment and, as such, in core in this study is seen to commonly grade vertically into planar laminated sandstone (Sh), ripple laminated sandstone (Sr) and planar laminated mudstone (Fl) (cf. Miall, 1985; Bristow, 1993). Figure 3.11c shows an example of Sp from within a high-energy channel complex.

Planar-laminated sandstone (Sh): This lithofacies is characterised by very-fine- to fine-grained pale-brown sandstone (Figures 3.11b and 3.11d). Mud and carbonaceous drapes are common, as well as plant material. Beds are

commonly on a decimetre scale and can have either erosive or gradational bases. This lithofacies is commonly associated with ripple-laminated sandstone (Sr) and laminated mudstone (Fl).

This facies is most commonly present at the top of channel deposits. It is interpreted to have been deposited under waning-low flow-regime conditions. Where present as part of bay-fill assemblages, this lithofacies is tentatively interpreted as representative of the fill of distal distributary channel and mouth-bar elements (Adamson et al., 2013; cf. Coleman & Gagliano, 1960; Coleman et al., 1964; Hyne et al. 1979; Tye & Hickey, 2001).

Massive sandstone (Sm): This lithofacies is expressed as dm-thick, sharp, erosive based beds of very-fine, pale-grey to brown sandstone (Figure 3.11d). Beds typically exhibit weak fining-upward trends. Rarely, cm- to dm-thick beds with pronounced normal grading are present.

Lithofacies Sm is interpreted as being deposited rapidly in discharges with high sediment-to-water ratios typical of hyperconcentrated or gravity-driven flows (Miall, 1978; 2000; 2006), either in channel or overbank areas. In this study, facies Sm is most commonly interpreted as being deposited by unconfined, overbank flow, although they are also identified as forming part of channel fill. Deposits of lithofacies Sm in non-confined, overbank settings are commonly associated both with crevasse splays (Mjøs et al., 1993), as splay channel or sheet deposits, often forming part of the 'splay belt' running parallel to fluvial channel deposits (Fielding, 1984), and with bay-fill in more distal areas, where they represent storm or flood events, where incidences of pronounced normal grading indicate pulsed flow (Collinson et al., 2006). Figure 3.11d shows an example of Sm associated with bay-fill.

Ripple laminated sandstone (Sr): This lithofacies is characterised by 0.1 to 2.0m-thick beds of very-fine- to fine-grained light-grey silty sandstone (Figure 3.11e). This facies is commonly burrowed and root mottled, especially toward the tops of beds. Sand filled rhizoliths are common. Mud drapes on ripple laminae are common.. Rarely, sets of climbing-ripple strata can be identified in core.

This lithofacies is interpreted as lower-flow regime fluvial deposits, representing the downstream migration of small sandy bedforms – microforms (Miall, 1985; 1988). These deposits are interpreted as resulting from (i) both confined flow in low-energy channels (Smith & Pérez-Arlucea, 1994), primarily in shallow areas of active channels (Miall, 2006), (ii) unconfined flow on the surfaces of crevasse splays (Hyne at al., 1979; Smith & Pérez-Arlucea, 1994), and (iii) bay-fill deposition (Hyne at al., 1979). Mud drapes indicate variations in flow energy. Figure 3.11e shows a well-developed section of Sr lithofacies from a low-energy channel fill.

De-watered and convoluted sandstone (Sdc), de-watered mud and silt (Fdc): Lithofacies Sdc is characterised by siltstone to very fine silty sandstone, and is commonly associated with finer-grained deformed facies Fdc (Figures 3.11f and 3.11g). Dewatering structures include convolute lamination, flame structures, disrupted laminations and overturning of beds. Fdc and Sdc sediments are typically cm-dm thickness (maximum thickness occurrence in the studied core is 0.4 m). The extent of deformation is usually confined to a single bed, and many such beds are erosionally truncated by overlying beds. Facies Fdc commonly contains siderite nodules and iron staining. Original bedding can be obscured, depending on the severity of the deformation.

Soft-sediment (plastic) deformation due to dewatering is implied by the sharp, upwards-pointing folds of the majority of the convolutions (Collinson et al., 2006) and is attributed to rapid deposition and loading on saturated deposits (Dzulynski & Smith, 1963; Collinson et al., 2006). This is interpreted as likely being due to rapid deposition of sediment during flood events. Facies Sdc and Fdc are commonly identified in this study in bay-fill deposits. Facies Sdc more rarely occurs in the studied core within channel deposits; this current convolute bedding likely developed very soon after deposition (Allen, 1982; Collinson et al., 2006).

Laminated mudstone (FI): This lithofacies is characterised by silty, dark-grey mudstone with silt to very-fine sand grade laminae and rare to common carbonaceous root traces. Beds typically range in thickness from 0.2 m to 1.5 m. Rhythmic, pinstripe laminae are common, with coarser, silt to very fine sandstone grade laminae ranging from approximately 0.2 to 1.0 cm thickness.

Examples of this facies are interpreted as mudrocks of lacustrine origin, whereby the fine-grained sediments settled out of suspension (Collinson et al., 2006). Coarser laminae were likely deposited by pulsed flow into a lake e.g. seasonal climatic variations controlling sediment supply (Collinson et al., 2006). This facies is also interpreted as the finer-grained part of bay-fill deposits (Horne et al., 1978). Figure 3.11h shows a typical example of FI.

Massive siltstone and mudstone (Fm): This facies is characterised by decimetre thickness individual beds that stack to form bedded deposits that are collectively several metres thick, of dark grey, massive siltstone-dominated mudstone (Figure 3.11h). This facies has either no discernable bedding or very indistinct bedding, often grading into facies FI. Low diversity bioturbation is

common at the top of beds (carbonaceous root traces and indistinct burrows – possibly *Planolites*). Metre-thick beds of massive, siltstone-dominated mudstones with absent bioturbation are also present.

This facies is interpreted as floodplain fines (Fielding, 1984), and can be interpreted as floodplain siltstones and mudstones, distal crevasse delta mudstones and anoxic lake floor mudstones (Fielding, 1984). The paucity of bioturbation (e.g. burrows and root traces) within the beds indicates a lack of vegetation and fauna, favouring an interpretation of facies Fm as floodplain lake mudrocks, deposited by settling out of suspension, with no discernable coarse sediment input. The preserved root traces at the top of beds (often extending down from overlying heavily rooted, siltstone and sandstone beds), indicates the establishment of vegetation as the local accommodation within the lakes and ponds became filled. Figure 3.11h shows an example of Fm overlaying Fl.

Discontinuous wavy laminated siltstone (Flr): This lithofacies is characterised by light-grey to dark-grey siltstone, commonly with mud lining the discontinuous internal laminae of the siltstone. Beds range in thickness from 0.1 to 0.6 m, and may stack with thinner (typically <0.1 m thickness) beds of mudstone to form multi-metre-thick accumulations of stacked heterolithic strata (Figure 3.11i). Flr beds are commonly burrowed (typically brackish water ichnofacies including possible *Diplocraterion*) and root-mottled (grey), containing carbonaceous root traces (preserved length <1.0 m) which frequently disrupt the original bedding structures. Flr is commonly associated with Sr and Sp.

This lithofacies commonly occurs at the top of coarser-grained channel elements and in sandy and muddy crevasse splay elements. Facies Flr is

interpreted as the deposits of waning-flow regimes during channel abandonment. It can also be attributed to very low energy, periodically (possibly seasonally) active distributary and crevasse channels and unconfined crevasse-splay deposits (Fielding, 1984), forming part of crevasse-splay delta and inter-distributary bay assemblages. The grey colour, mottling and preservation of carbonaceous root traces indicates a poorly-drained setting (Kraus & Hasitosis, 2006). Figure 3.11i shows an example of Flr that has not been burrowed or disturbed by root traces.

Sand-prone heterolithics (Hs) and mud-prone heterolithics (Hf): Lithofacies

Hs is characterised by dm-scale light-grey siltstone and very-fine sandstone that occurs interbedded with cm-scale dark grey siltstone to silty mudstone (Figures 3.11i and 3.11j.). Facies Hs is present both as sub-horizontal deposits and as inclined heterolithic cross-stratification (IHS), foresets of which are inclined at angles up to 20°. This lithofacies is commonly bioturbated with burrows in finer-grained beds and rhizoliths (sand-filled rhizoliths and rhizoliths containing preserved carbonaceous root traces) in coarser-grained beds. Indistinct wavy and ripple laminations are common.

Lithofacies Hf is characterised as cm- to dm-scale, interbedded siltstone, mudstone and very fine sandstone (Figure 3.11j and 3.11k). Sedimentary features include ripple laminations, rare hummocky cross-stratification (HCS) and dewatering structures. Bioturbation (both horizontal and vertical burrows, notably *Diplocraterion*, *Planolites*, *Chondrites*, *Zoophycos* and *Technichnus*) and mid- to dark-grey root mottling with carbonaceous root traces, are common in sub-horizontal Hf, but less so in IHS examples of facies Hf.

Facies Hs is attributed to unconfined deposition by low-stage, but varying energy flow. This facies is present as part of both proximal and distal crevasse-splay deposits (Fielding, 1984, 1986; O'Brien & Wells, 1986; Smith et al., 1989; Mjøs et al., 1993). IHS is also interpreted as tidally-influenced fluvial channel deposits (e.g. Thomas et al., 1987; Smith, 1987, 1988; Johnson & Dashtgard, 2014).

Lithofacies Hf is interpreted principally as a more distal expression of facies Hs (Stear, 1983; Fielding, 1984) and is present as crevasse-splay deposits (Bristow et al., 2002). In some cases, associated inclined heterolithic cross-stratification (IHS) has been interpreted as the inclined toes of crevasse-splay delta foresets, and as bay-fill (Hillier et al., 2007; Adamson et al., 2013). Figure 3.11j shows an example of facies Hf relating to crevasse splay deposits, and Figure 3.11k shows Hf as bay-fill deposits.

Mudstone, siltstone and very fine sandstone, with root traces (Fro): This lithofacies is most commonly present as very-fine sandstone and siltstone, with mid to dark grey mottling and in-situ carbonaceous rootlets. Preserved length of the traces is typically 0.3 to 1.0 m (the best example of which is found at 4092 m in Well-11; the preserved length is ~1.0 m in length, where the primary root can be seen to give rise to second and third order rootlets (Figure 3.11l). Depending on the intensity of the rooting, original bedding features are either disrupted or completely destroyed.

This lithofacies is found throughout the formation, and where the roots are well developed. This facies is interpreted as fine-grained overbank deposits, including crevasse splay deposits (Bristow et al., 2002). This lithofacies is also present in the uppermost deposits of channel complexes, where overlain by

floodplain deposits. The preservation of carbonaceous root traces implies a relatively poorly-drained depositional setting (Kraus & Hasitosis, 2006). Figure 3.11l shows an example of Fro, with an exceptionally well-preserved carbonaceous root trace in a silty sandstone crevasse splay deposit.

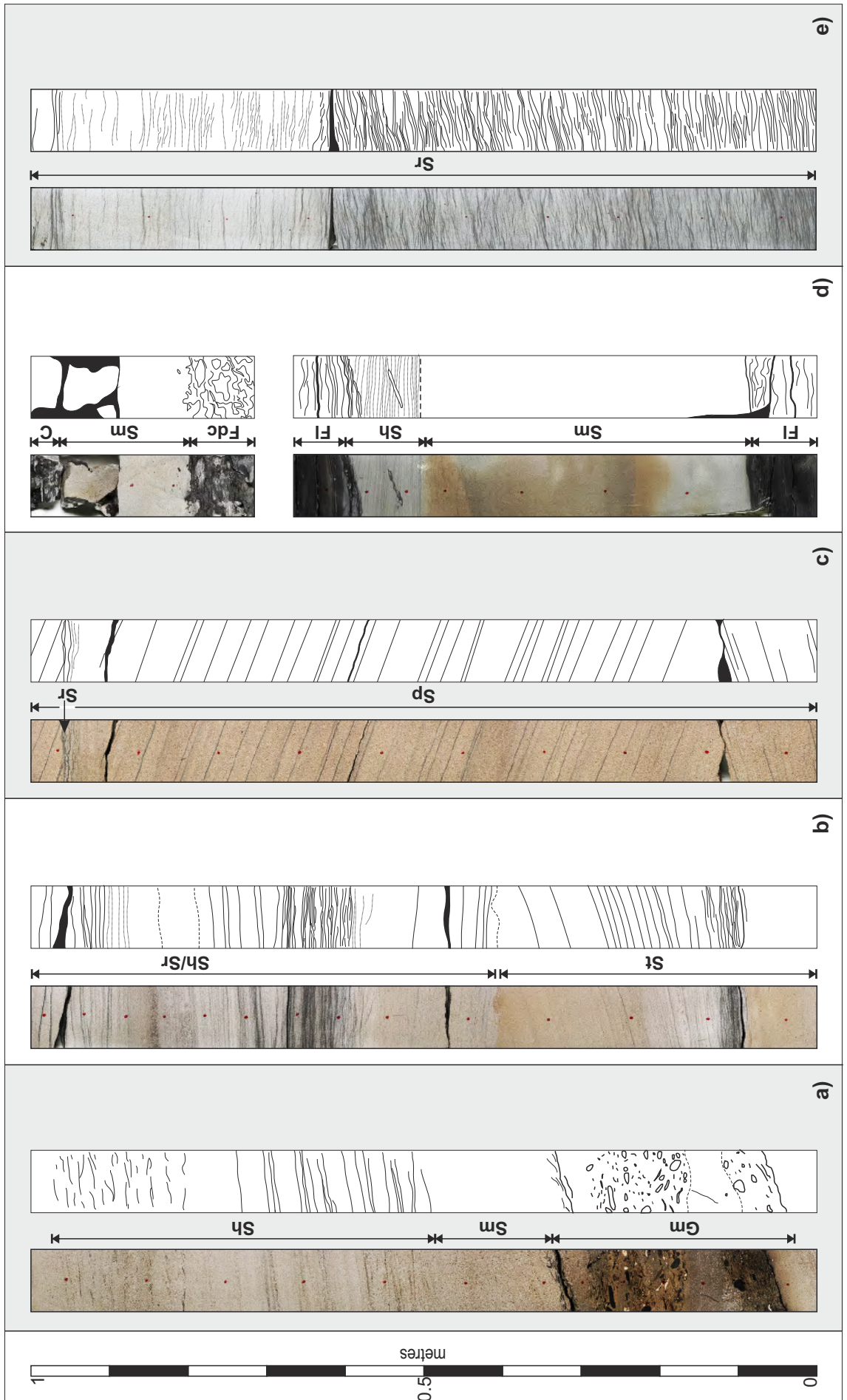
Gleysol (Pg): Facies Pg consists of palaeosol beds that are typically 0.5 to 1.5 m thick. The grain size of this lithofacies is typically siltstone-grade (Figure 3.11m). Colour varies from grey to green-grey to dark-grey. Beds are commonly pyritic and contain siderite nodules up to 10 cm diameter. Root mottling affecting part or the whole of the bed and rhizoliths preserved as iron-oxide precipitates and carbonaceous root traces (preserved length approximately 0.3 to 1.0 m) are abundant in this lithofacies, as are fragments of carbonaceous plant material.

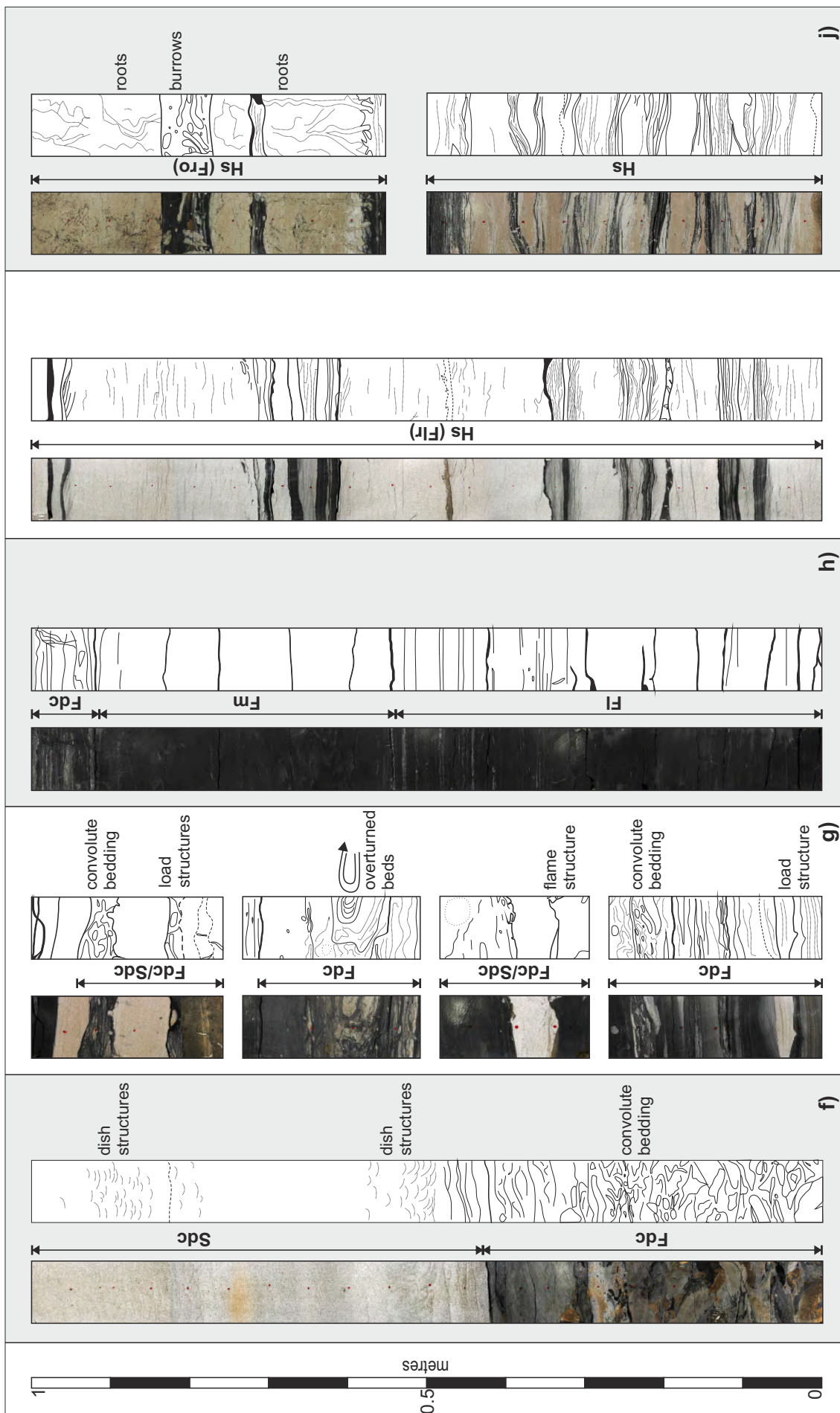
The reduced (grey) colour of the matrix, in conjunction with abundant organic fragments are indicative of very poorly drained, gleyed palaeosols (Kraus, 1998), Rhizoliths preserved as yellow-brown tendrils (Figure 3.11m) indicate that the soil matrix was sufficiently poorly-drained to reduce and solubilized iron which is precipitated as goethite, lending the rhizoliths their yellow-brown colour (Kraus & Hasitosis, 2006). Carbonaceous root traces are more commonly found in very poorly-drained palaeosols; the preservation of the organic matter being highly dependent on anoxic conditions in waterlogged soils (Kraus & Hasitosis, 2006). This lithofacies is interpreted as gleysol accumulating in poorly-drained floodplain and marsh conditions, with variations in colour attributed to mineral leaching. Facies Pg is commonly associated with (i) crevasse-splay deposits, where it occurs both above and below the splay deposits (Slingeland & Smith, 2004), and in this study of the Mungaroo Formation has been found in close association with (ii) lacustrine, (iii) coal and (iv) bay-fill deposits. Figure 3.11m

shows an example of Pg with mottling due to iron (possible goethite) staining and sideritized root traces.

Coal and carbonaceous mud (C): This lithofacies is typified by dark grey to black, cm to dm-thickness beds of carbonaceous mudstones and borderline coals, commonly with a blocky/rubby texture (Figure 3.11n). Carbonaceous root traces and sand to granule grade fragments of plant material are common. This lithofacies is often closely associated with, and grades into facies Pg.

These borderline (poor-quality) coals and carbonaceous muds are interpreted as accumulating in waterlogged settings, e.g. swamp or marsh conditions (cf. Horne et al., 1978; McCabe, 1984; Ethridge et al., 1981; Slingerland & Smith, 2004). Figure 3.11n shows lithofacies C, where it is in association with facies Pg and Fm.





i)

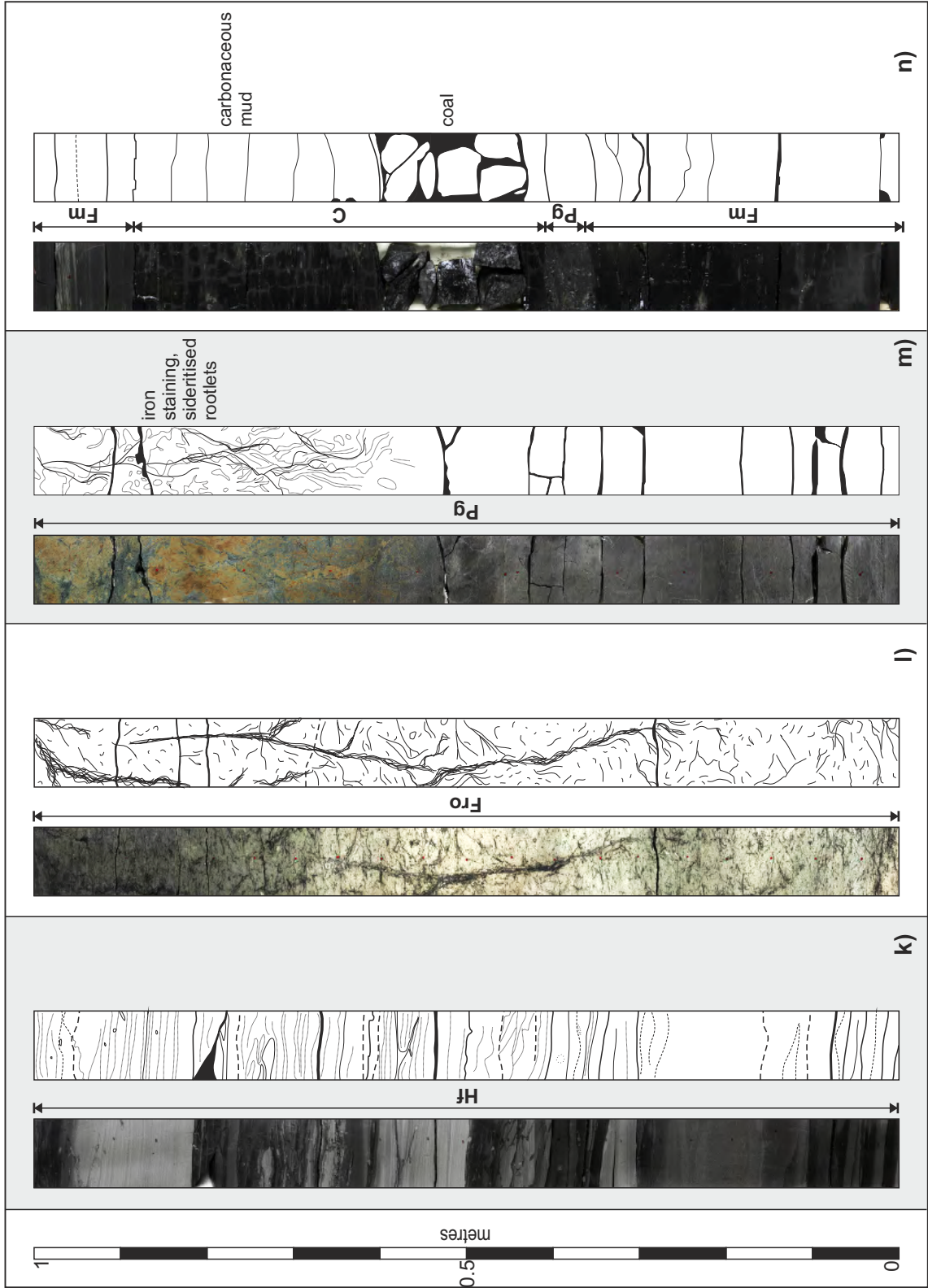


Figure 3.11: Facies photos and accompanying sketches highlighting key features from Well-11 penetrations of the Mungaroo Formation: **a.** Gm, Sm, Sh; **b.** St, sh; **c.** Sp, Sr; **d.** Sm, Sh; **e.** Sr; **f.** Sdc, Fdc; **g.** Fdc, Sdc; **h.** Fl, Fm; **i.** Hs; **j.** Hs; **k.** Hf; **l.** Fro; **m.** Pg; **n.** Fm, Pg, C.

Table 3.3 provides descriptions of each of the above lithofacies.

Table 3.3: Characteristic lithofacies of the Mungaroo Formation.

Code		Facies	Description	Interpretation
Gm		Conglomerate (matrix-supported)	Very coarse sand to pebble-sized clasts composed of mud, silt, fine sandstone or carbonaceous material. Commonly contains scattered plant material. Matrix commonly fine to medium sandstone.	Commonly found at the base of channel elements. Entrainment and reworking of locally derived sediment; can occur as basal lags of channel fill.
St		Low-angle-inclined cross-bedded sandstone trough	Fine to medium grained, pale-brown to grey sandstone. Foresets inclined <15° with clasts common at the base of beds.	Occurs in channel complexes. High-energy fluvial flow; downstream migration of bars.
Sp		Planar sandstone cross-bedded	Very-fine to medium grained sandstone, pale-brown to grey colour. Mud drapes and clasts along cross-bed surfaces are common. Commonly grades vertically into facies Sh, Sr and Fl.	Prevalent in channel deposits. Downstream migration and lateral accretion of sediment in both high- and low-energy channel settings.
Sh		Planar laminated sandstone	Very-fine to fine pale-brown sandstone. Mud and carbonaceous drapes common. Associated with facies Sr and Fl.	Lower flow regime sands; present at the top of channel deposits; possible distal mouth bar deposits.

Code		Facies		Description	Interpretation
Sm	Massive sandstone	Very-fine, pale-grey to brown sandstone; rarely normally-graded. Typically sharp-based.		Unconfined overbank sands. Associated with splays where they may form either minor splay channel deposits or sheet deposits, and bay-fill where they represent storm or flood events. Rarely present as dewatered sediments at the base of channel deposits.	
Sr	Ripple laminated sandstone	Very-fine to fine light grey sandstone; commonly burrowed; root mottled and with rhizoliths.		Low flow regime fluvial deposits representing the migration of small sandy bedforms. Present as both confined flow in low-energy channel deposits, and unconfined flow in crevasse splay and bay-fill deposits.	
Sdc	De-watered and convoluted sandstone	Siltstone to very fine sandstone. Dewatering structures include convolute bedding, flame structures, disrupted laminations and overturned beds.		Dewatering occurs as the result of post-depositional loading on water-saturated unconsolidated sediment. Likely due to rapid loading of sediment during flood events. Common in bay-fill deposits.	
Fdc	De-watered mud and silt	Convolute bedded mudrocks; original bedding obscured; siderite nodules and iron staining; overturned beds common. Commonly associated with facies Sdc.		Occurrence in gleysol facies underlying facies Sdc channel sands. Response to rapid loading of sediment on water-saturated fines.	

Code		Facies	Description	Interpretation
Fl	Laminated mudstone	Silty mudstone with silt to very-fine sand laminae. Pinstripe and rhythmic laminae common.	Lacustrine mudrocks commonly with rhythmic pinstripe laminae; rare occurrence as part of bay-fill successions.	
Fm	Massive mud and silt	Massive siltstone-dominated mudrocks with no discernable bedding.	Lacustrine mudrocks; settling of sediment out of suspension.	
Flr	Discontinuous wavy- or ripple-laminated siltstone	Light- to dark-grey siltstone; commonly burrowed and/or rooted; commonly associated with facies Sr and Sp.	Commonly occurring at the top of channel elements and in crevasse splay elements. Represent waning flow fluvial regimes during channel abandonment, or deposits of very low energy, episodically active distributary or crevasse splay channels. Also associated with crevasse splay deltas.	
Hs	Interbedded siltstone and very-fine sandstone (sand-prone heterolithic strata)	Silt to very fine sandstone; light grey; commonly burrowed or rooted.	Unconfined deposition with low-energy but varying flow. Proximal and distal crevasse splay deposits. Also present in bay-fill successions.	
Hf	Interbedded silty sandstone and mudstone (mud-prone heterolithic strata)	Interbedded siltstone, mudstone and sandstone. Commonly ripple laminated; rare HCS; commonly rooted or burrowed; rare dewatering structures.	Distal crevasse splay deposits and bay-fill.	

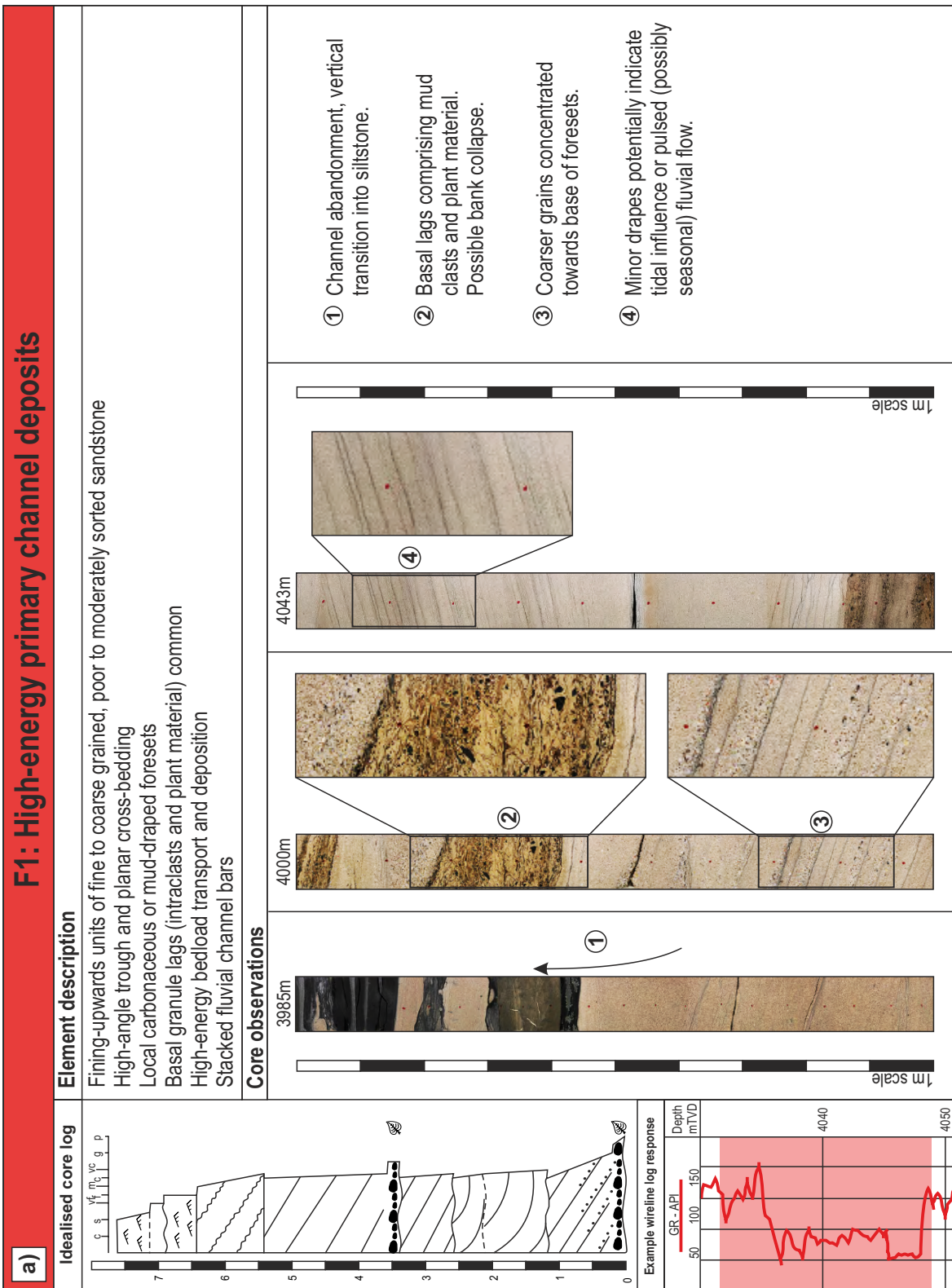
Code		Facies		Description	Interpretation
Fro	Mud, silt and very-fine sand with root traces	Mottled very-fine sand and silt, with in-situ carbonaceous rootlets, disrupting original bedding structures.	Fine-grained overbank deposits including crevasse splay deposits.		
Pg	Palaeosol (gleysol), locally with siderite nodules, mottled texture, roots	Typically siltstone-grade; colour ranges grey, green-grey, dark-grey; commonly intensely mottled; common carbonaceous beds and lenses; abundant plant material; rarely pyritic; common siderite nodules.	Gleysol; poorly-drained floodplain and swamp or marsh facies.		
C	Coal and carbonaceous mud	Poor-quality coals; cm-dm scale beds; commonly associated with facies Pg; root traces and fragments of plant material common.	Poor quality coals and carbonaceous muds deposited in swamp or marsh conditions.		

3.6 Lithofacies associations

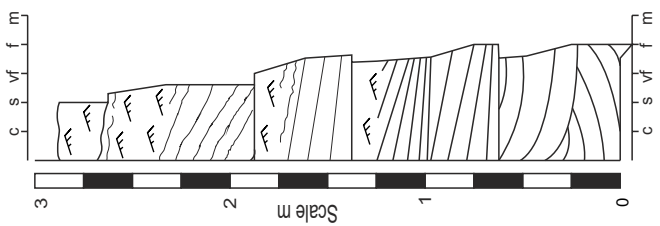
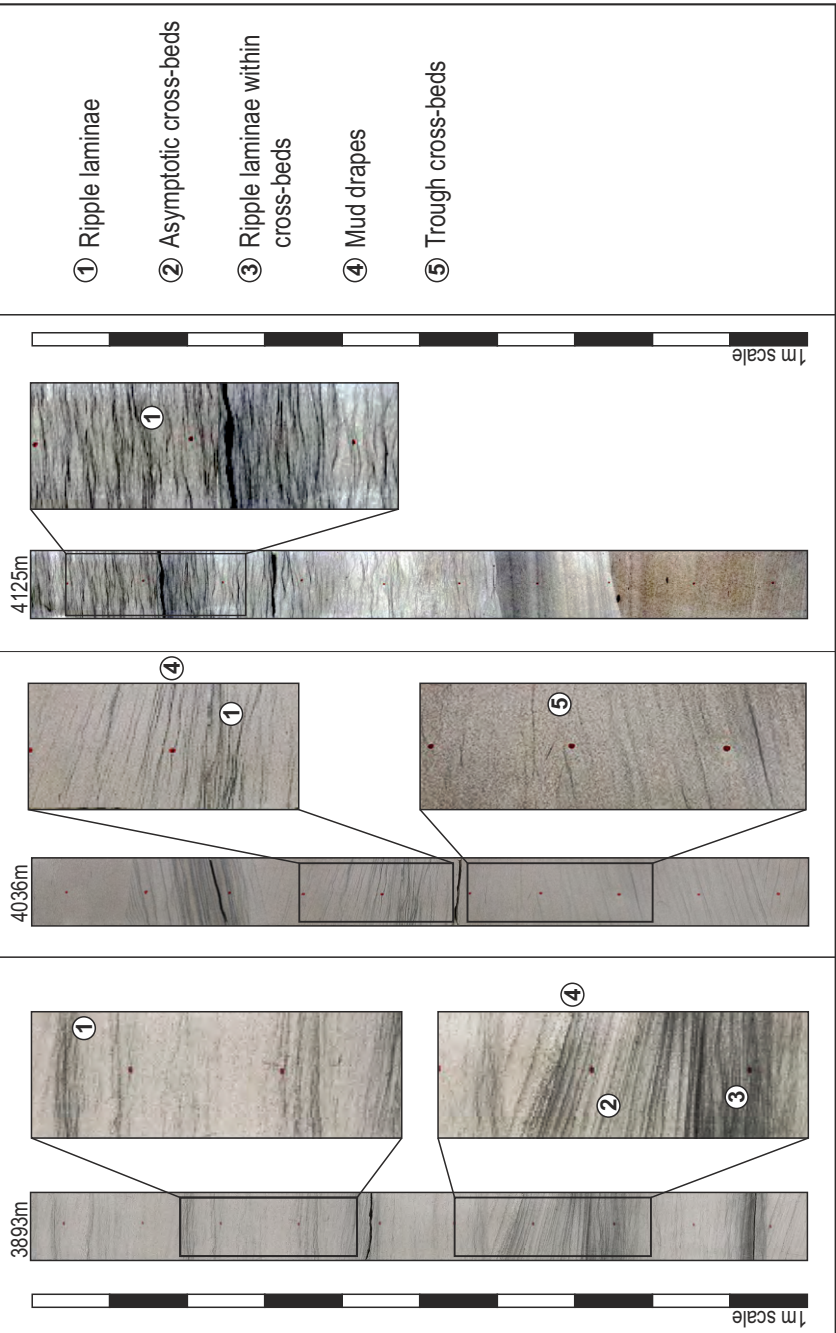
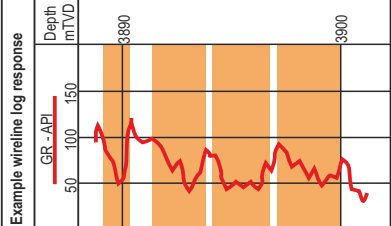
Facies associations, comprising commonly occurring successions of lithofacies are interpreted as successions of genetically-related strata that represent the preserved record of depositional sub-environments (Walker and James, 1992). Seven facies associations have here been interpreted from the Mungaroo Formation and these associations have been recognised based on lithology, the occurrence of sedimentary and biogenic structures, and on stacking patterns of the individual lithofacies types. The typical expression of the facies associations on wireline logs has also been investigated.

Table 3.4 lists and describes the seven facies associations recognised in the Mungaroo Formation, and lists the lithofacies present in each facies association. Figure 3.11 shows core photos of the facies associations, as well as idealised logs and gamma-ray wireline log responses.

Figure 3.12: Facies associations of the Mungaroo Formation, incorporating sedimentary and wireline logs, as well as core photo examples and brief description of typical sedimentary features and interpreted depositional processes: **a.** High-energy channel (F1); **b.** Low-energy channel (F2); **c.** proximal crevasse splay (F3); **d.** distal crease splay (F4); **e.** gleysol, swamp and coal (F5), and floodplain lake (F6); **f.** Inter-distributary bay heterolithics (F7).

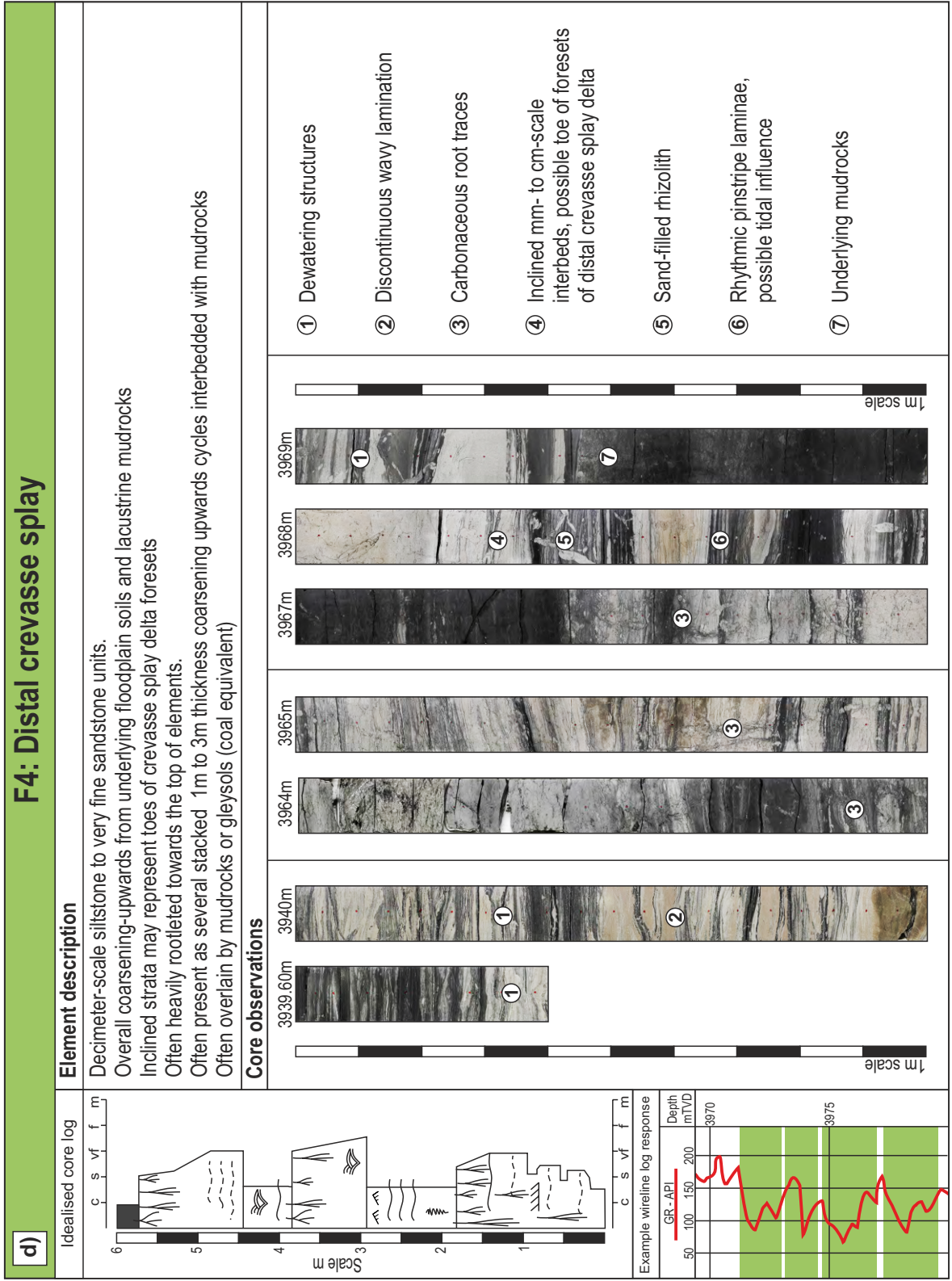


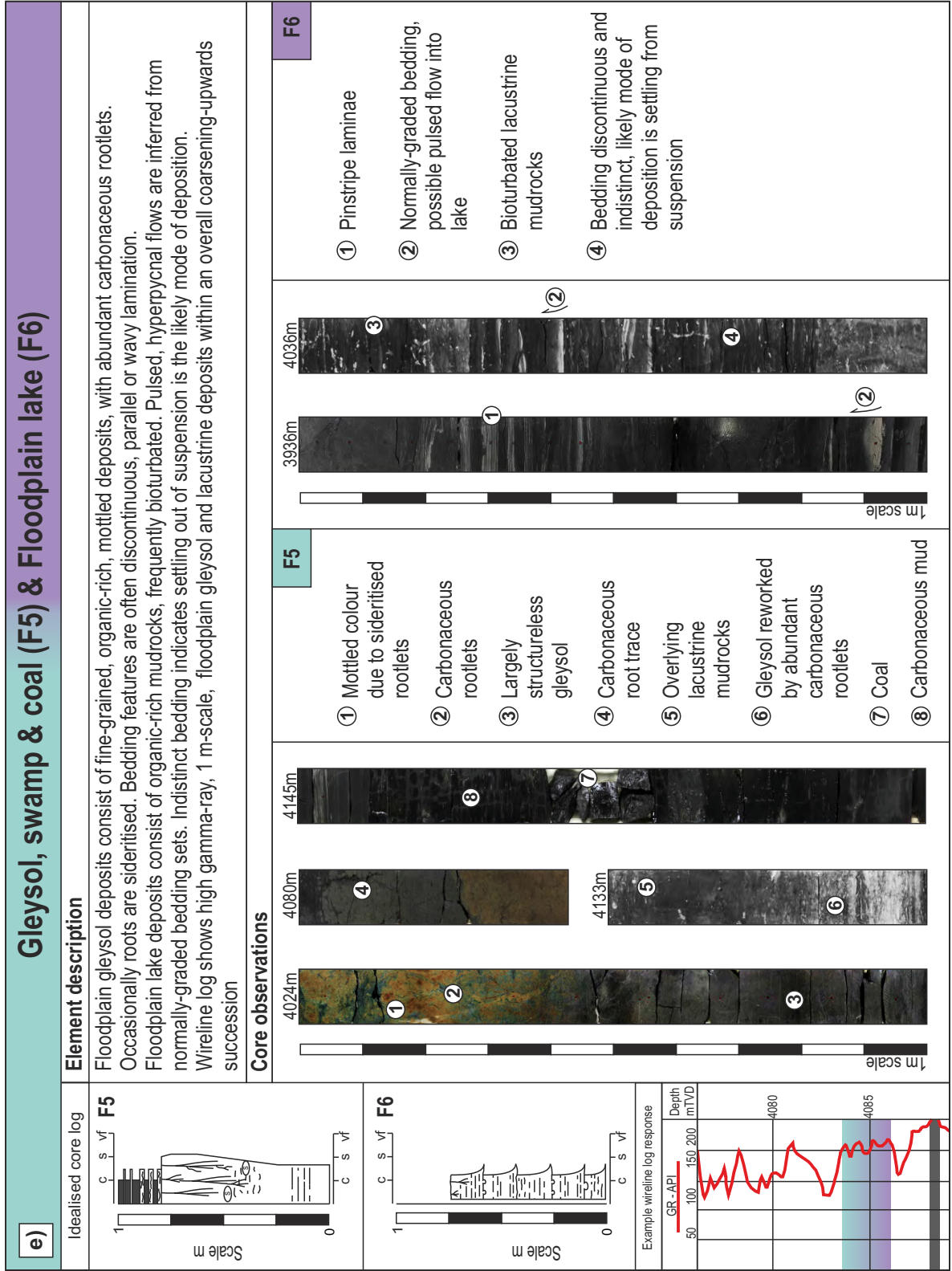
b) F2: Low-energy channel deposits (Secondary or tertiary distributary channels)

<p>Idealised core log</p> 	<p>Element description</p> <p>Fining-upwards, fine sand to silt grain size, moderately well sorted units High-angle planar & trough cross-beds towards the base of units and ripple-laminations (frequently draped) towards the top Possible fluctuations in flow rate (seasonal discharge) and weak tidal influence in some cases (delta plain distributary channels) Abundant carbonaceous & muddy drapes Moderate-energy bed to mixed load transport and bar deposition within a more sluggish 'lazy' river channel. Interpreted as moderate to low energy channel deposits, secondary or tertiary distributary channels.</p>	<p>Core observations</p>  <ul style="list-style-type: none"> ① Ripple laminae ② Asymptotic cross-beds ③ Ripple laminae within cross-beds ④ Mud drapes ⑤ Trough cross-beds
<p>Example wireline log response</p> 		

c) F3: Proximal crevasse splay

c)	Element description	
<p>Idealised core log</p>	<p>Deposits tend to be upwards-coarsening, with overall increase in thickness of sandstone beds</p> <p>Sandstone tends to be silty, very fine- to fine-grained</p> <p>Fining-upwards, massive sandstone beds 1m to 2m thickness may represent channel deposits within crevasse splay deltas</p> <p>Dewatering structures are common</p> <p>Tops of units may be heavily reworked by roots, obscuring sedimentary structures</p>	<p>① Overall fining-up sequence often topped with soils and lake deposits</p> <p>② Roots common at top of beds</p> <p>③ Load casts</p> <p>④ Discontinuous wavy lamination and convolute bedding (dewatering) common in mud-rich beds</p>
<p>Example wireline log response</p>	<p>Core observations</p>	<p>① Lake (possibly inter-distributary-bay) deposits overly splay deposits often containing roots</p> <p>② Silt/sand-filled rhizolith</p> <p>③ Decimetre-scale fine, often silty sandstone units, often massive, structureless</p> <p>④ Discontinuous wavy lamination</p> <p>⑤ Dewatering structures and mud clasts. Possible bank collapse assemblage</p> <p>⑥ Carbonaceous root traces. The original sedimentary structures (including wavy lamination) of this sandstone unit are mostly destroyed due to extensive reworking by roots.</p>





F7: Inter-distributary Bay (Heterolithics)

f)	Idealised core log	Element description	
	<p>a</p> <p>b</p>	<p>Inter-distributary bay-fill deposits are heterolithics with marine and tidal indicators, often include distributary mouth bar deposits. F7a: Tidally-influenced. Tidal indicators include rhythmic bundling of laminae (although this is often indistinct, indicating a weak tidal influence) and synaeresis cracks, indicative of fluctuating salinity levels. Minor bioturbation, low-diversity ichnofauna (possible <i>Chondrites</i> and <i>Planolites</i>) and rhizoliths are present. Deposition in a restricted, brackish setting. F7b: Marine-influenced. HCS visible in cm-dm scale of sand beds. Intense bioturbation by moderate diversity ichnofauna (including <i>Zoophycos</i>, <i>Chondrites</i>, <i>Planolites</i>, <i>Diplocraterion</i>) indicates a less restricted bay setting with access to marine water.</p>	<p style="text-align: right;">F7a</p> <div style="display: flex; justify-content: space-between;"> <div style="width: 45%;"> <p>① Bioturbation</p> <p>② Sand-filled rhizoliths</p> <p>③ Synaeresis</p> <p>④ Rhythmic laminae</p> </div> <div style="width: 50%;"> </div> </div>
		<p style="text-align: right;">F7b</p> <div style="display: flex; justify-content: space-between;"> <div style="width: 45%;"> <p>① Interbedded heterolithics</p> <p>② Possible wave ripples</p> <p>③ Relict laminae</p> <p>④ Moderate- to- intense bioturbation</p> <p>⑤ <i>Diplocraterion</i></p> <p>⑥ <i>Zoophycos</i></p> <p>⑦ <i>Planolites</i></p> <p>⑧ Possible distributary mouth bar</p> </div> <div style="width: 50%;"> </div> </div>	
		<p>Core observations</p>	
	<p>Example wireline log response</p>		

Table 3.4: Lithofacies and facies associations of the Mungaroo Formation.

Facies association	Lithofacies present	Description
F1: High-energy channel deposits	Gm, St, Sp, Sh, Sr, Fir	<p>These fining-upwards units of fine to coarse grained sandstone are typically poorly to moderately sorted, and frequently feature basal erosional surfaces and granule lags of intraclasts, carbonaceous material and plant material. High-angle trough and planar gross bedding grades upwards into ripple-laminated very fine sandstone and silt where abandonment facies are preserved. Fine-grained drapes on individual cross beds indicate fluctuating flow, possibly from seasonal or tidal influences. Channel deposits can be single multi-storey. The relatively coarse grain-size indicates a relatively high-energy channel system.</p> <p>Idealised core log, typical wireline log expression and core photo examples of this facies association are featured in Figure 11a.</p>

Facies association	Lithofacies present	Description
F2: Low-energy channel deposits	St (rare), Sp, Sh, Sm, Sr, Sdc (rare), Flr	<p>These fining-upwards units of fine sand to silt-grade sandstones are moderately to well sorted, sometimes with basal scour surfaces. High angle planar and trough cross-bedding grade vertically into wavy bedded and ripple cross-laminated siltstones and silty sandstones. Abundant muddy and carbonaceous drapes indicate a fluctuating flow regime, possibly influenced by seasonal or tidal flow. May be present as single storey or more rarely multi-storey deposits. These fine-grained channel deposits are interpreted as being formed by low-energy channels, such as secondary or tertiary distributary channels.</p> <p>Idealised core log, typical wireline log expression and core photo examples of this facies association are featured in Figure 11b.</p>
F3: Proximal crevasse splay deposits	Sm, Sr, Sdc, Flr, Fdc, Hs, Fro	<p>These typically coarsening-upwards units of very fine-fine silty sandstone may be massively bedded, or feature sedimentary structures such as ripple lamination, discontinuous wavy bedding and dewatering structures. The tops of these units are typically bioturbated by both burrows and carbonaceous root traces, as well as sand-filled rhizoliths.</p> <p>Idealised core log, typical wireline log expression and core photo examples of this facies association are featured in Figure 11c.</p>

Facies association	Lithofacies present	Description
F4: Distal crevasse splay deposits	Sr, Flr, Fdc, Hs, Hf, Fro	<p>These fine-grained units feature both fining upwards and coarsening-upwards siltstone and very fine sandstone beds. Discontinuous wavy lamination and dewatering/convolute bedding are common. Carbonaceous root traces are abundant, with root mottling frequently obscuring original bedding at the tops of units. This facies association is often present as several stacked metre-scale, coarsening-upwards cycles, interbedded with mudrocks. These deposits are interpreted as the distal expression of facies association F3.</p> <p>Idealised core log, typical wireline log expression and core photo examples of this facies association are featured in Figure 11d.</p>
F5: Gleysol, swamp and coal deposits	Fdc, Fro, Pg, C	<p>Poorly-drained floodplain deposits are present as the following: Gleysol deposits, which are present as fine-grained, organic-rich, mottled deposits, with abundant carbonaceous rootlets. Sedimentary features include discontinuous wavy or parallel lamination and siderite nodules, carbonaceous and silty mudrocks, and thin, poor-quality coal deposits.</p> <p>Idealised core log, typical wireline log expression and core photo examples of this facies association are featured in Figure 11e.</p>

Facies association	Lithofacies present	Description
F6: Floodplain lake deposits	Fl, Fm, Fro	<p>Floodplain lake deposits consist of organic-rich mudrocks, which are frequently moderately bioturbated. Pulsed, hyperpycnal flows are inferred from normally-graded bedding sets. Bedding features are indistinct, indicating settling out of suspension is the likely mode of deposition.</p> <p>Idealised core log, typical wireline log expression and core photo examples of this facies association are featured in Figure 11e.</p>
F7: Inter-distributary bay deposits	Sh, Sm, Sr, Sdc, Fl, Hs, Hf, Fro	<p>Inter-distributary bay deposits are interpreted where there are heterolithics with marine and tidal indicators. Tidal indicators include rhythmic laminae and syneresis cracks, while marine indicators include sedimentary features indicative of wave action, and a more diverse ichnofacies. The distinction between more marine or tidally-influenced bay-fill is not investigated further within the scope of this study, although periods of greater and lesser tidal influence are described.</p> <p>Idealised core log, typical wireline log expression and core photo examples of this facies association are featured in Figure 11f.</p>

3.7 Depositional environment

In this section, the depositional environment of the Mungaroo Formation is discussed, in particular tidal influence and sedimentary indicators thereof, and the different styles of channel system interpreted from core deposits.

3.7.1 Tidal indicators

Sedimentary features: The following sedimentary features, whilst alone are merely indicators of changing flow conditions, where several are found in close association, are judged to be indicators of tidal influence on a fluvial regime.

- Double and single mud drapes on cross beds (Willis, 2005; van den Berg et al., 2007). Downdip, low-energy tidal bar complexes tend to be relatively finer-grained and contain higher abundances of mud drapes and mudstone rip-up clasts (Cheadle & McCrimmon, 1997).
- Inclined, heterolithic cross-stratification (IHS), common in channels in the fluvial-tidal transition zone (Thomas et al., 1987), in river-dominated channels (Smith et al., 2009, 2011; Sisulak & Dashtgard, 2012), mixed river and tidal channels (Smith, 1987, 1988; Thomas et al., 1987; Sisulak & Dashtgard, 2012; Johnson & Dashtgard, 2014) and tide-dominated channels (Choi et al., 2004; Dalrymple & Choi., 2007; Choi, 2010; Shiers et al., 2014). Finer deposits in IHS can be attributed to downstream fining in a reversing current in mixed tidal-fluvial settings (Johnson & Dashtgard, 2014). Rhythmic bedding (alternating sand-rich and mud-rich beds) and bundling of mud laminae on a mm to cm scale may be attributed to diurnal and semi-diurnal tidal changes (de Boer et al., 1989; Ainsworth & Walker, 1994; Choi et al., 2004; Dalrymple & Choi, 2007).

- 'Tidal bundles' in cross-stratified sets indicating increasing and waning tidal strength, formed in response to spring and neap tides (Collinson et al., 2006).
- Reactivation surfaces: erosional surfaces between cross-strata formed in response to current reversals and variations in flow strength (Collinson et al., 2006).
- Bi-directional current indicators, including herringbone cross bedding and current-ripple lamination (van den Berg et al., 2007; Collinson et al., 2006).
- Wavy, flaser and lenticular bedding indicative of repeatedly changing energy levels associated with flows of different strengths such that sand is moved and deposited during the flood or ebb tide, whereas mud is deposited from suspension during the turning of the tide (van den Berg et al., 2007).
- Synaeresis cracks, indicating fluctuating salinity levels (Burst, 1965; Pemberton & Wightman, 1992), with both saline and fresh water inputs to the system.
- Low diversity trace-fossil assemblages indicative of saline influence, e.g. Glossifungites and Skolithos ichnofacies (Pemberton & Wightman, 1992).

Tidal indicators have been identified in core, where available. Indicators present in the Mungaroo formation are: (i) single and paired mud/silt drapes on cross beds; (ii) His; (iii) wavy bedding and flaser bedding; (iv) ripple-laminated

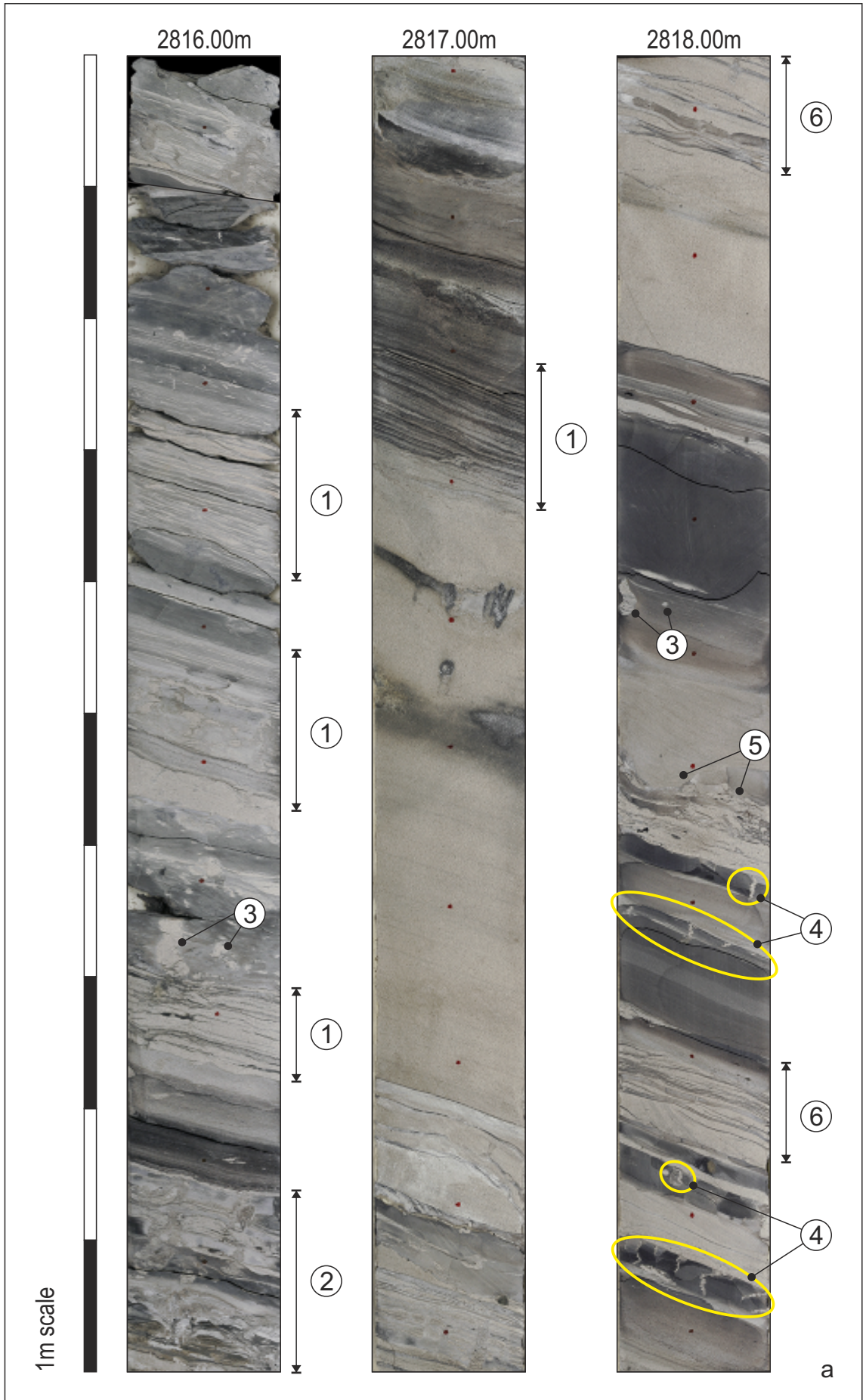
foresets indicative of possible current reversals; (v) syneresis cracks; (vi) trace fossil ichnofacies indicative of saline influence.

Figure 3.13 shows some of the more well-developed examples of some of the above features from Mungaroo Formation cores (Well-09), including sandy and mixed IHS, syneresis cracks, brackish water trace fossils, wavy-flaser bedding, paired and single mud drapes.

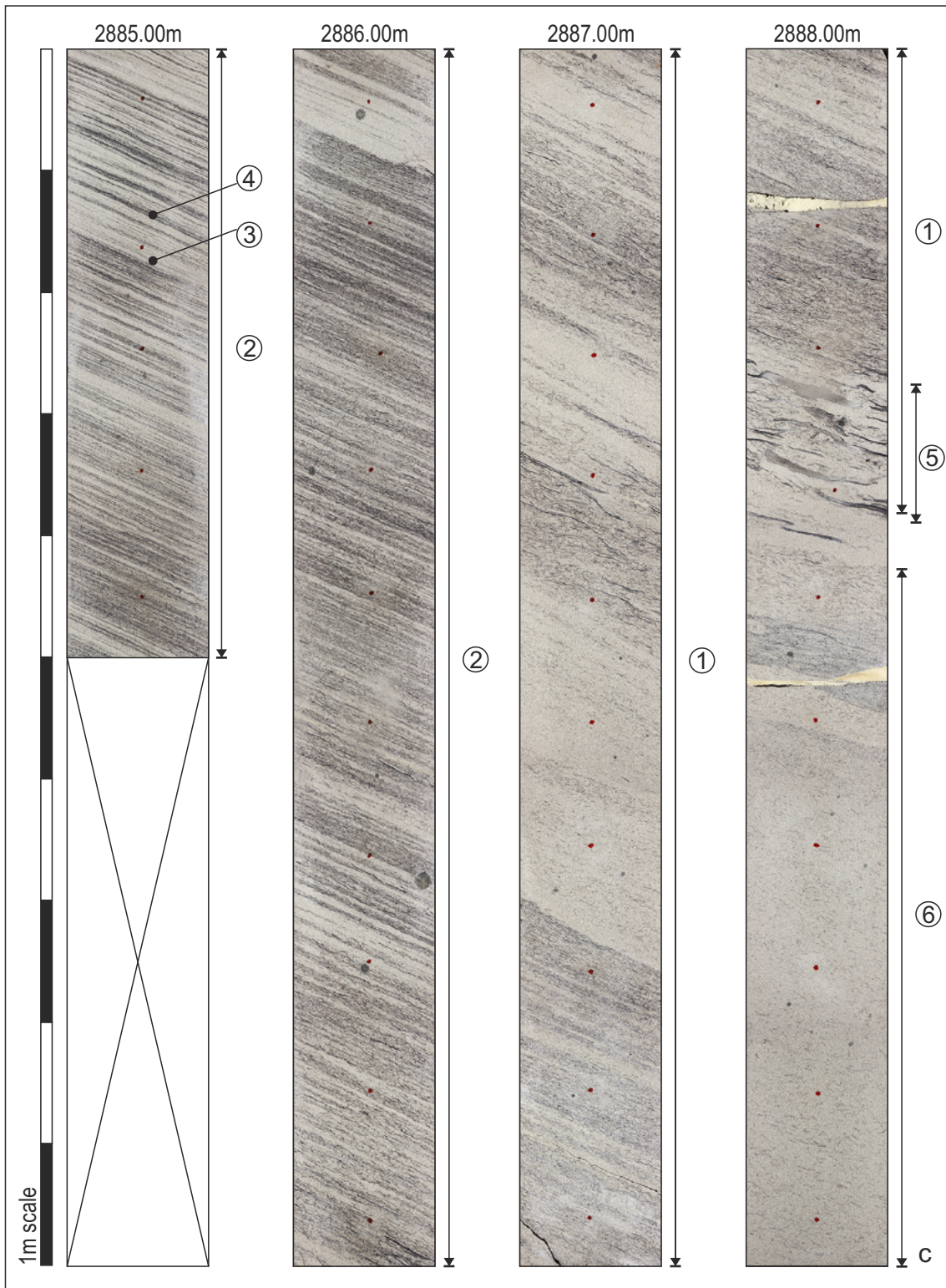
Limitations: Caution must be taken when inferring tidal influence from often subtle and cryptic sedimentary features, as many of them, taken on their own, can potentially be explained by other processes. For example: although mud drapes on cross beds are indicative of fluctuating current energy, they could be attributed to seasonal fluctuations in the flow regime (Jablonski & Dalrymple, 2014), rather than tidal fluctuations. As such, these structures are common in certain fluvial settings (e.g., Collinson et al., 2006). Wavy and lenticular bedding can also be attributed to seasonal discharge patterns (e.g., Cain and Mountney, 2009). Syneresis cracks can be confused with desiccation cracks. However given the dominantly poorly-drained floodplain facies of the Mungaroo Formation (which are dominated by gleysols, coals and floodplain-lake deposits), syneresis cracks are interpreted with high confidence where identified in core in this study.

Synthesis: The presence of syneresis cracks, together with brackish and marine ichnofauna within the Mungaroo Formation indicates that a marine-influenced setting was prevalent at times, lending confidence to interpretations of sedimentary features such as mud drapes as indicators of a tidally-influenced regime. Where subtle mud drapes and wavy bedding are present but not in association with bioturbated beds or syneresis cracks, this is interpreted as

Figure 3.13: Annotated photographs from the S6-S7 interval (Well-09) showing sedimentary features interpreted as tidal indicators. **a:** Mixed IHS deposits featuring: (1) single and double mud drapes; (2) convolute bedding due to dewatering; (3) trace fossils (probable *Teichichnus*); (4) synaeresis cracks; (5) ball and pillow structures; (6) flaser bedding. Interpreted as sharp-based mouth-bar deposits. **b:** Mixed IHS coset from the S6-S7 interval, featuring: (1) paired mud couplets; (2) tidal bundling of mud laminae; (3) IHS sets formed of alternating mud-prone and sand-prone subsets; (4) ripple laminations; (5) flaser bedding; (6) lenticular bedding, possible dewatering; (7) possible current reversals (NB broken core, so could have twisted to give this appearance). Probable tidal channel-bar deposits. **c:** Probable tidal channel-bar deposits from the S6-S7 interval: (1) Sandy IHS set grading vertically into mixed (2) IHS set with both single (3) and double (4) fine-grained laminae. In this case the fine-grained sediment is plant material fragments, possibly indicating a peat substrate on the floodplain. Lenticular/flaser bedding (5) is present at the base of the IHS coset. IHS channel-bar deposits underlain by very fine grained sandstone, indistinct bedding with scattered plant material fragments (6), possible low-energy channel deposit.







resulting either from seasonally fluctuating, or weakly tidally-influenced flow. Where IHS, paired mud drapes, syneresis cracks and wavy/flaser bedding are well-developed, a stronger tidal influence, in a more down-dip setting is interpreted.

3.7.2 Trace fossils and bioturbation

Trace fossils identified in the S2-S3 interval of the Mungaroo Formation are *Diplocraterion*, *Planolites*, *Chondrites*, *Zoophycos* and *Technichnus*, which are found primarily in bay-fill packages in the core, although they have also been identified in IHS, lake-fill and distal crevasse-splay deposits. *Diplocraterion* is part of the *Skolithos* and *Glossifungites* ichnofacies and can be found in a variety of depositional settings, in saline or brackish water. *Planolites*, *Chondrites*, *Zoophycos* and *Technichnus*, are found in brackish settings (Beynon & Pemberton, 1992) and in more marine settings.

Bioturbation records the deformation and reworking of the primary depositional fabric of sediments. The degree of reworking can be measured as a percentage of the original sediment, and presented as a bioturbation index value (Taylor and Goldring, 1993). Table 3.5 presents a summary of Taylor & Goldring's (1993) bioturbation index scheme.

Table 3.5: Bioturbation index (BI) describing the proportion of deformation and reworking of a sedimentary package by bioturbation. From Taylor and Goldring (1993).

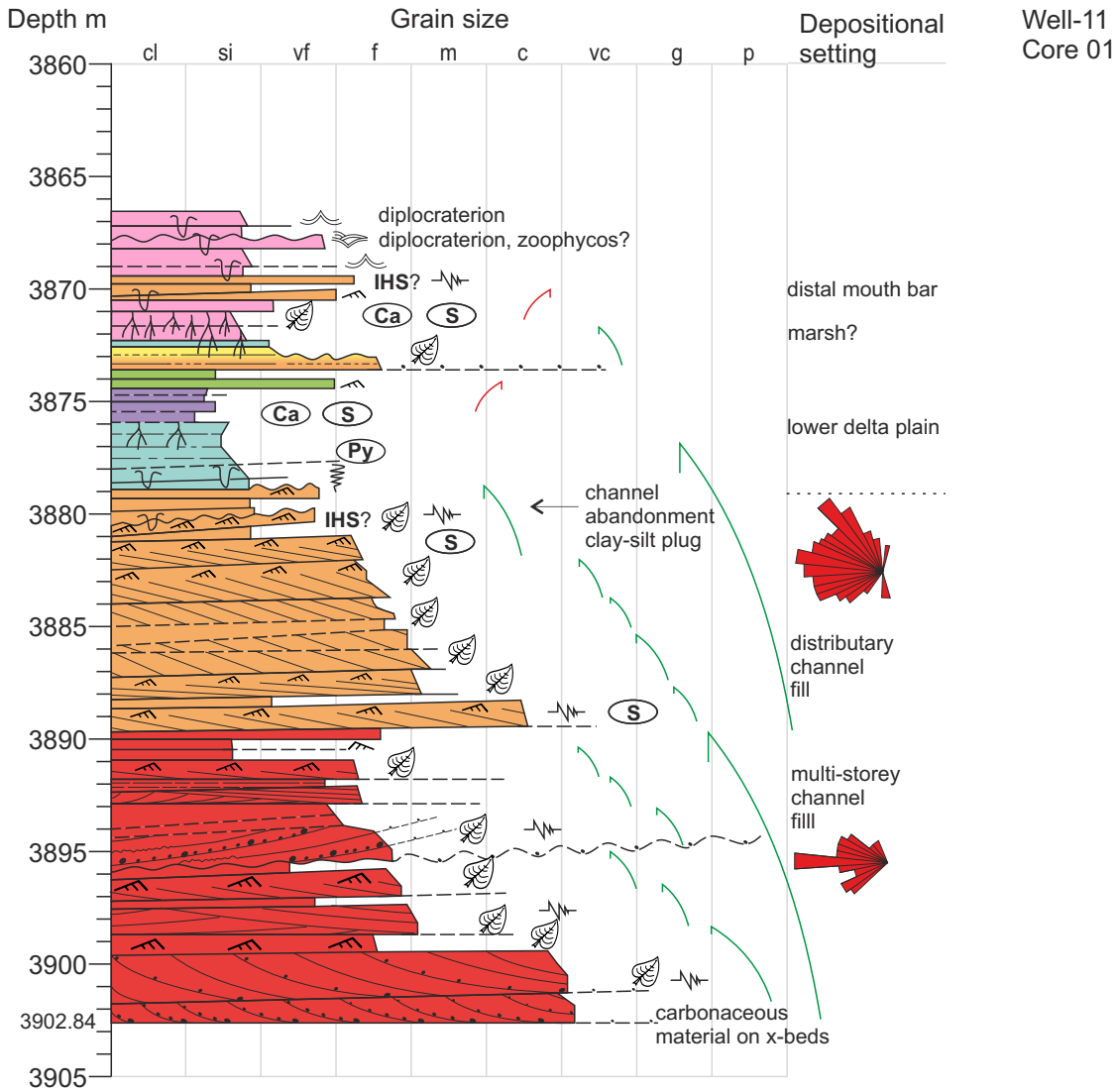
BI grade	Fraction bioturbated (%)	Description
0	0	No bioturbation
1	1-4	Sparse bioturbation: few discrete traces and/or escape structures.

BI grade	Fraction bioturbated (%)	Description
2	5-30	Low bioturbation: bedding distinct, low trace density, escape structures often common.
3	31-60	Moderate bioturbation: bedding boundaries sharp, traces discrete.
4	61-90	High bioturbation: bedding boundaries indistinct, high trace density with overlap common.
5	91-99	Intense bioturbation: bedding completely disturbed (just visible), limited reworking, later burrows discrete.
6	100	Complete bioturbation: sediment reworking due to repeated overprinting.

Bay-fill packages with very low diversity and a bioturbation index (BI) of 2-3 are typical of restricted, brackish bay settings (Pemberton & Wightman (1992) and are herein most readily attributed to facies association F7a. Bay-fill packages with higher diversity and moderate to intense bioturbation (BI 2-4 – typically grade 3 – at colonisation beds) are herein interpreted as bay settings with open access to marine water, examples of which can be seen in facies association F7b.

3.7.3 Interpreted logs

Graphic logs have been recorded for more than 250 m of succession from the Mungaroo Formation, encompassing 4 cores from well Well-11, which penetrates the TR21.1-TR22.2 (S2-S3) interval. Stacking patterns of lithofacies, additional sedimentary features (including tidal indicators such as paring and



Symbol key

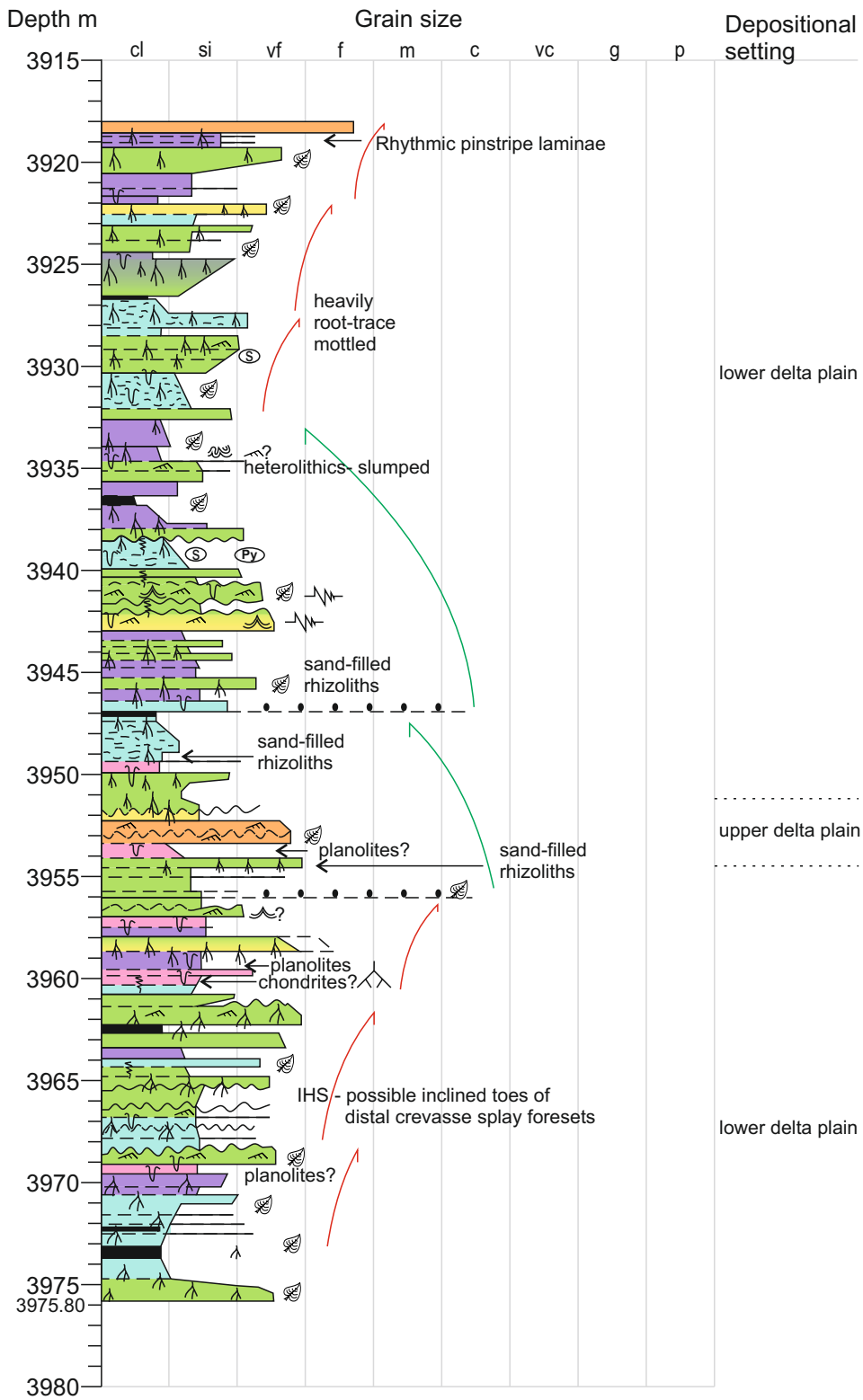
				c			
IHS inclined heterolithic x-stratification	Ca calcite cement	Py pyrite	S siderite				

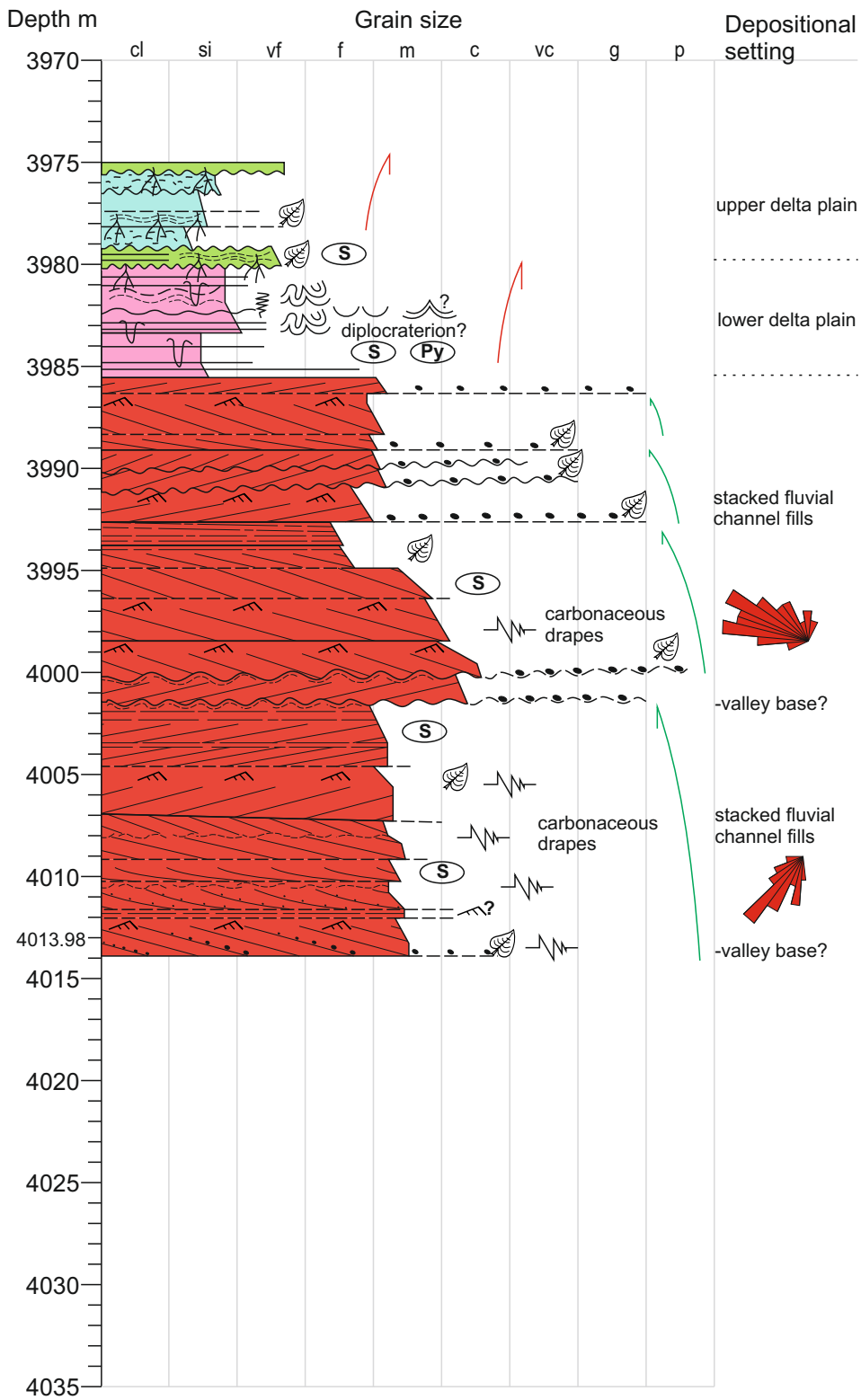
Lithofacies association

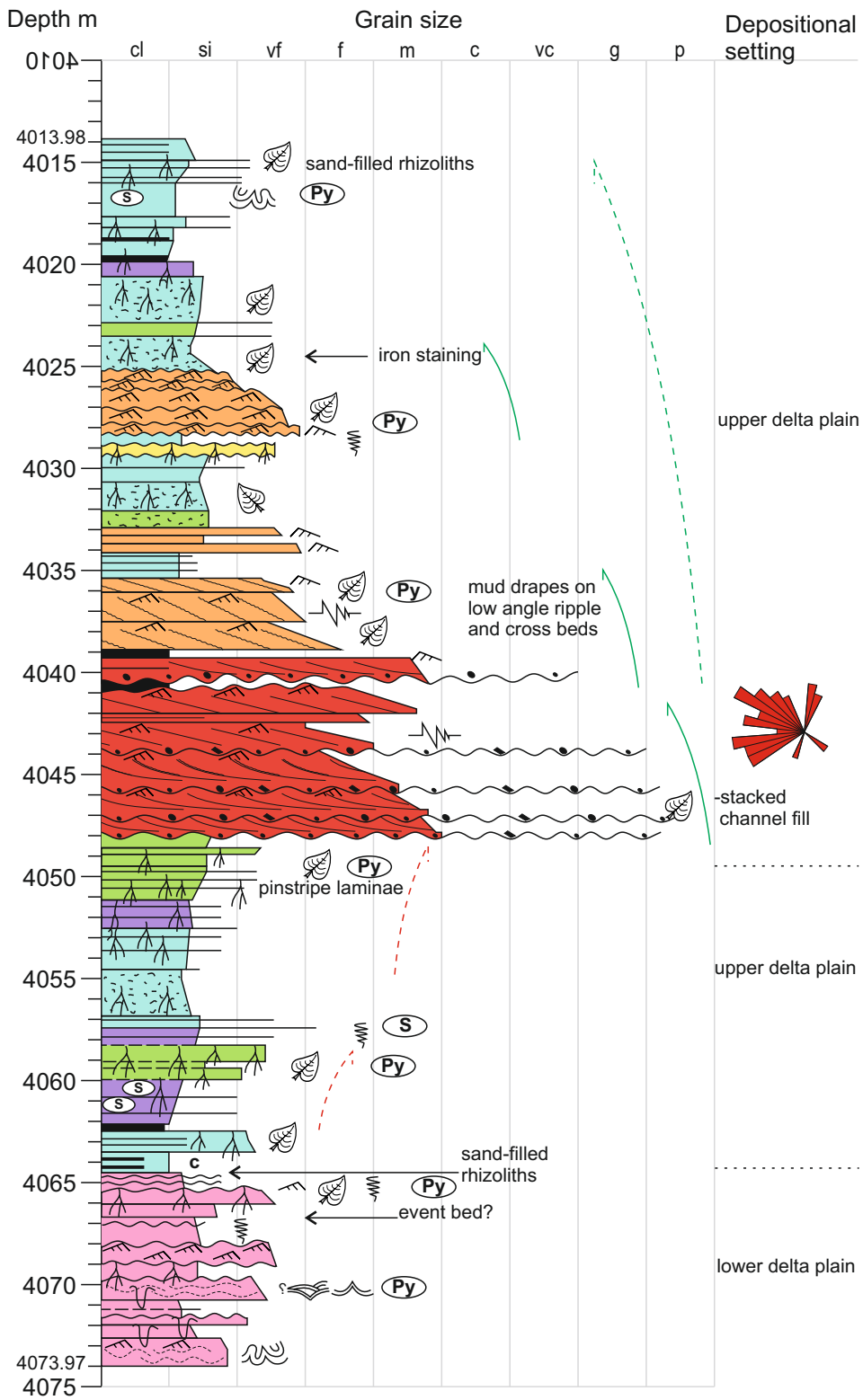
	High-energy channel		Gleysol
	Low-energy channel		Lake
	Proximal splay		Bay-fill
	Distal splay		Coal

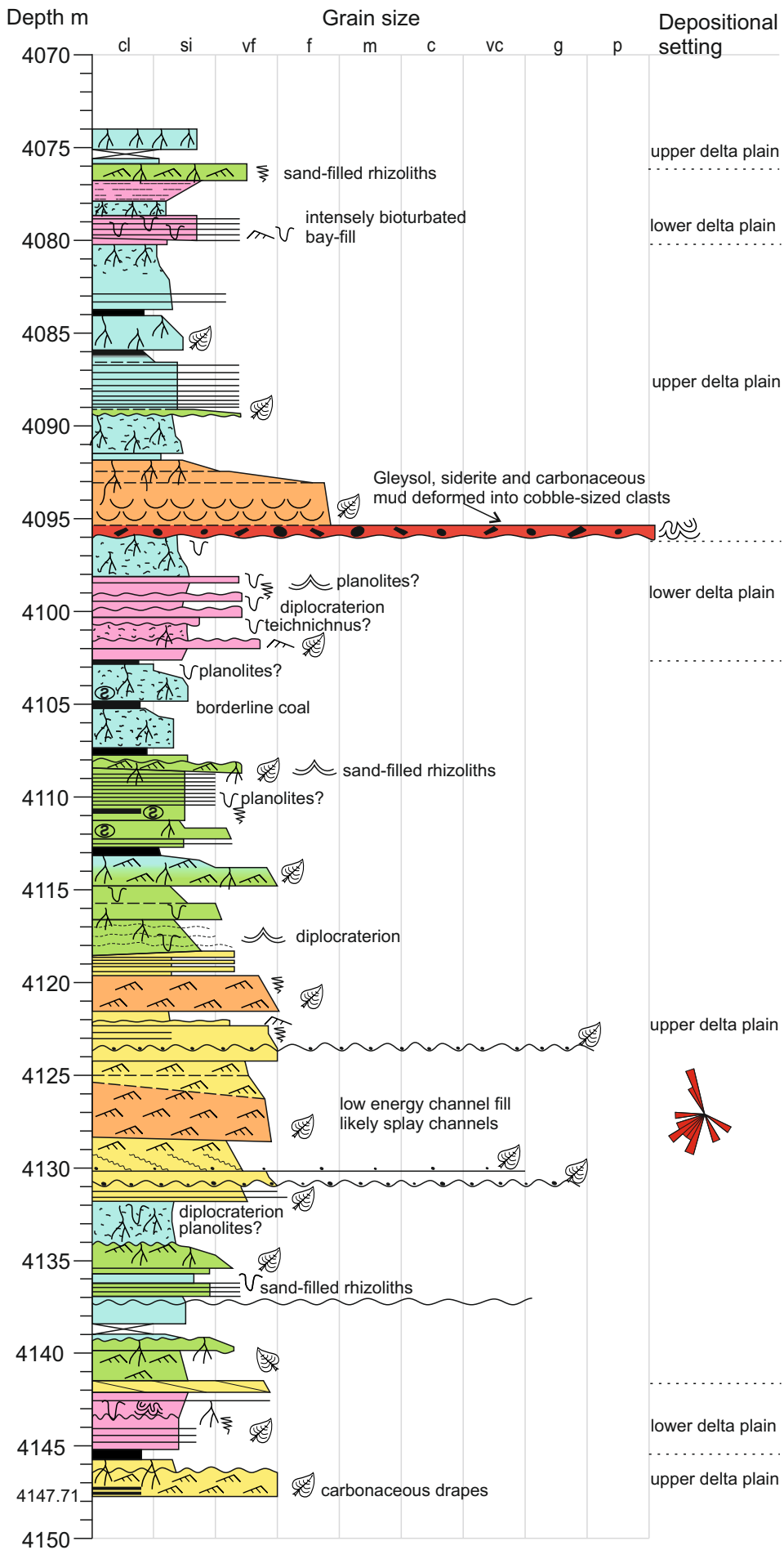
Figure 3.14: Graphic logs for the cored section of the Mungaroo Formation from Well-09/Noblige-2: **a.** core 1; **b.** core 2; **c.** core 3, part 1; **d.** core 3, part 2; **e.** core 4.

a









bundling of laminae), biogenic features (such as trace fossils) and fining or coarsening-up trends have been used to interpret facies associations and the larger scale depositional setting of discernable intervals. Figures 3.14a-3.14e show the interpreted core logs. For reference, Appendix 2 shows the core photos for the well used in this study (Well-11), with the interpreted lithofacies noted (same key as core graphic logs).

3.7.4 Facies association proportions within the logged section of the Mungaroo Formation

Facies associations proportions have been calculated in the S2-S3 interval from logged thickness (Figure 3.15a). Thirty per cent of the logged formation is classified as channelized deposits (Figure 3.15b), of which 63% are high-energy channel deposits (lithofacies association F1) from primary and secondary fluvial and distributary channels. Thirty-seven per cent of channelized deposits are low-energy channel deposits (lithofacies association F2), attributed to distributary and crevasse splay channels. Seventy per cent of the logged formation is classified as non-channelized (lithofacies associations F3 to F7). Figure 3.15b gives a breakdown of facies associations present in the non-channelized portion. Of the strata represented by non-channelized facies associations, only proximal crevasse splay deposits (F1, 8%) and, less frequently, bay-fill heterolithics (F7, 17%) are sand-prone; the remaining 75% of the non-channelized facies associations consist of silt-prone to mud-prone lithofacies.

3.7.5 Depositional setting

The general and regional depositional setting has been interpreted for large (metre to tens of metres scale) stacked units of interpreted facies associations,

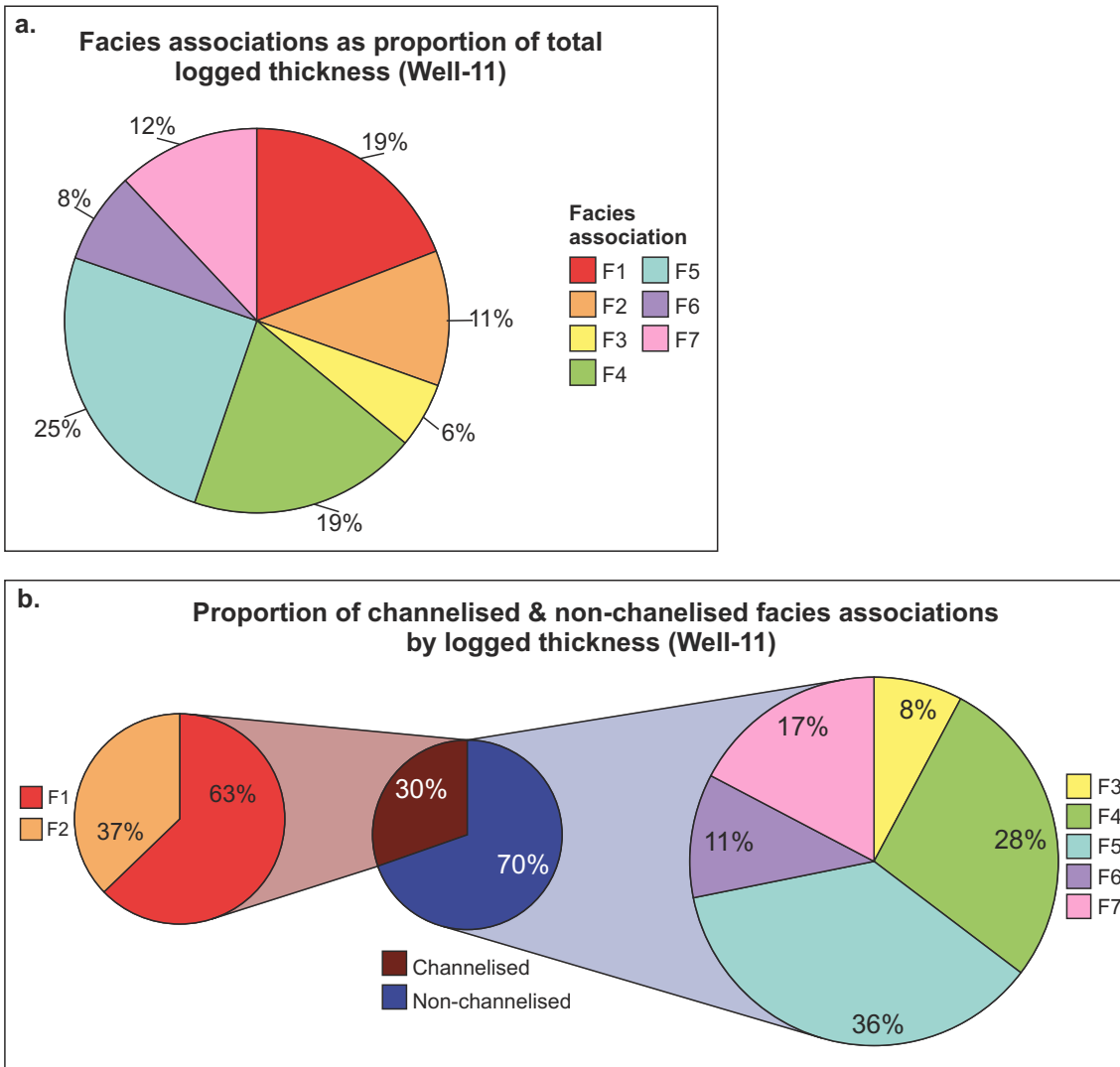


Figure 3.15a: Facies association proportions calculated from logged thickness (Well-11). **b:** Proportion of channelised and non-channelised elements and their constituent facies associations, as measured from logged thickness.

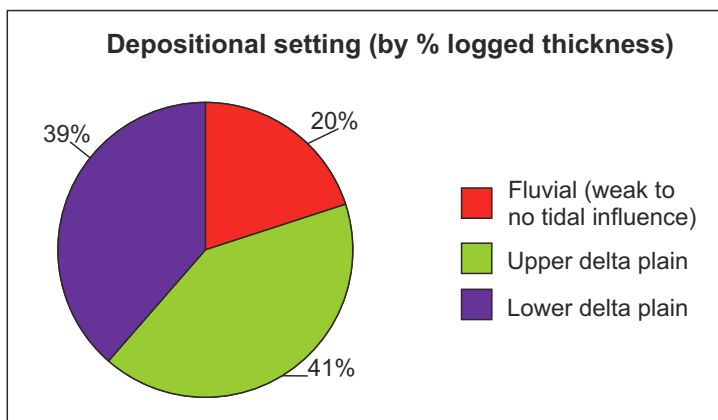


Figure 3.16: Proportions of the cored Mungaro Formation assigned to fluvial, upper delta plain and lower delta plain settings, as calculated from logged thickness.

and split into three broad classes: fluvial channel fill, upper delta plain and lower delta plain.

Eighty per cent of the deposits within the S2-S3 logged section are interpreted as deltaic (Figure 3.16): 41% upper delta plain, with more sand-prone successions of crevasse splays, minor channels and soils; 39% lower delta plain with more silt-prone successions of distal splays, swamps, lakes and bay-fill. The remaining 20% of the logged section comprised stacked fluvial channel fill, representing valley fill and stacked channel belts (cf. Holbrook, 2001). Weak tidal influence is inferred in the S2-S3 channel fill from the presence of mud drapes along cross-beds, as well as some (tentatively interpreted) bundling of laminae. The tidal indicators within the channel deposits are weak and poorly-developed: Although varying flow is indicated by mud drapes and IHS, the majority of interpreted 'tidally-influenced' channel deposits do not show evidence of current reversals, thus are interpreted as the deposits of a fluvially-dominated, rather than tidally-influenced system. This indicates a very weak (if any) tidal influence (cf. Johnson & Dashtgard, 2014; Jablonski & Dalrymple, 2014). More deltaic-influenced and more fluvially-influenced intervals can be inferred from their constituent facies association. Figure 3.17 illustrates the proportions of infill by each facies associations, for fluvial channel fill, upper-delta-plain and lower-delta-plain settings. The facies association proportions demonstrate how depositional setting influences reservoir distribution and preserved deposits: without considering the large-scale, multi-storey channel belt and valley deposits, of which all facies associations are sand-prone, 30% of upper-delta-plain deposits are sand prone (F1, F2 and F3), whereas only 4% of lower-delta-plain deposits (F2 and F3) are sand prone.

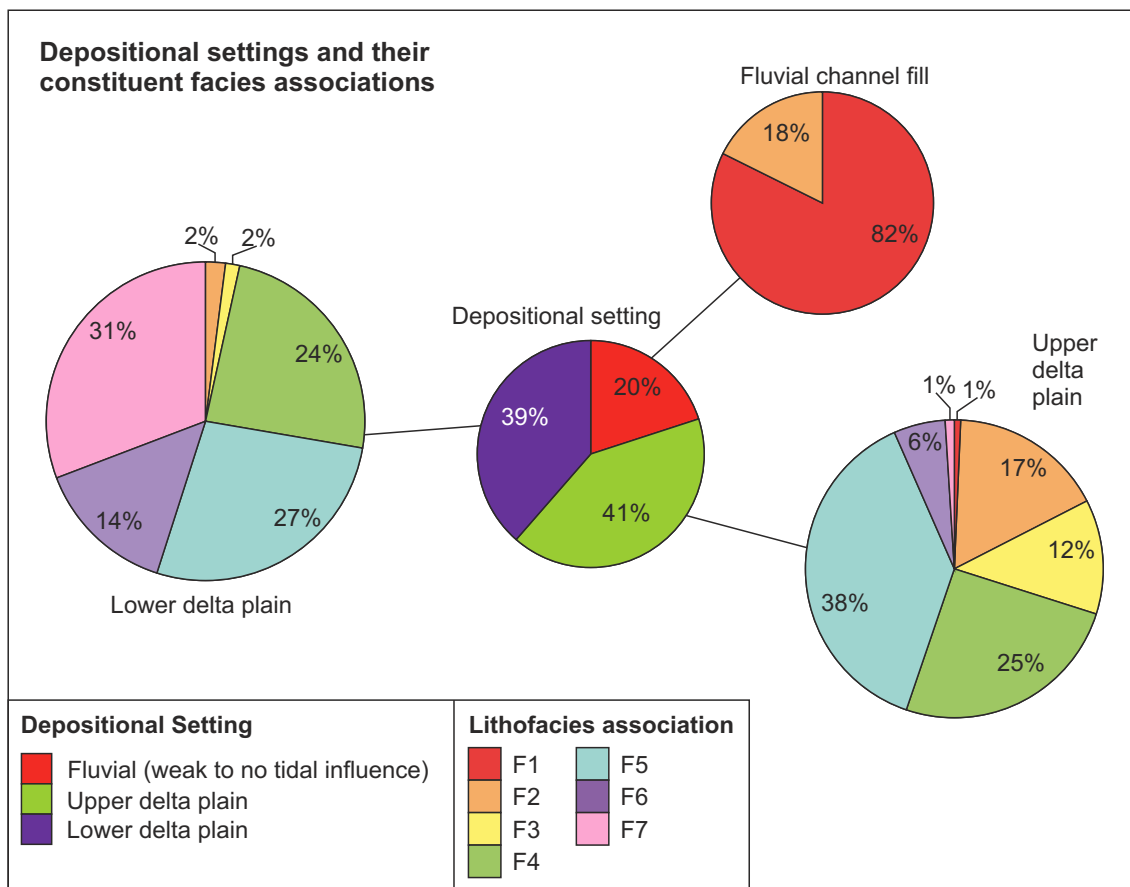


Figure 3.17: Illustrating the contrasting proportions of infill by each facies association (measured by logged thickness) within the three broad depositional settings of fluvial channel fill, upper delta plain and lower delta plain.

Previous studies of the Mungaroo Formation (Adamson et al., 2013; Payenberg et al., 2013) interpret the Mungaroo Formation as dominantly deltaic. Adamson et al. (2013) in particular cite evidence for tidal influence on the fluvial deposits. Within this study, although some overbank-dominated intervals (particularly bay-fill) indicate a marine or tidal influence, possible tidal features in channelized deposits are typically subtle or cryptic, with channel deposits indicating a unidirectional, episodically fluctuating flow. These deposits were likely formed in the innermost (up-dip) part of the fluvial-to-marine transition zone, in a fluvially-dominated, weakly tidally influenced setting. Figure 3.18 attempts to place the Mungaroo within the fluvial-tidal transition, in a fluvially-dominated, tidally influenced, fresh-to-brackish water setting. The broad range given for the Mungaroo Formation within the tidal-fluvia transition is because the studied interval spans a period over which the shoreline likely transgressed and retrograded many tens if not hundreds of km. As such, the position on the depositional profile shown in Figure 3.18 would have varied considerably for different intervals.

3.8 Palaeocurrent analysis

3.8.1 Channel complex paleocurrent readings

Dip logs (measuring dip azimuth of cross-beds, calibrated with image logs) were available for the channel deposits with well-developed cross-beds, and were used to infer palaeocurrent direction. Summary rose plots are presented on the graphic logs (Figure 3.14). The rose plots reveal localised variations in palaeocurrent directions and therefore fluvial style within the logged section. A wider spread of palaeocurrent directions indicates a more sinuous channel,

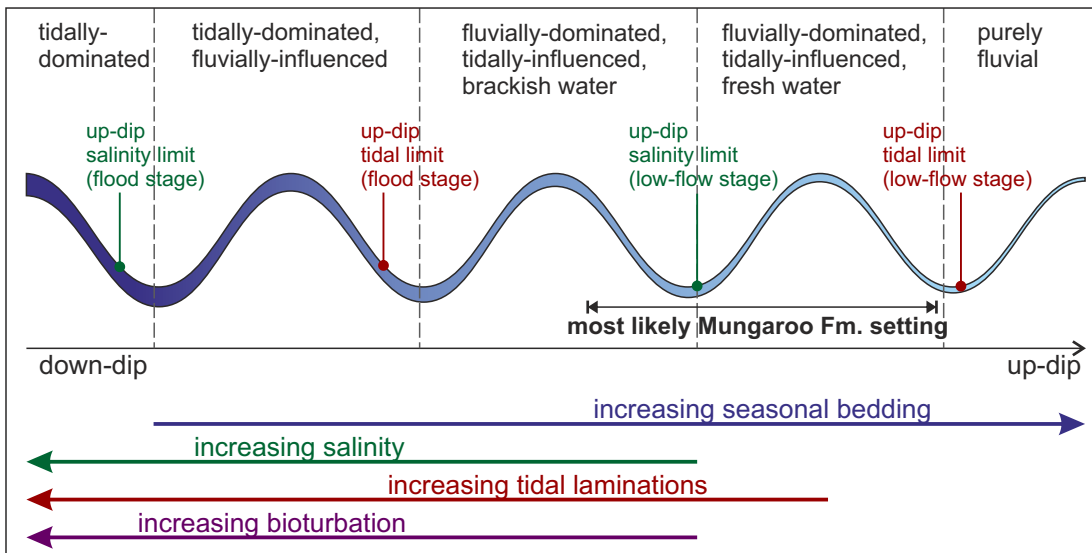


Figure 3.18: Schematic diagram illustrating the tidal-fluvial transition (Modified after Martinus & Gowland, 2013 and Jablonski & Dalrymple, 2014), illustrating the variation of depositional structures (seasonal bedding, tidal laminations, bioturbation) and conditions (salinity) resulting from varying tidal and fluvial influences.

likely with both downstream and laterally migrating bedforms. A narrower range of palaeocurrent directions is interpreted as relating to lower sinuosity channels, with dominantly downstream migrating bedforms. Similar patterns were identified for the Mungaroo Formation by Adamson et al. (2013), who report that palaeocurrents interpreted from image logs and core are consistent with the orientation of large channel and channel belt geobodies identified using seismic data, favouring an interpretation of predominantly downstream-migrating bedforms. Bal et al. (2002) similarly utilised image logs and core, and found that most bar-forms interpreted in their study of the Mungaroo Formation were downstream-accreting.

Channel complex 1 (3881.40 - 3889.75 m): This complex has an 8.35 m succession of stacked low-energy channel deposits (Figure 3.14a). Modal paleocurrent direction is 280° (west) with a palaeocurrent range of 195° (80 readings were taken from image logs). The wide spread of palaeocurrents indicates a relatively sinuous channel system, with downstream and laterally migrating bedforms.

Channel complex 2 (3889.75 – 3902.84 m): This complex comprises 13.09 m of stacked, high-energy fluvial channel deposits (Figure 3.14a), with a modal palaeocurrent direction of 270° (west), and a 110° spread of palaeocurrents (44 readings were taken). There is a much stronger trend of readings taken due west, with fewer readings taken to the southwest and northwest. The spread of readings indicates relatively low-sinuosity channels, with predominantly downstream migrating bedforms.

Channel complex 3 (3985.48 – 4001.50 m): This channel complex comprises 16.02 m of stacked, high-energy fluvial channel deposits (Figure 14c), with a

modal palaeocurrent direction of 290° (WNW) and a 140° spread of palaeocurrents. The majority of palaeocurrent readings are between 275° and 310°, with a weakly developed bi-directionality at 280° and 300° (74 readings were taken). The palaeocurrent distribution indicates a low-sinuosity channel system with predominantly downstream migrating bedforms.

Channel complex 4 (4001.50 – 4013.98 m): This channel complex is amalgamated with channel complex 3 and comprises 12.48 m of stacked, high-energy fluvial channel deposits with a modal palaeocurrent of 220° (southwest), and a palaeocurrent spread of 90° (55 readings were taken). These deposits likely represent a low-sinuosity channel system with predominantly downstream migrating bedforms.

Channel complex 3 and 4 jointly comprise 28.5 m of stacked fluvial deposits. Given the thickness and relatively coarse-grained nature of the deposits (medium to coarse grained), they are likely stacked valley deposits. The change in palaeocurrent direction from southwest in the lower part of the valley fill towards the WNW in the upper part is interpreted as recording an avulsion event, re-orienting the valley to the northwest.

Channel complex 5 (4039.25 – 4048.35 m): This channel complex comprises 9.10 m of stacked, high-energy channel deposits (Figure 3.14d), with a modal palaeocurrent direction of 290° and a spread of 260° (51 readings were taken). The palaeocurrent appears bi- or possibly tri-directional, with trends towards the southwest, northwest, and a (tentative) minor trend to the northeast. This channel complex was likely deposited by a moderately sinuous channel system, with a combination of downstream and laterally migrating bedforms.

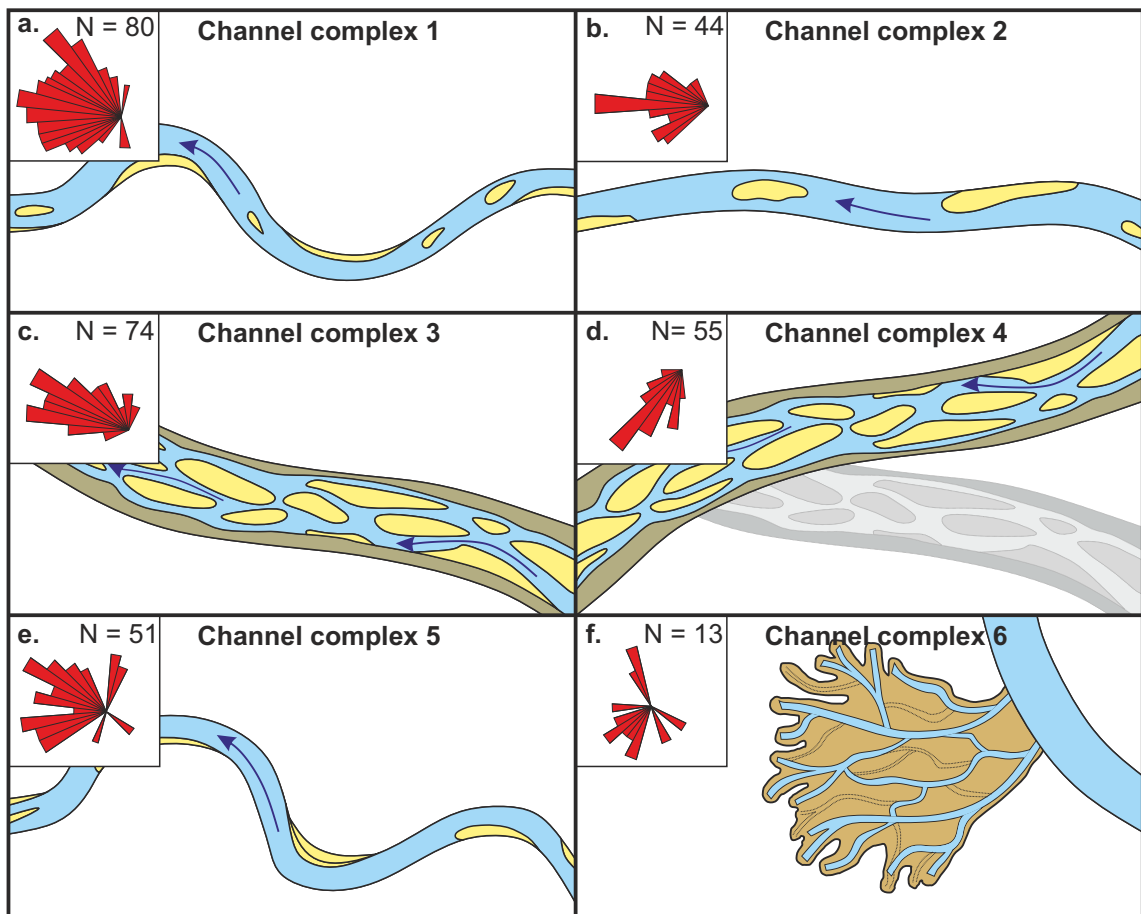


Figure 3.19: Summary rose plots and sketch models of fluvial style for 6 channel complexes identified in core from the Mungaroo Formation. **a:** Channel complex 1 fluvial style is interpreted as moderate sinuosity channel with both laterally and downstream migrating bedforms. Paleoflow is to the west. **b:** Channel complex 2 fluvial style is interpreted as a low sinuosity channel with downstream migrating bedforms. Paleoflow is to the west. **c:** Channel complex 3 fluvial style is interpreted as low sinuosity-braided, with downstream migrating bedforms. Paleoflow is to the northwest. **d:** Channel complex 4 is interpreted is shown as analogous to that of complex 3, and is interpreted as forming a stacked, multi-valley fill, amalgamated with that of complex 3. Complex 4 is shown as a braided valley deposit overlying that of complex 3, following an avulsion. **e:** Channel complex 5 fluvial style is interpreted as moderate sinuosity with predominantly laterally migrating bedforms. **f:** The range of paleocurrent orientations can be explained by this small channel deposit's location within crevasse splay deposits. The channel deposits are interpreted as very low energy crevasse channel sands.

Channel complex 6 (4125.80 – 4131.20 m): These deposits are interpreted as 5.40 m of low-energy, crevasse splay channel deposits (Figure 3.14d), with a modal palaeoflow of 230° and a spread of 230° (13 readings were taken). Palaeocurrent appears tri-directional, with trends to the southeast, southwest and northwest, although the uneven spread of palaeocurrents could be biased and due to the relatively small sample size in this bed (13 cross-bed dip readings). These deposits are likely from stacked crevasse channels with multiple nodal avulsions within a crevasse delta with low-moderate sinuosity, low-energy crevasse splay channel deposits.

3.8.2 Fluvial style summary

The cored section of the Mungaroo Formation, although representing only a small portion (stratigraphically limited section) of the extensive Mungaroo Formation, exhibits considerable variability in fluvial style as is inferred from paleocurrent data. Low, moderate and high-sinuosity channels are present, with both laterally migrating and downstream migrating bedforms preserved. There is an apparent tendency towards lower sinuosity in high-energy channel deposits (channel complexes 2-4), and higher sinuosity in lower energy deposits (channel complexes 1 and 6). Figure 3.19 summarises the palaeocurrent trends and inferred fluvial styles responsible for each of the above channel complexes.

3.9 Chapter summary

- The Mungaroo Formation is characterised by a mixed fluvio-deltaic succession. The distribution of lithofacies and facies associations within the formation demonstrates systematic and predictable transitions from more fluvial-dominated to more deltaic-dominated episodes of accumulation.

- Sixteen distinctive lithofacies identified within the Mungaroo Formation can be used to interpret seven discreet facies associations, the proportions and vertical stacking patterns of which can be used to distinguish depositional settings such that fluvial-channel, upper-delta-plain and lower-delta plain-settings are each identified.
- Tidal influence has been interpreted in some sections of the Formation, as evidenced by (i) single and paired mud/silt drapes on cross beds; (ii) His; (iii) wavy bedding and flaser bedding; (iv) ripple-laminated foresets indicative of possible current reversals; (v) synaeresis cracks; (vi) trace fossil ichnofacies indicative of saline influence.
- In addition to the ability to recognise switches between relatively more and less deltaic-influenced settings, the lithofacies analysis undertaken within this study has enabled several alternations in fluvial style to be recognised within the deposits of the Mungaroo Formation. Identified fluvial styles include: relatively more sinuous channel bodies characterised by deposits arising from lateral (and downstream) migrating bedforms; relatively less sinuous channel bodies characterised by deposits arising from downstream migrating bedforms. The formation also records at least one major avulsion of a fluvial valley system.
- The core sections studied in this chapter demonstrate that the formation exhibits many small-scale changes in depositional style, many of which, at a scale less than 10 m, are unlikely to be resolvable on seismic data. Chapters 5 and 6 investigate larger-scale depositional styles of the Mungaroo Formation, over a larger stratigraphic extent, utilising a combination of seismic and well-data analysis.

Chapter 4 Seismic geomorphology and sedimentology of fluvial environments in the subsurface: fluvio-deltaic Triassic Mungaroo Formation, North West Shelf, Australia

Research question: What are the broad variations in depositional environment at key intervals of the Mungaroo Formation? Can seismic facies be used to distinguish between fluvial and fluvio-deltaic deposits?

4.1 Chapter Overview

Fluvial and fluvio-deltaic successions of the Late Triassic Mungaroo Formation accumulated in a long-term transgressive system tract. The formation represents the principal reservoir for a major gas play offshore northwest Australia, the key reservoir characterization challenge for which is to better understand the style and distribution of sand-prone channelized depositional elements. This study addresses this challenge by mapping architectural bodies within a high-resolution 3D seismic volume from the Exmouth Plateau of the Northern Carnarvon Basin. Interpretations of the palaeoenvironmental significance of these bodies are supported by analyses of lithofacies observed in core and wireline data. Specific objectives of this study are to: (i) catalogue sub-seismic-scale fluvial and deltaic architectural elements in core and wireline log data; (ii) map the plan-form morphology of seismic-scale fluvio-deltaic elements; (iii) classify key stratigraphic intervals according to their accommodation setting; (iv) match the studied intervals to likely modern analogues for the purpose of characterizing palaeoenvironments.

Seven sub-seismic-scale architectural elements are identified in core: primary (high-energy) channel, low-energy channel, proximal crevasse splay, distal

crevasse splay, gleysol (swamp), lake, and inter-distributary bay. Flattening the seismic cube on key horizons has enabled visualization of stratally-aligned slices, within which identified architectural element types have been mapped; attribute analysis highlights fluvial elements. Valley and channel belt, valley margin, floodplain, and gleysol (mire) seismic elements were identified and mapped in GIS. Analyses of well-log data confirm that valley-margin elements contain sub-seismic scale sand-prone intervals of probable crevasse-splay and accessory channel origin.

The dimensions of seismic elements are used to assess likely accommodation conditions within which the systems accumulated for different stratigraphic intervals. Apparently higher-accommodation settings led to the progressive fill of multi-lateral channel and valley elements (<7 km width), as well as the establishment of distributary channel networks and widespread gleysol development. Low-accommodation settings resulted in laterally constrained (<1 km width) channel elements that potentially accumulated within incised valleys, with associated valley-margin elements. Settings that experienced negligible rates of accommodation generation are characterized by a complex mosaic of overprinted channel elements and only minimal preservation of overbank elements.

4.2 Introduction

4.2.1 Project background

Detailed reconstruction of fluvial palaeoenvironments using datasets derived solely from subsurface settings is challenging using relatively low-resolution of subsurface seismic data (10-30 m vertical resolution) to discern the shapes of architectural bodies. Although any accompanying well data are of relatively high

resolution, they are essentially one dimensional in form, are generally (sub) vertical and reveal little about the shapes of geo-bodies (architectural elements) which are known to vary predictably according to the preserved geomorphic form represented by the preserved fluvial succession (cf. Bridge 2003; Miall 1996). This is especially the case in subsurface regions for which the number of wells is small and/or the spacing between individual wells is large (Gundesø & Egeland, 1990; Pranter et al, 2007).

Reconstruction of complex fluvial palaeoenvironments in the subsurface usually requires adoption of a holistic approach that incorporates a varied range of subsurface data types (Leeder, 1993). Such interpretations typically also draw comparisons with modern and ancient analogues, to support inferences made regarding the likely dimensions of the various architectural elements present and the geometrical relationships between these elements. However, the choice of appropriate analogues is notoriously problematic because successions that appear similar in their vertical profiles commonly exhibit marked differences in terms of the three-dimensional arrangement of their geobodies (Alexander, 1993). Thus, there exists a need to glean as much detailed information as possible from seismic data to better quantify geometrical relationships between geobodies.

Since the early 2000s a growing trend has emerged in hydrocarbon exploration relating to the recognition of smaller 'thin-bed pay' targets, especially in maturing hydrocarbon provinces where most of the larger 'primary' reservoir targets have been identified (Zhu et al., 2014). For example, Cuba et al (2013) assess point-bar, crevasse-channel, and crevasse-splay deposits from a tight gas reservoir perspective. In fluvial environments, this philosophy extends to the recognition of

minor distributive channel and crevasse-splay complexes, the deposits of which are typically well below seismic resolution (Bridge & Tye, 2000; Ethridge & Schumm, 2007). Given the wide spacing of well data and the relatively low average width of minor distributive channels, these bodies are rarely intersected by exploration wells, and may be overlooked where intersected due to their thin nature (Klein, 1996). However, secondary and tertiary channel bodies and crevasse-splay networks can form a significant proportion of the sand content of some fluvial systems, for example the Permian Rangal Coal Measures (Fielding et al, 2003; Stuart et al, 2014) of Queensland, Australia and the Westphalian Coal Measures of England (Fielding, 1986). Such systems are being increasingly targeted for hydrocarbon exploration and CO₂ sequestration, with research into both modern and ancient analogues having been undertaken by Donselaar et al (2011), Blowles & Moslow (1999). One such example is the Oligocene Frio Formation which hosts the Seeligson Field, Texas (Ambrose et al, 2008). A thorough understanding of the relationships known to occur between primary channel elements, minor channel elements and their relationship to the surrounding overbank must be applied to identifiable subsurface data to reduce uncertainty range and enable properties to be extrapolated from well control, lending increased accuracy to the interpretation of the precise depositional setting of such accumulations. In turn, this results in the development of more realistic and higher-resolution reservoir models.

The aim of this study is to demonstrate how a combination of seismic and well data can be used to define the sedimentology and geomorphology of a complex fluvio-deltaic succession (the Triassic Mungaroo Formation) known only from the subsurface and to show how the developed workflow can be applied to other

similar datasets. Detailed, core-based sedimentological and stratigraphic analysis are needed as they aid in the understanding of sub-seismic details of the depositional system of interest. Specific objectives of this investigation are as follows: (i) to describe the sub-seismic scale sedimentology of the fluvial and fluvio-deltaic deposits through assignment of a lithofacies scheme based on available well data (ii) to develop a seismic element scheme which incorporates both seismic facies response and seismic geomorphology, integrating well data where available; (iii) to apply the seismic element scheme to map out seismic-scale fluvial and fluvio-deltaic deposits in three key intervals; (iv) to use the seismic element maps to assess the depositional setting at each of the key intervals and to account for the depositional style in terms of accommodation setting.

The principal results of this study are novel, timely, significant and of broad appeal to those working on subsurface characterization more generally for the following reasons: (i) the exceptionally high-quality seismic dataset enables visualisation of fluvial deposits even at depths of several kilometres; (ii) the workflow employed sets out a method for fast, efficient screening of large datasets to highlight stratally-aligned deposits; (iii) the generally applicable method demonstrates how geomorphology and sedimentology can be efficiently combined to allow interpretation of depositional environments to a greater level of detail than has traditionally been possible.

4.3 Study area and data

The study focuses on a 3D seismic data cube (Colmbard) from a 3000 km² area of the Woodside operated block WA-404-P, situated on the Exmouth Plateau, in the Northern Carnarvon Basin (Figure 4.1). A succession of the fluvial-deltaic Mungaroo Formation (>1 km thickness) is covered by the dataset. Supporting data in the form of wireline logs from 11 wells within the block, as well as core from one well were analysed. Figure 4.2 depicts a typical expression of one of the interpreted horizons from the Colmbard dataset, and shows the locations of the wells. The core data presented in Chapter 3 covers the entire S2-S3 interval. Core data illustrating tidal-fluvial point bar deposits (Figure 3.12) are from the S6-D7 interval. As such, the seismic data covers a greater stratigraphic range than the core data. Wireline log facies and seismic facies are therefore used to link the wider Mungaroo Formation geology to the deposits encountered in the S2-S3 and S6-S7 core.

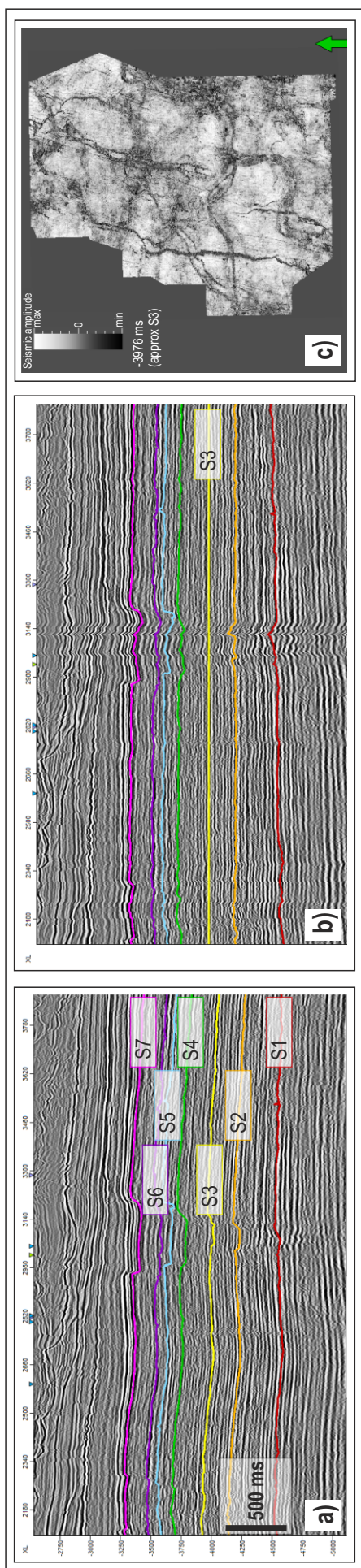


Figure 4.6: Workflow for viewing stratal slices. The volume (in depth domain, (a)) is flattened on key stratal surfaces (b). The resulting flattened volume allows visualisation of stratal slices (c), capturing the fluvial deposits of the Mungaroo Fm.

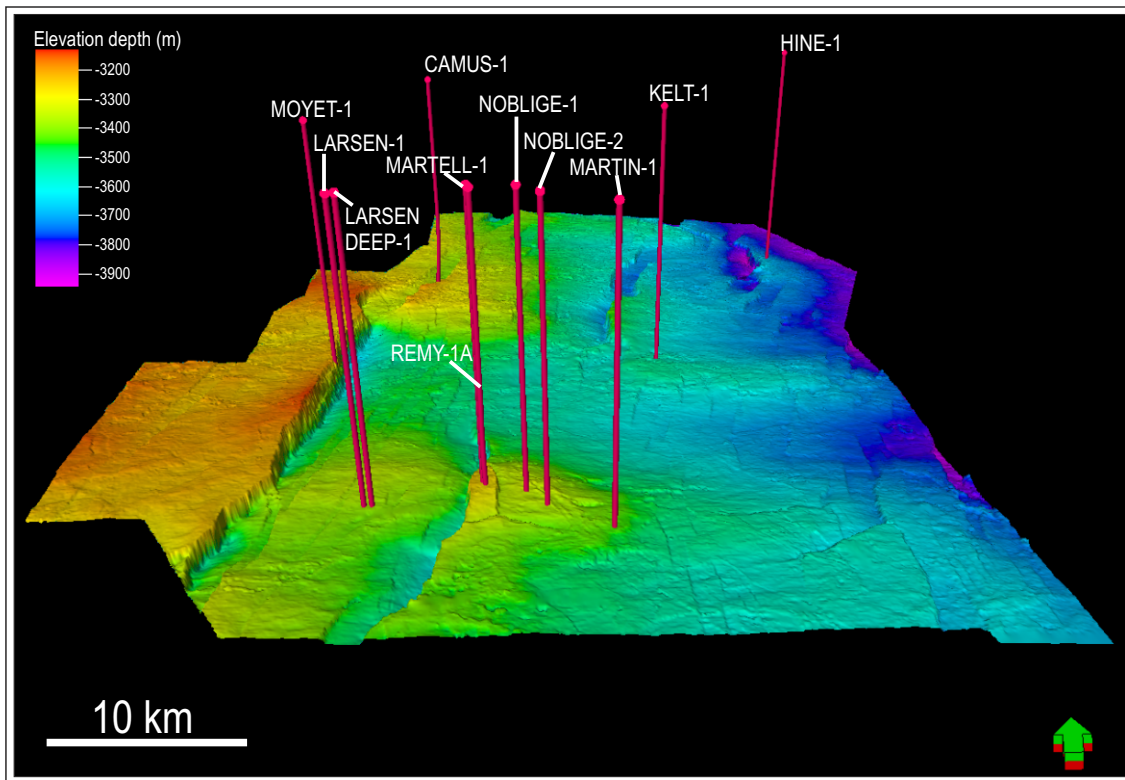


Figure 4.2: Depth map from within the Colmbard dataset, showing the locations of 11 wells with Triassic penetrations.

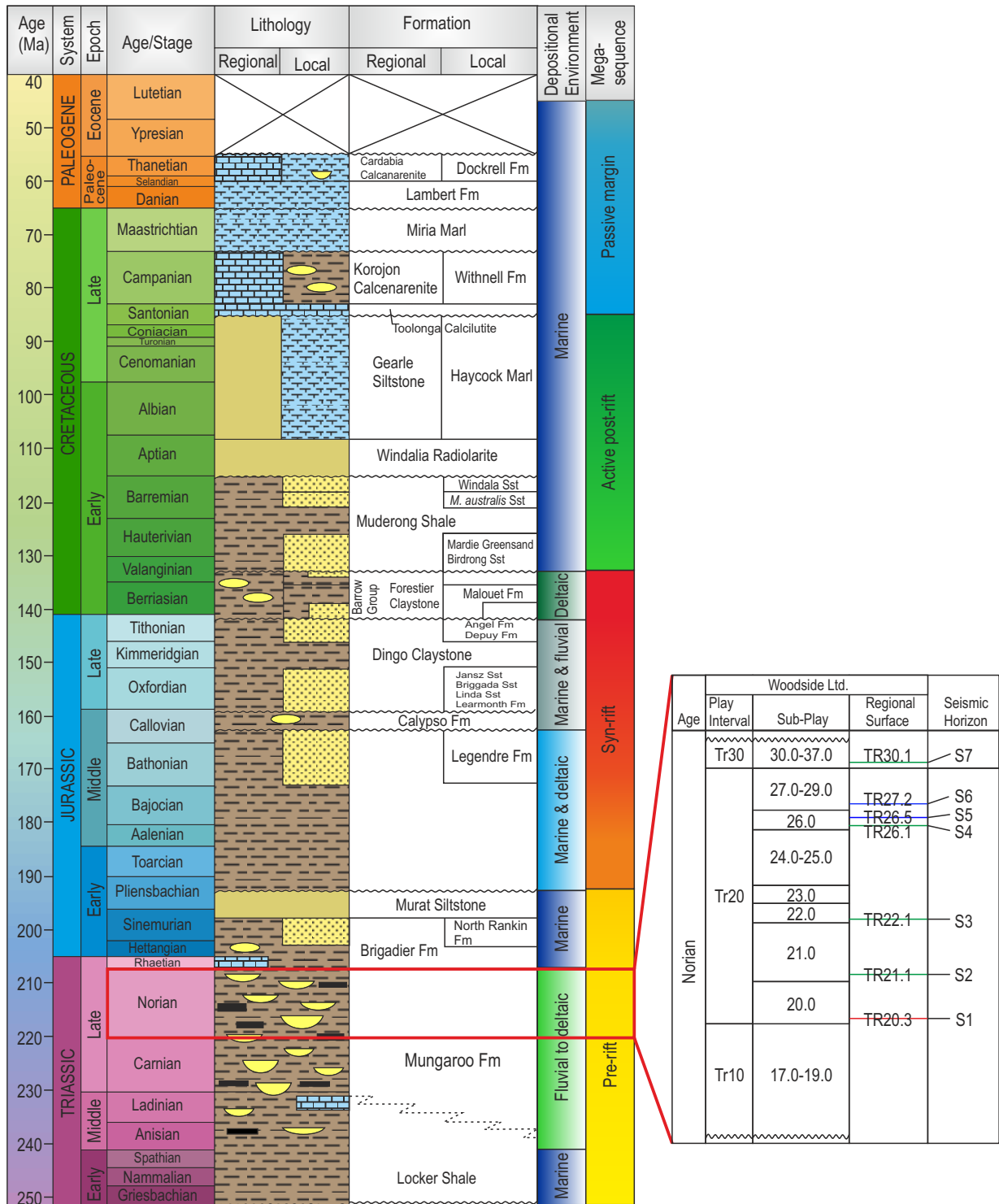


Figure 4.3: Stratigraphy of the Northern Carnarvon Basin (after Longley et al., 2002) Inset lists stratigraphic nomenclature for key horizons used in this study (after Marshall & Lang, 2013). Red lines denote surfaces of regional extent and seismic horizons that represent sequence boundaries; green lines denote transgressive surfaces; blue lines denote maximum flooding surfaces. Seismic surfaces used in this study (S1-S7) correlate to region-wide stratigraphic surfaces.

4.3.1 Geologic setting

The Northern Carnarvon Basin is located in the southern-most part of the North West Shelf, and is one of four basins that form the “Westralian Basin”: the Northern Carnarvon, Browse, Bonaparte and Offshore Canning/Roebuck basins (Yeates et al., 1986; Westphal & Aigner, 1997; Longley et al., 2002; Lewis & Sircombe 2013; Marshall & Lang, 2013). Bounded to the east by the Precambrian Craton and to the west by the Gascoyne Abyssal Plain (Hocking et al., 1987; Falvey & Veevers, 1974), the Northern Carnarvon Basin is filled with a succession of Mesozoic and younger strata up to 10 km thick (Marshall & Lang, 2013). The Basin formed in response to pre-rift and rifting events related to the breakup of Gondwana (Westphal & Aigner, 1997). Figure 4.3 shows a tectonostratigraphic column for the Northern Carnarvon Basin. The offshore Northern Carnarvon Basin is 535,000 km², and is structurally subdivided into the Barrow-Dampier, Exmouth, Dixon and Beagle sub-basins and the Exmouth Plateau (Longley et al., 2002).

During the accumulation of the Mungaroo Formation in the Late Triassic, the Northern Carnarvon Basin evolved as a large, Westerly dipping, flat ramp cratonic margin, forming part of the southern Tethyan Continental Margin (Figure 4.4; Blakey 2013). The climate in the Late Triassic is interpreted to have been temperate-warm, humid and monsoonal, with wet and dry episodes (Dickens, 1985; Bradshaw et al., 1994; Payenberg et al., 2013, Preto et al., 2010; Arche &

López-Gómez, 2013). The Carnian to Norian fluvial to fluvio-deltaic Mungaroo Formation is generally interpreted to be sourced from the Ross High (Jablonski, 1997) in eastern Australia, with a drainage system that developed through the Canning region and from the Pilbarra Cratonic Rock (Seggie et al., 2007) passing towards a palaeoshoreline that lay to the west, including material sourced from long distance hinterland areas, reworked glacials and also first cycle material from the basement terrains that fringe the Canning Basin and Western limits of the Northern Carnarvon Basin. However, an alternative regional palaeogeographic drainage pattern has also been suggested by Lewis & Sircombe (2013) who argue for a south-to-north draining system, based on U-Pb provenance studies, although this disagrees with channel trends observed in both core and seismic data. The drainage system feeding the fluvio-deltaic deposits of the Mungaroo Formation is interpreted to have developed on a comparable scale to that of the present-day Mississippi drainage network (Jablonski, 1997), with predominantly low-sinuosity rivers.

A comprehensive internal chronostratigraphy and lithostratigraphy of the Mungaroo Formation (Figure 4.3) has been proposed by Marshall & Lang (2013), who built on work by Jablonski (1997) and Longley et al., (2002), applying an alpha-numeric stratigraphic nomenclature, using sedimentological, micropalaeontological and palynological observations to present a new regional stratigraphic framework. The framework integrates major hydrocarbon play intervals by fitting key regional surfaces to a third-order sequence stratigraphic model, using sedimentological, biostratigraphic and seismic data. Chapter 3 describes the stratigraphy and sedimentology of the Mungaroo Formation.

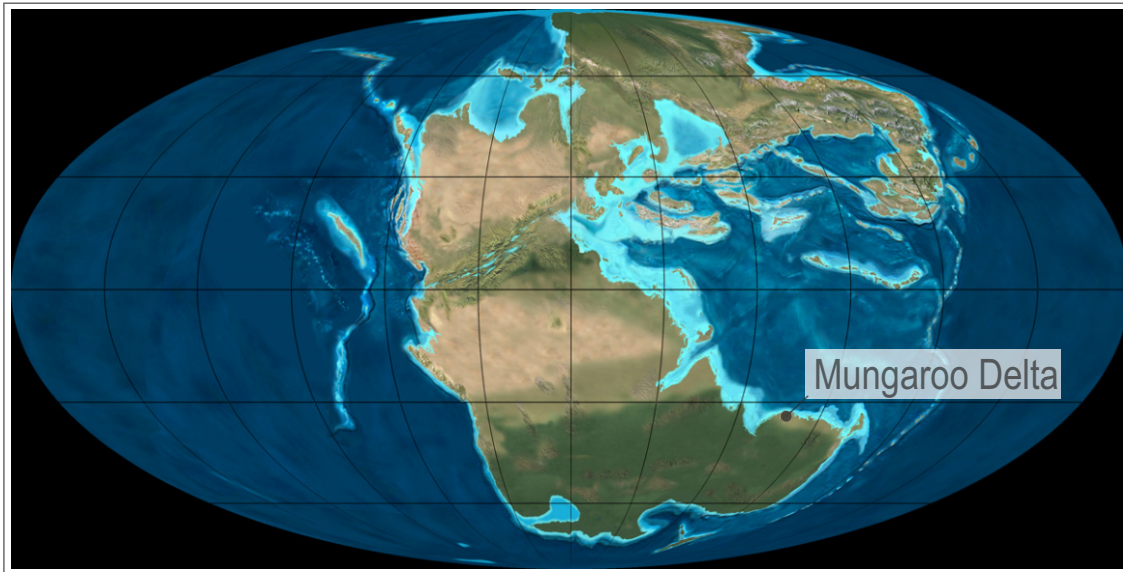


Figure 4.4: 220Ma paleogeographic map (Blakey, 2013), given for paleogeographic context, showing the approximate location of the Mungaroo Delta, on the southern margin of Tethys.

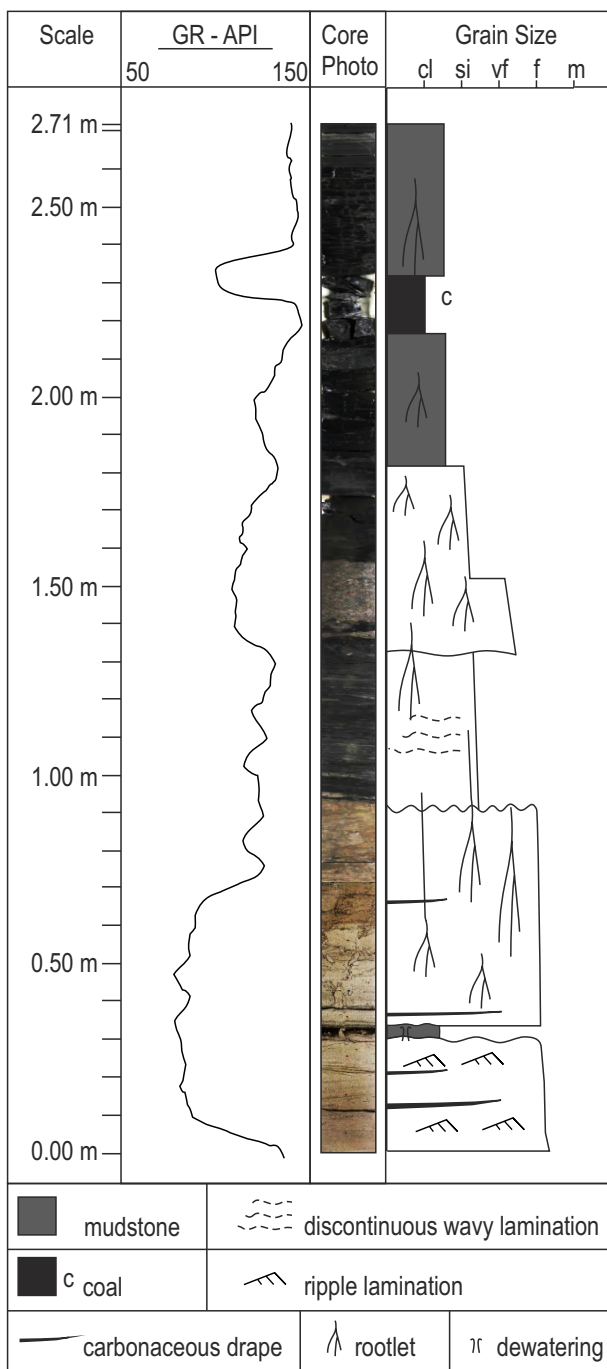


Figure 4.5: Well data set example: wireline log, core photo and sedimentary log from a representative low net-to-gross interval of the Mungaroo Fm.

The Mungaroo Formation records the preserved stratigraphic expression of numerous cyclical changes in accommodation space within the context of an overall long-term rise throughout the Norian to Rhaetian (Longley et al., 2002).

4.4 Methods

4.4.1 Well-log interpretation

Core from a distal well of the Mungaroo Formation (Well-11, Figure 3.2), sited within the boundary of Colmbard dataset was described in order to interpret lithofacies and architectural elements, based on the facies scheme devised by Adamson et al. (2013). Sedimentary lithofacies and architectural elements were matched to corresponding wireline log packages, facilitating interpretation of lithofacies associations and depositional environments for regions where core was not available. Figure 4.5 shows a representative section of core photos, together with wireline-log and lithological-log signatures from a low net-to-gross section of the Mungaroo Formation.

4.4.2 Seismic Interpretation & Attribute Analysis

Seven horizons were recognised within the Mungaroo Formation and used to interpret the fluvial deposits of the formation. The Mungaroo Formation has proved difficult to interpret in the past due to the discontinuous nature of accumulations of fluvial deposits apparently filling incised-valley systems associated with sequence boundaries (Payenberg et al., 2013). For this reason, the surfaces that are most useful for correlation purposes tend to be transgressive surfaces, these being the most continuous events visible in the seismic volume. Following the stratigraphic

nomenclature developed by Marshall & Lang (2013), the surfaces used in this study are from the TR20 play interval. Table 3.1 lists the stratigraphic surfaces and the corresponding seismic horizons and summarizes whether they are transgressive surfaces, sequence boundaries or maximum flooding surfaces.

Stratal slicing of 3D seismic data by creating flattened volumes serves as the basis for a fast and efficient method for screening 3D seismic datasets to gain an improved understanding of depositional environments and geomorphology of deposits (Possamentier, 2005; White et al., 2012). In this study, seven horizons were used to create flattened volumes for near, far and full stack data, such that stratally-aligned slices could be viewed, enabling clearer imaging of the planform geomorphology of contemporaneous fluvial deposits. The near stack volume most clearly imaged the channelized deposits of the Mungaroo Formation. Figure 4.6 shows the workflow employed in the flattening and viewing of stratal slices. Flattening the volume on correlatable horizons made it possible to visualise stratally aligned fluvial deposits above and below those horizons.

The flattened seismic cube was used to identify three intervals where the fluvio-deltaic deposits were most clearly imaged. The analysed intervals related to horizons S6, S3 and S1. Amplitude ranges corresponding broadly to different lithologies were highlighted to better delineate fluvial deposits. For the seismic volume that was flattened using the deepest (near base S1-S2 interval) S1 surface, where stratal slices did not adequately resolve the deposits, attributes including maximum positive amplitude were extracted for a 50ms window below the horizon to better visualise the fluvial deposits.

The horizon slices used for S3 and S6 are extracting amplitudes at a discrete depth (as they are time-slices taken from a flattened volume). The amplitude map extracted beneath S1 represents a 50ms time window. As such they represent discrete intervals within stratigraphic intervals, rather than amalgams of all the deposits within that interval. The interpretations of depositional environment made therefore represent a specific 'snapshot' in time, and may not be representative of the whole stratigraphic succession.

A joint seismic geomorphological and seismic sedimentological approach was employed to identify both channelized and non-channelized deposits, and to assign them to seismic-scale elements. This involved combining analyses of planform geomorphologies and seismic facies response of different horizon slices, using an approach similar to that employed by Zeng (2001). The seismic elements were calibrated using core and wireline logs to confirm lithology. Seismic slices and attribute maps from key stratigraphic intervals were exported to Arc GIS, and georeferenced. The seismic elements were then mapped to contrast depositional environments within the succession.

Using GIS to map geobodies visible on seismic slices and attribute maps allowed geospatial analysis of the mapped elements. Measurements were taken, including element proportions, channel-body length, width, sinuosity and palaeo-drainage orientation to further characterize the fluvial components present within the studied intervals and to relate them to likely depositional and accommodation settings.

4.5 Mungaroo Fm Lithofacies associations

Seven sub-seismic scale non-marine lithofacies associations were interpreted from studied core and wireline logs, describing the rocks in terms of their lithology, texture, and sedimentary features, as well as evidence of bioturbation. The lithofacies associations are: (i) high-energy, primary channel deposits representing stacked fluvial bars, (ii) low-energy channel deposits (secondary or tertiary splay and distributary channels), (iii) proximal crevasse-splay deposits, (iv) distal crevasse-splay deposits, (v) gleysol (local coal equivalent indicating swamp/mire environment), (vi) floodplain-lake deposits, and (vii) inter-distributary bay deposits.

Table 3.1 and Figure 3.11 provides a detailed description of each facies association, detailing conceptual sedimentary logs, wireline logs and core photograph examples. Figure 4.7 links the previously interpreted facies associations to seismic expression of those deposits.

Lithofacies associations identified here are considered to represent distal expressions of the lithofacies associations described by Adamson et al. (2013) focussing on a more inboard section of the formation. They are also deemed to correspond to the facies associations described by Heldreich et al. (2013) approximately 100km SW of the Colmbard dataset, and those identified by Payenberg et al. (2013). As such, the scheme utilised here is considered to be representative of the fluvial and fluvio-deltaic system present on a basin-wide scale.

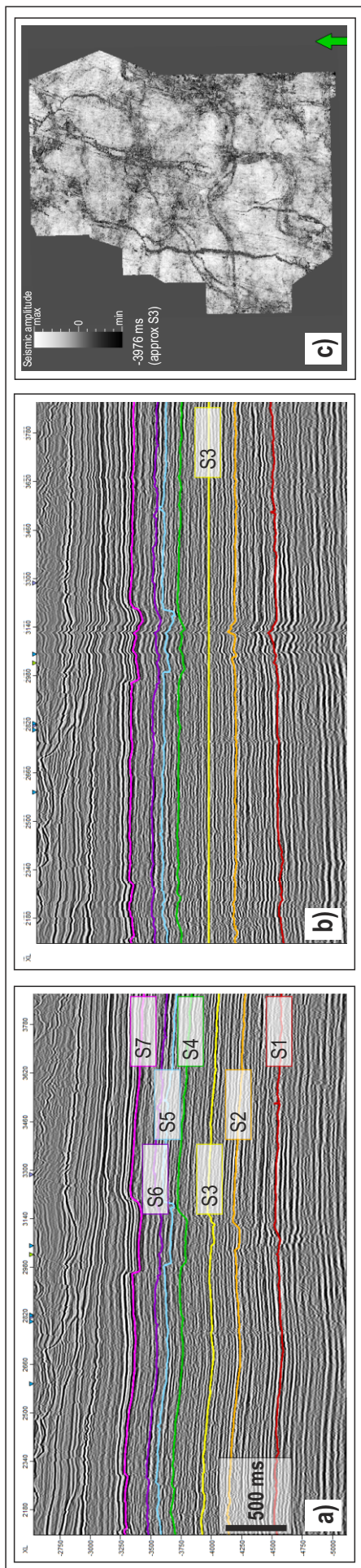


Figure 4.6: Workflow for viewing stratal slices. The volume (in depth domain, (a)) is flattened on key stratal surfaces (b). The resulting flattened volume allows visualisation of stratal slices (c), capturing the fluvial deposits of the Mungaroo Fm.

4.6 Seismic element mapping

4.6.1 Seismic element scheme

Seismic-scale channel bodies and valleys are identifiable by virtue of their sinuous planform geomorphologies (Figure 4.7), although it is difficult to distinguish between channel-belt and incised-valley deposits. Within the studied intervals, the elongate trends of these features are generally aligned E-W. One way to distinguish between channel-belt deposits versus valley-fill deposits is the associated presence of thin-bedded sandstones that likely correspond to crevasse-splay and minor distributary channel deposits in areas laterally adjacent to major channels. Such 'channel-margin' elements are characterized by a 'messy' seismic facies, and are represented by thinly-bedded sandstone packages where wells penetrate the facies (Figure 4.7). Gleysols represent waterlogged, marshy floodplains, and are sometimes present in conjunction with cm-scale minor coal lenses. They have a distinct seismic facies: such elements appear 'bright' on near stack data, and 'dim' on far stack data (Figure 4.7). Seismically homogeneous zones are interpreted as undifferentiated floodplain deposits. Post-depositional faults are visible as generally N-S trending features imaged as high-amplitude lineations.


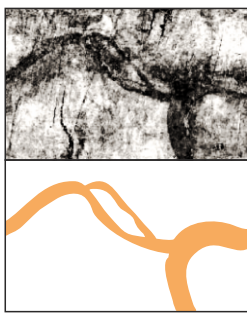


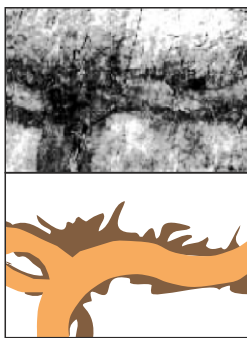
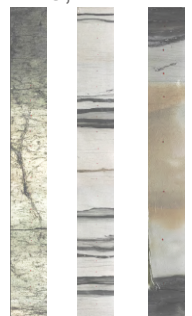

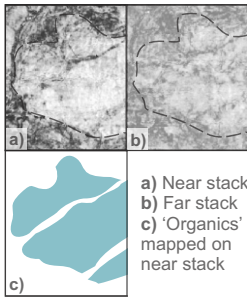


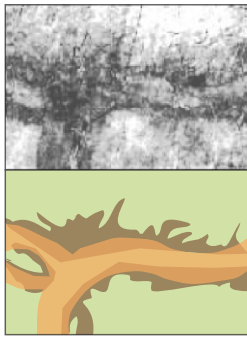
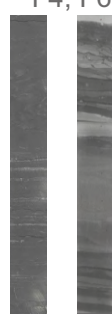

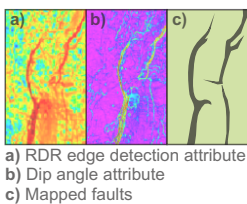
Seismic Element	Seismic Expression	Example	Measurements	Lithofacies
 Fluvial channel and valley deposits	~100m to 20km wide, low to moderate sinuosity features with clear boundaries. Positive amplitude. Clearer on near stack data than far stack.		Width Length Area Sinuosity Orientation	F1, F2 
 Margin	Discontinuous, “messy” seismic facies. Positive amplitude, lower amplitude than channel elements. Adjacent to channel deposits. Indicates splay belt and sub-seismic scale channels at the margin of channel belts.		Width Axial length Area	F3, F4 
 Gleysol, coal organic-rich mudrocks	Class IV AVO: Appear as bright spots on near stack data, dim on far stack data, away from channel deposits.	 <p>a) Near stack b) Far stack c) 'Organics' mapped on near stack</p>	Area	F5, F6, F7 
 Floodplain: Undifferentiated deposits	Dim or homogenous seismic facies, with no discernable gleysol or channel elements. Represents floodplain fines.		Total area	F4, F6 
 Faults	N-S aligned, very high amplitude, linear features. Identifiable using attributes including variance, RDR edge detection and dip angle.	 <p>a) RDR edge detection attribute b) Dip angle attribute c) Mapped faults</p>	NA	NA

Figure 4.7: Seismic-scale fluvial-deltaic deposits have been assigned to mapable ‘seismic elements’ to aid in identifying depositional settings at several stratigraphic intervals. The seismic element scheme incorporates planform geometry and seismic facies, with reference to wireline data and lithofacies where possible. The facies associations (interpreted in Figure 3.11) relevant to each seismic element are noted.

4.6.2 S1

S1 is the deepest of the horizons used to create the flattened volumes (mean elevation -4510 msTWT). Due to the reduced resolution of the data at this depth, the stratal slices were not able to clearly resolve the fluvial deposits. To counter this limitation, a maximum amplitude (maximum positive peak) attribute was extracted on a 50ms window beneath the horizon (Figure 4.8a), thereby enabling resolution of the large-scale geomorphology of the fluvial system for this time interval. Large (>8 km-wide), low-sinuosity geobodies, interpreted as valleys and primary channels are clearly visible, as is a very large (38 km-wide) feature interpreted as a possible overprinted multivalley or stacked multivalley complex (Blum & Price, 1998; Holbrook, 2001), (i.e., a multilateral and amalgamated valley fill over a regionally smooth erosional surface, in this case the S1 sequence boundary). Some tentative 'channel-margin' elements are interpreted close to channel geobodies, but because there were no well penetrations at this level in the study area, neither core- nor well-log-based analysis of the seismic facies has been possible. Figure 4.8 shows both the uninterpreted attribute map and the interpreted seismic element map for the S1 horizon slice.

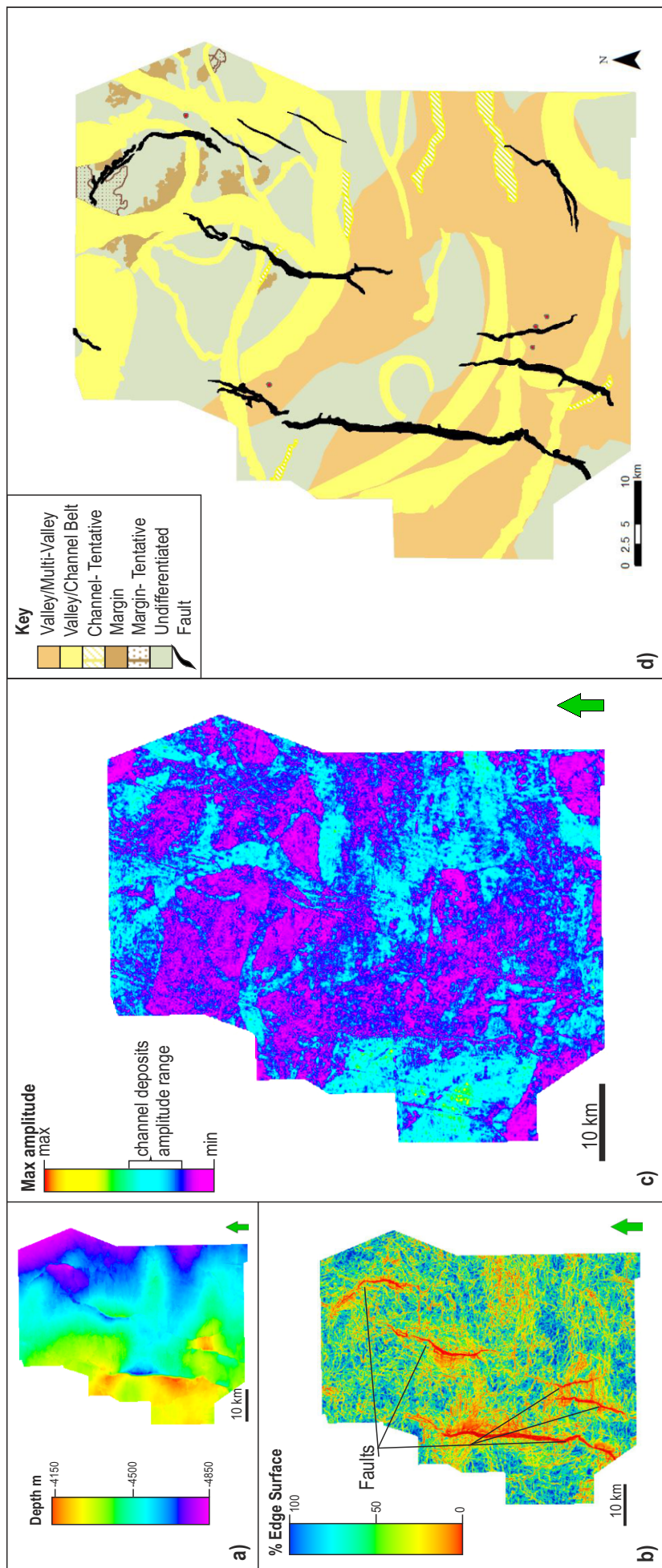


Figure 4.8: Seismic maps used to construct the seismic element map, and the finished element map. **a)** S1 depth map. **b)** RDR Edge detection attribute map highlighting faults at S1 level. **c)** Attribute map representing maximum amplitude (maximum positive peak) for a 50ms window below the S1 surface. **d)** Interpreted seismic element map showing elements interpreted from the maximum amplitude map (c) and positions of interpreted faults.

4.6.3 S3

Stratal slices derived from the seismic volume following flattening at the S3 horizon clearly delineate some large-scale fluvial features (Figure 4.9a), as well as areas of less coherent seismic facies that are shown to correspond to sandstones of crevasse splay origin where penetrated by a well. Smaller channel geometries are also visible. Areas with a strong, 'bright' response are interpreted as gleysols corresponding to a waterlogged, marshy floodplain setting. Colouring the amplitude ranges according to seismic facies further delineates both channel and overbank deposits. Nevertheless, distinguishing between valley-fill and channel-belt deposits from the seismic data where there are limited well penetrations remains difficult. Figure 4.9b shows the S3 seismic element map, highlighting channel, margin, floodplain and gleysol deposits.

Distinguishing between valley and channel-belt deposits is important as it has implications for what deposits may be preserved adjacent to the valley or channel belt. Channel belt deposits may also have a coeval splay belt, which may be preserved (as in Figure 4.9). These splay belt deposits can be sand-rich (c.f. Figure 3.11c) and may represent additional, thinly-bedded reservoirs, or provide connectivity between adjacent channel belts.. Valley deposits are laterally constrained within the incised valley and as such repeatedly overprint, potentially leading to higher net:gross amalgamated sand-fill, but with no adjoining 'fringe' or splay-belt deposits. Therefore, the identification of a preserved splay-belt necessitates the interpretation of a channel belt, rather than valley deposit.

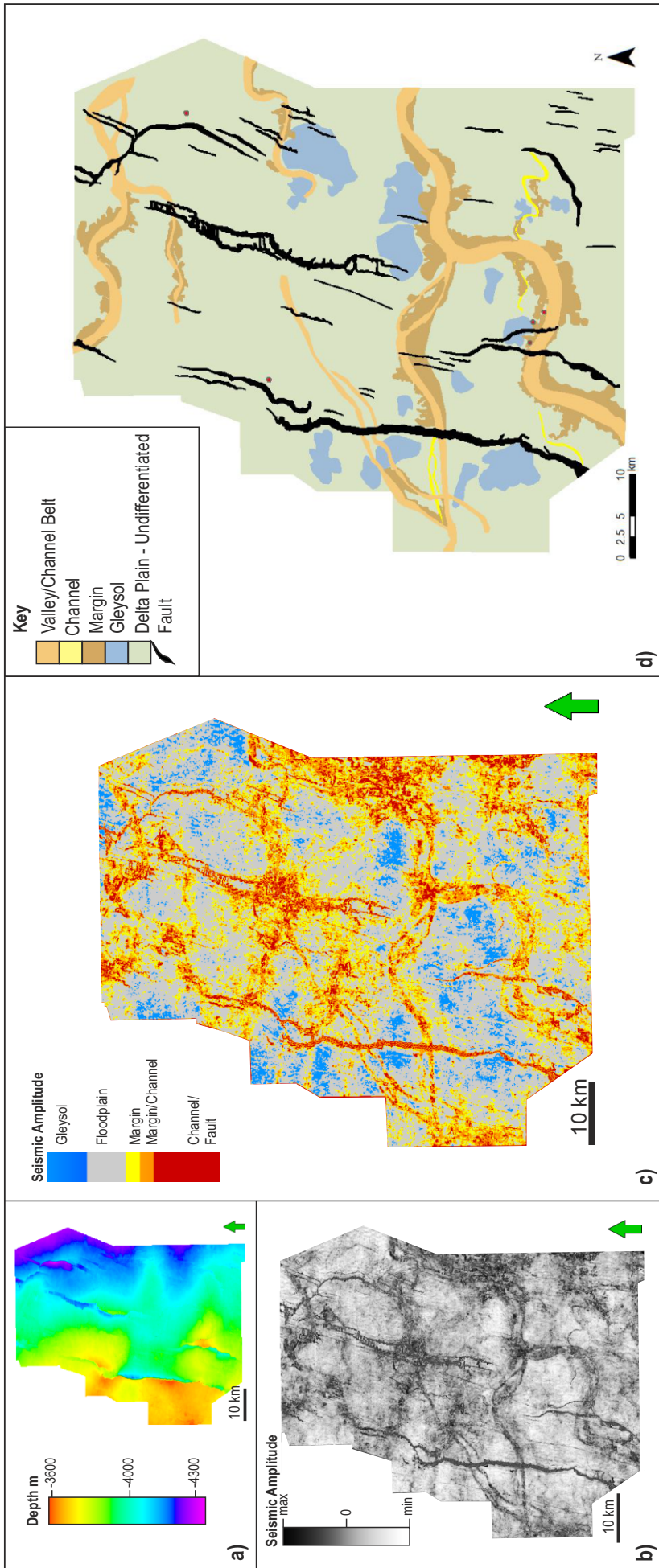


Figure 4.9: Seismic maps used to construct the seismic element map, and the finished element map. **a)** S1 depth map **b)** Horizon slice at approximate S3 sequence boundary, showing N-S trending, linear faults, and E-W trending, sinuous fluvial features. **c)** Different elements of the fluvial system are highlighted by their amplitude ranges. **d)** Interpreted seismic element map showing fluvial elements, overbank elements and faults.

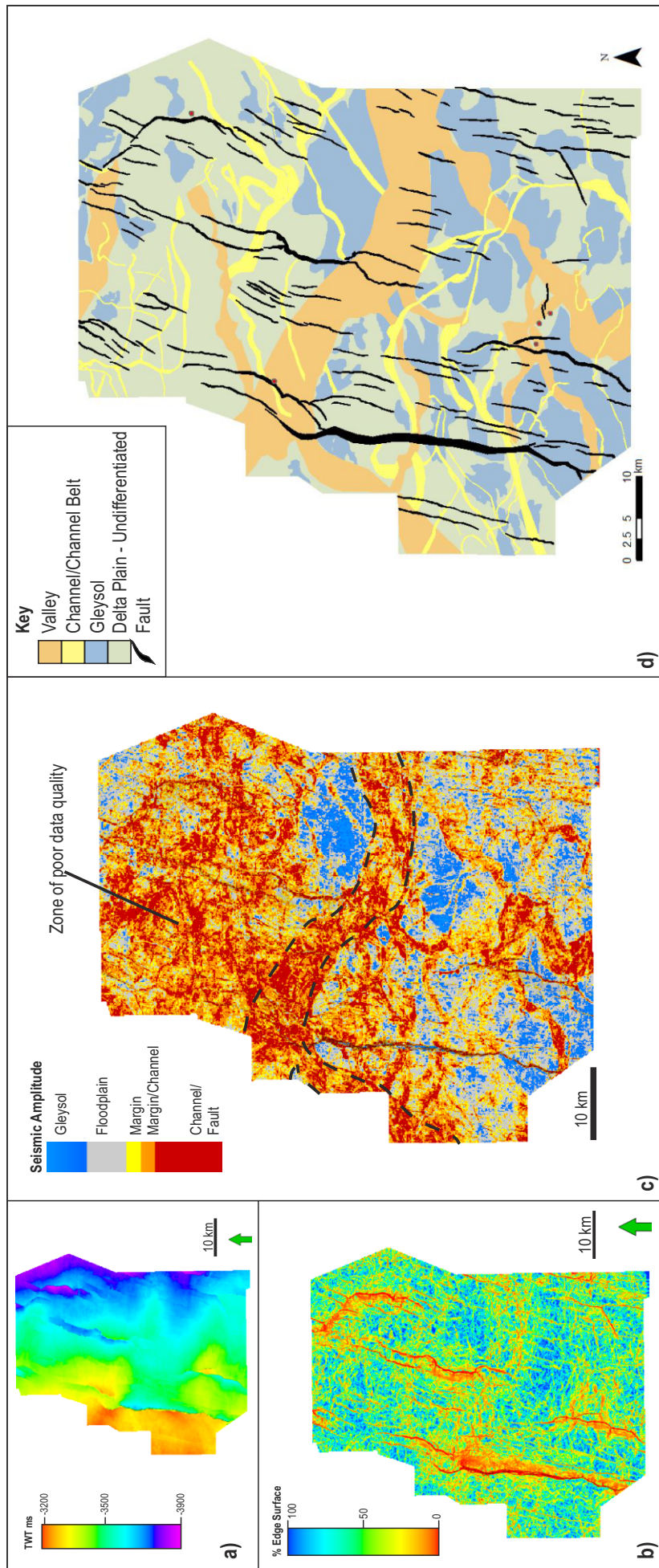


Figure 4.10: Seismic maps used to construct the seismic element map, and the finished element map. **a)** S6 depth map **b)** RDR edge detection attribute map at the S6 surface highlighting faults (red). **c)** Horizon slice below S6, taken from the Near Stack flattened volume. Different elements of the fluvial system are highlighted by their amplitude ranges. Dashed line delineates a wide, low sinuosity feature with visible internal overprinting of higher sinuosity deposits. Probable multi-valley or amalgamated channel belt. A zone of poor data quality towards the north of the slice is due to thickening of deposits between horizons in the cube. **d)** Interpreted seismic element map showing fluvial elements, overbank elements and faults.

4.6.4 S6

A stratal slice taken below S6 reveals a markedly different planform geomorphology to those of the S1-S2 and S2-S3 intervals. Channel and valley geobodies have an apparently distributive morphology, and exhibit a greater variety of channel orientations. A large (7 km-wide), low-sinuosity feature shows internal overprinting and can be interpreted as amalgamated, multi-lateral, multi-story channel-belt deposit. The nature of the overbank seismic facies also contrasts with that of the S2-S3 study interval, being characterized by an apparent dominance of gleysol deposits. Figure 4.10 shows both the uninterpreted stratal slice and the seismic element map for this interval. Figure 4.11 shows the cross-section view of the deposits interpreted in Figures 4.8-4.10. Large-scale incised features and organic-rich floodplain deposits can be identified.

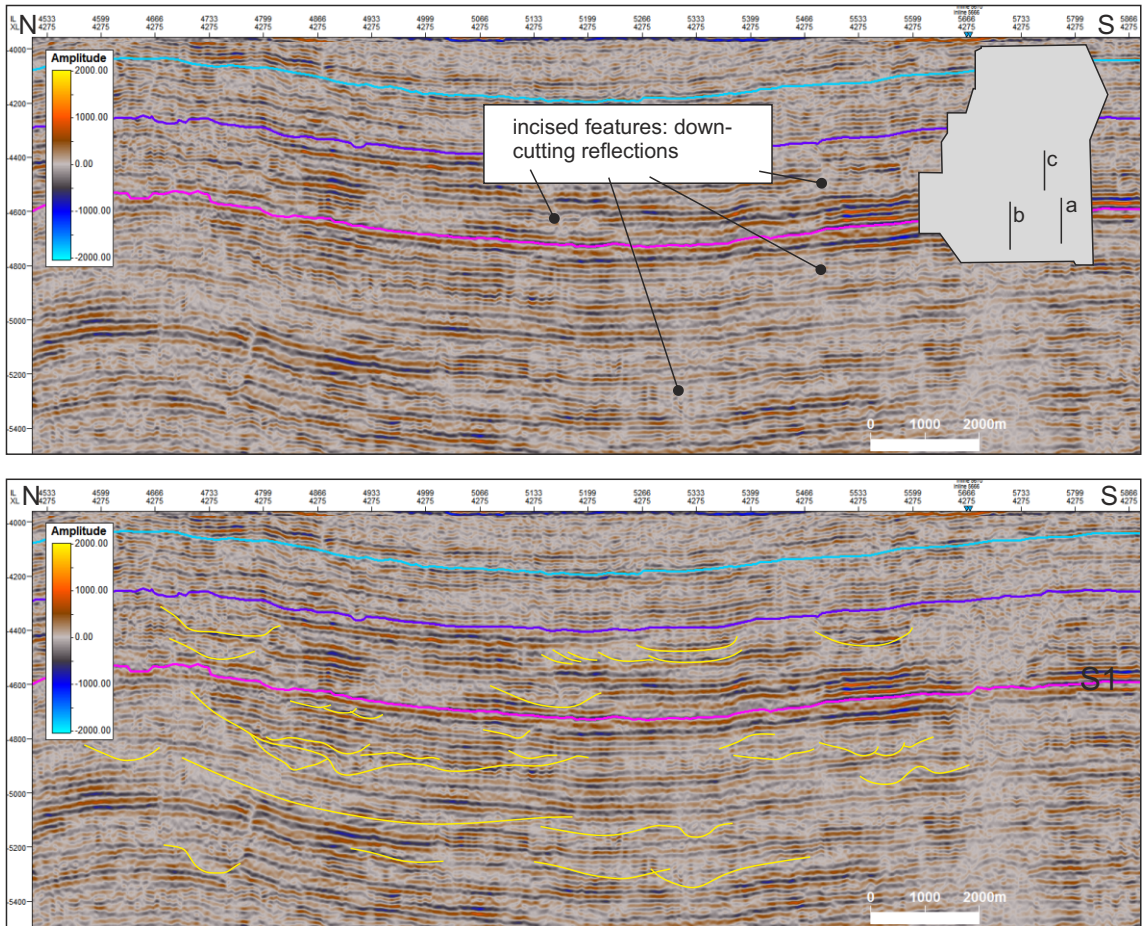


Figure 4.11a: Seismic profile (uninterpreted above, interpreted below) illustrating some of the incised features interpreted in Figure 4.8. Cross-cutting reflections indicate incised events, some of these are laterally extensive (several km wide) and may represent incised valleys. The locations of seismic profile takes from the Colmbard 3D survey for Figure 4.11 (a-c) are shown inset.

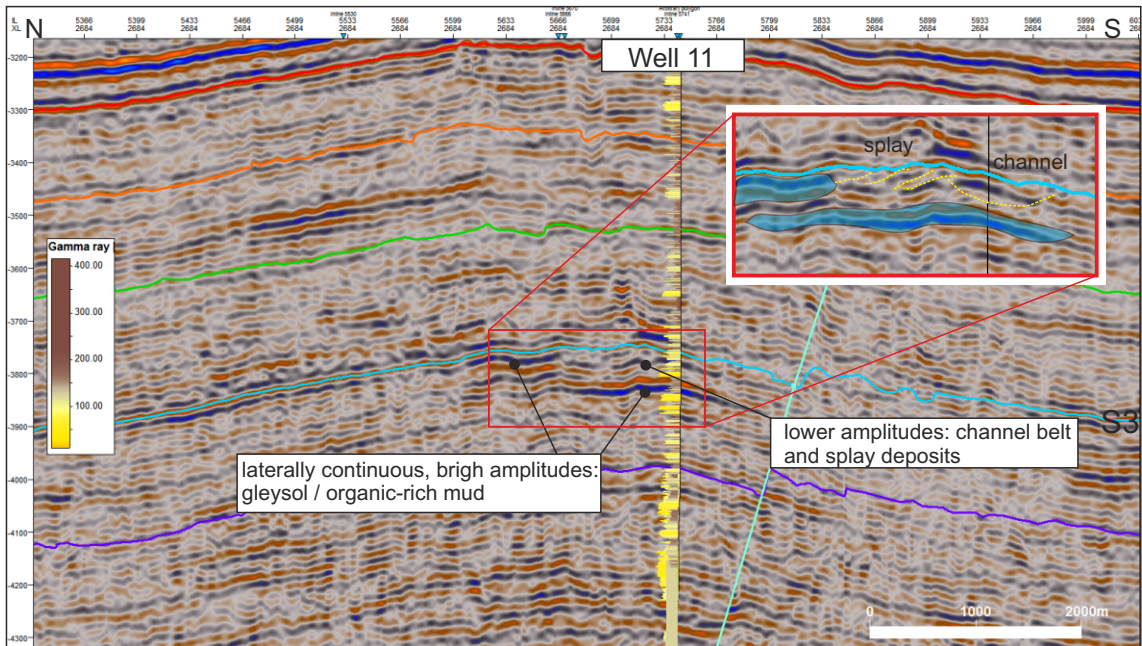


Figure 4.11b: Seismic profile through Well-11, illustrating the seismic facies typical of the channel belt, splay belt and gleycol deposits in the S2-S3 interval, interpreted in Figure 4.9.

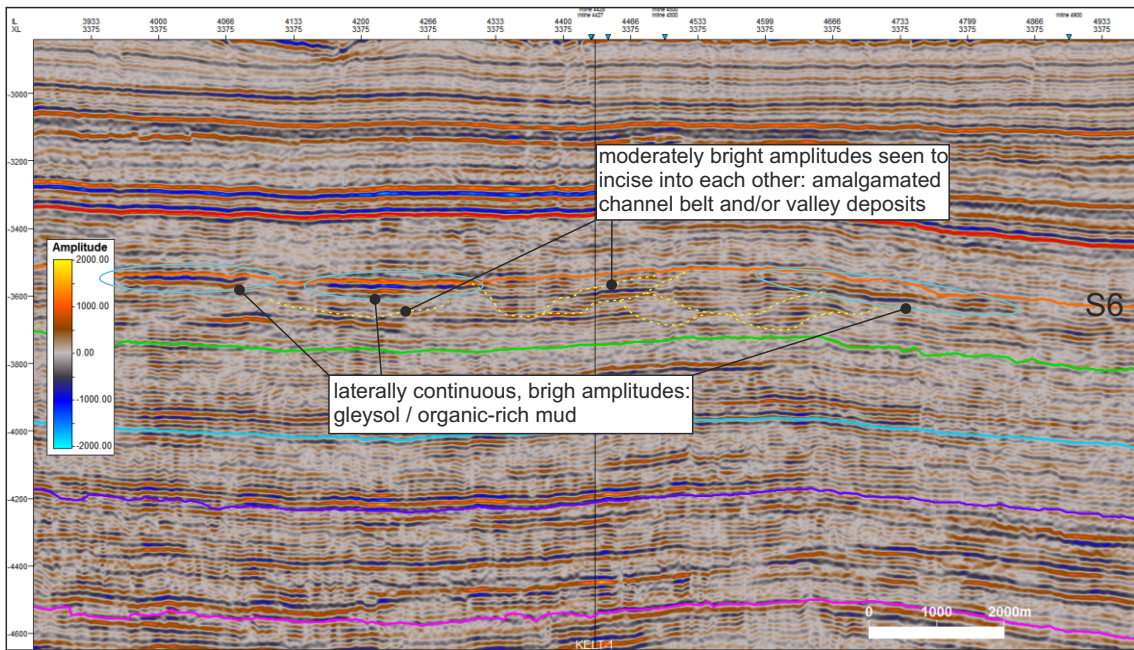


Figure 4.11c: Seismic profile illustrating the cross-section expression of the amalgamated channel belt and gleysol deposits interpreted in map view in Figure 4.10.

4.7 Statistical Analysis

4.7.1 Element proportions

Relative proportions of seismic elements were measured to further highlight differences in fluvial style between the three mapped intervals (Figure 4.12).

The S1-S2 interval is dominated by channel and valley deposits, notably due to the presence in the region of a large multi-valley fill at this level, which accounts for 37% of the mapped area. Channel bodies and floodplain interfluvial areas are of similar proportion, accounting for 32% and 29% of the map, respectively. Channel-margin deposits account for only 2% of the mapped area and are not likely to contribute significantly to sand volume in this interval.

The S2-S3 interval is dominated by undifferentiated floodplain deposits, which account for 81% of the mapped area. The narrow valley and channel-belt elements account for only 9%. The thinly-bedded channel-margin elements associated with channel-belt deposits account for 5% of the mapped area. The small, restricted gleysol elements account for 5% of the mapped area.

Within the S5-S6 interval, a substantially greater proportion of the mapped area is represented by gleysols (25%), indicating a poorly-drained setting within which channel development was not confined to entrenched valleys, as indicated by the divergent, distributive pattern of channels visible on the stratal slices. Amalgamated channel belts and distributive channel elements account for 28% of the mapped area. Channel-margin elements were not recognized in this interval.

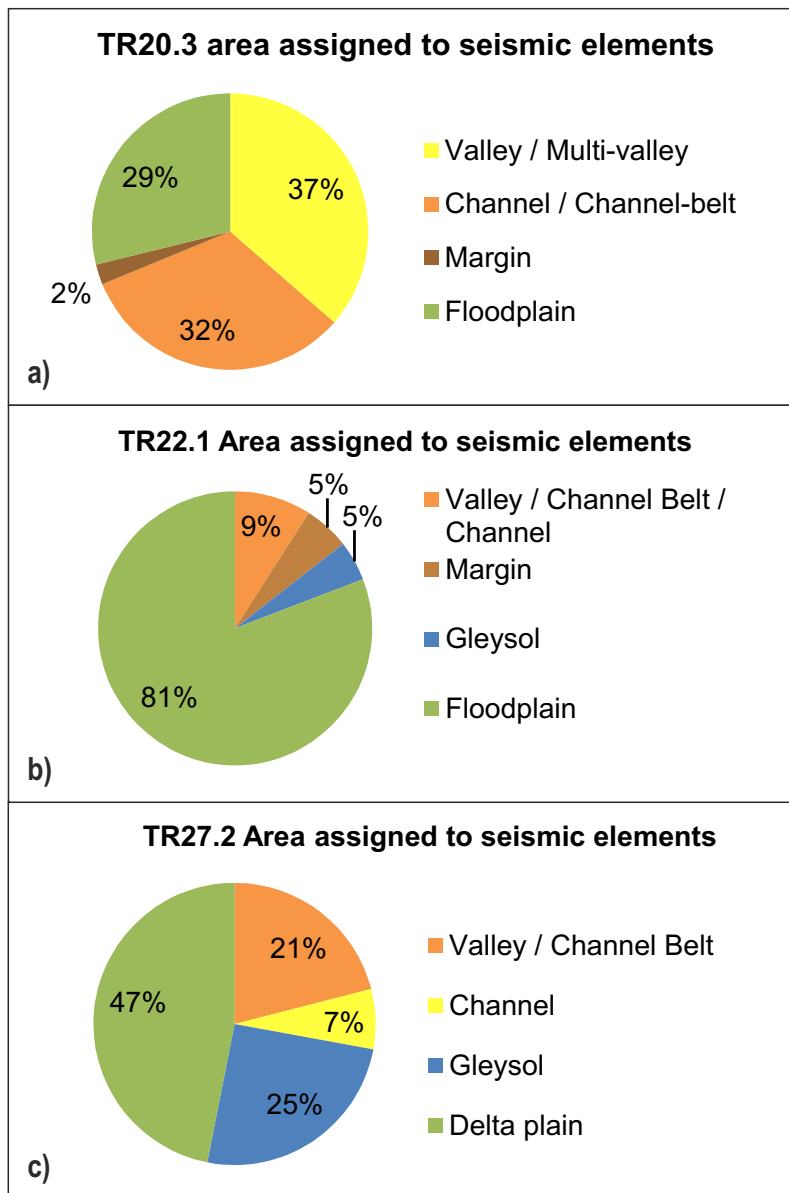


Figure 4.12: Relative proportions of seismic elements at each mapped interval. **a)** S1-S2 interval is dominated by valley and channel elements. **b)** S2-S3 is dominated by 'undifferentiated' floodplain deposits. The mapped area interpreted as channel margin sands is proportionally significant compared to the percentage of the mapped area interpreted as channels/valleys. This may indicate the preservation of splay belts at the margin of channel belts. Restricted gleysol development indicates a well-deained floodplain. **c)** S5-S6 has a far higher proportion of mapped area interpreted as gleysol, indicating a poorly-drained, swampy floodplain, potentially in a delta plain setting. The development of a distributary network of channels at various scales accounts for the high proportion of channel and valley elements.

Dimensional attributes relating to the identified elements, including width, length, area and sinuosity of visible portions of elements within the bounds of the survey, are summarised in Tables 4.1 – 4.3.

Table 4.1: Dimensions of seismic elements for the S1-S2 interval

Measurement	min	max	mean
Channel Length (km)	4.4503	43.0942	16.4544
Channel Sinuosity	1.0117	2.0811	1.1056
Channel Max Width (km)	0.6294	8.6175	2.3264
Channel Area (km ²)	2.2067	147.4713	35.1831
Valley Width (km)		39.1888	
Valley Area (km ²)		1149.4950	
Margin Axial Length (km)	0.7351	6.1674	2.2505
Margin Max Width (km)	1.9298	5.2872	2.5076
Margin Area (km ²)	0.7448	21.7747	4.5613

Table 4.2: Dimensions of seismic elements for the S2-S3 interval

Measurement	min	max	mean
Channel/Valley Length	5.0181	60.0100	23.8133

Channel/Valley Sinuosity	1.0210	1.5714	1.1732
Channel/Valley Max Width	0.2780	1.8819	0.9171
Channel/Valley Area	1.1159	111.5643	22.1458
Margin Axial Length	0.1904	4.0307	1.2801
Margin Max Width	0.5074	13.7958	3.7663
Margin Area	0.1549	18.5012	3.0622
Gleysol Area	2.5058	42.0169	13.6911

Table 4.3: Dimensions of seismic elements for the S5-S6 interval

Measurement	min	max	mean
Channel Length (km)	0.88518	39.38414	11.29873
Channel Sinuosity	1.003423	1.520827	1.07308
Channel Max Width (km)	0.101419	1.996168	3.158849
Channel Area (km ²)	0.119218	22.07021	4.478524
Valley Length (km)	10.67798	67.63019	25.89899
Valley Sinuosity	1.013609	1.090761	1.063554
Valley Width (km)	1.12043	9.344592	3.158849

Valley Area (km ²)	10.83576	383.841	75.56158
Gleysol Area (km ²)	1.335652	173.4524	21.10325

4.7.2 Channel and valley orientations – palaeodrainage

Reconstructed orientations of channelized and valley elements were measured for the features present in each of the three intervals (Figure 4.13).

Overall, there is an E-W trend in drainage orientation. The S2-S3 interval shows the least variation in drainage orientation, with two distinct trends to the SW and NW. However, this may be biased by the comparatively small number of channel bodies mapped at this interval. As indicated by the element map, the S5-S6

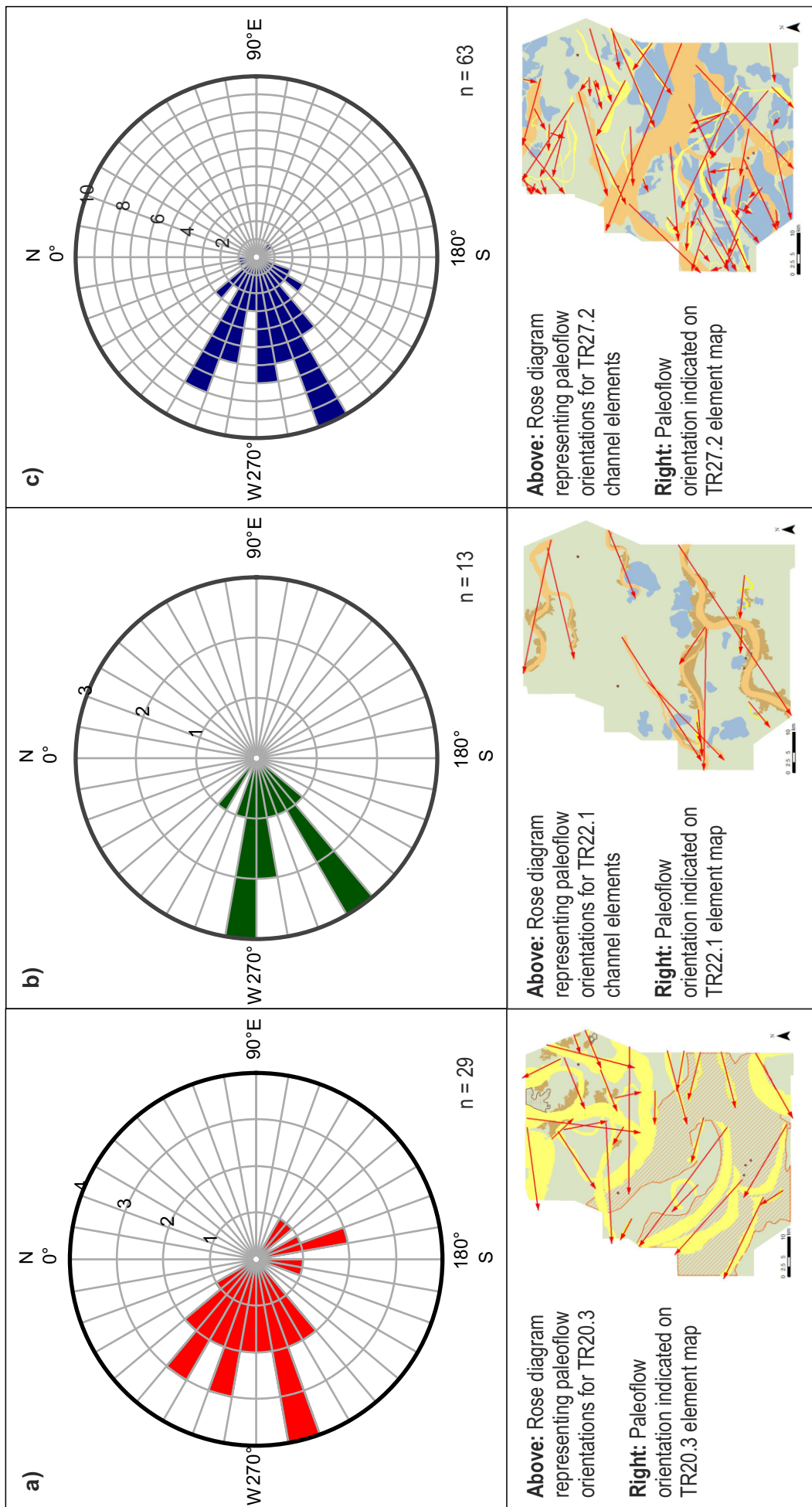


Figure 4.13: Channel orientation rose diagrams for **a) S1, b) S3, and c) S6.**

interval has a relatively evenly distributed spread of channel-body orientations, ranging from 230° to 310°. The S1-S2 interval exhibits the greatest range of orientations, with the bulk of the channel bodies orientated between 230° and 320°, and a secondary, minor trend of channels orientated to the SE, between 120deg and 200°.

4.8 Depositional environment

4.8.1 S1-S2

The channel elements mapped in the S1-S2 interval are larger than those seen in the stratigraphically higher intervals. This, together with the lack of significant areas of preservation of overbank deposits (notwithstanding the possibility that the resolution may simply be too low at this depth to image them), is interpreted to represent deposition within large, incised valleys. The 'undifferentiated' elements likely represent interfluvial areas, and are considered unlikely to contain significant crevasse-splay or minor distributary-channel elements because deposition would have been confined to within the incised valleys. Large, incised valleys may suggest a purely fluvial regime in a more proximal position at this time.

4.8.2 S2-S3

The relatively small-scale of the channel elements (<2km width) at this interval and their association with channel-margin elements suggests that these deposits likely represent channel belts with associated splays and distributary channels that are present at the sub-seismic scale. Restricted development of gleysols indicates a relatively well-drained floodplain. This interval is interpreted as having accumulated during a relatively dry episode, with overbank sedimentation restricted to splay belts possibly formed by seasonal flood events (Slingerland & Smith, 2004).

4.8.3 S5-S6

The widespread development of gleysols in this interval indicates a relatively poorly-drained floodplain in which swamp/marsh zones likely developed. This interval shows a large multi-lateral channel belt feature with overprinted, sinuous deposits forming the internal architecture. Many small, relatively low-sinuosity channels are also identified. Given the numerous minor channels, the distributive pattern of channel orientations, and seemingly wetter depositional setting, this interval is best interpreted as representing an upper delta plain. Payenberg et al., (2013) also interpret delta plain deposits at this interval.

4.9 Ambiguity in interpretations

A major challenge in this study has been the establishment of unambiguous criteria with which to reliably distinguish between valley-fill and channel-belt successions. In cases where wells penetrate such seismic elements, the thickness of the deposit may assist with the identification of likely valley-fill deposits from single- and multi-storey channel-belt deposits. The width of the seismic element might additionally be useful in assisting with recognition but caution should be exercised: it is possible to have a 1 km-wide valley just as it is possible to have a 10 km-wide channel belt. Indeed, studies such as those by Gibling (2006) and Colombera et al. (2012, 2013) demonstrate a large overlap in widths of channels, channel belts and valleys from both modern settings and the ancient preserved record.

Although primary channel-element and valley deposits can be interpreted with confidence, and discerned from gleysols – chiefly by virtue of the distinct geomorphological expression of channel-element and valley deposits, and the

characteristic seismic facies response of the gleysols – other elements, including channel-margin deposits should be interpreted more tentatively, due to their small-scale and spatially restricted and discontinuous nature.

Within this study the overprint of post-depositional faulting causes only minor imaging problems, mainly because preferred orientations of fault arrays are close to perpendicular to the trend of the major channels (Figure 4.13). Thickening of packages between horizons was also detrimental to the imaging of deposits as the ‘stratal slices’ become mis-aligned with the fluvial deposits where the thickness of the package is non-uniform (Figure 4.14). This effect is evident in the northern half of the S6 horizon slice. The flattened interval is thicker in the north of the dataset than in the south, hence slices taken through the dataset do not necessarily fully align with the fluvial deposits.

4.10 Conclusions

Using high resolution seismic data it is possible to identify a range of architectural elements present in subsurface fluvial and fluvio-deltaic successions using stratal slicing and attribute extraction techniques. Seismic facies can be linked to sedimentology through adoption of a holistic approach integrating wireline log, core log and seismic data. From careful analyses of planform geomorphology and assessment of relative proportions of seismic elements, it is possible to recognise key aspects of the depositional palaeoenvironment, namely: (i) wet versus dry substrate conditions, as indicated by the presence or absence of gleysols indicative of a poorly drained floodplain, as is seen at the S5-S6 interval; (ii) the presence of incised valley systems, as identified around S1, an interval with large

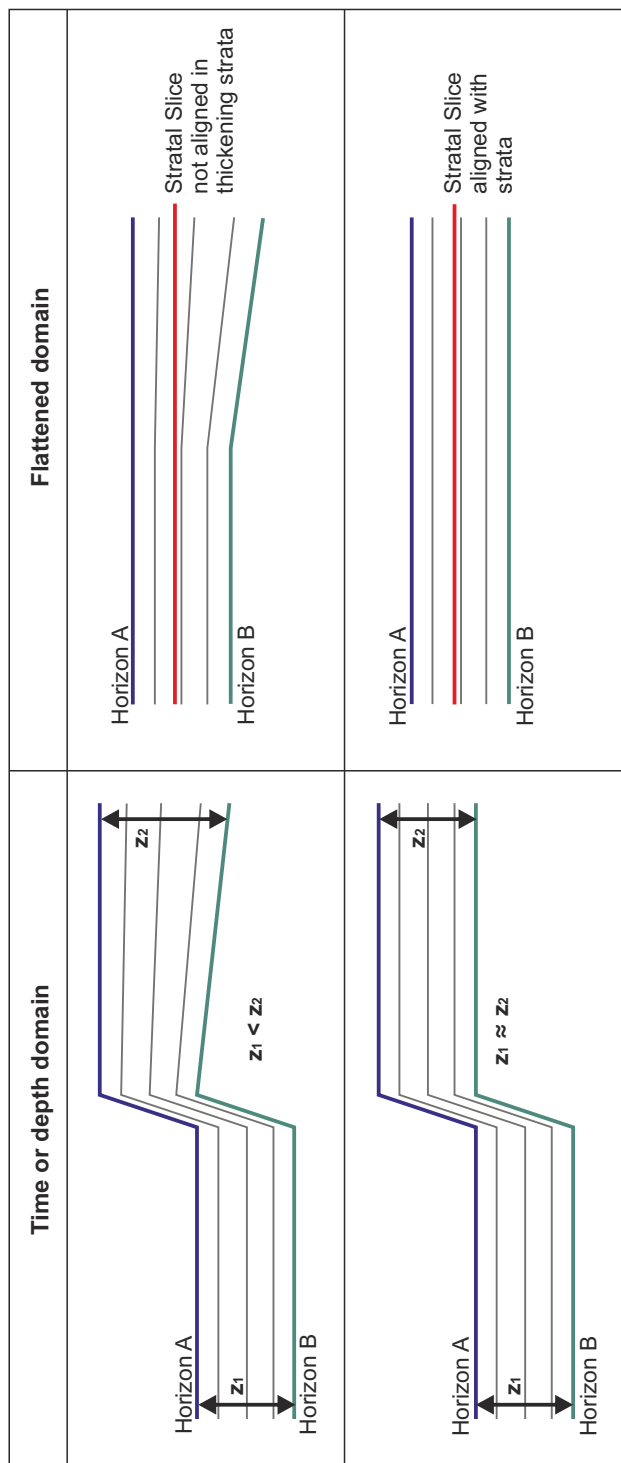


Figure 4.14: Flattening a seismic volume on a single surface will cause stratal slices to be mis-aligned in strata with a lateral change in thickness between surfaces. Flattening on multiple surfaces would avoid this problem. Multiple-surface flattening was not possible using the data packages available.

valley features, with negligible deposition away from the large features, indicating deposition is confined within them; (iii) aggradational delta plain, as indicated by fluvio-deltaic deposits accumulated across a broad floodplain area, as identified at near S6. It is, however very difficult to distinguish definitively and routinely between valley-fill and channel-belt deposits at this scale, especially at deeper levels where there are few well penetrations and where the relatively low-resolution of the seismic data hampers interpretation. For the three studied intervals, which represent 'snapshots' at key stages in the accumulation of the Mungaroo Formation, three distinct depositional palaeoenvironmental settings have been reconstructed: (i) the S1-S2 interval represents dominantly incised valley deposits; (ii) The S2-S3 interval represents dominantly channel-belt and associated splay deposits within a relatively well-drained floodplain setting; (iii) The S5-S6 interval represents large and small distributary channel networks present in a poorly drained upper delta-plain setting. The Mungaroo drainage system had a consistent E-W trend, with only minor systems developing draining to the south. Looking at the deposits interpreted moving up through the succession, the transition from valley fill, to relatively well-drained fluvial floodplain, to poorly drained delta plain, the Mungaroo Formation records several small-scale fluctuations in base-level but overall records a general base-level rise.

Chapter 5 Seismic interpretation techniques useful in the interpretation of subsurface fluvial deposits

Research question: What techniques can be employed to identify channelized deposits and non-channelized floodplain deposits at a range of scales? How can seismic interpretation techniques be used to enable more detailed interpretations?

5.1 Introduction

Channel deposits of fluvial and fluvio-deltaic systems are common targets in reservoir exploration (Shanley & McCabe, 1993; Miall, 2006, Wood, 2007). Examples of well-known fluvial channel reservoir plays include the Cretaceous (Campanian) McMurray Formation, Alberta, which comprises lateral-accretion deposits present in composite valley-fill features (cf. Fustic et al., 2012; Hubbard et al, 2011; Labrecque et al., 2011; Musial et al, 2012; Smith et al., 2009); Triassic Snadd Formation, offshore Norway (Klaussen et al., 2014) Pliocene and Miocene fluvial systems from the Gulf of Mexico (Wood, 2007; Zeng & Hentz, 2004), and the Triassic Mungaroo Formation, Australia, which comprise fluvio-deltaic deposits present across much of the North West Shelf region (Adamson et al., 2013; Heldreich et al, 2013; Jablonski, 1997; Seggie et al ,2007; Stoner, 2010).

Many past and current studies of fluvial deposits present in the subsurface have sought to define the location, size (geometry and lateral extent) and depositional style of such deposits by adopting a combined sedimentologic, stratigraphic and geomorphic approach (e.g. Chopra & Marfurt, 2008; Reijenstein et al., 2011; Posamentier, 2013).

Channel deposits can be laterally discontinuous, exhibiting complex lateral and vertical connectivities influenced by net:gross, channel element size, channel element 3D architecture and mud drapes (Colombera et al., 2012a, 2013; Gibling, 2006; Larue & Hovadik, 2006 Wood, 2007). Figures 2.9-2.11 illustrate the influence of varying channel configuration and net:gross on channel body connectivity. Figure 5.1 (after Orton & Reading, 1993) illustrates some of the basic fluvial depositional styles. The typical thickness of individual channel elements and channel-belt deposits is commonly <10 m (Colombera et al., 2012b; Gibling, 2006), meaning that many such examples are below seismic resolution. The boundaries of these complex, often erosive deposits can prove difficult to map using seismic data as continuous surfaces (Hardage et al, 1994; Roksandic, 1995; Payenberg et al., 2013). Although advances in 3D seismic acquisition, processing and analysis have advanced to the point of being able to detect geomorphic elements, the vertical resolution of conventional 3D surveys is not yet sufficient to detect bed-scale stratigraphic and sedimentary features (Reijenstein et al., 2011).

The aim of this chapter is to introduce the seismic interpretation methods utilised in this project that have proven useful in the identification and interpretation of subsurface fluvio-deltaic deposits of the Triassic Mungaroo Formation, North West Shelf, Australia. The methods employed include those for horizon interpretation, data conditioning, horizon slicing and spectral decomposition. Additionally, this chapter considers methods associated with the analysis of several further seismic attributes carried out in Petrel™ and Geoteric™ that are potentially useful when studying fluvial deposits, including edge detection, dip angle and azimuth, relative acoustic impedance, and two Geoteric™ attributes designed to enhance thin bedforms .

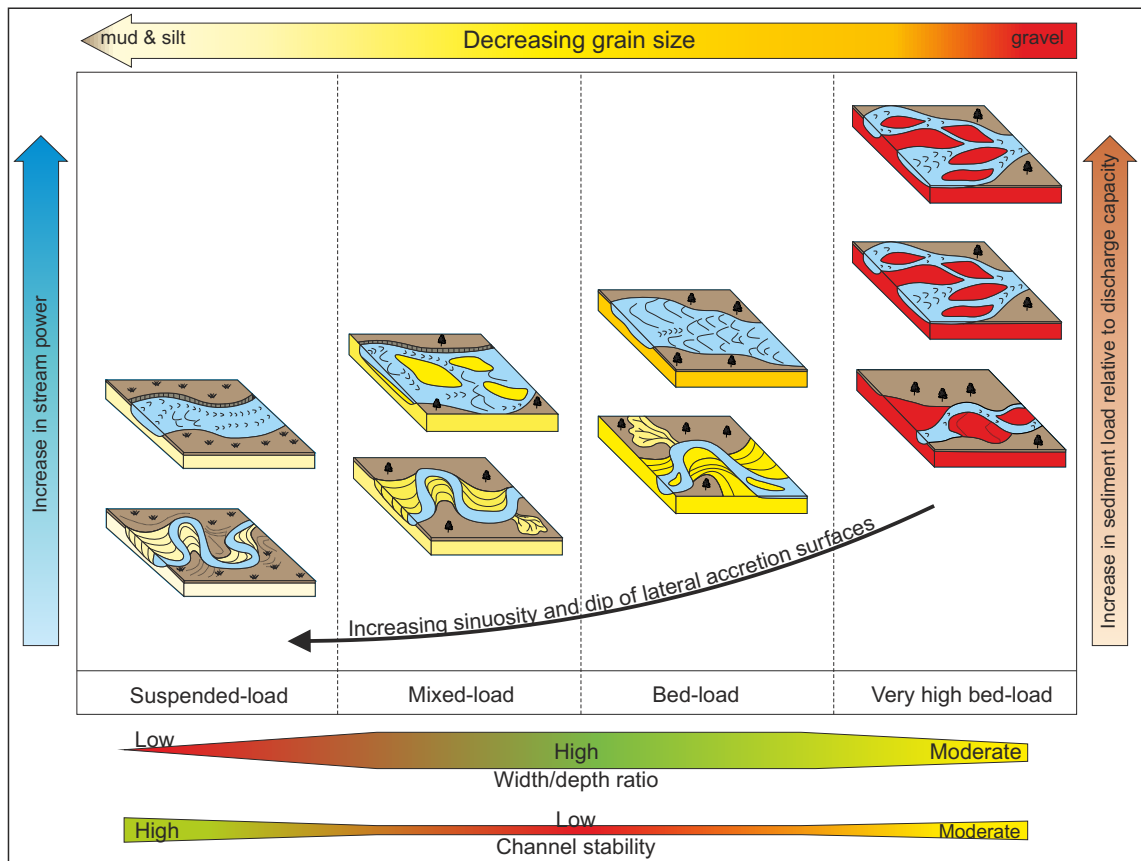


Figure 5.1: Simple block diagrams showing some of the varieties of suspended-load and bed-load fluvial architecture as relates to grain size, width/depth ratio, channel stability, sediment load and stream power (After Orton & Reading (1993).

5.2 Well-log correlation

Sequence boundaries are interpreted as: unconformity surfaces of regional extent and their correlative conformities (Vail & Mitchum, 1977, Mitchum et al., 1977), which are most commonly expressed in fluvial sequences as major erosion and incision to form valleys (Van Wagoner et al., 1990). These sequence boundaries were mapped with high detail in well logs provided by Woodside; however correlation problems have arisen when trying to map out seismic horizons corresponding to these sequence boundaries. Due to limitations in vertical seismic resolution, the cross-sectional expression of geomorphic elements such as incised channel and valley elements is often too crudely imaged in seismic data to delineate stratigraphic discontinuities (Reijnen et al., 2001). This is the case in the Colmbard 3D survey examined as part of this study. For this dataset, the vertical and lateral extent of fluvial valley and channel deposits is such that although they are readily identifiable in core and wireline log data, and are discernible on seismic data, they are typically not clearly expressed in seismic cross-section (Figure 5.2a). Additionally, the laterally confined nature of channelized deposits associated with the sequence boundaries gives rise to a laterally variable seismic reflection character (c.f. Payenberg et al., 2013) meaning that mapping over regional extents is problematic (Figure 5.2a & b). This is not a problem that is specific to the channelized deposits of the Triassic Mungraoo Formation, *per se* but is common to most subsurface fluvio-deltaic successions. To circumvent this problem, generally more recognizable, distinctive and laterally extensive have been used to map key seismic horizons within the succession. Flooding and atransgressive events have widespread, stratigraphic manifestations and so the resultant thin but recognisable flooding and transgressive surfaces provide

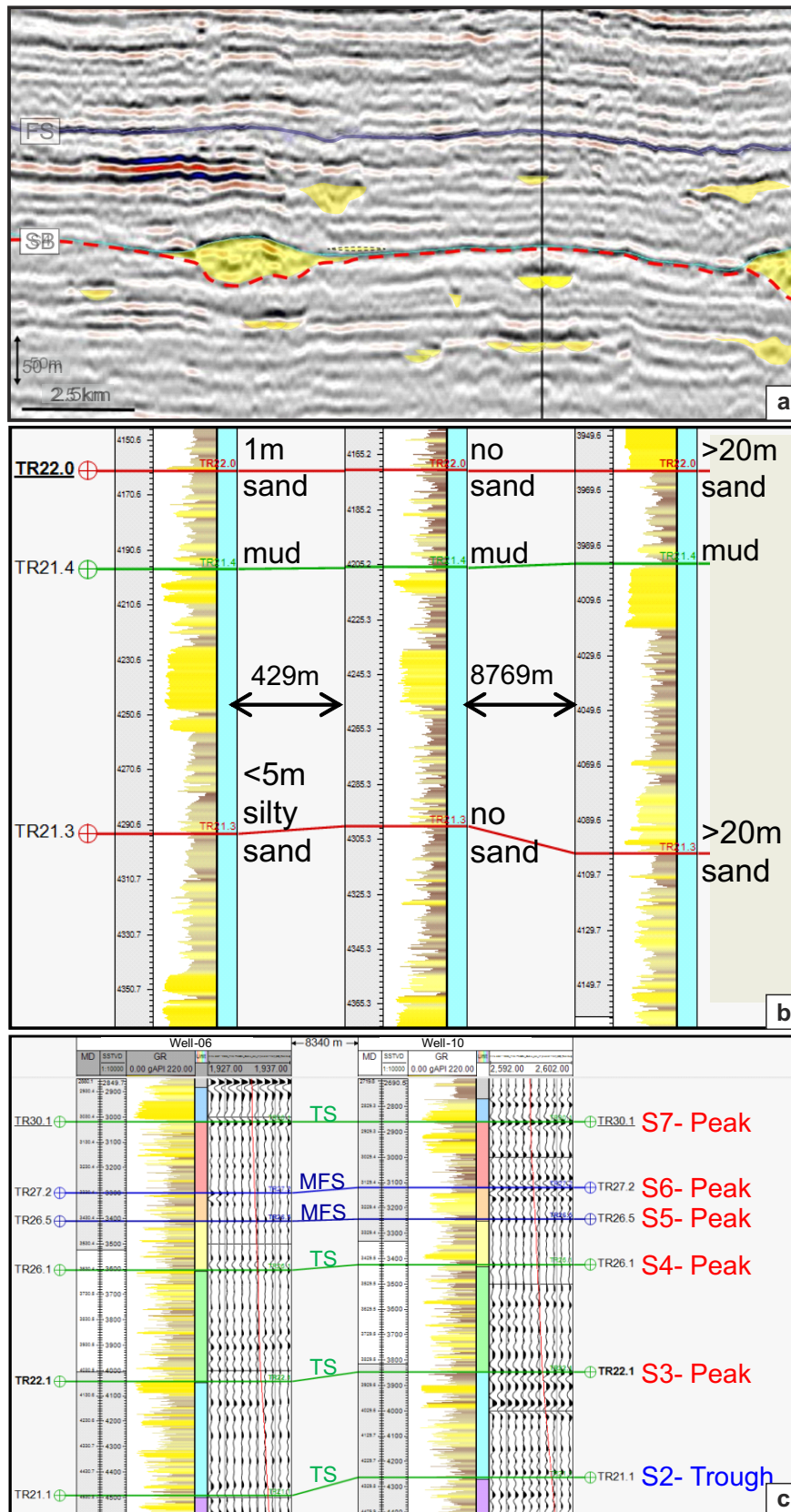


Figure 5.2a: Expression of laterally discontinuous fluvial bodies on a seismic cross-section. The base of the major incised valleys represents a sequence boundary but it is hard to distinguish between these and entrenched channel belt features from seismic cross-section alone. The discontinuous and variable seismic character means that confident correlation is problematic. **b:** Channel-related sand bodies do not necessarily correlate between adjacent wells. **c:** Key stratal surfaces were tied as closely as possible to seismic events prior to horizon interpretation in the 3D cube. Abbreviations: TS (Transgressive Surface), MFS (Maximum Flooding Surface), SB (Sequence Boundary).

particularly useful time-stratigraphic markers for regional correlation (Galloway, 1989a, 1989b) The flooding and transgressive surfaces within the Mungaroo Formation are associated with gleysols, coals, and mud-prone sediments that can be regionally correlated in wells (Adamson et al, 2013) and having a more continuous, uniform seismic character such that they can be mapped as surfaces of regional extent. In the Colmbard survey, 7 horizons relating to regionally correlateable transgressive and flooding surfaces were interpreted within the Mungaroo Fm (Figure 5.2c); these serve as the basis for the subdivision of the Formation into study intervals used in this study. Further detail of the interpreted horizons and how they link into the chronostratigraphic framework of the Mungaroo Formation can be found in Chapter 3, Figures 3.4-3.6.

5.3 Seismic methods

5.3.1 Data conditioning

Before detailed interpretation of the volume could be undertaken, steps were taken to reduce the noise present in the volume, and enhance the resolution of the volume.

5.3.1.1 Noise reduction

Noise reduction was carried out using GeoTeric™, to reduce coherent noise (including linear noise and multiples) and random noise. Two noise filters used in the study are: (i) TDiffusion, which removes random noise while preserving structural details such as edges; (ii) SO FMH (Structurally Orientated: Finite Mean Hybrid filter), which reduces random and coherent noise while preserving edges and dipping features. This filter uses dip and azimuth steering volumes to steer the filter, so has higher fidelity than traditional filters (such as Petrel™

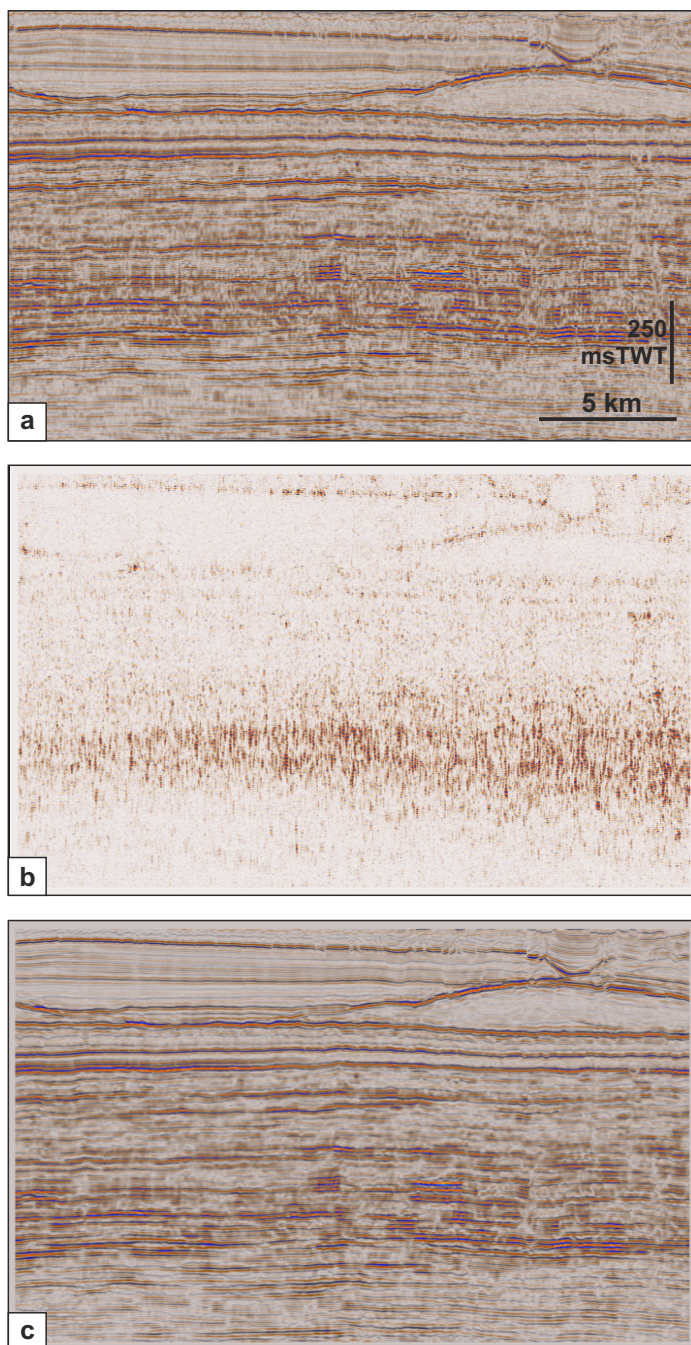


Figure 5.3: Comparison of the seismic volume before and after noise reduction. **a:** Example seismic cross section from the Colmbard 3D (Near Stack) volume. Reflections are highly discontinuous with considerable noise. **b:** The same cross section showing the noise removed from the volume. **c:** The resultant structurally smoothed, noise-filtered cross section. Reflections appear more laterally continuous, whereas edges of features are preserved and not smeared through over-smoothing, as can occur as a result of traditional smoothing techniques.

structural smoothing filter), and is less likely to confuse subtly dipping features with noise. This filter gives a similar output to the OpendTect™ dip-steered median filter. Figure 5.3 compares a seismic cross-section from the original volume with that of the noise-filtered volume, and depicts the same cross-section to demonstrate how noise has been removed from the volume.

5.3.1.2 Spectral enhancement

The vertical resolution of seismic data is partially dependent on the frequency content of the seismic signal (Partyka et al., 1999). Maximising the mean frequency and bandwidth of the seismic data by enhancing the higher frequency content of the seismic volume can aid the delineation of seismic events that were poorly resolved in the original seismic volume (FFA, 2013). The Geoteric™ Spectral Enhancement workflow produces a more balanced frequency spectrum with a higher vertical resolution. Figure 5.4 compares a seismic cross section from the noise cancelled volume with that of the spectrally enhanced volume. The equivalent process in Petrel™ utilizes the Graphic Equalizer volume attribute.

5.3.2 Horizon slicing (Petrel™)

In seismic surveys where deposits are horizontal to sub-horizontal, and have not been post-depositionally deformed, time slices can be used to visualise fluvial channel-belt deposits (c.f. Miall, 2002; Posamentier, 2005; Ethridge & Schumm, 2007; Reijenstein et al., 2011), particularly where deposits are shallowly buried (c.f. Reijenstein et al., 2011). The quality of image produced decreases with depth. Figure 5.5 compares a shallow time slice (~125 m SS) from Reijenstein et al. (2011) with a deep (~1500 m SS) slice from Wood (2007), showing how the level of detail of the deposits discernable within a

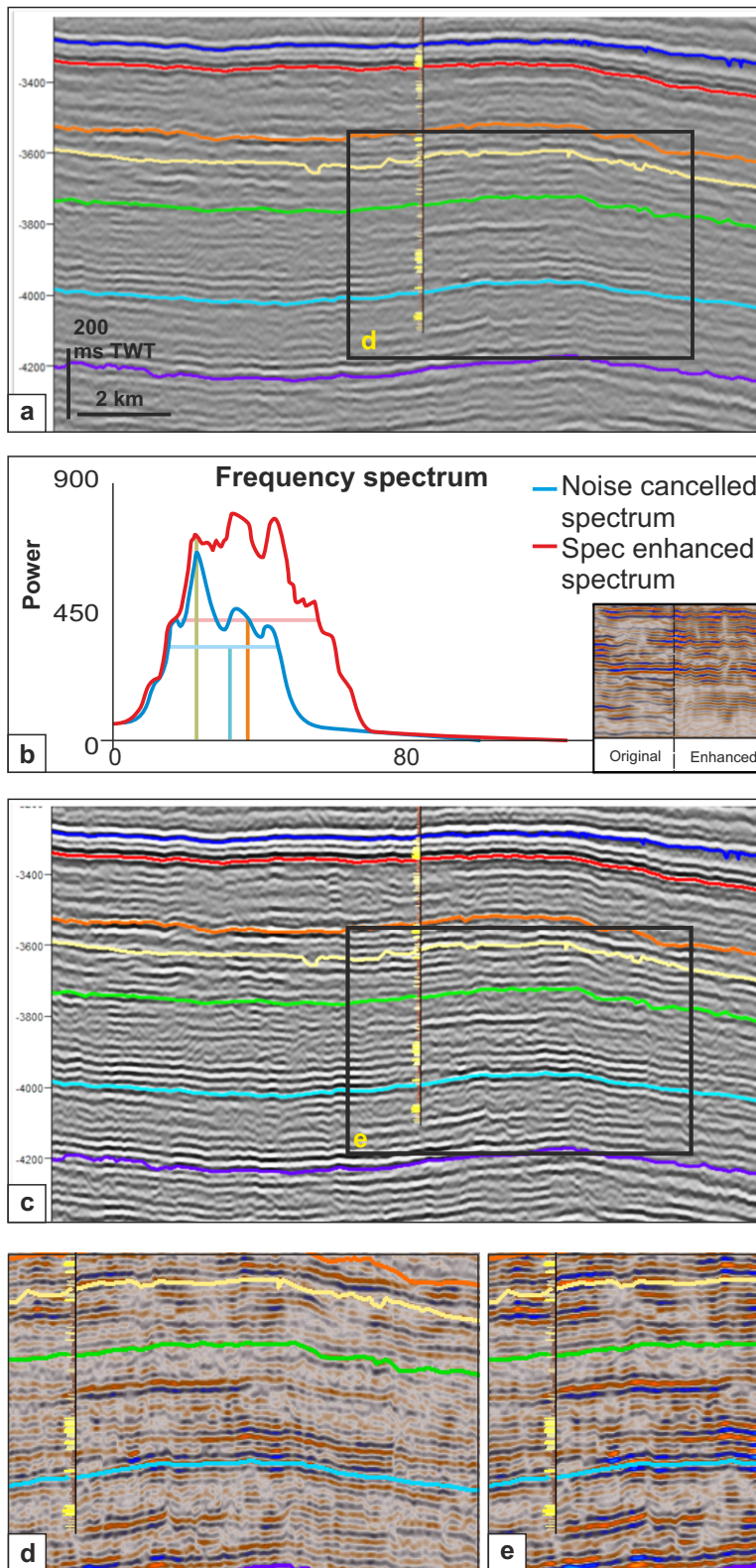


Figure 5.4: Demonstrating the effects of the Spectral Enhancement workflow. **a:** Seismic cross section from the noise-filtered seismic volume. **b:** Frequency spectra for the original and enhanced volumes. The mean frequency and bandwidth have been enhanced by increasing the input from higher frequencies, whilst keeping the dominant frequency as close to the original as possible. The inset figure shows enhanced reflections relating to thinly bedded strata. **c:** The same cross section as in **a**, from the spectrally-enhanced volume. Reflections appear crisper; some previously discontinuous reflections are more laterally continuous. **d:** Detailed view of poorly imaged, discontinuous reflections. **e:** Detailed view of better resolved, more laterally continuous reflections.

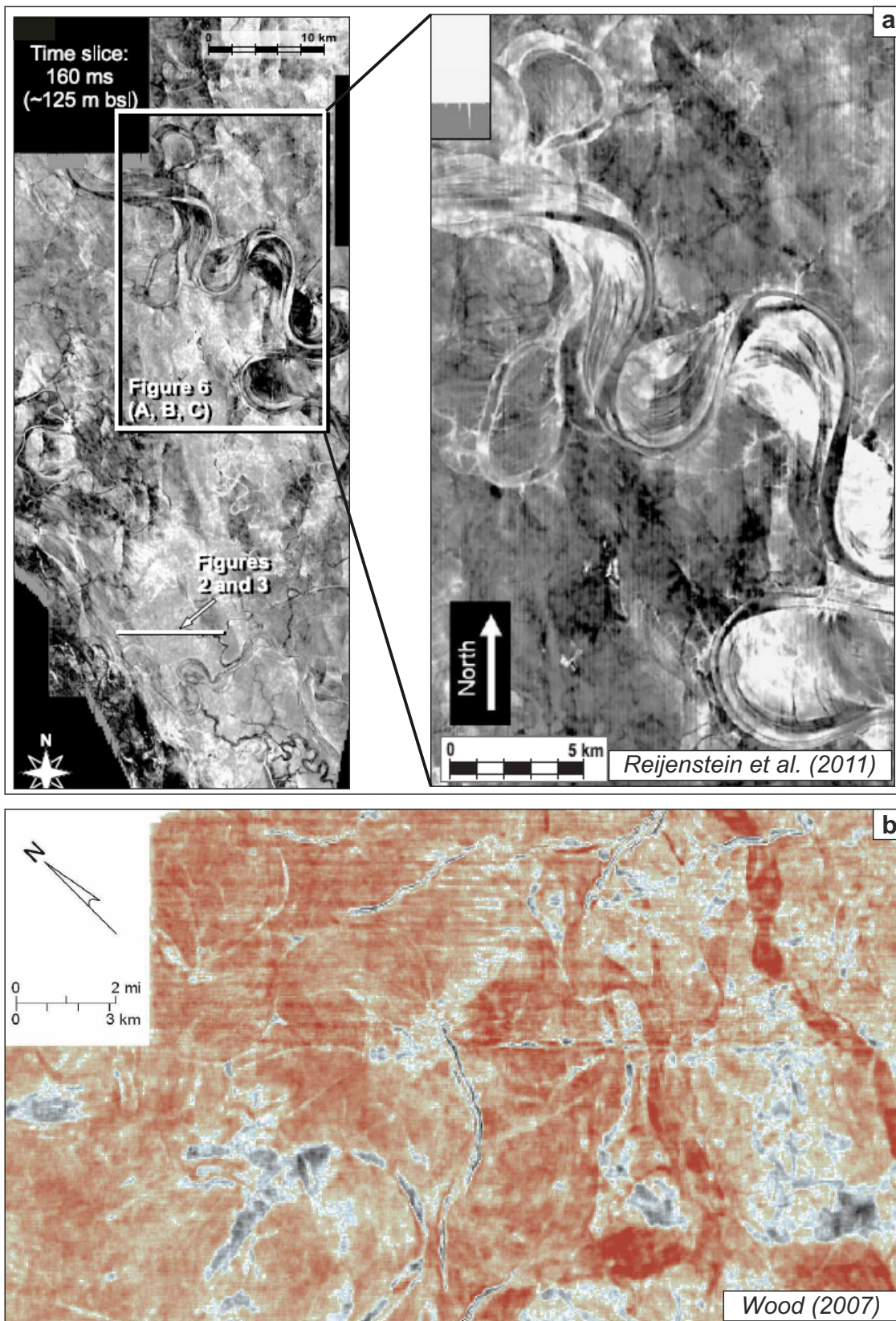


Figure 5.5: Comparison of (a) a shallow (~125 m SS) and (b) a deeper (~1500 m SS) time slice, illustrating the fluvial features visible at the different depths. **a:** Very shallow time slice from the Gulf of Thailand (reproduced from Reijnen et al., 2011) shows the detailed geomorphology of meandering channel and point bar deposits in an exceptionally well-imaged volume. **b:** This deeper slice from the Gulf of Mexico (reproduced from Wood, 2007) shows less detail of the fluvial deposits, although both large and small channel and channel belt bodies can be discerned.

seismic cube is less in more deeply-buried deposits than in shallowly buried deposits.

The Mungaroo Formation has been subject to post-depositional faulting, the result of which is that the fluvial deposits cannot be visualised using conventional time slices. The method employed in this study to visualise the deposits is horizon slicing. To achieve this, a series of sub-volumes were created, flattened on individual seismic horizons (Figure 5.6 shows the horizon slicing workflow). Time slices taken within the flattened volumes are effectively horizon slices, and show deposits that are stratally aligned with the flattened horizon (Hardage, 1994). Horizon slices are only effective in cases where strata are parallel to the interpreted seismic horizon (Zeng & Ambrose, 2001). This method is effective for the Colmbard 3D survey as deposits of the Mungaroo Formation are parallel to sub-parallel.

5.3.3 Proportional slicing and amplitude extraction (Petrel™)

Where flattened slices did not image the deposits, proportional slices extracting amplitudes over a larger window were used to capture large-scale features. Proportional slices are stratal slices taken aligned with strata between two seismic horizons (Zeng et al., 1998). Figure 5.7 (after Zeng & Hentz, 2004) illustrates the difference between time slices, horizon slices and stratal slices. In very deep sections of the dataset (>4000 msTWT), resolution was reduced such that visualisation of the fluvial deposits was not possible. For very deep (>4000 msTWT) sections, amplitudes were extracted over a window around a proportional slice in order to image the large-scale geometry of the fluvial deposits. Figure 5.8 compares the amplitude map of a proportional slice, from the deepest interval of the Mungaroo Formation investigated in this study, with an amplitude map where the values (in this case, a maximum amplitude

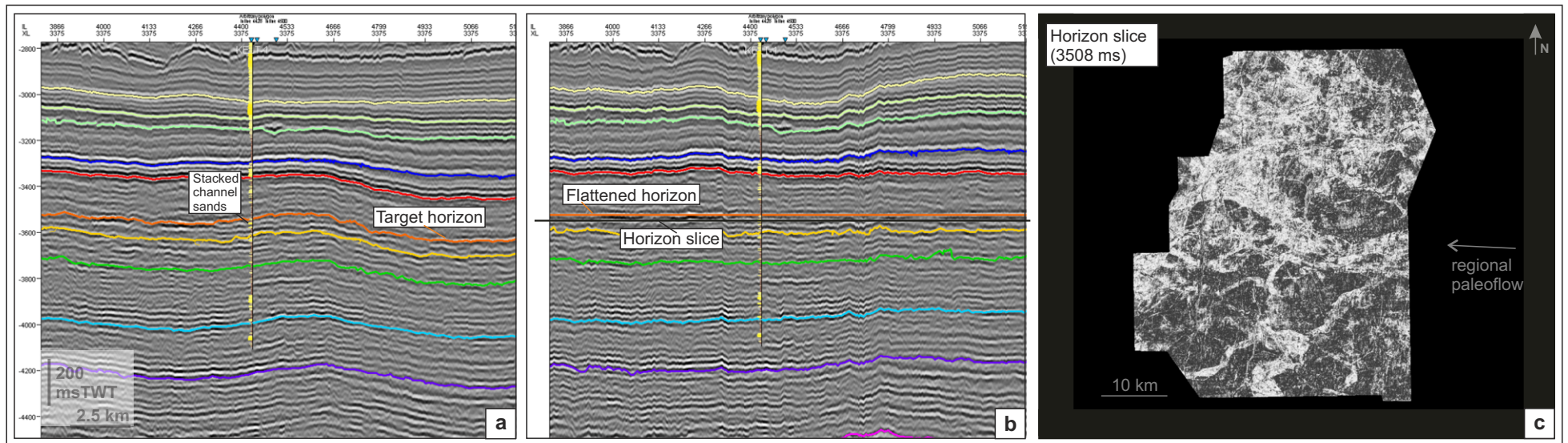


Figure 5.6: Flattening workflow used on the Colmbard 3D survey. **a:** Seismic cross-section showing interpreted seismic horizons. The horizon to be flattened (target horizon), and some stacked, channelized sand bodies identified in well logs are labelled. **b:** Cross-section view showing the flattened volume (flattened on the orange horizon), and the location of a horizon slice taken below the flattened horizon. **c:** The horizon slice is able to image a distributary network of channels and channel belts, at the approximate stratigraphic location of the stacked, channelized sand bodies encountered in the well.

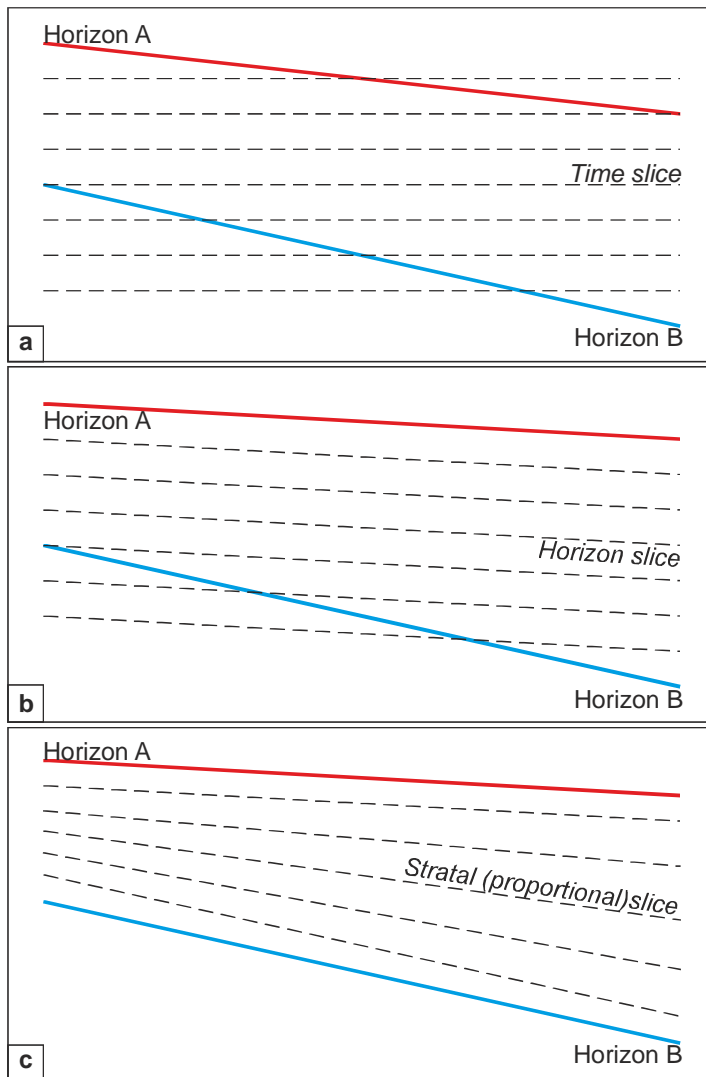


Figure 5.7: Comparison of time, horizon and stratal-slicing techniques (after Zeng & Hentz, 2004). **a:** As neither horizon is horizontal, time slices cross the dipping horizons and would not reveal time-equivalent strata. **b:** Horizon slices aligned with horizon A are conformable with stratigraphy when taken close to horizon A, but as the lower horizon B is dipping at a higher angle, they are not stratally-aligned lower down. This is common where there are lateral changes in the thickness of the stratal package. If the two horizons are close to parallel, horizon slices would be stratally conformable throughout the interpreted package. **c:** Stratal (proportional) slices are conformable with both horizons, and provide a 'best' fit through dipping strata with lateral thickness changes.

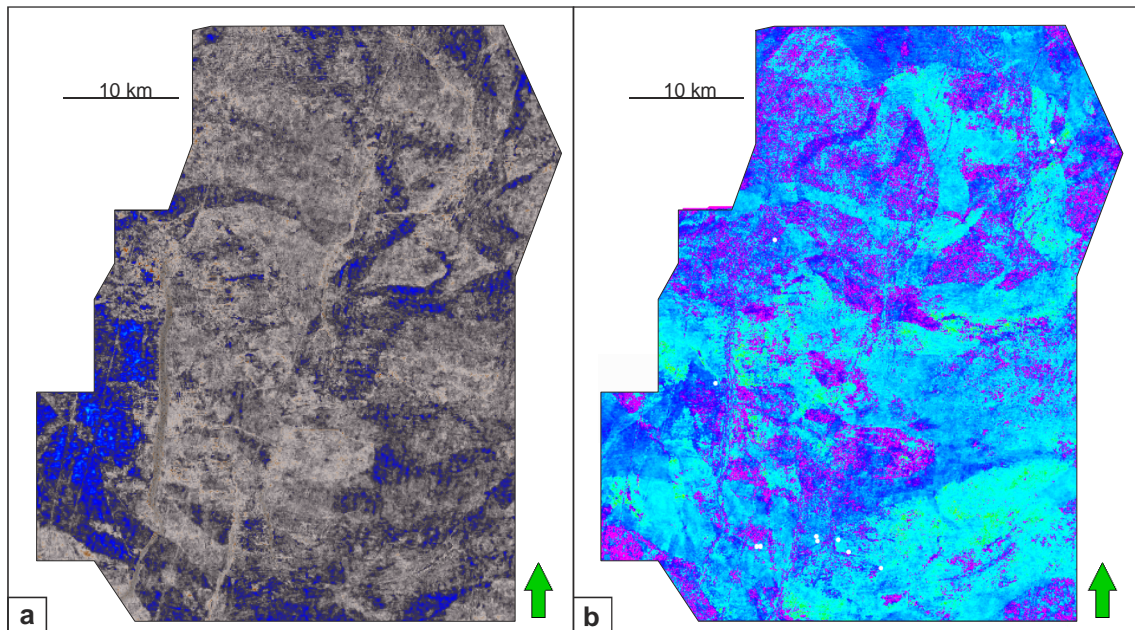


Figure 5.8a: Proportional (stratal) slice showing poorly-imaged, laterally discontinuous geobodies relating to fluvial deposits. **b:** Amplitude map for the same slice as in **a**, with a maximum amplitude attribute extracted over a 50 ms window, showing more laterally continuous and clearly defined features, some measuring >10 km width, interpreted as valley deposits.

attribute – maximum positive peak value – extracted over a 50 ms window). Large-scale, likely palaeovalley, geobodies are visible in both slices, but are clearer and more continuous in the 50 ms window. Implementation of this technique meant that large-scale features were able to be imaged, that would otherwise have remained undetected.

5.4 Spectral (frequency) decomposition (Geoteric™)

Spectral decomposition breaks down a seismic volume into its constituent frequencies and then creates amplitude volumes tuned around specific frequencies. Application of this method makes it possible to visualise the same seismic interval (and the deposits within it) at different frequencies (Partyka et al., 1999; Henderson et al., 2008). Thickly bedded features tend to have relatively higher amplitude at lower frequencies, whereas thinly bedded features tend to have higher amplitude at higher frequencies (Partyka et al., 1999). Spectral decomposition can help to delineate features that fall below normal seismic resolution. Two methods of spectral decomposition were used in this project, using Geoteric™. The methods are explained in detail by McArdle & Ackers (2012) and McArdle et al. (2014), and are summarised below with examples from this study.

5.4.1 RGB blending

A region of interest around a seismic slice is defined (Figure 5.9a), from which a frequency spectrum is generated. Next, a series of frequency bands are projected onto the spectrum (Figure 5.9b). The minimum frequency, maximum frequency and number of bands can be altered. The distribution of the frequency bands depends on the decomposition method chosen: the Constant Bandwidth method produces equally sized and spaced frequency bands within the minimum and maximum range defined (Figure 5.9b); Uniform Constant Q

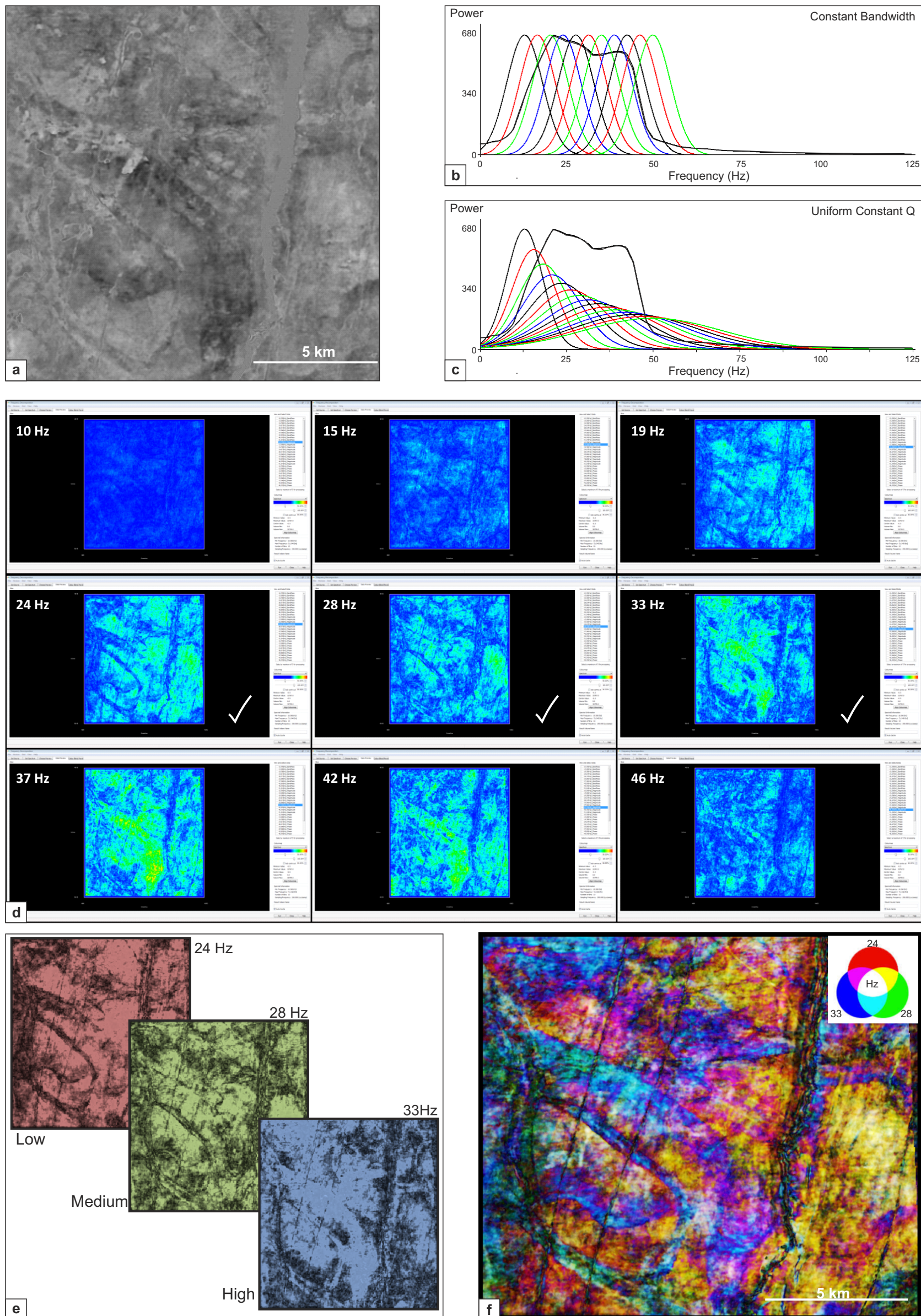


Figure 5.9: Stages in the creation of an RGB blended volume. **a:** Target horizon slice (seismic amplitude), poorly imaged. **b:** Frequency spectrum with Constant Bandwidth frequency bands. **c:** Frequency spectrum with Uniform Constant Q frequency bands. **d:** Preview slices from frequency band volumes. Those at 24, 28 and 33 Hz show different details of features. **e:** Chosen input volumes for the blended volume are coloured red, green and blue respectively. **f:** RGB blended volume showing much more detail than the horizon slice (**a**), with contrasting channel (blue) and overbank (yellow) deposits.

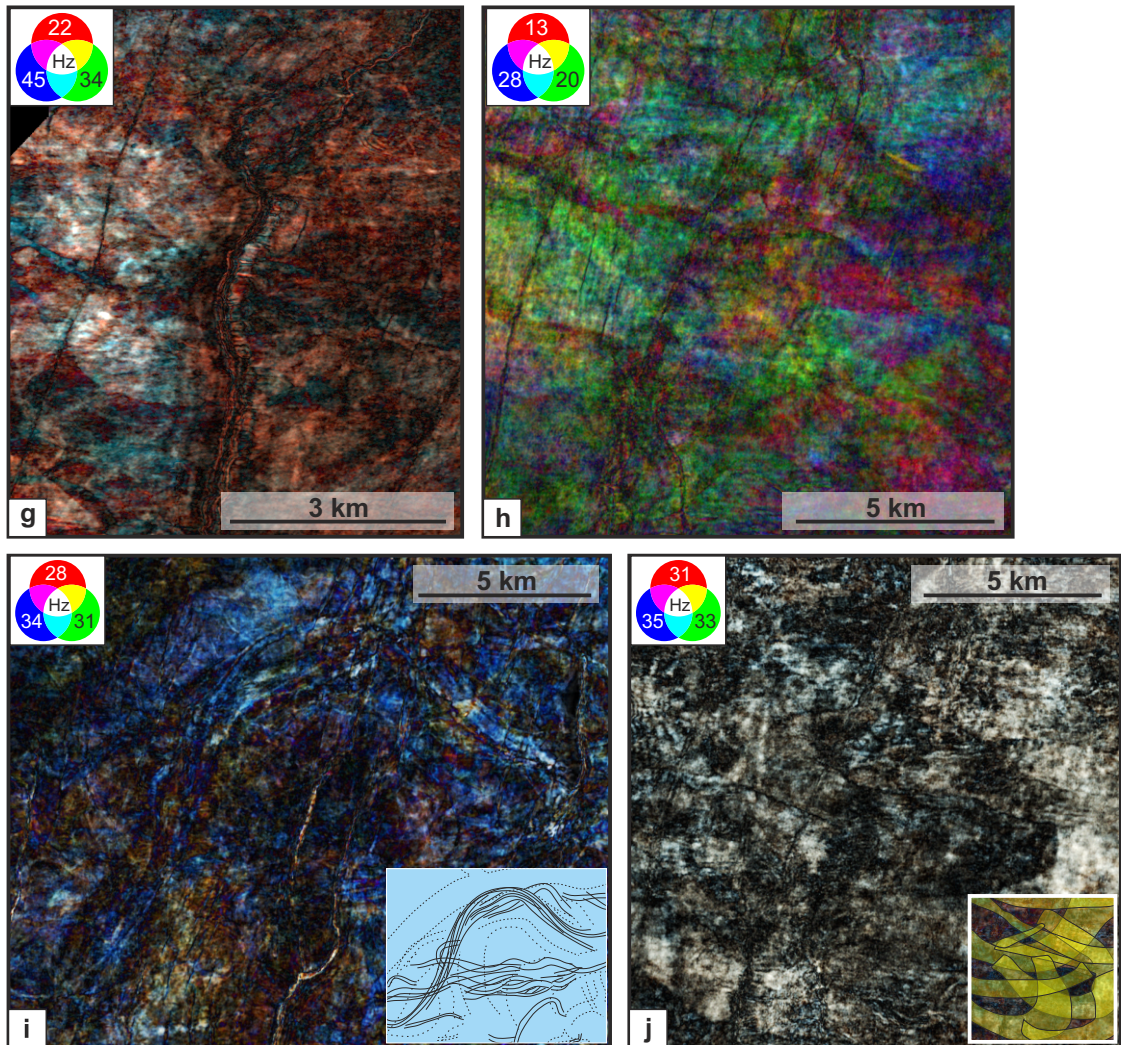


Figure 5.9 continued: Improperly balanced RGB colour blends. **g:** Colour blend biased towards the lower frequency (red). **h:** Colour blend biased towards the middle frequency (green). **i:** Colour blend biased towards the higher frequency (blue). Inset figure shows sketched outlines of channel belt deposits. **j:** Colour blend where frequencies are too close together, giving a grey colouration. Inset figure shows sketch outline of valley geobodies.

(analogous to Fast Fourier Transform) increases the bandwidth of the frequencies by a constant amount (Figure 5.9c). This latter method gives a better vertical resolution than Constant Bandwidth, but less separation of frequency colours.

A series of magnitude volumes is generated (one for each of the frequency bands defined on the spectrum), which show the same seismic slice at different frequencies (Figure 5.9d). Three magnitude volumes are selected, from a low, medium and high frequency, these are coloured red, green and blue, respectively (Figure 5.9e). Volumes that show different, contrasting features should be selected. When blended together, the RGB blended volume highlights features corresponding to the three frequency channels. Where the volume has a strong response from all three frequencies, the volume appears white; a red, green or blue hue indicates a bias towards a particular frequency. The resulting volume highlights features that were not discernable using the original seismic volume (Figure 5.9f), with contrasting colours corresponding to the frequency responses of different lithologies and fluid content.

5.4.2 HD frequency decomposition (HDFD)

High-definition frequency decomposition (HDFD) is based on a matching pursuit algorithm (McArdle & Ackers, 2012). This method of frequency decomposition is useful in fluvial settings where thinly-bedded deposits abound as greater vertical resolution is achieved with less vertical 'smearing' of the data, thereby giving better delineation of subtle features (Figure 5.10). However, the contrast between frequencies is not as great as with RGB blending, and the process is considerably more time-consuming. Chapter 6 details a case study where HDFD lends more detail to the interpretations of depositional architecture made.

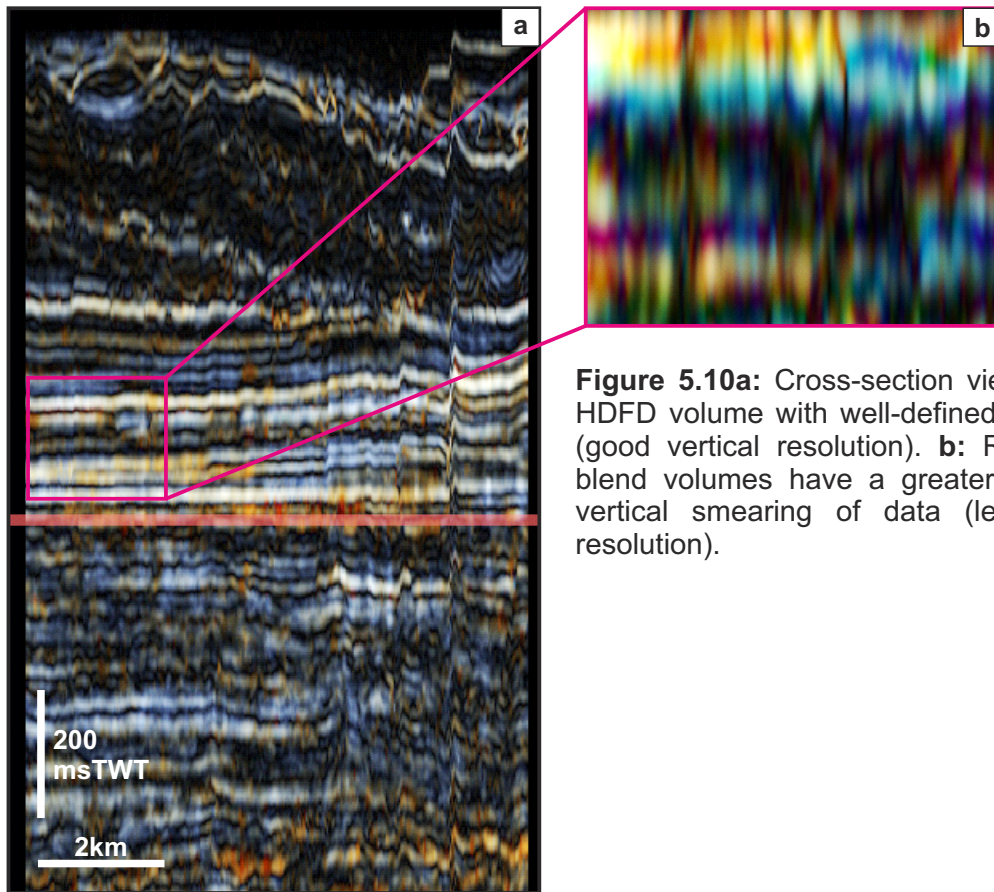


Figure 5.10a: Cross-section view from an HDFD volume with well-defined reflections (good vertical resolution). **b:** RGB colour blend volumes have a greater degree of vertical smearing of data (less vertical resolution).

5.5 Additional seismic methods: attributes

This section briefly considers other seismic attributes that may be useful in the interpretation of fluvial and fluvio-deltaic deposits, but were not focussed upon in this project. The attributes discussed herein were computed in Petrel™ and Geoteric™.

5.5.1.1 RDR Edge Detection (Petrel™)

This surface attribute highlights sharp edges in seismic data and is typically used to identify faults (which are expressed as approximately N-S aligned lineaments in the Colmbard survey Mungaroo Formation). The attribute also appears to have highlighted some individual meander loops within channel belt deposits (Figure 5.11).

5.5.1.2 Dip angle (Petrel™)

The dip angle was calculated as a surface attribute, highlighting higher-angle inclined reflections associated with faults and channel belt deposits (Figure 5.12). Relatively high-angle dipping features that may represent individual incision events by mobile channels within the channel belt are highlighted. Care must be taken when inferring such deposits in cases where the dipping beds are at the channel-belt margin, as the dip angles may simply be responding to the edge of the channel belt rather than a smaller channel body nested within it.

5.5.1.3 Dip Azimuth (Petrel™)

The dip azimuth, calculated as a surface attribute, reveals a structural trend within the Colmbard survey, aligned E-W (Figure 5.13), that is not associated with N-S aligned, post-depositional extensional faulting, and may be exerting a

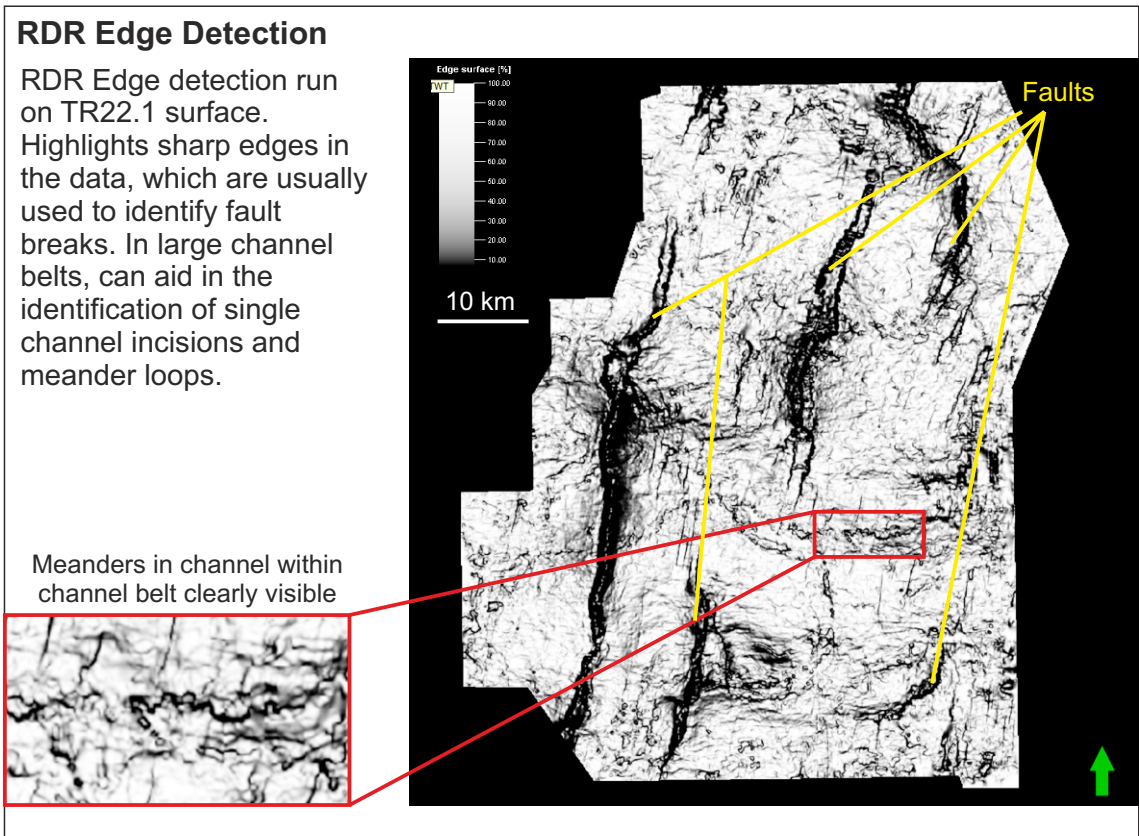


Figure 5.11: RDR Edge Detection surface attribute, highlighting sharp edges in the data, including faults and incised channel features.

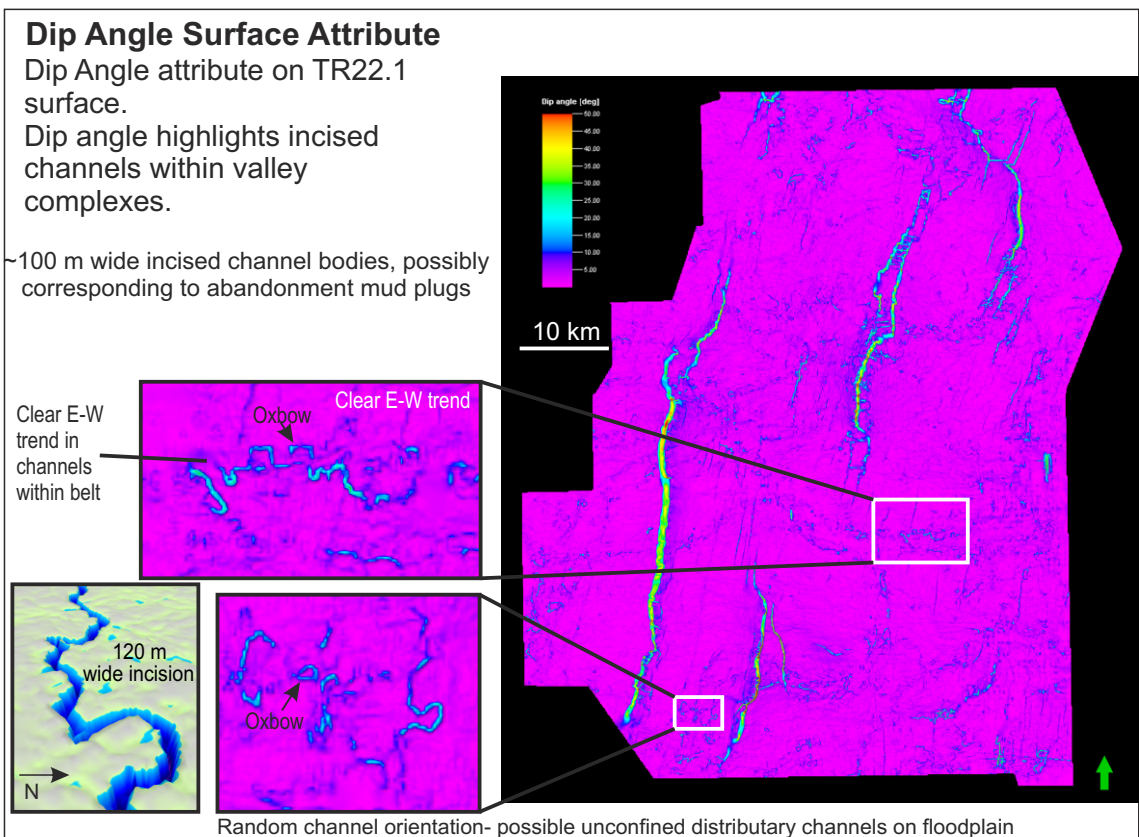


Figure 5.12: Dip angle surface attribute highlighting faults and other relatively high-angle inclined features. Two possible incised, meandering channel features are highlighted.

subtle structural control on the orientation of regional drainage patterns (regional Mungaroo Fm palaeoflow is approximately east-to-west).

5.5.1.4 Relative Acoustic Impedance (AI) (Petrel™)

Relative acoustic impedance indicates apparent acoustic contrast, and can highlight variations in porosity and fluid content. Figure 5.14 shows an example from one of the channelized sand-bearing intervals, where channel-belt deposits have a positive RAI and overbank deposits have a negative RAI. This attribute can indicate sand-rich areas, but does not delineate the overall plan-form geometry of the deposits in as much detail as horizon slices.

5.5.1.5 Bedform (Geoteric™)

The bedform attribute is a phase-based attribute (ffA, 2013). Lineaments are extracted along their minimum and maximum phase. This can aid in resolving discontinuous, thin events into a continuous, mapable reflection. Figure 5.15 shows a cross-section view of the bedform attribute. Reflections are relatively continuous across the cross section. An area showing multiple phases of infill within an entrenched valley or channel-belt feature is highlighted.

5.5.1.6 Terrace Thickness (Geoteric™)

Where 2 beds of thinly bedded deposits show as a doublet rather than two discrete wavelets, the terrace attribute attempts to resolve the inflection points of the doublets into discrete wavelets. The resulting output is displayed as voxels (Figure 5.16). Terrace thickness is a measure of the difference between inflection points on a trace. Thickness of beds is represented as a colour response. Darker colours indicate thicker beds. Application of this technique can help to identify discrete channelized bodies.

Dip Azimuth

Dip azimuth attribute produced for seismic horizon S7. Similar trends are seen on other horizons.

Dip azimuth reveals E-W / SE-NW structural trend.

Possibly influencing Triassic drainage network orientation (Mungaroo Fm regional paleoflow approx E-W).

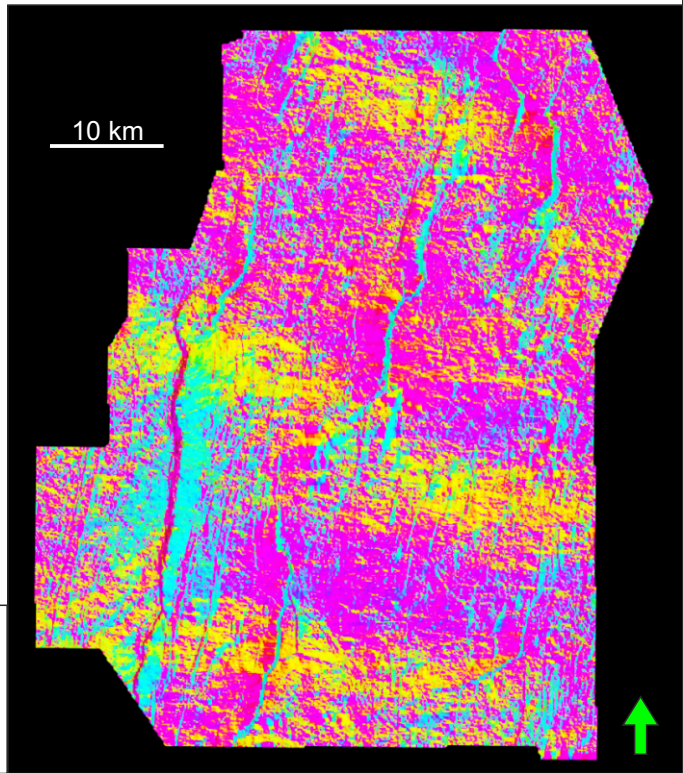
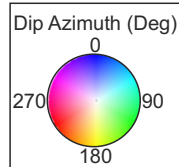


Figure 5.13: Dip azimuth surface attribute highlighting local (N-S faults) and regional structural trends.

Relative Acoustic Impedance

Positive relative acoustic impedance at ~4000 m within sinuous channel form relates to 40 m fluvial channel sand intersected by well Martin-1 at 3942-3982 m TVDSS (responding to higher porosity, sand-prone deposits).

Martin-1: Channel Sand

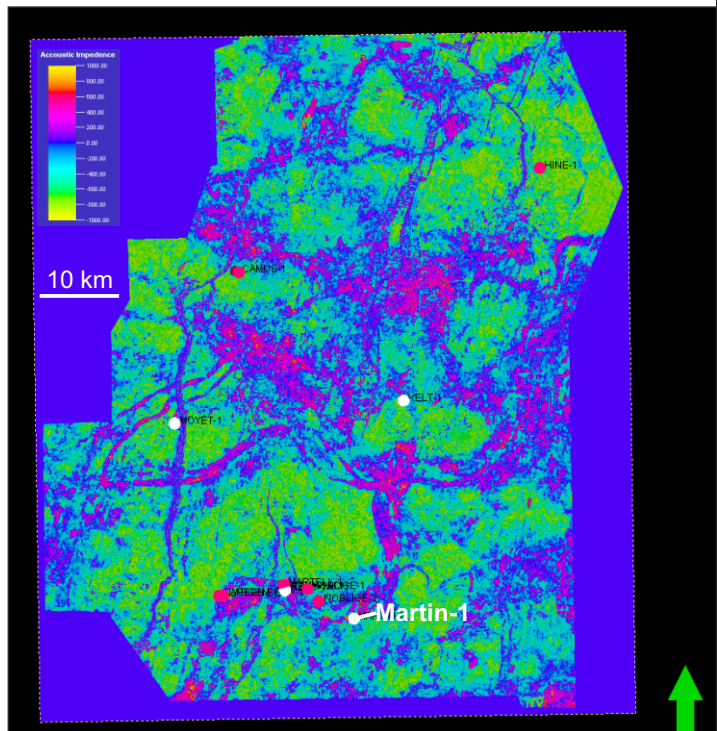
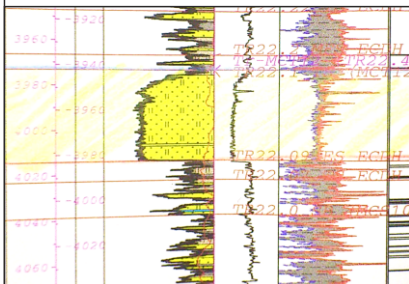


Figure 5.14: Relative acoustic impedance attribute responding to porosity contrasts within the formation.

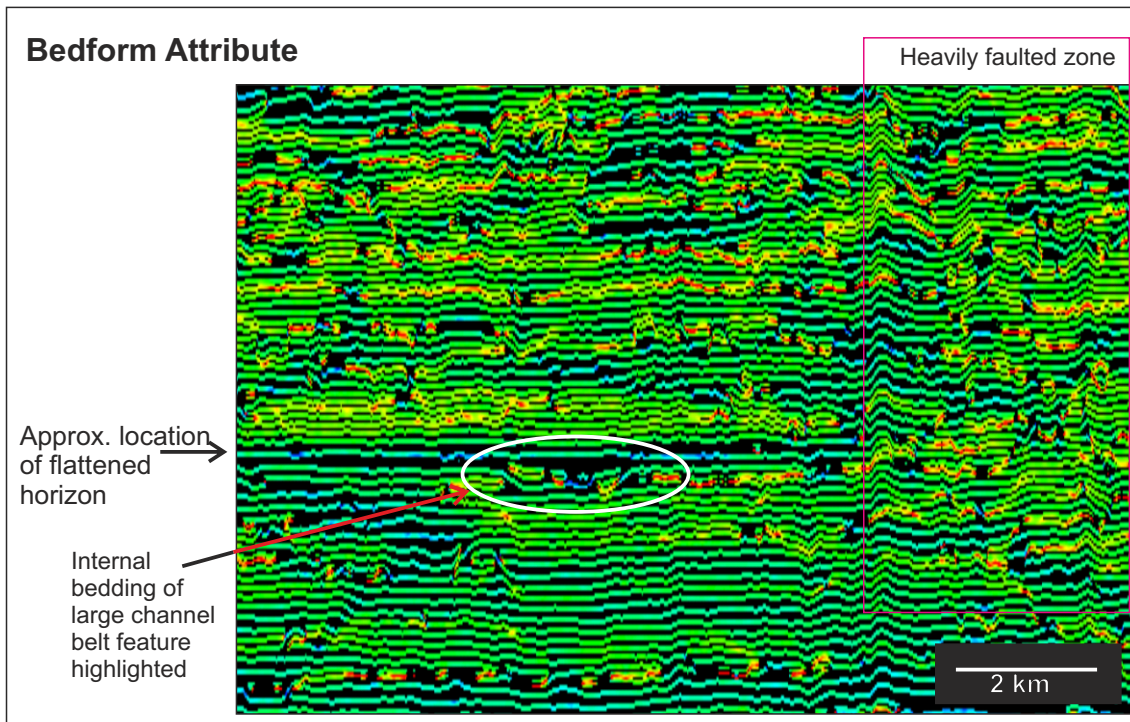


Figure 5.15: Bedform attribute (bedform frequency) showing continuous beds and, circled, fluvial deposits with multiple phases of fill below a flattened horizon.

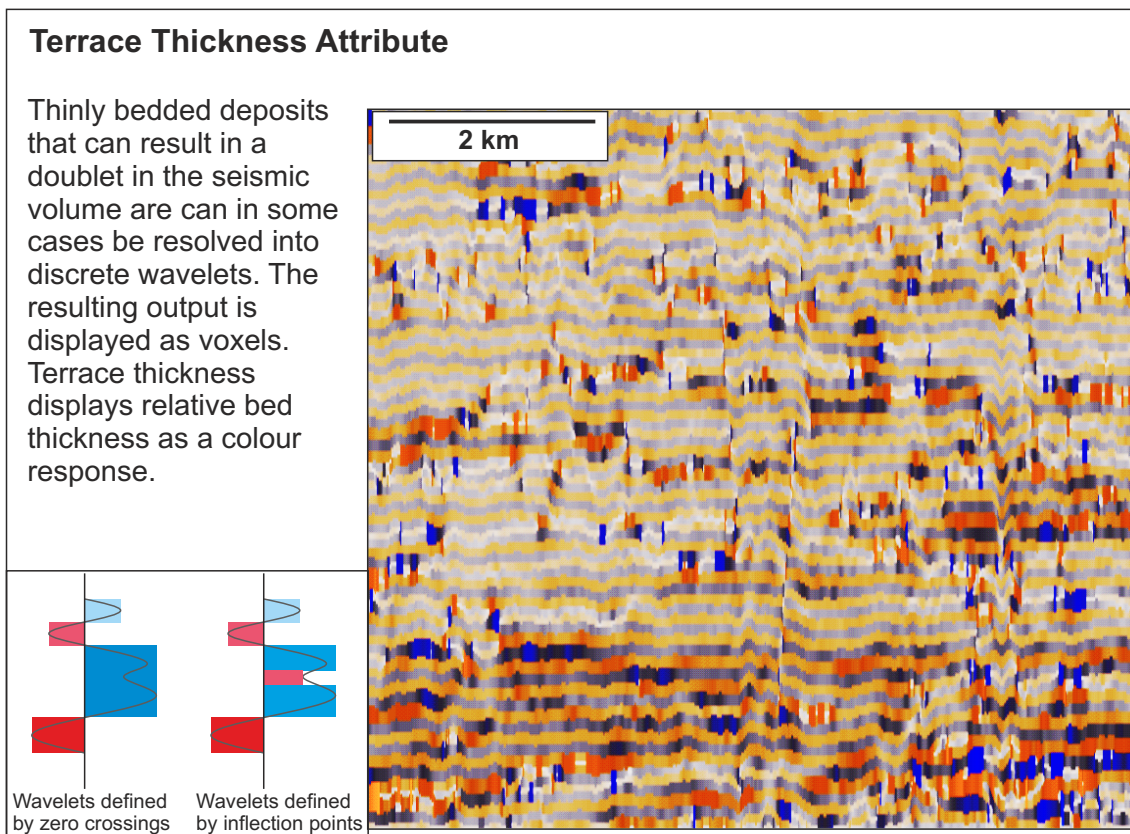


Figure 5.16: Terrace thickness attribute. Darker areas indicate thicker deposits.

5.6 Chapter summary

Accurate interpretation of fluvial deposits using seismic data requires integration with well log data, including wireline and core, and, where possible, placing the deposits within a sequence stratigraphic context. Flooding and transgressive surfaces, being regionally continuous and recognizable both in seismic data and well logs, form more reliable well correlation and seismic interpretation horizons than sequence boundaries. Noise reduction and frequency enhancement workflows can aid in enhancing thinly-bedded deposits, while horizon slicing and proportional slicing reveal stratally aligned deposits. Frequency decomposition enables the visualisation of deposits that are below normal seismic resolution by allowing the viewer to focus on specific frequency ranges revealing subtle features. The aforementioned techniques proved the most consistently reliable while studying the Mungaroo Formation, however a number of other structural, signal processing and stratigraphic attributes have also been shown to aid in the identification and interpretation of fluvial deposits, most notably dip angle, tentatively identifying single channel bodies within channel belts, and relative acoustic impedance, distinguishing between higher porosity sand-rich channel belt deposits, and lower porosity overbank fines.

Chapter 6 Architecture of a fluvio-deltaic succession investigated with seismic attribute analysis and spectral decomposition: Late Triassic Mungaroo Formation, offshore Western Australia

Research question: How can a range of seismic interpretation techniques, including spectral decomposition, be used to resolve the internal architecture of channel-belt deposits? Can these techniques provide further insight into fluvial styles, distinguishing between entrenched valleys and amalgamated channel belts?

6.1 Chapter Overview

Many reservoir targets in relatively low net-to-gross fluvio-deltaic successions comprise thinly bedded sandstone bodies with complex geometries; such architectural elements are, typically, poorly imaged using conventional seismic interpretation techniques. The Late Triassic Mungaroo Formation present in the subsurface offshore Western Australia comprises a succession of fluvial and deltaic architectural elements at a variety of scales. Reliable interpretation of the paleoenvironmental significance of these deposits requires a combined stratigraphic and geomorphologic approach using core, wireline and seismic data. The high-resolution Colmbard 3D seismic cube (block WA-404-P) encounters fluvial-deltaic deposits between ~3000 and 5000 ms TWTSS and within this interval the succession has been studied in detail from 3400 - >4300 ms TWT. A workflow is presented for the recognition and interpretation of fluvial deposits from subsurface datasets that involves data conditioning, horizon slicing (domain transform) and spectral decomposition. The preserved Mungaroo Formation has been interpreted at 3 different intervals, representing

two fluvial and one deltaic paleoenvironment. Interpreted deposits include: multi-story, multi-lateral meander-belt deposits contained within incised valley systems, vertically amalgamated channel-belt deposits, and successions composed of individual meandering channels with associated point-bar deposits. Results from analysis of reflectivity horizon slices are compared to spectrally decomposed horizon slices: spectral decomposition more clearly images valley, channel-belt and even individual channel features, at depths >3 km. Interpretations made using spectral decomposition have significance in planning well placement. Morphological components of the modern Peace River, Alberta, Canada, are analogous to the meandering channel and bar elements. The deposits represent lowstand systems tracts (incised valley and low accommodation lateral accretion deposits) and highstand systems tracts (high accommodation delta plain distributary deposits) that can be interpreted within the framework of a series of stacked buffer zones and transgressive events that, themselves, record repeated base-level rise and fall.

6.2 Introduction

6.2.1 Context

Most fluvial successions include sandstone bodies that can be laterally constrained on a scale of several tens of meters to hundreds of metres. Many such bodies are thinly-bedded (commonly <10 m) and commonly exhibit complex lateral and vertical connectivity relationships (Colombera et al., 2012, 2013; Gibling, 2006; Wood, 2007). As hydrocarbon exploration increasingly targets smaller, thin-bed pay, it has become ever more important to glean as much geologic information from subsurface core, well-log and seismic data as possible, by adopting an integrated sedimentology, stratigraphy and geomorphology approach (Chopra & Marfurt, 2008; Posamentier, 2013).

From the standpoint of imaging fluvial bodies using seismic techniques, thin-bedded units are those that are near or below seismic resolution. If a sand body is thinner than $\frac{1}{4}$ wavelength (λ) of the seismic wavelet, the top and bottom of the unit are difficult to resolve independently (Widess, 1973; Kalweit & Wood, 1982). $\lambda/8$ is generally considered the limit of seismic resolution (Widess, 1973), although greater resolution has been demonstrated in experimental setups (Chopra et al, 2006).

Currently employed seismic interpretation techniques have developed from 2D seismic sequence stratigraphy (Vail et al, 1977), which assumes that seismic reflections are stratigraphically significant surfaces, thereby allowing the interpretation of genetic depositional units. The advent of 3D interpretation techniques has incorporated attribute analysis and stratigraphic techniques such as 3D and 4D Wheeler diagrams, computed from 3D seismic data (e.g., de Groot et al, 2010; Qayyum et al, 2014). Spectral decomposition – a technique to improve seismic imaging by breaking down the seismic signal into its component frequencies – can be used to reveal geologic information in 3D seismic datasets that cannot be fully resolved using standard reflectivity data (McArdle & Ackers, 2012), particularly where clastic deposits have sharp impedance contrasts (Partyka et al, 1999). Spectral decomposition allows the visualization of the seismic response at discrete frequency intervals. Decomposing seismic data into its spectral components can reveal stratigraphic and structural details that are often poorly imaged in the seismic volume. Frequency responses can be interpreted; for example, lower frequencies typically image thicker beds, whereas thinner beds are best imaged at higher frequencies (Partyka et al, 1999; Van Dyke, 2010).

The use of stratal slicing (Zeng et al., 1998^a; Zeng et al., 1998^b; Zeng et al., 2001) and domain transforms (Dorn, 2011; 2013) to produce flattened horizon and stratal cubes allows for the visualization of complex or subtle depositional geomorphologies (Posamentier, 2013) that cannot be seen on time slices. Stratal slicing and domain transforms overcome some of the visualization problems associated with time slicing; principal among these is that to view stratal geometries, time slices need to be time-conformable with seismic-stratal events but this is rarely the case due to the structural dip and thickness variations of deposits (Zeng et al., 2001). Stratal slices are proportionally sliced between interpreted horizons. In a proportionally flattened cube, the cube is viewed in the stratal domain such that time slices are effectively stratal slices. In a cube that is flattened on one horizon, time slices are 'horizon slices'. These stratal viewing techniques are particularly useful in analysis of fluvial successions (Hardage & Remington, 1999; Wood et al, 2000; Wood, 2007), where discontinuous, erosive deposits prove difficult to map as continuous seismic horizons (Hardage et al, 1994; Roksandic, 1995; Payenberg et al., 2013).

6.2.2 Aim and objectives

The aim of this study is to present a workflow whereby seismic data can be conditioned, stratally interpreted and spectrally decomposed to better image relatively thinly-bedded fluvial deposits, more fully resolving features that are near or below conventional seismic resolution. Specific objectives are as follows: (i) identify areas within the formation that are likely to be composed internally of a substantial proportion channelized architectural elements of fluvio-deltaic origin; (ii) to illustrate how frequency decomposition can be used to better resolve the external geometry and internal architecture of a range of

complex sandstone geo-bodies of fluvio-deltaic origin; (iii) to outline a technique for the identification of deposits revealed by the spectral analysis; (iv) to present a method for the classification of fluvial channel styles; (v) to show how a range of integrated seismic analysis techniques can be applied to provide further insight into the depositional environment of the Late Triassic Mungaroo Formation of the NW shelf of Australia.

This chapter develops the observations and interpretations presented in Chapter 4 by allowing a more detailed view of the internal architecture of channel belt and valley deposits: Frequency decomposition allows the visualization of features that are below the normal resolution of seismic data. This chapter also attempts to place the more successful techniques employed in Chapters 4 and 5 in a concise, repeatable workflow. Study area & geological setting

6.2.3 Study area & data

The study area is the ~3000 km², Woodside Endergy Ltd operated, offshore block WA-404-P, on the Exmouth Plateau, NW Australia (Figure 6.1), which is imaged by the Colmbard 3D seismic survey. The Colmbard survey is a pre-stack depth-migrated, zero-phase, 3D seismic reflection survey. The inlines and cross-lines are oriented E-W and N-S, with spacings of 15 m and 12.5 m, respectively. This study uses the Near Stack volume of the survey. The survey has negative polarity, such that a downward increase in acoustic impedance (hard kick) corresponds to a negative amplitude reflection and a downward decrease in acoustic impedance (soft kick) is represented by a positive amplitude reflection. For the purpose of this study, positive amplitudes are shown as red or black, negative amplitudes are shown as blue or white. The study area has an average water depth of 1.3 km.

This study focuses on a ~1200 km² subset of the survey area, studying a >1 km-thickness succession of the Late Triassic Mungaroo Formation. The study additionally makes use of 11 wells with wireline log suites, 2 of which also have core (Figure 6.2). The approximate vertical resolution of the Colmbard dataset at the depth of the Mungaroo Formation is 20 m.

6.2.4 Geological setting

The NW Shelf of Australia spans >2400 km along the NW margin of Australia (Figure 6.1b) and forms part of the Westralian Basin. The NW Shelf comprises four offshore basins: Northern Carnarvon Basin, Roebuck Basin, Browse Basin and Bonapart Basin (Yeates *et al.*, 1986; Westphal & Aigner, 1997; Longley *et al.*, 2002; Marshall & Lang, 2013). The Exmouth Plateau forms the outboard section of the Northern Carnarvon Basin. The Northern Carnarvon Basin is bound to the north, west and southeast by the Argo, Gascoyne and Cuvier Abyssal plains, and to the east by the Australian Craton (Hocking *et al.*, 1987).

The Triassic deposits of the NW Shelf comprise the Locker Shale, Mungaroo Formation and Brigadier Formation (Jablonski, 1997). At this time the pre-rift sag Northern Carnarvon Basin formed a large, westerly dipping, flat ramp cratonic margin, and constituted part of the continental margin on the NE edge of Gondwana (Westphal & Aigner, 1997). Drainage from the east may have originated from the Ross High in central Australia and passed through the Canning Region, and also from the Pilbarra Craton (Seggie *et al.*, 2007; Payenberg *et al.*, 2013). Triassic sediments are known to be up to 4 km thick in the inboard NW Shelf, and are suggested to be up to 6 km thick in some parts of the Exmouth Plateau (Adamson *et al.*, 2013).

The Mungaroo Formation is a Carnian-Norian age fluvio-deltaic system that developed to a size similar to that of the modern Mississippi delta system (Jablonski, 1997). The climate in the Late Triassic is interpreted to have been temperate-warm, humid and monsoonal, with wet and dry episodes (Dickens, 1985; Bradshaw *et al.*, 1994; Payenberg *et al.*, 2013, Preto *et al.*, 2010; Arche & López-Gómez, 2013). Studies of the Mungaroo Formation identify a variety of depositional styles associated with multi-valley complexes (i.e. multi-phase valley fills; multilateral and amalgamated valley fill over a regionally smooth erosional surface, cf. Holbrook, 2001). Multi-phase valley fills (Marshall & Lang, Adamson *et al.* 2013; Payenberg *et al.* 2013) have been interpreted in areas penetrated by relatively more in-board wells in an up-dip location relative to WA-404-P (Figure 6.1). Both large (≤ 2 km wide, ≤ 15 km long) and small-scale (250-750 m wide, 50-10 km long), predominantly low-sinuosity channels have been interpreted in the Mungaroo Fm ~200km to the south of the study area by Heldreich (2013), as have tidally-influenced and deltaic deposits (Longley *et al.*, 2002; Marshall & Lang, 2013).

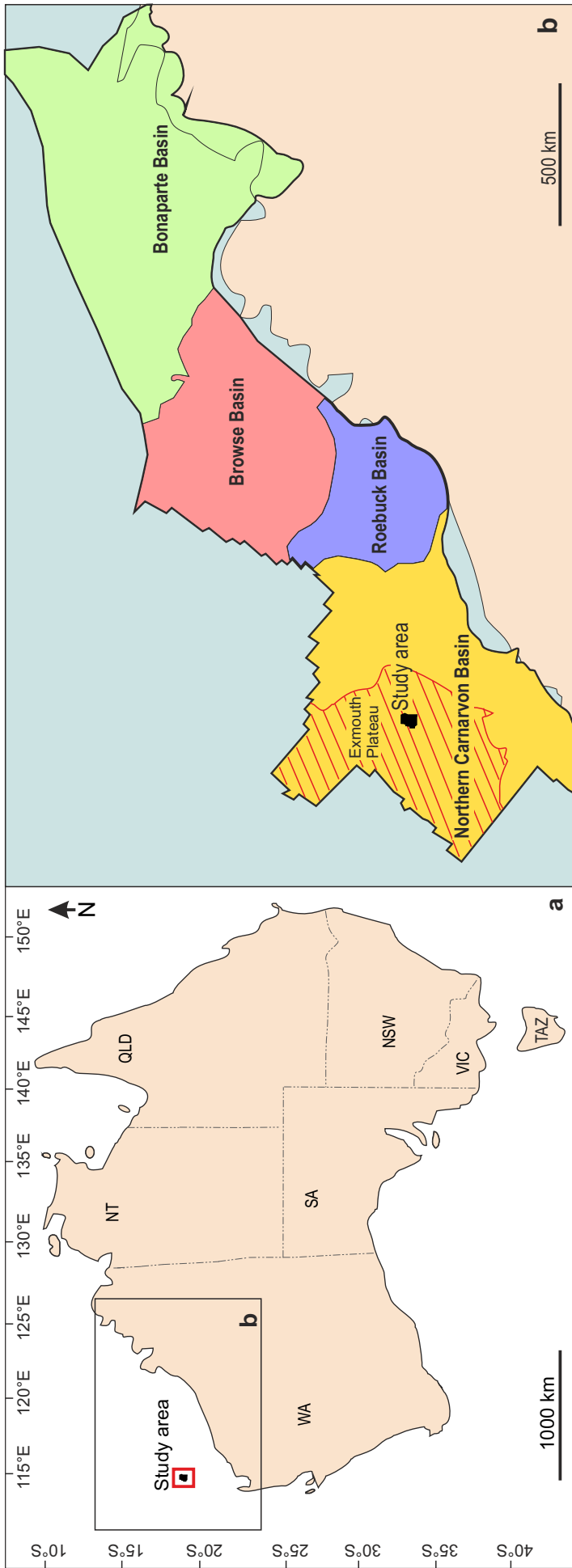


Figure 6.1: (a) Location of the study area, offshore NW Australia. (b) Overview map showing the location of sedimentary basins on the Exmouth Plateau; the study area is located in the Northern Carnarvon Basin.

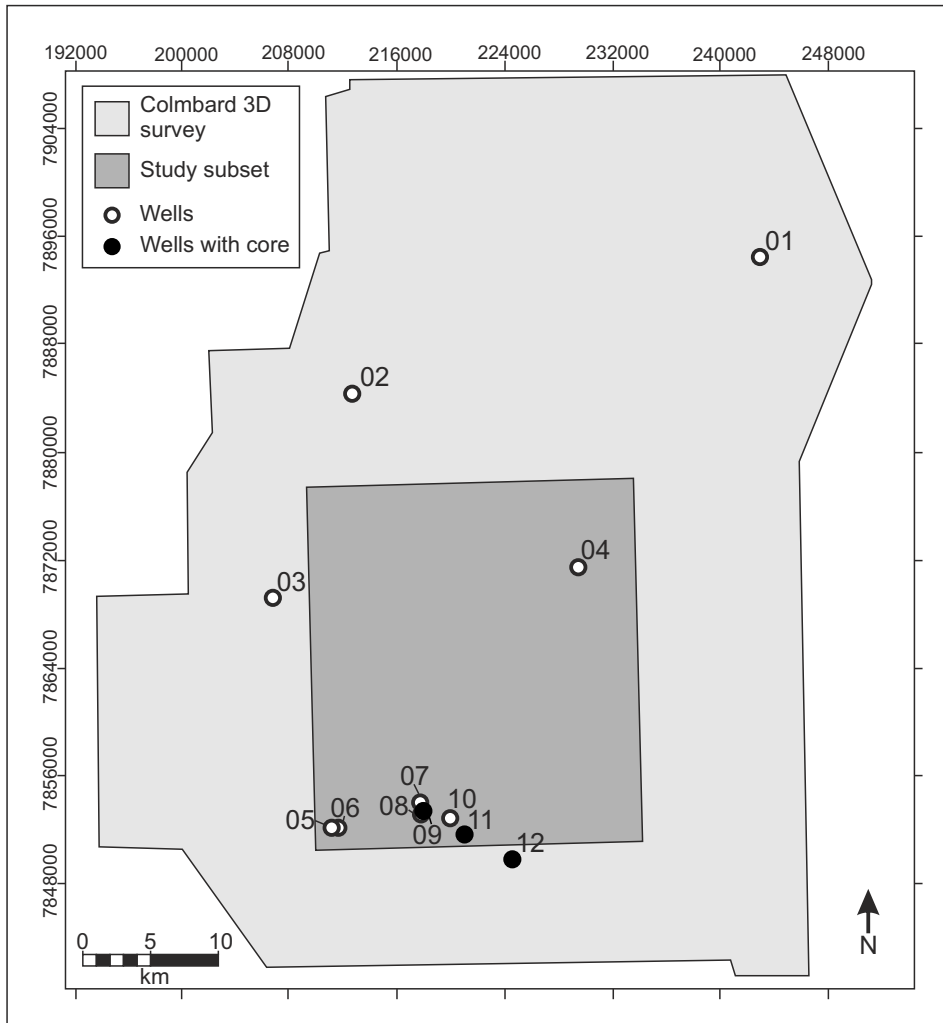


Figure 6.2: Location of wells and study subset within the area covered by the Colmbard 3D seismic survey. Grid measurements are given in m (UTM zone GDA94_50S).

6.2.5 Stratigraphy

The Mungaroo Formation records the overall transgression of a fluvio-deltaic system (Payenberg et al., 2013). Within this overall trend, several high-frequency transgressive-regressive cycles are recorded and these have been identified using seismic and well data (Adamson et al., 2013; Marshall & Lang, 2013). The stratigraphy of the Mungaroo Formation has been described by Marshall & Lang (2013) and Adamson et al (2013). Using a combination of seismic, sedimentological and palynological data, these authors describe third-order cyclicity within the formation whereby cycles are bound by key stratal surfaces linked to regionally correlatable seismic horizons. In the Marshall & Lang (2013) study, the Triassic is split into three regional play intervals, TR10 (252.2-237.0 Ma), TR20 (237.0-209.9 Ma) and TR30 (209.5-201.3 Ma) that are themselves split into sub-plays. Within the sub-plays, third-order stratal surfaces were identified. This study examines the TR20 play interval, investigating the Norian deposits of the Mungaroo Formation. Figure 6.3 shows a chronostratigraphic column for the region, and highlights the stratigraphy and seismic horizons studied. The Mungaroo Formation stratigraphy is summarized in further detail in Chapter 3.

6.3 Methods

The workflow adopted is set out in Figure 6.4. Six of the regionally-defined key stratal surfaces (c.f. Marshall & Lang, 2013) were interpreted in the TR20 play interval in this study; one surface was interpreted from the TR30 interval. Due to the discontinuous nature of the accumulations of sand-prone fluvial deposits, many of which apparently fill incised-valley systems associated with major incision events (Payenberg et al., 2013), sequence boundaries proved difficult to map in the seismic data. The majority of the surfaces interpreted are

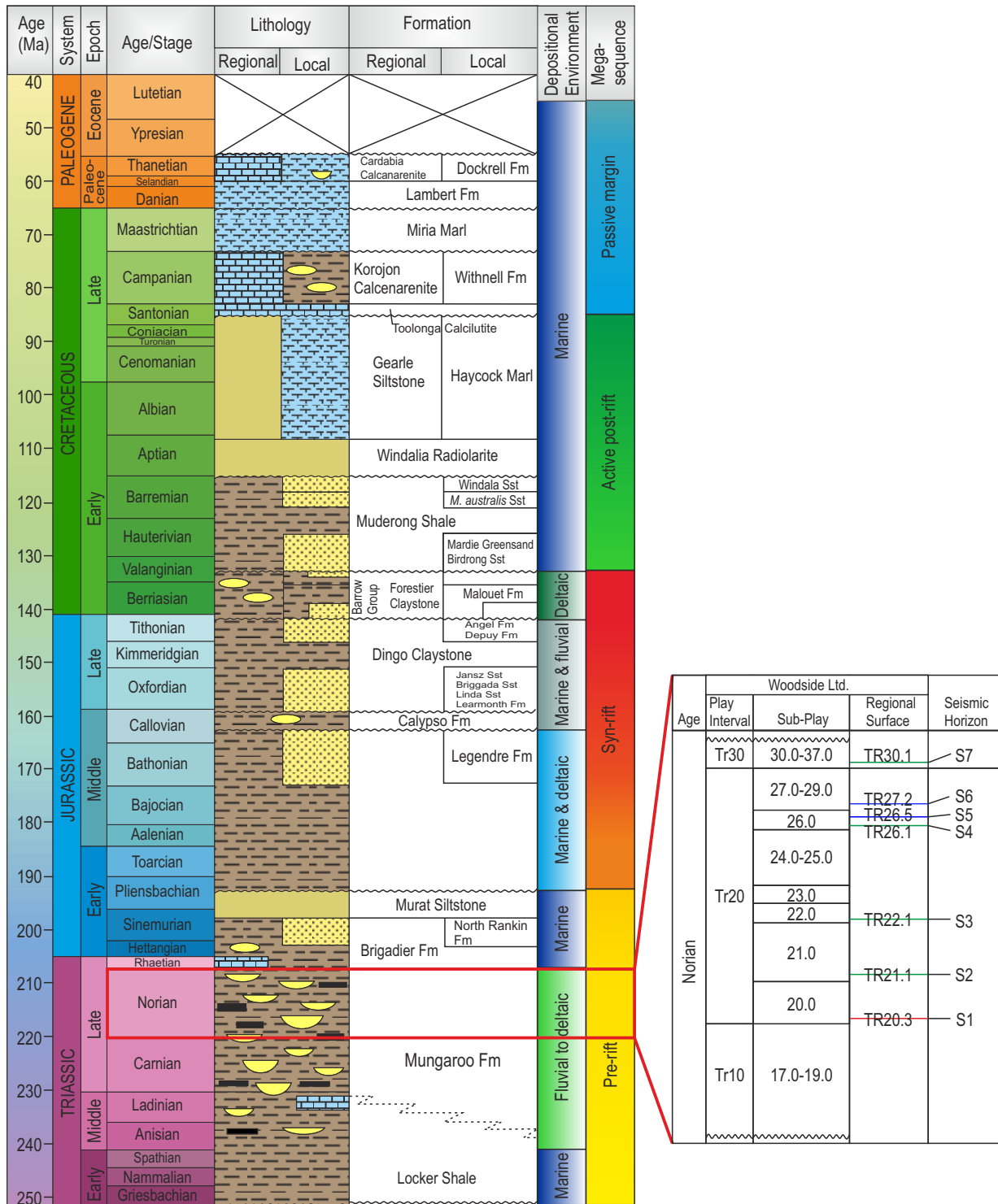


Figure 6.3: Stratigraphy of the Northern Carnarvon Basin (after Longley et al., 2002) Inset lists stratigraphic nomenclature for key horizons used in this study (after Marshall & Lang, 2013). Red lines denote surfaces of regional extent and seismic horizons that represent sequence boundaries; green lines denote transgressive surfaces; blue lines denote maximum flooding surfaces. Seismic surfaces used in this study (S1-S7) correlate to region-wide stratigraphic surfaces.

transgressive surfaces (TS), as these were the most laterally continuous and readily traceable seismic events. Table 6.1 lists the stratigraphic surfaces and the corresponding seismic horizons (S1-S7) interpreted. These stratigraphic surfaces were identified in well logs and used in a seismic-to-well-tie (Figure 3.7)

Table 6.1: Stratigraphic surfaces used in the study.

Seismic horizon	Mean Elevation (-ms TWT)	Stratigraphic surface	Bounding surface type	Stage
S7	3335	TR30.1	Transgressive surface	Norian
S6	3517	TR27.2	Maximum flooding surface	Norian
S5	3592	TR26.5	Maximum flooding surface	Norian
S4	3713	TR26.1	Transgressive surface	Norian
S3	3955	TR22.1	Transgressive surface	Norian
S2	4175	TR21.1	Transgressive surface	Norian
S1	4510	TR20.3	Sequence boundary	Norian

Figure 6.4: Summary of workflow undertaken in the study involving noise cancellation, horizon slicing (flattening on stratal surfaces), and spectral decomposition.

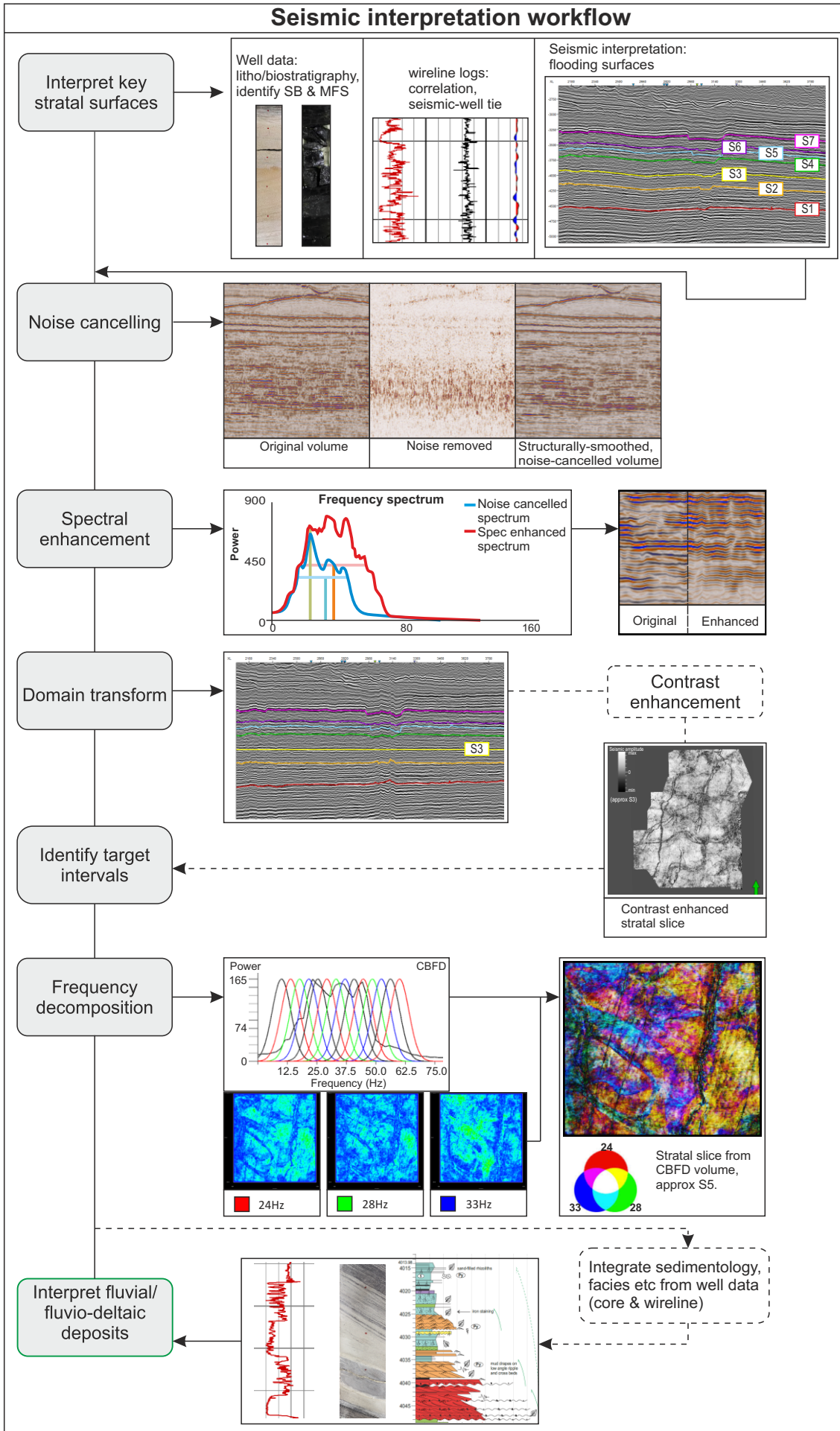


Figure 6.4: Seismic interpretation and frequency decomposition workflow.

A subset from the central region of the seismic data cube measuring 30 km x 40 km and encompassing the TR20 and TR30 play intervals was selected for detailed analysis (location shown on Figure 6.2). The subset volume was conditioned to eliminate structural and random noise. The resultant noise-cancelled volume was spectrally enhanced to boost the higher frequency data and improve the vertical resolution of the data. This was undertaken to better image thin beds in the higher frequency ranges.

Flattened volumes were then created for each horizon. This domain transform enabled the visualization of horizon slices, imaging channelized deposits that were approximately time-conformable with the flattened surface. Horizon slicing is deemed appropriate where formations are relatively sheet-like, but not flat-lying (Zeng & Hentz, 2004). The sub-parallel nature of the key horizons in the Mungaroo Formation lends itself to this method. The flattened cubes were used to identify target intervals for spectral decomposition. Contrast enhancement (Kidd, 1999), which involved re-scaling the color scale to fit the range responding to the fluvio-deltaic deposits, was carried out where necessary in zones with low contrast between channelized and non-confined (i.e. floodplain) deposits.

Spectral decomposition was performed over target intervals around the S2, S6 and S7 horizons. Three methods of spectral decomposition were employed, using GeoTeric™ software. The methods are explained in some detail by McArdle & Ackers (2012) and McArdle et al. (2014). Two band-pass filtering decomposition methods were employed: (i) Constant Bandwidth frequency decomposition (CBFD), in which an identical bandwidth is assigned to each frequency decomposition band; and (ii) the Uniform Constant Q (UCQ) method, analogous to Fast Fourier Transform (FFT), where the bandwidth of the

frequencies increases by a constant amount. High-definition frequency decomposition (HDFD) is based on a matching pursuit algorithm (McArdle & Ackers, 2012), which is useful for visualizing thin-bedded deposits, since there is less vertical 'smearing' of the data.

The reflectivity attribute maps shown in Figure 6.5 are horizon slices, taken from a flattened volume and as such represent amplitude extractions at discrete depths. The flattened volume has been frequency decomposed and colour blended, so that the same horizon slice may be viewed in the frequency domain.

Fluvial and fluvio-deltaic deposits were identified in the spectral decomposition volumes. The architecture of key deposits was mapped out such that the depositional environment could be interpreted for each studied interval.

6.4 Results

6.4.1 Comparison of seismic reflection to frequency decomposition data

The results of frequency decomposition applied to three key target intervals (S1-S2, S5-S6, S6-S7) within the subset volume are shown in Figure 6.5. The locations of wells are shown within the subset. Although the fluvial and fluvio-deltaic deposits are poorly imaged on the (flattened) seismic volume, the corresponding spectral decomposition volumes more clearly imaged these deposits. The poor realization of the deposits on reflectivity data is most likely due to the relatively thin nature of some of the deposits: individual channel-belt architectural elements range 6 m to 12 m thick in core and are composed of fining-upwards units of fine to coarse grained, poor to moderately sorted sandstone with high-angle inclined trough and planar cross-bedding (Stuart et al, in review). The subsurface depth of the study intervals (interpreted flattened

slices) range from -3414 ms TWT to -4320 ms TWT. The lithology of many of the relatively low-energy channel bodies is characterized by heavily cemented siltstones, giving a poor impedance contrast between these channels channel and concurrent silt-prone overbank deposits.

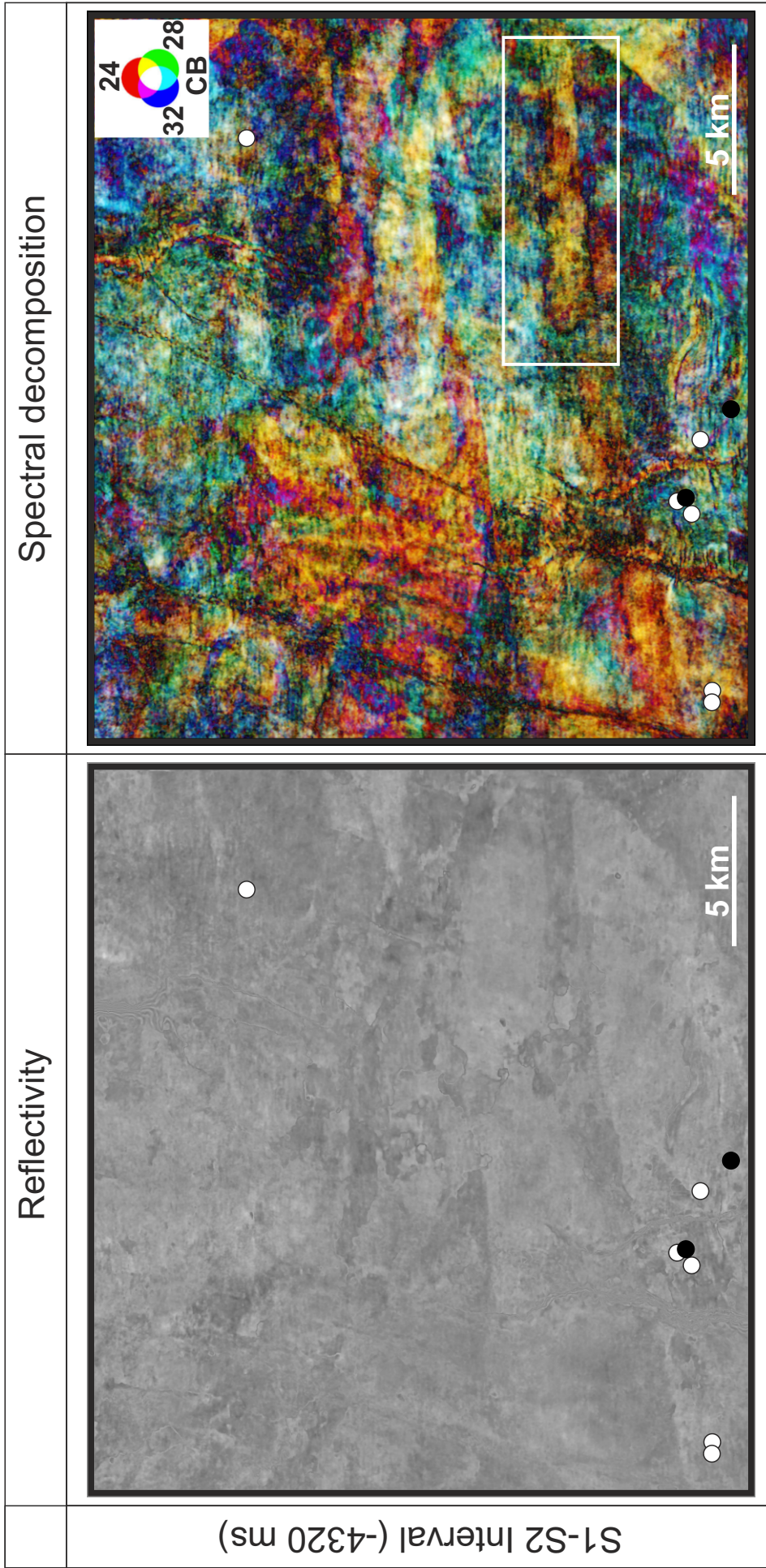


Figure 6.5: Reflectivity and spectral decomposition stratal slices from the S1-S2, S5-S6 and S6-S7 intervals, taken at -4320, -3458 and -3414 ms TWT from the subset volume, respectively (location shown on Figure 2). The three volumes used were flattened on S2, S6 and S7, respectively. Deposits are poorly imaged on the reflectivity volumes, but much more clearly imaged on their respective spectral decomposition volumes. Outputs from CBF, UCQFD and HFD are shown. The stratal slices shown from the spectral decompositions represent the best imaged volumes. The positions of wells are shown. **a:** Reflectivity and RGB blended stratal slices from the S1-S2 interval used for comparison of visible features. The white box in the S1-S2 slice defines a region of interest (ROI) for interpretation.

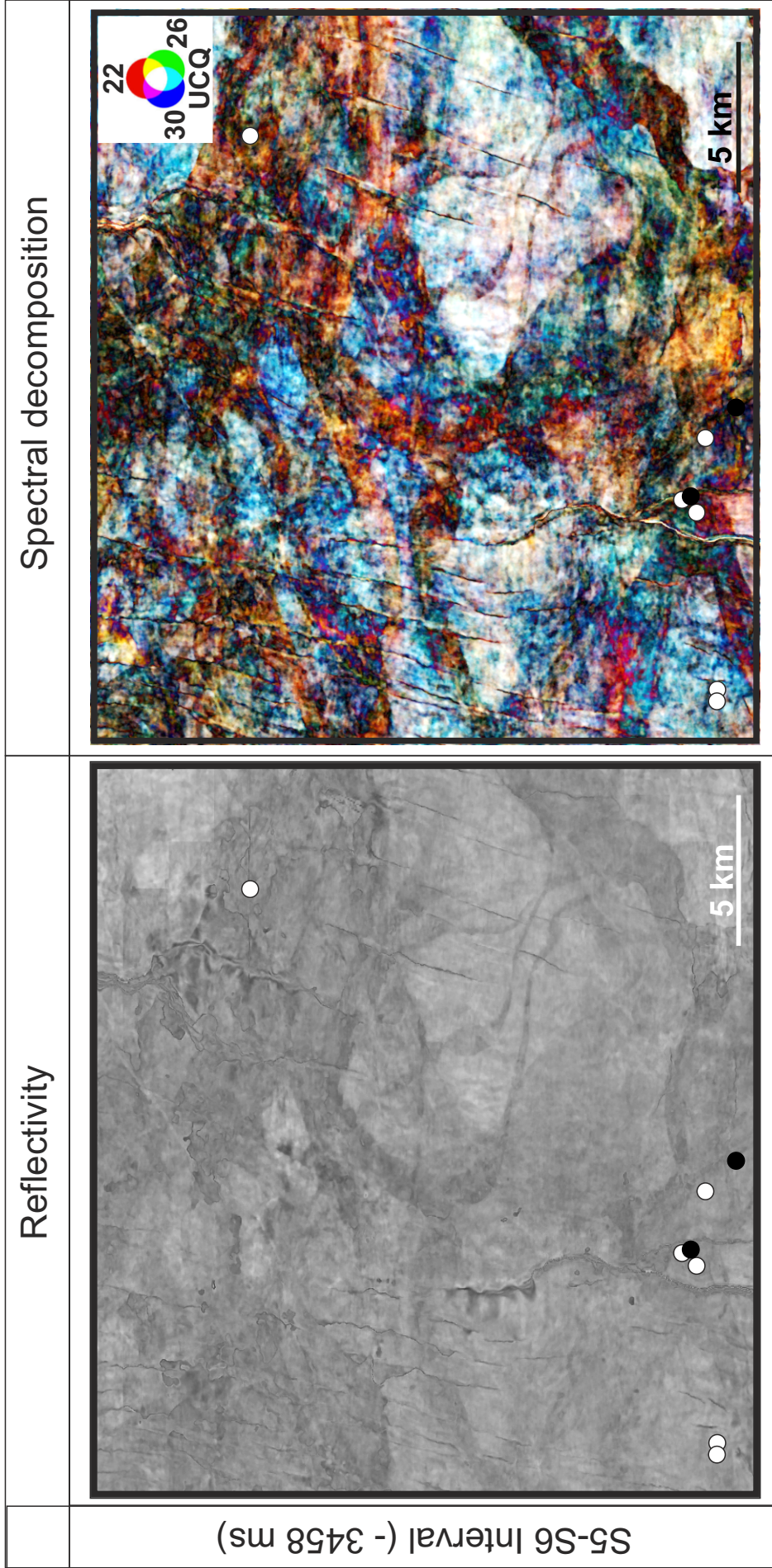


Figure 6.5b: Reflectivity and RGB blended stratal slices from the S5-S6 interval used for comparison of visible features.

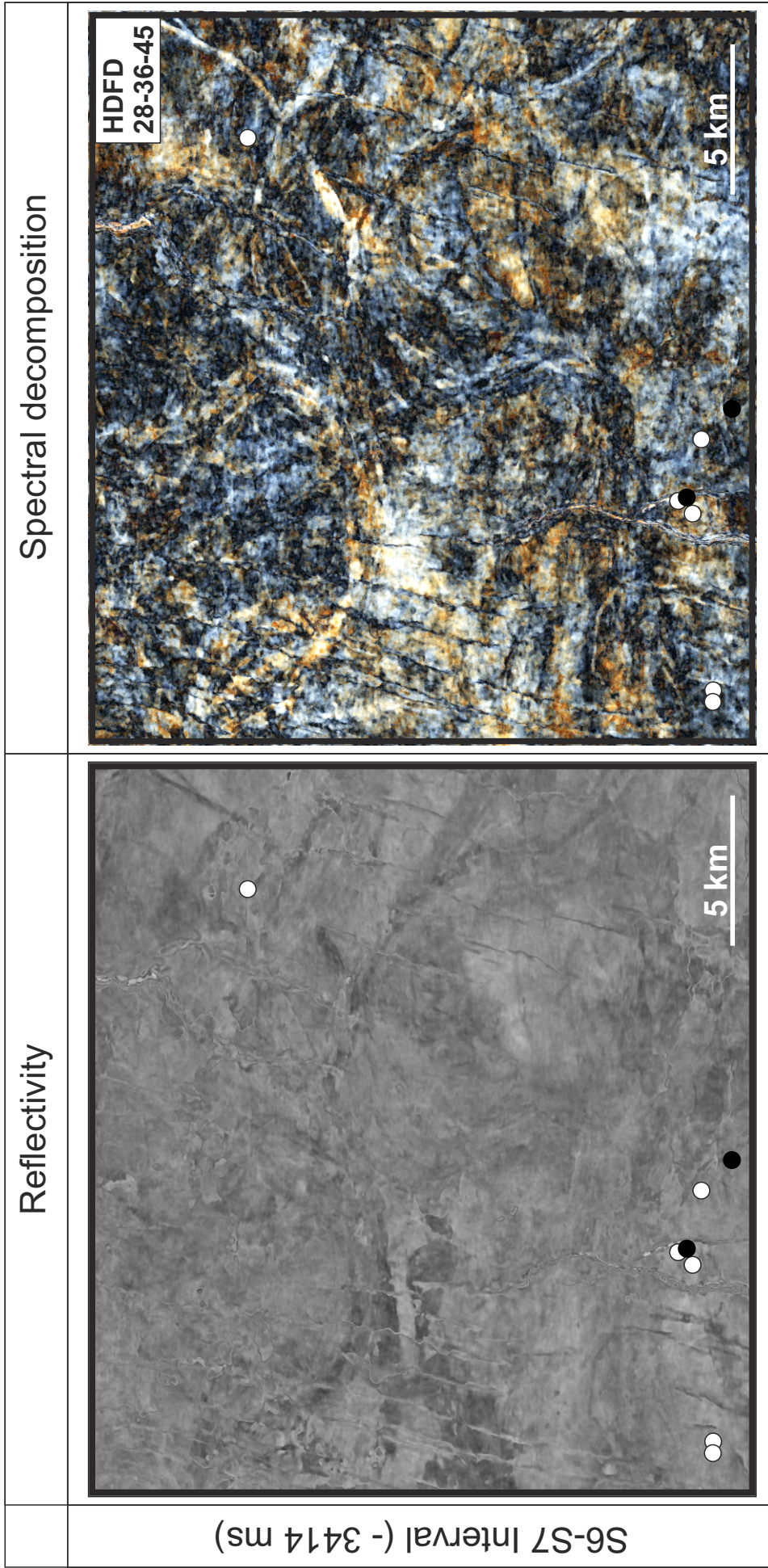


Figure 6.5 c: Reflectivity and HDFD blended stratal slices from the S6-S7 interval used for comparison of visible features.

The S1-S2 interval deposits were best imaged with the Cbfd method. The lower vertical resolution of this method was well suited to the large-scale deposits, which are encountered over a 40ms window. The greater separation of frequencies offered by this method (McArdle & Ackers, 2012) gives rise to high-contrast, vivid output. Figure 6.5 shows the reflectivity and Cbfd slice at -4320 ms TWT from the stratally flattened volume (flattened on S2).

The UCQFD method gave the sharpest imaging of the deposits in the S5-S6 interval. Figure 6.5 shows a representative stratal slice at -3458 ms TWT, taken from the volume flattened on S6. The large, unclear deposits visible on the reflectivity data are resolved into numerous, contrasting deposits with spectral decomposition.

A stratal slice taken from the S6-S7 interval at -3414 ms TWT shows deposits that appear to have an overprinting form, but these are poorly imaged on the reflectivity slice. Both UCQFD and HDFD techniques were employed; the greater vertical resolution of the output from HDFD most clearly imaged the form of the overprinting deposits.

6.5 Fluvio-deltaic architectural elements

6.5.1 Meander belts (S1-S2)

Description. Horizon slices from the S2 flattened volume reveal several large (~2 km-wide), very-low sinuosity features (Figure 6.6a). Two of these features are orientated ENE-WSW and are almost straight. A region of interest (ROI) is identified around the southern-most of these features. Within the valley, a bright, apparent higher sinuosity feature can be identified and was mapped on horizon slices over a 44 ms window (Figure 6.6b-f). As the feature is traced on successively shallower slices, it can be seen to migrate laterally.

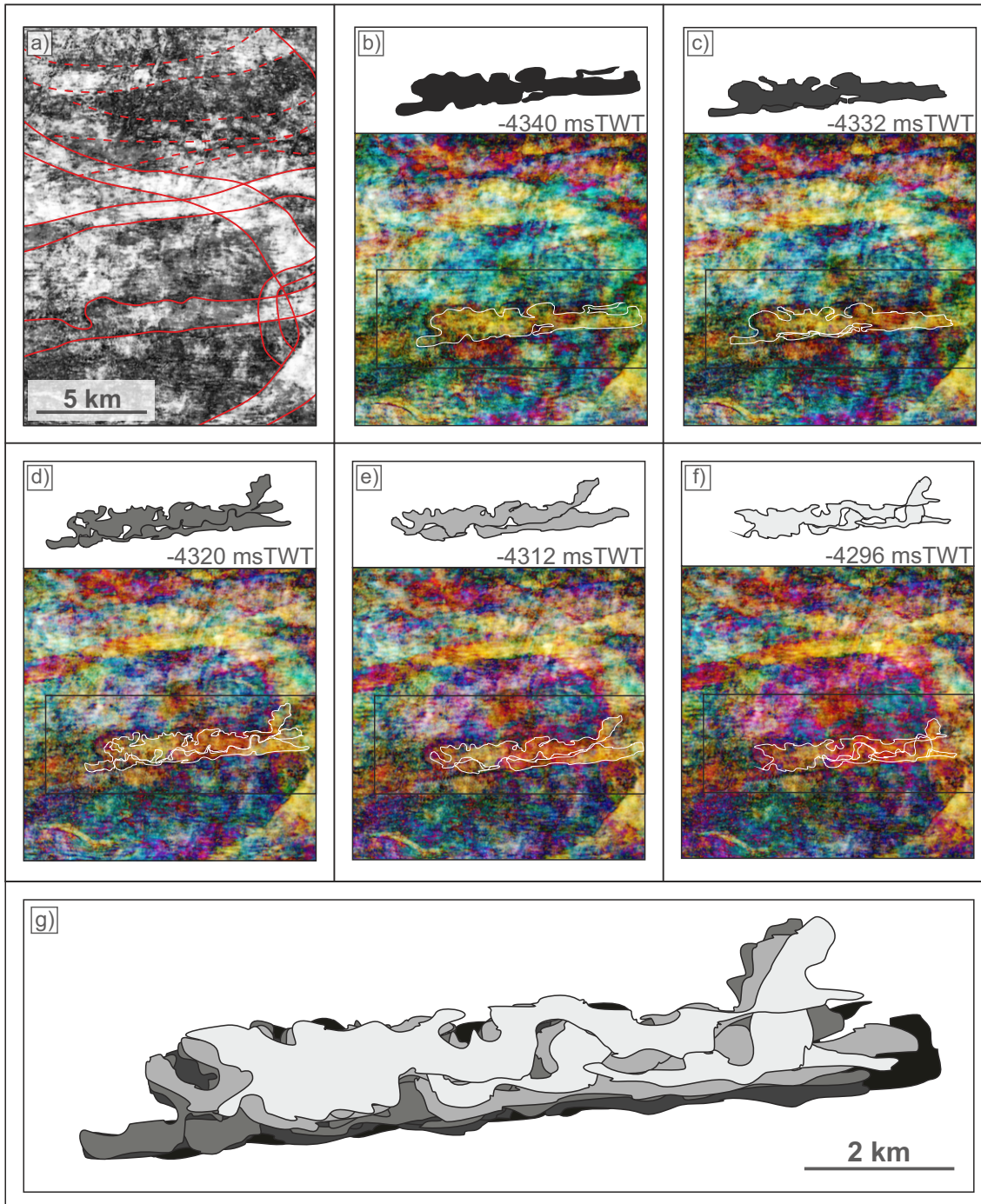
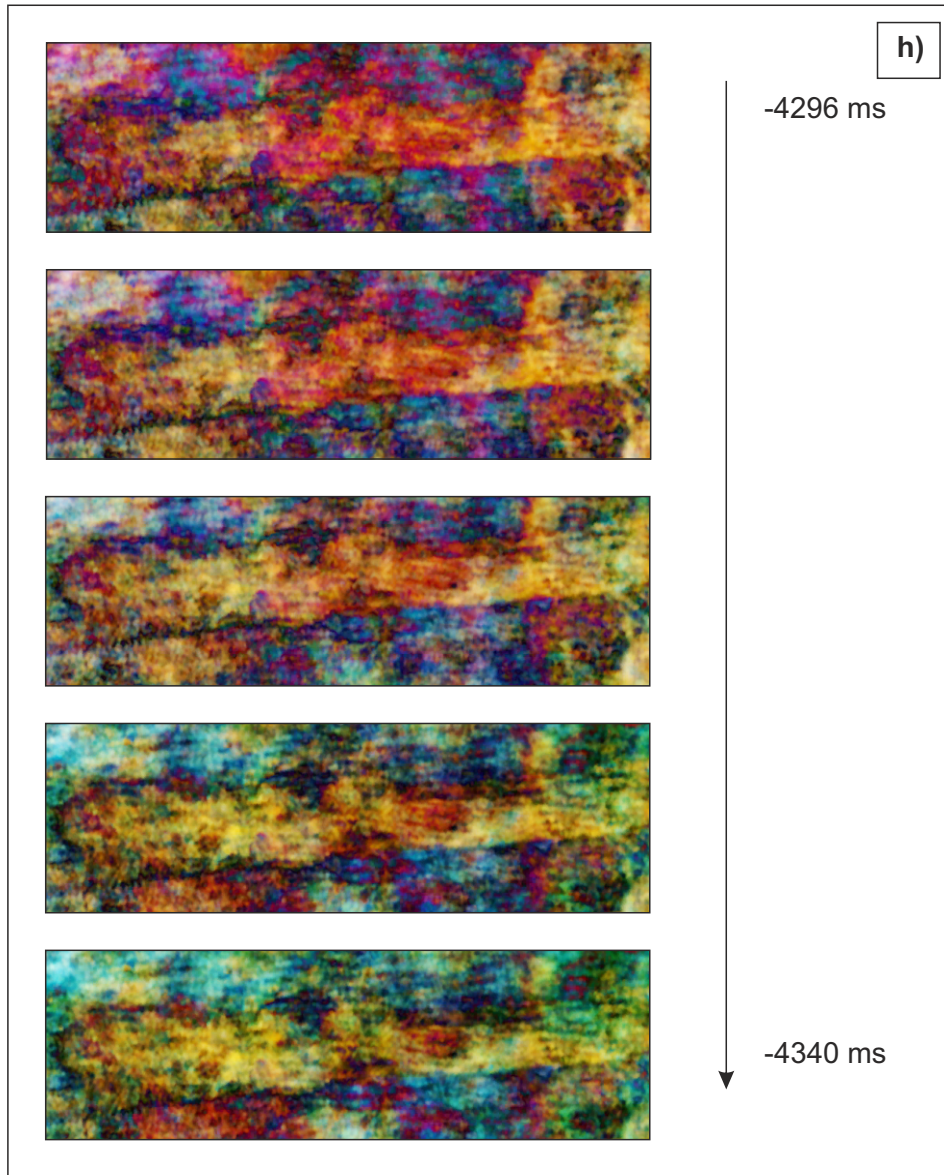


Figure 6.6: Interpretation of fluvial features identified in Figure 6.5a. Several low-sinuosity features can be mapped on CB frequency decomposition data (a) features highlighted by solid lines are interpreted with higher confidence than those with stippled outlines. (b) to (f) show slices from the same CB volume, moving up through a 40 ms window. Within the channel belt, a brighter area is interpreted as meander-belt deposits, with only the brightest areas outlined (ROI outlined in white, and shown in inset diagram). (g) These deposits accumulated via lateral migration. (h) over-page, uninterpreted view of the ROI between -4296 and -4340 ms.



Interpretation. The feature is interpreted as having undertaken some lateral migration and comprises vertically stacked channel belt deposits, within the confines of an incised valley (Figure 6.6a). Other incised features from this interval can be seen in profile in Figure 4.11a. The criteria for the interpretation of incised valleys at this interval are as follows: (i) presence within a regionally identified lowstand systems tract, as interpreted by Adamson et al. (2013); (ii) the border of the features appear sharp, and much more well-defined than those of the internal 'bright' features (interpreted as the sand-rich meander belt); (iii) absence of visible splay belt, lacustrine or other alluvial plain deposits associated with non-confined fluvial deposits. Incised valleys commonly contain fluvial deposits at their base (Posamentier, 2001), transgression and erosion typically leads to poor, patchy preservation of these deposits (Allen, 1991; Allen & Posamentier, 1993; Zaitlin et al., 1994). Posamentier (2001) suggests that two mechanisms for the exceptional preservation of fluvial deposits within incised valleys: firstly, rapid transgression would cause high energy coastline deposits to pass swiftly over the fluvial deposits, minimizing the potential to erode the underlying fluvial deposits; secondly, a low energy coastal system would also have a lower potential to erode

Although only the large-scale valley and channel belt morphologies can be seen in the spectrally decomposed volume (and not the small-scale, individual channel morphology), an attempt can be made to classify the types of channels active in the system. The planform geomorphology of the meander belts provides some insight into the nature of the deposits. The channel-belt rugosity (Payenberg et al, 2014) can be used as a means to estimate the nature of the rivers that formed the deposits. Payenberg et al. (2014) use rugosity to describe how dissimilar the opposing sides of a fluvial channel belt are in planview:

rugosity is used as a measure of *smoothness*, whereby the more rugose a channel belt, the less parallel two sides of the channel belt, and the less smooth the channel-belt profile. Via analysis of modern analogues, Payenberg et al. (2014) demonstrated how an increased prevalence of lateral accretion barforms from higher sinuosity channels formed higher rugosity channel belts than those formed by low-sinuosity or braided rivers with downstream accretion. Qualitative assessment of meander belts interpreted in the S1-S2 interval, –reveals a highly rugose form. Rugosity (R) can be assessed quantitatively (Payenberg et al., 2014):

$$R = (L1+L2)/(2*D) \quad (1)$$

Where L1 & L2 are the lengths of the channel belt margins and D is the straight-line distance between the end points of the channel-belt length (L3). The amount that the channel belt wanders (i.e. a measure of its sinuosity) can be quantified as:

$$\underline{W = L3/D} \quad (2)$$

W affects the value of R. Large values of wandering (W), will artificially increase the value of R. In cases of channel belts where W is high, a value of rugosity weighted for W is more appropriate:

$$Rw = (L1+L2)/2*L3 \quad (3)$$

Figure 6.7 demonstrates the method for measuring rugosity. Channel-belt dimensions have been determined by tracing and rugosity has been measured for 5 interpreted channel belt deposits from the S1-S2 interval. Table 2 shows the results of the rugosity calculations. The channel belts interpreted in the S1-

S2 interval have a R value range of 1.275-1.735. There is little difference between the values of R and R_w due to the low (<1.10) wandering (W) value.

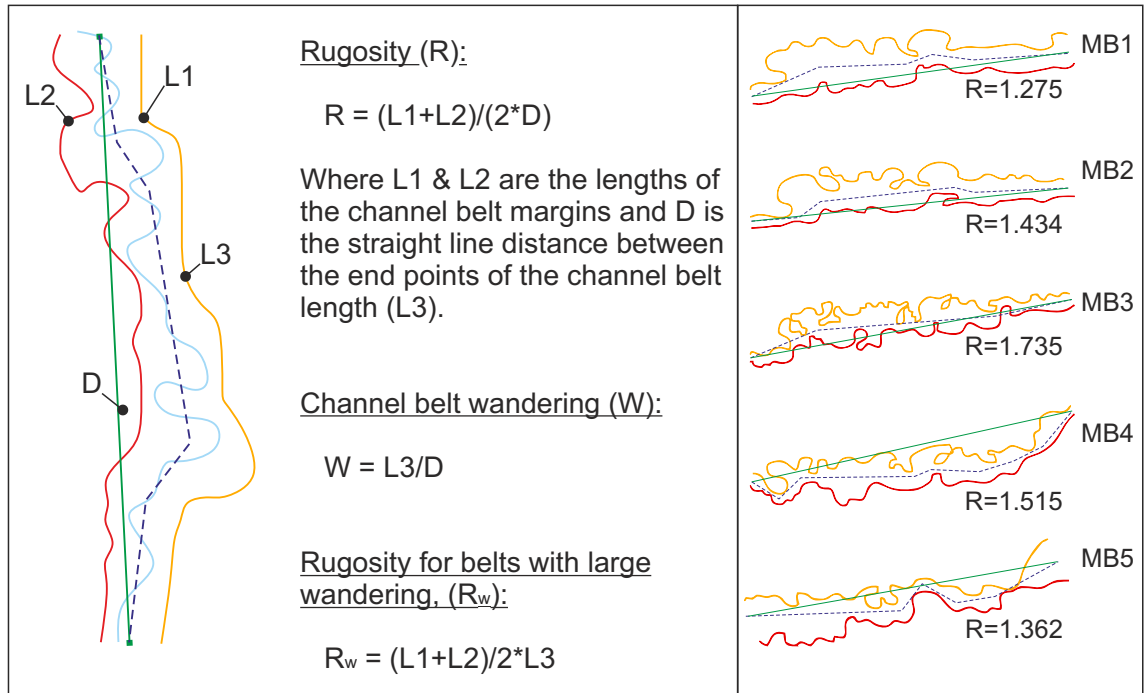


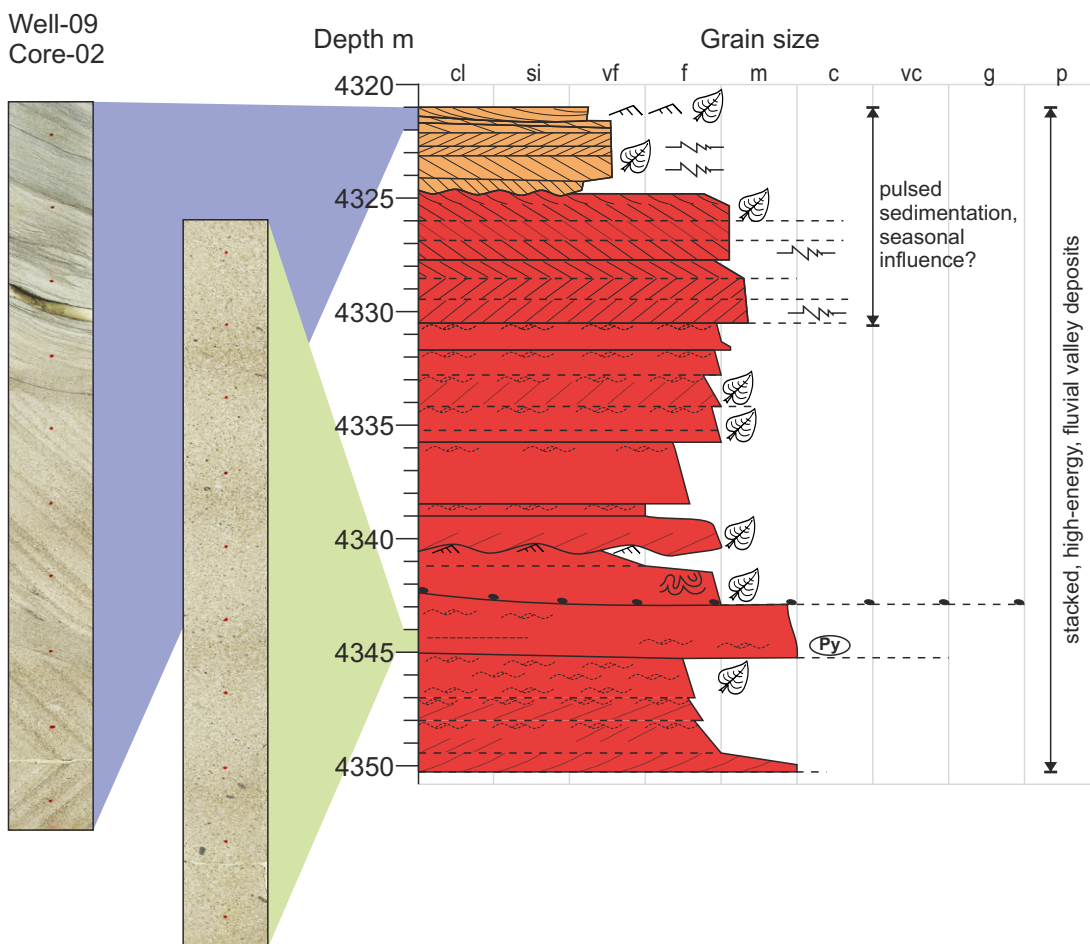
Figure 6.7: Method for determining the rugosity of an interpreted channel belt as described by Payenberg et al. (2014), using the traced S1-S2 channel belt deposits shown in Figure 6.6. Rugosity is used as a measure of how dissimilar the two opposite margins of a channel belt are. The higher the value of rugosity, the greater the disparity between the two margins. Laterally accreting bar forms from higher sinuosity channels form higher rugosity channel belts than those formed by low-sinuosity or braided rivers with downstream accretion. Using the cutoffs of Payenberg et al. (2014) whereby low- and high-sinuosity rivers are characterized by $R < 1.1$ and $R > 1.3$, respectively, the rivers responsible for the S1-S2 meander belts were most likely moderate to high sinuosity.

Table 6.2: Rugosity measurements for meander belts of the S1-S2 interval

Meander Belt	Elevation (TWTms)	L1 (km)	L2 (km)	L3 (km)	D (km)	$R = \frac{L1+L2}{2*D}$	$W = \frac{L3}{D}$	$Rw = \frac{L1+L2}{2*L3}$
MB_01	4340	15.103	11.454	10.824	10.411	1.275	1.040	1.227
MB_02	4332	16.575	11.923	10.049	9.936	1.434	1.011	1.418
MB_03	4320	20.886	14.323	10.185	10.147	1.735	1.004	1.728
MB_04	4312	16.138	11.187	9.362	9.018	1.515	1.038	1.459
MB_05	4296	11.881	10.701	8.854	8.292	1.362	1.068	1.275
					Mean:	1.464	1.032	1.422

Using the cutoffs of Payenberg et al. (2014) whereby low- and high-sinuosity rivers are characterized by $R < 1.1$ and $R > 1.3$, respectively, the rivers responsible for the S1-S2 channel belts were most likely moderate sinuosity, although the relatively long reach of channel belt used in the measurements may have biased towards a higher rugosity value.

The interpretation of the S1-S2 interval deposits as stacked fluvial valley deposits is further supported by the core and interpreted core log of Well-09 (Figure 6.8) which penetrates stacked channel deposits with no preserved overbank deposits at this interval. The lack of tidal indicators also supports the interpretation of this interval as purely fluvial rather than within the tidal-fluvial transition zone, pulsed sedimentation is instead interpreted here as an indicator of seasonal flow variation. It should be noted that a predominance of downstream accreting barforms seen in the core may indicate



Symbol key

				c			
IHS inclined heterolithic x-stratification	Ca calcite cement	Py pyrite	S siderite				

Lithofacies association

	High-energy channel		Gleysol
	Low-energy channel		Lake
	Proximal splay		Bay-fill
	Distal splay		Coal

Figure 6.8: Interpreted sedimentary log from Well-09 and supplementary photographs, showing the typical sedimentology of the S1-S2 channel deposits. The upper portion of the log shows pulsed sedimentation with regular variations in grain size, possibly indicating seasonal variations in flow conditions. The relatively coarse grain size indicates a high-energy setting. No overbank deposits were preserved in the cored interval. Infrequent changes in orientation of the planar cross beds favours the interpretation deposits formed through downstream accreting bar forms. No tidal, brackish or marine indicators.

that while moderately sinuous channel belts are indicated by their rugosity value, the rivers within them were more likely to have formed bars through downstream, rather than lateral migration.

6.5.2 Amalgamated channel belts (S5-S6)

Description. Figure 6.9 shows a horizon slice from the S5-S6 interval (Figure 6.9a), two spectral decomposition horizon slices (Figure 6.9b-c), a map of deposits based on reflectivity data alone (Figure 6.9d), a sample well log (Well 04, position given on Figure 6.2), and a map of deposits interpreted from reflectivity and spectral decomposition data. The flattened volume (Figure 6.9a) shows several broad linear to arcuate features, most notably a large (~7 km wide), SE-NW trending feature in the NE of the subset. Well 04 penetrates the feature. The features seen in the flattened volume are significantly more clearly imaged in both the UCQ (Figure 6.9b) and the HDFD (Figure 6.9c) volumes. Both spectral volumes resolve the SE-NW trending feature into several smaller (~0.5-2 km width) features.

Interpretation. Through analysis of the flattened volume alone (Figure 6.9a), the feature in the north of the subset appears to be a large, NE trending, valley deposit. Given the width (9.3 km) and vertical extent (>50 ms) of the feature, the interpretation based on analysis of the flattened cube alone was a large, multi-valley deposit, i.e. a multilateral and amalgamated valley fill over a regionally smooth erosional surface (Blum & Price, 1998; Holbrook, 2001).

The two spectral decomposition volumes (UCQ and HDFD, Figure 6.9b-c) allow an alternative interpretation, since they clearly show numerous, amalgamated, channel belt deposits (~1 km to 2km width), rather than one large valley deposit. This feature can be seen in profile in Figure 4.11c. Based on the interpretation of a large, multivalley accumulation from the reflectivity data (Figure 6.9d), Well 04, situated within the bounds of the 'multivalley', should therefore contain high net:

gross fluvial sands at this interval. Instead, the wireline logs at this interval (Figure 6.9e) show low net:gross, silty deposits. The low net:gross deposits intercepted by the well are explained by its position on the margin of one of these channel belts (Figure 6.9f). Other well penetrations in the SW of the subset show that the bright, features relate to high organic content gleysols. The general arrangement of the channel belts indicates anabranching patterns (Stuart et al., in review), typical of fluvio-deltaic distributary channels. Other overbank deposits interpreted from well logs at this interval (Adamson et al, 2013) included heterolithic bay-fill, with tidal indicators and bioturbation, indicating a poorly-drained, delta plain setting.

6.5.3 Lateral migration (S6-S7)

Description. Although the flattened volume struggles to resolve any deposits at this interval (Figure 6.10a), the UCQ (Figure 6.10b) and HDFD (Figure 6.10c) volumes image several sinuous features (≤ 1.5 km wide), several of which appear to overprint each other. The UCQ volume shows these features as relatively low frequency (red features) whose extents have been traced on the HDFD volume.

Interpretation. Fluvial deposits imaged in the S6-S7 interval are interpreted as predominantly moderate sinuosity (mean sinusosity 1.28, sinuosity range 1.05-1.61), 0.5 to 1.5 km-wide channel bodies (Figure 6.10). Where seismic reflectivity (Figure 6.10a) shows a poorly imaged 'footprint' of some of the larger features, spectral decomposition (Figure 6.10b-c) is able to more clearly image individual channel deposits with multiple phases of overprinting demonstrating the action of lateral migration and accretion (Figure 6.10d). Deposits interpreted with greater confidence are shown in solid outlines; those interpreted with less confidence are denoted by dashed lines, and possibly relate to deposits underlying or overlying the horizon slice shown.

Figure 6.9: Reflectivity data (a) shows a broad, SE-NW aligned feature, interpreted as a wide channel belt or valley deposit, as well as some smaller features (most likely channel belts), which are more clearly resolved with a contrast-enhanced slice. Frequency decomposition (b) - (c) resolves the large 'valley' feature into a series of low-sinuosity, overprinting, stacked and amalgamated channel belts. Other features are also more clearly resolved using the frequency decomposed data compared to reflectivity data. Interpretations of channel-belt deposits using only reflectivity data are shown (d). Wireline logs from Well 04 (e) show low net:gross deposits at this interval. The interpretation of channelized deposits incorporating reflectivity and frequency decomposition data has been made (f). The positions of wells are shown on all the figures.

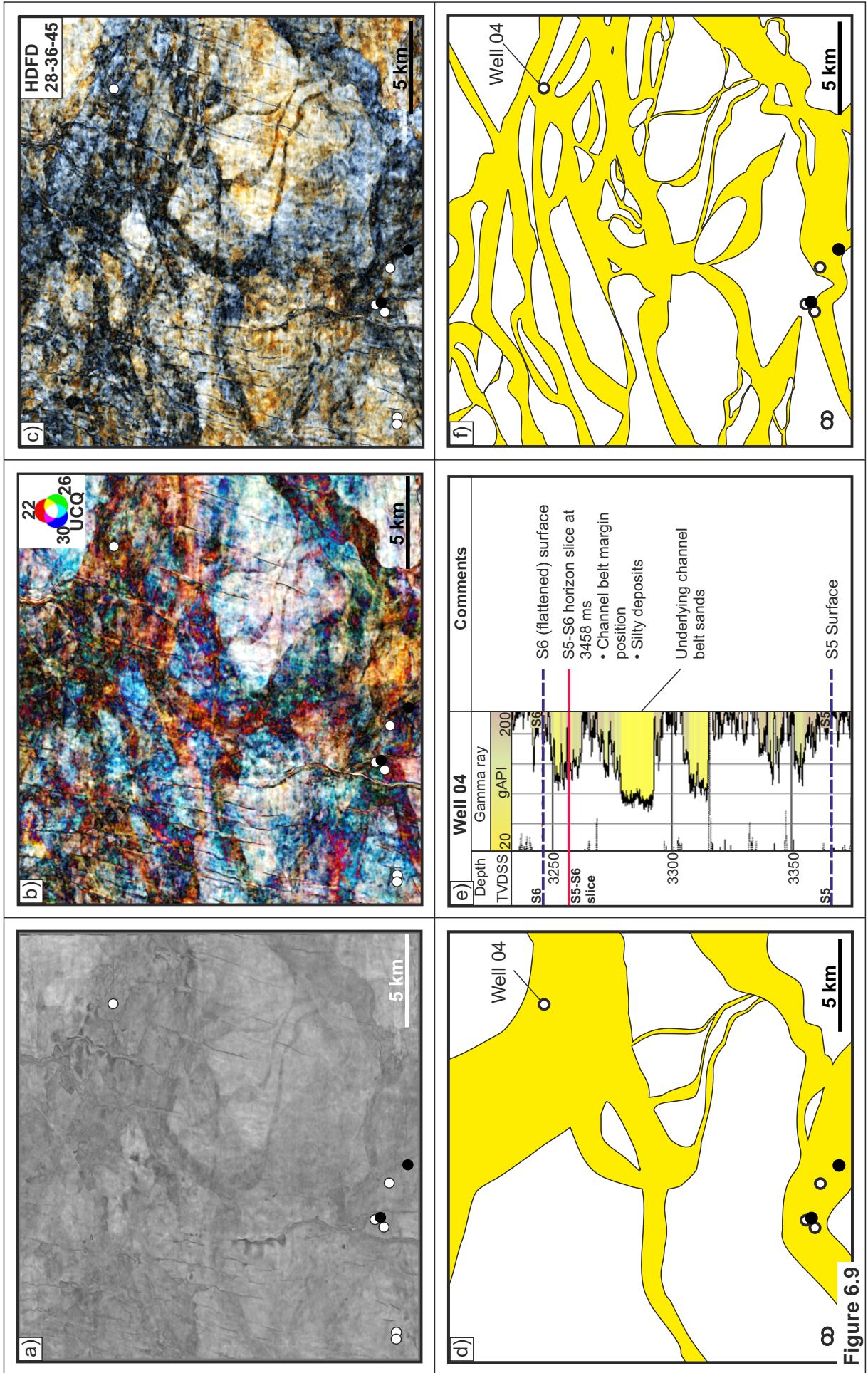
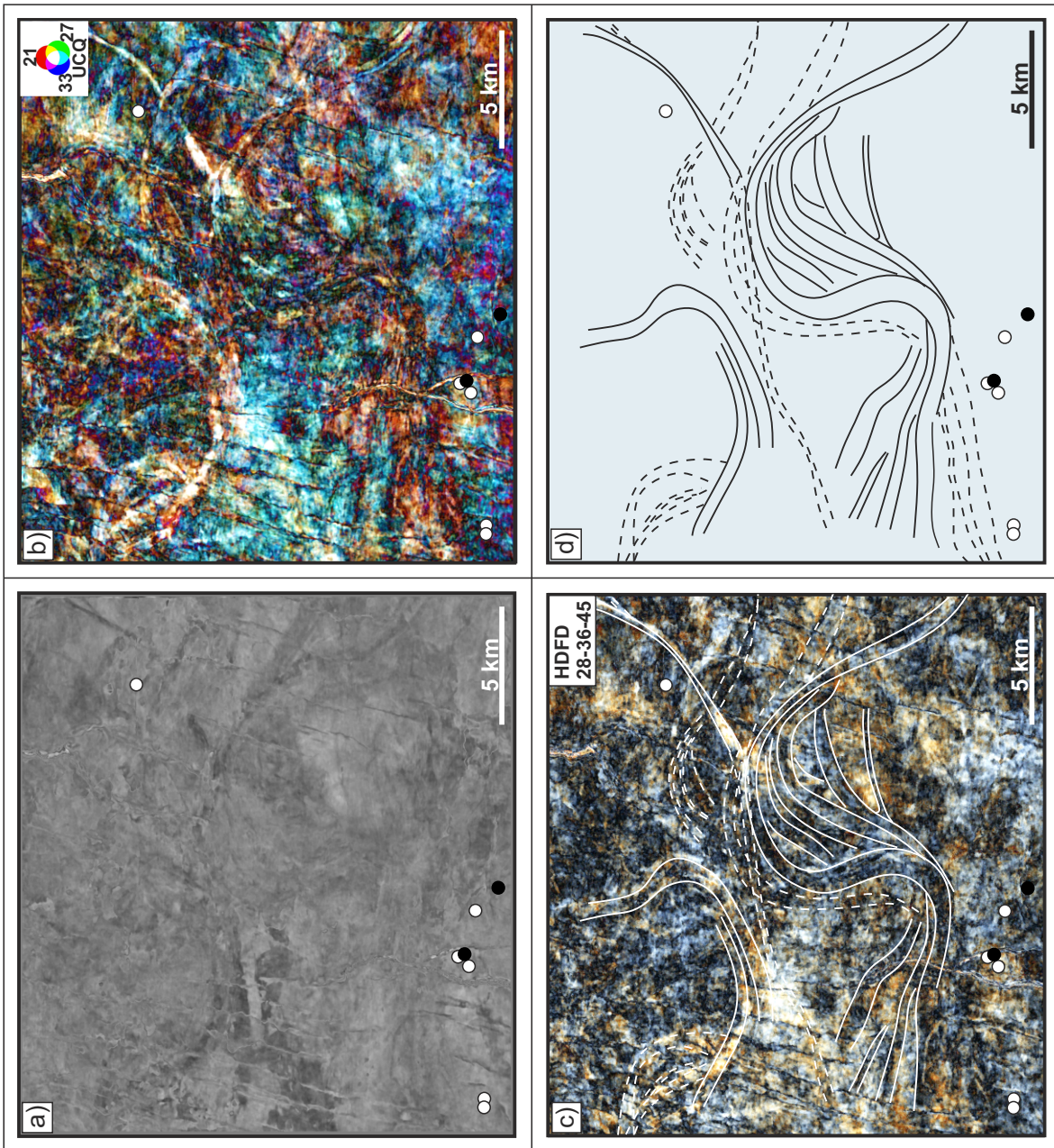


Figure 6.9

Figure 6.10: (a) Lateral accretion deposits are tentatively identified from stratigraphically flattened reflectivity data but the features are poorly resolved; reflectivity shows only faint, arcuate forms, likely channel-belt deposits. (b) UCQ frequency decomposition was better able to resolve these deposits, confirming the presence of large-scale lateral accretion channel-belt deposits. Large-scale, moderately sinuous channel bodies are imaged, with evidence for lateral migration of channel belts over time. This image also shows overprinting of deposits from above and below. (c) HD frequency decomposition has less vertical smearing so better isolates the deposits at the S6-S7 interval. (d) Final interpretation of fluvial point-bar and channel architecture.



Similar features have been noted in the Cretaceous McMurray Formation of Alberta, Canada (Smith et al, 2009; Hubbard et al, 2011), where they have been interpreted as point-bar and counter-point-bar deposits. The channels interpreted in the S6-S7 interval of the Mungaroo Formation are of a comparable scale to those described from the McMurray Formation and Smith et al (2009) and Hubbard et al (2011) cite the Peace River, Alberta, Canada as a possible modern analog for the McMurray. Analogous channel and bar deposits of the modern Peace River have been traced (Figure 6.11) and have a similar plan-form geomorphology to similar elements imaged in the Mungaroo Formation (Figure 6.10). Assuming an analogous depositional setting to that of the current Peace River, the S6-S7 deposits (Figure 6.10) are in sharp contrast to the lower sinuosity valley (S1-S2) and deltaic (S5-S6) deposits, and are interpreted as lateral accretion deposits relating to several phases of channel migration and abandonment. This interpretation is considered representative of this section, but not the Mungaroo Formation as a whole: Adamson et al. (2013) interpret the majority of the Mungaroo Formation using image logs and dip-meters as low sinuosity, with downstream-migrating bars. The interpretation of the S6-S7 deposits as 'McMurray-type' point bar deposits is further supported by the Well-09 core at this interval (Figure 6.12). The core shows inclined heterolithics with paired mud drapes and bundling of mud drapes, leading to the interpretation of the S6-S7 interval deposits as tidal-fluvial point bars.

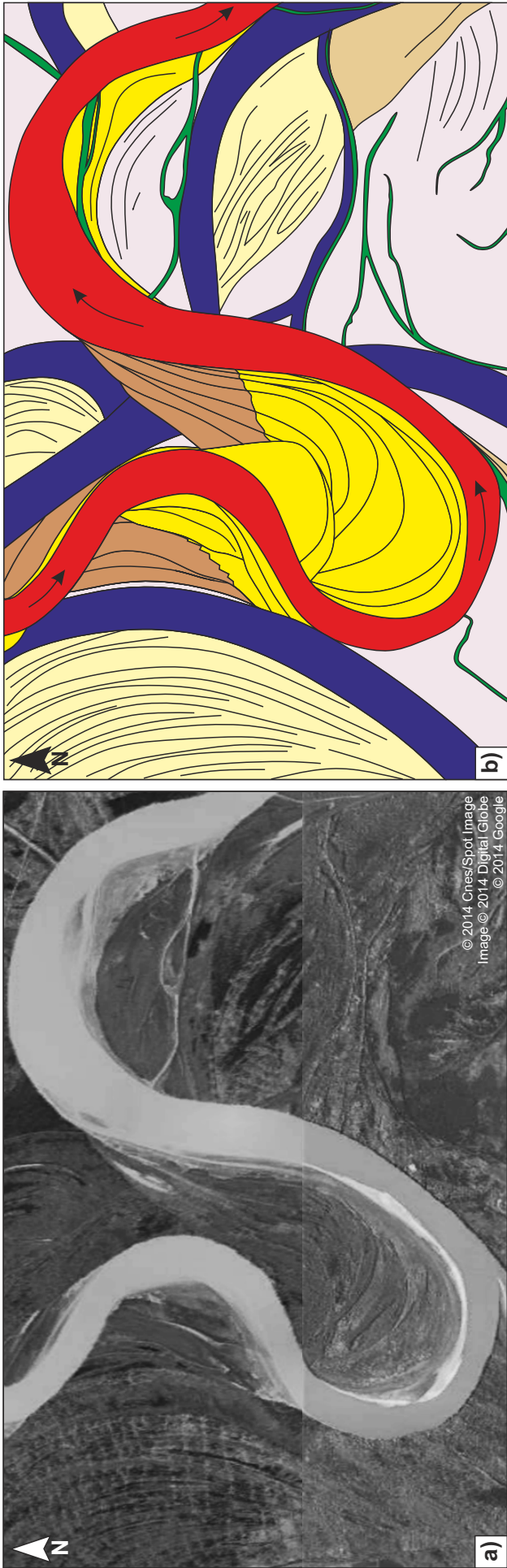
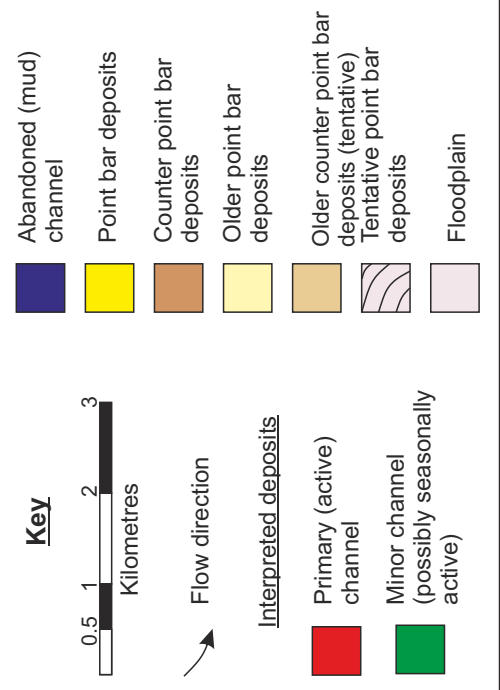


Figure 6.11a: Google Earth image showing point-bar and counter-point-bar deposits of the meandering Peace River, Alberta, Canada (see also Smith et al., 2009). **b:** Interpretation of deposits associated with the present-day Peace River and past phases of lateral migration and channel abandonment, showing similar planform geomorphology to those identified in the S1-S2 interval of the Mungaroo Formation.



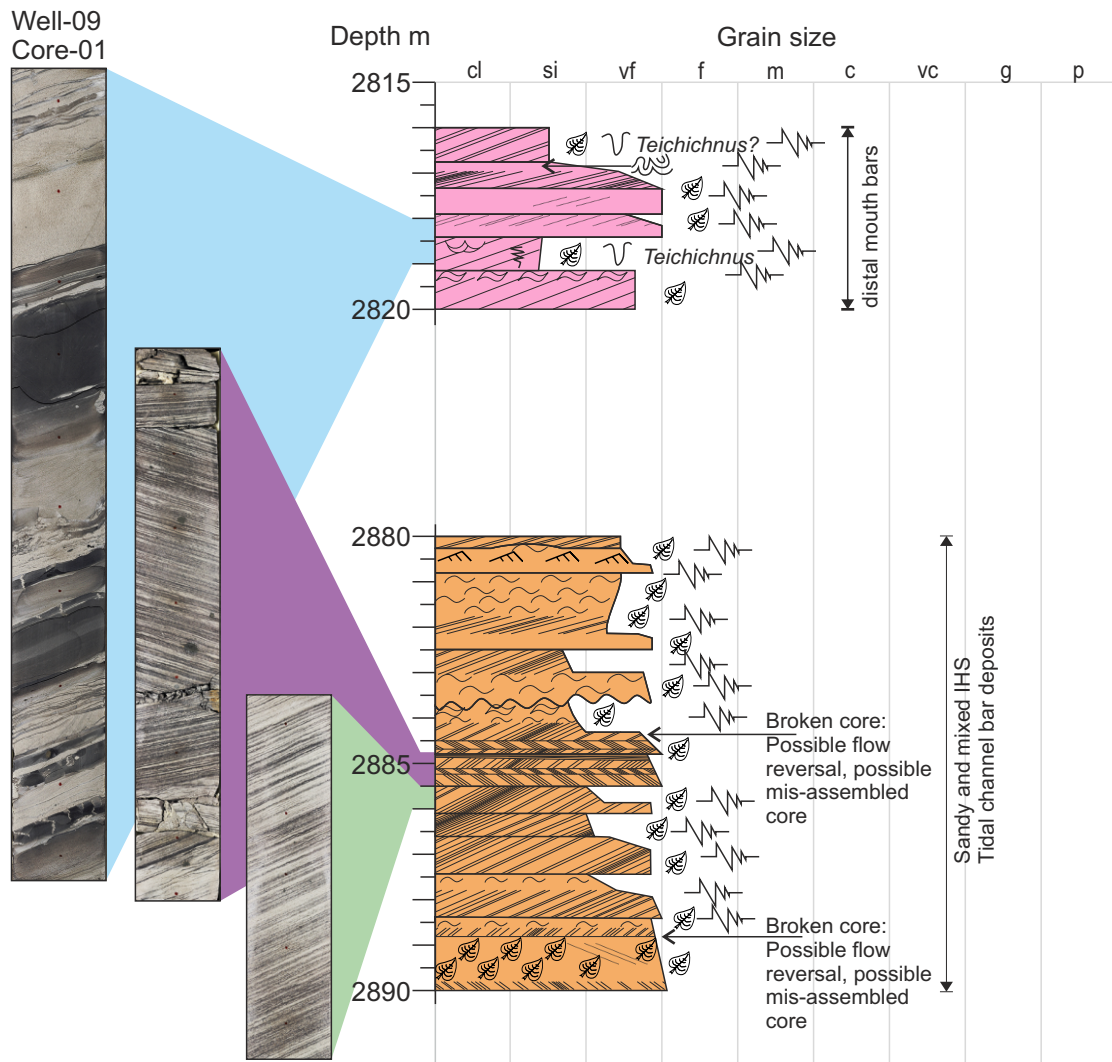


Figure 6.12: Interpreted sedimentary log and supplementary core photographs from Well-09, showing typical channelized and non-channelized deposits from the S6-S7 interval. In the upper core log, tidally indicators including rhythmic bedding and synaeresis cracks are present, as are marginal marine trace fossils e.g. *Teichichnus*. mud-prone heterolithics are interpreted as interdistributary bay fill, with distributary mouth bars interpreted where relatively clean, dm-thickness sandstone beds are present. The lower log shows the typical expression of the channelized deposits of the S6-S7 interval. This core is from the approximate location of the S6-S7 stratal slice (Figure 6.10). Rhythmic bedding, paired mud-drapes, wavy bedding and (tidal) bundling of laminae support the interpretation of these sand-prone IHS deposits as tidally-influenced lateral accretion deposits.

6.6 Discussion

6.6.1 Sequence stratigraphic setting

The horizon slices used in this study are taken at discrete depths, as such they cannot be used to reconstruct a high-resolution model of relative sea—level variations: the slices represent ‘snapshots’ in time during the deposition of the Mungaroo Formation. The contrast in depositional style between the different slices has however been used to tentatively interpret the stratigraphic setting.

Each of the three interpreted intervals fluvial deposits of the Mungaroo Formation are here placed within the context of a sequence stratigraphic model (Figure 6.13), by adapting the idealized incised valley system models of Zaitlin et al (1994). The S1-S2 interval is represented by Figure 6.13a-b. Base-level fall led to the creation of narrow and relatively straight incised valley system via fluvial down-cutting that culminated in sediment bypass to a new lowstand shoreline fan (Figure 6.13a). The S1-S2 deposits represent the lowstand system tract, where fluvial deposition commenced within the incised valley as base-level stabilized at lowstand. Within the valley system, a fluvially-dominated delta likely passed up-dip through a zone of meandering and braided fluvial system development within the confined incised valley before emerging as a non-confined fluvial system in the relatively up-dip part of the system. The meander belt morphology interpreted in the S1-S2 interval suggests a relatively low sinuosity river within the valley. The proposed position of the deposits is shown in Figure 6.13b.

The S5-S6 deposits within the studied subset are interpreted as upper delta-plain deposits, with channels able to migrate across the delta plain, with no evidence of confinement within a valley system. As such, they are interpreted

as having accumulated in a highstand system tract, where the earlier valley system had been filled and buried, thereby allowing the deposits to extend beyond the confines of the former paleo-valley (Adamson et al., 2013; Stuart et al., in review), and these would likely pass up-dip into the alluvial plain deposits (Figure 6.13c).

The S6-S7 intervals feature highly overprinted channel deposits. This, together with a lack of preserved interpreted overbank deposits indicates a relatively low-accommodation setting, and these are interpreted as having accumulated during a relative lowstand, within a much larger system than the S1-S2 deposits (S1-S2 valley is ~2 km wide; S6-S7 individual channel bodies are 0.5-1.5 km wide). The idealized position of the tidally-influenced fluvial S5-S6 deposits on the delta plain is shown in Figure 6.13d.

6.6.2 Buffers and buttresses model

An alternative model that can be used to explain the stacking patterns of the Mungaroo Formation is the buffers and buttresses model (Figure 6.14; Holbrook et al, 2006, Holbrook, 2009), which accounts for the creation of accommodation through repeated episodes of base-level change. The model assumes that fluvial sediment storage must be contained within an upper and lower buffer profile, which constrains the limits of a buffer zone (Figure 6.14a). The profiles of a river recorded at given instants for so-called instantaneous profiles that lie within the buffer zone, and the limits of this buffer zone delineate the preservation space where fluvial sediment can be stored. The upper and lower limits of the buffer zone meet down-dip at the level of a buttress (e.g. sea level, lake level). A rise or fall of this buttress level will induce a shift in buffer and will therefore impact preservation space. Figure 6.14b demonstrates the effect of a rise in buttress (sea level). Preservation space is created by a rise in buttress.

This effect would be greater in proximity to the buttress, and reduces up-dip away from the buttress.

Within the context of this study, it has not been possible to define whether tectonics or eustasy is driving the inferred sea level changes, however previous studies have interpreted a relatively rate of subsidence (0.03 mm/yr) during the Late Triassic (Kaiko & Tait, 2001), indicating that tectonics may have been the controlling factor.

Figure 6.14c shows a generic model demonstrating a typical sequence of stacked buffer zones (B) and transgressions (T) in a down-dip region. The stacking patterns of the Mungaroo Formation are represented by Figure 6.14d,

Figure 6.13: Four schematic models demonstrating the effect of base level change on incised valley fill as relates to the three interpreted intervals of the Mungaroo Formation (based in part on Zaitlin et al., 1994). (a) Model depicting a falling-stage system tract and the generation of an incised valley similar to those that confine the S1-S2 deposits; generation of relatively straight, narrow sediment bypass features. (b) Model depicting a lowstand system tract with fluvial accumulation within the valley as a fluvially-dominated lowstand delta that passes up-dip through meandering and braided fluvial deposits within the incised valley, to non-confined fluvial deposits. The S1-S2 deposits are interpreted as low-sinuosity deposits within the incised valley. (c) Model depicting a highstand system tract, representative of the S5-S6 deposits, where the incised valley has been filled allowing the development of a largely unconfined delta-plain, characterized by distributary channel networks and inter-distributary bays that pass up-dip into alluvial-plain deposits. (d) Model for the S6-S7 deposits in which fluvial systems form laterally accreting, low accommodation fluvial deposits in a low-accommodation, lowstand setting.

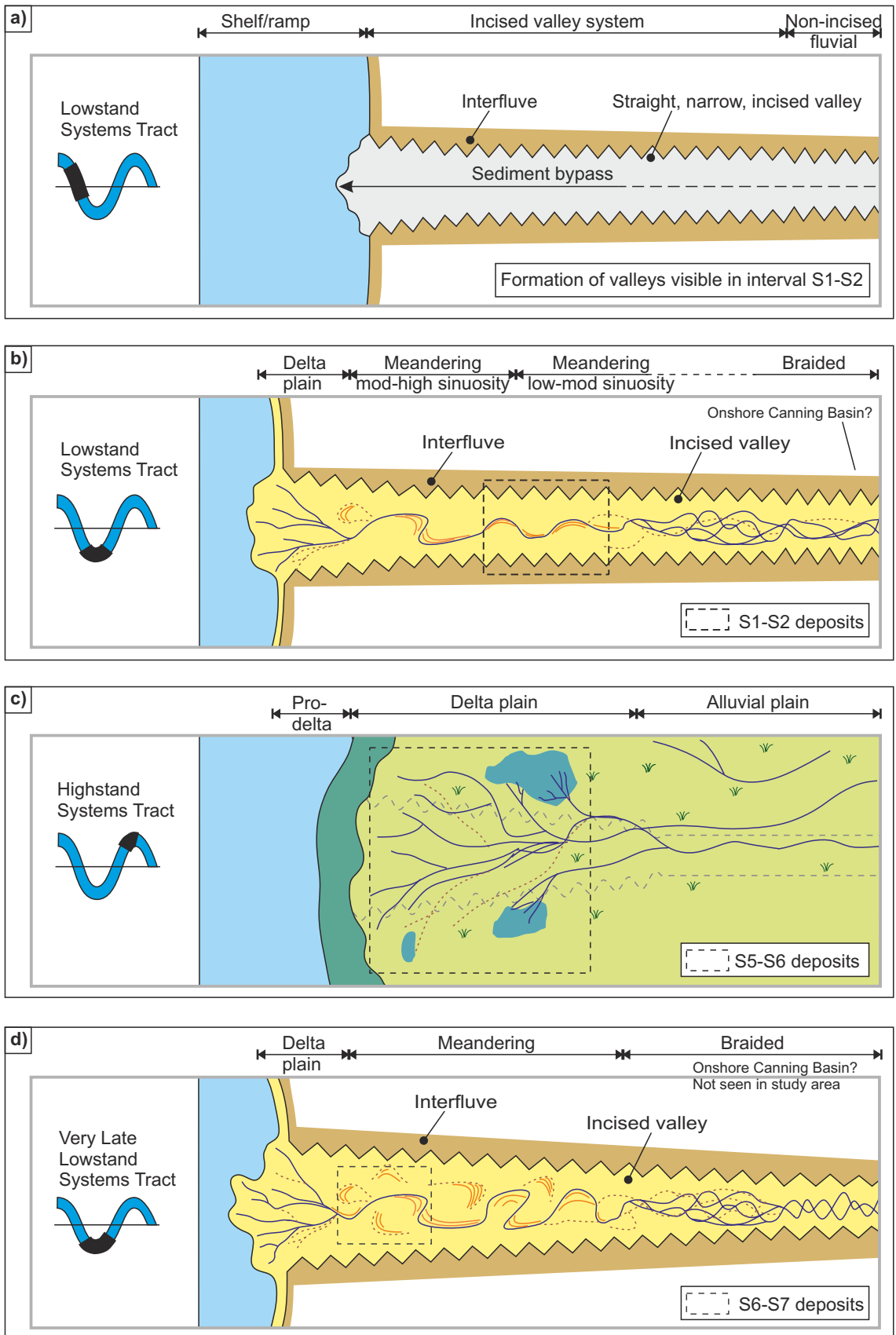


Figure 6.13

Figure 6.14: Buffers and buttresses model, adapted from Holbrook et al (2006). **a:** The buffer and buttress model argues that fluvial sediment storage must be contained within an upper and lower buffer profile, which constrain the limits of a buffer zone. The profiles of a river recorded at given instants (instantaneous profile) will lie within this buffer zone, and delineate the preservation space where fluvial sediment can be stored. Buffer zones meet down-dip at the level of a buttress (e.g. sea level, lake level). **b:** A rise or fall of the buttress level will cause a shift in buffer and therefore preservation space. The effect of a rise in buttress level (sea level) is shown. Preservation space is created by a rise in buttress. This effect is greater in proximity to the buttress, and reduces up-dip away from the buttress. **c:** Generalized model demonstrating stacked buffer zones (B) and transgressions (T) in a down-dip region of a fluvio-deltaic system. **d:** Buffers and buttresses model demonstrating the aggradation of the Mungaroo Formation as a result of successive incremental but punctuated rises in buttress level. The location of the three studied intervals is annotated. The resultant formation is a series of stacked buffer zones and transgressions. The model represents only the down-dip section of the buffers present in the study area.

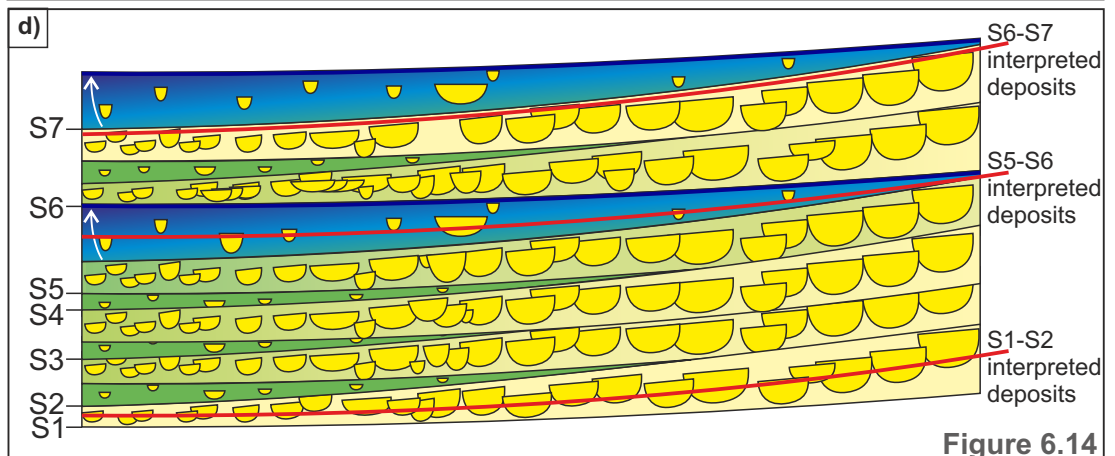
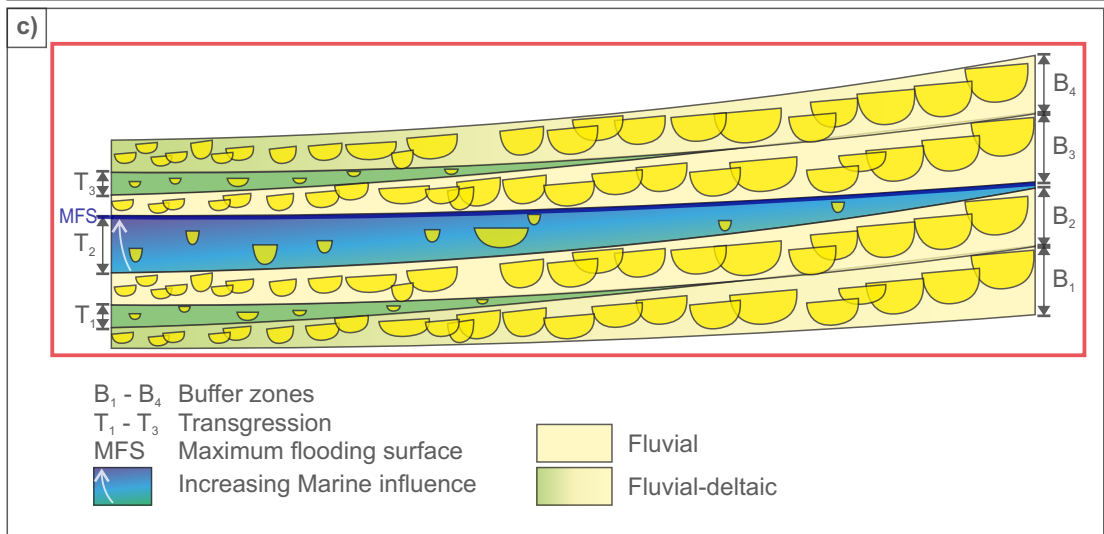
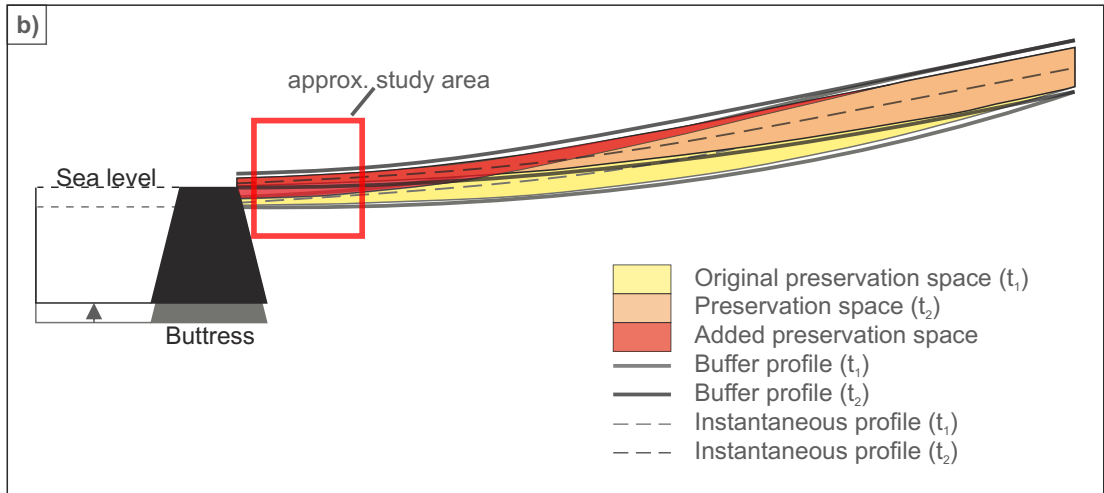
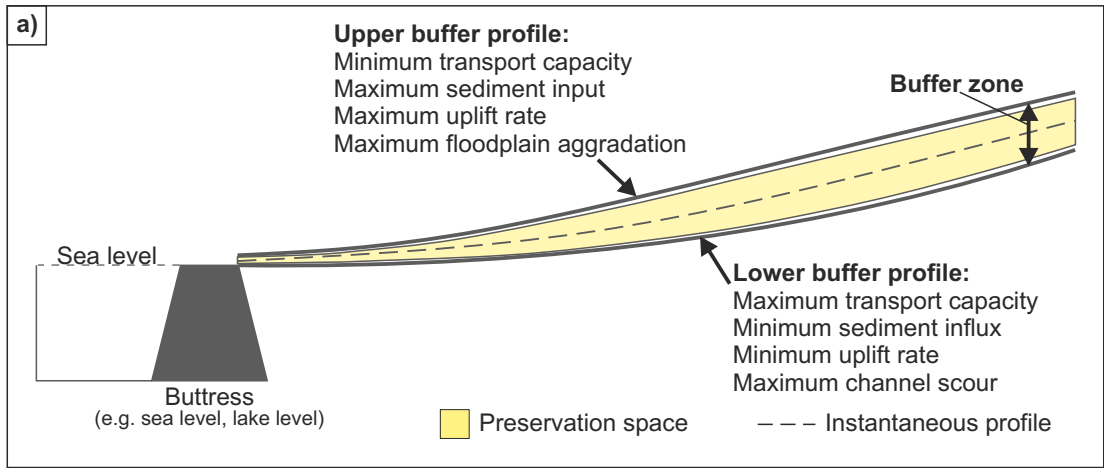


Figure 6.14

a buffers and buttresses model demonstrating the overall net aggradation of the Mungaroo Formation in response to a series of progressive but punctuated rises in buttress level as recorded by the preserved architectural style in the study area. This architectural style is representative of the relatively down-dip setting within the overall Mungaroo system studied here. The location of the three studied intervals has been annotated. The resultant formation is a series of stacked buffer zones and transgressions, recording the cyclical movement of buffers driven by punctuated rises in buttress.

6.7 Conclusions

Attribute analysis and horizon slicing is a useful tool for identifying fluvial deposits on seismic data. Reflectivity data alone cannot properly image thinly bedded or deposits of fluvial bodies for which there is poor contrast with surrounding facies. Spectral decomposition can more clearly image valley, channel-belt and even individual channel features, even at depths >3 km. The interpretations made using spectral decomposition have significance in terms of well placement decisions. The preserved Mungaroo Formation has been interpreted at 3 different intervals, representing two fluvial and one deltaic paleoenvironment. Interpreted deposits include (i) migrating, stacking meander belt deposits within an incised valley (interval S1-S2), (ii) amalgamated channel belts (interval S5-S6), and (iii) individual fluvial channel and point-bar elements (interval S6-S7) that are analogous to the modern Peace River, Alberta in terms of scale and geometries and may also form an analogue to the tidally-influenced McMurray Formation. The S1-S2 and S6-S7 deposits represent low accommodation settings, whereas the S5-S6 fluvio-deltaic deposits are interpreted as representing a highstand systems tract with higher accommodation conditions. The preserved deposits of the Mungaroo Formation

can also be described as a series of stacked buffer zones (higher net:gross intervals dominated by alluvial deposits) and zones influenced by transgressions (lower net:gross intervals with increased marine influence).

Chapter 7 Discussion: Controls on depositional style of fluvio-deltaic deposits: case study of the Mungaroo Formation

Research question: What are the possible allogenic and autogenic controls on fluvio-deltaic successions? Which combination of allogenic and autogenic controls best explain the variations in depositional style seen in the Mungaroo Formation? What can this tell us about fluvio-deltaic depositional systems in general?

7.1 Chapter overview

This chapter discusses the possible influence of autogenic and allogenic forcing mechanisms that acted to determine the preserved fluvio-deltaic stratigraphic expression of the Mungaroo Formation, in terms of the overall pattern of stacking of architectural elements present in the formation, as well as the detailed architectural expression of key stratigraphic intervals and surfaces. The chapter will discuss the applicability of these findings to generalised models of fluvio-deltaic stratigraphy and will draw comparisons to the morphology and style of evolution of analogous modern systems.

7.2 Introduction

Fluvio-deltaic stratigraphy is ultimately controlled by the interplay of autogenic (intrinsic) and allogenic (extrinsic) processes (van Dijk et al., 2009; Karamitopoulos et al., 2014). Understanding the relative importance of autogenic vs. allogenic controls on sedimentation is crucial for understanding how such mechanisms are responsible for determining the resulting depositional architecture (Blum & Törnqvist, 2000; Stouthamer & Berendsen,

2007; Hajek et al., 2012). Traditional thinking around the controls on fluvial deposition link fluvial stratigraphy to basin boundary conditions, i.e. climate, tectonics and sea level (Shanley & McCabe, 1994; Jerolmack & Paola, 2010; Abels et al., 2013). However, recent research has assigned greater significance to the influence of autogenic controls, with many studies recognising how continental successions exhibit patterns of stratal architecture that are most readily explained by self-organisation behaviour over basin-filling time scales of 10^3 - 10^6 years (Blum & Törnqvist, 2000; Muto & Steel, 2001; van Dijk et al., 2009; Van De Wiel, 2010; Stouthamer et al., 2011; Hajek et al., 2012; Straub & Wang, 2013). The major challenges in unravelling the relative influence of autogenic vs. allogenic processes are (i) the lack of quantitative understanding of autogenic processes and their interactions with allogenic forcing mechanisms (Karamitopoulos et al., 2014; Kim et al., 2014), and (ii) the ability of the deposits formed by autogenic processes to overprint and obscure and be confused with the results of allogenic processes, such as basin subsidence and sediment supply (Hajek et al., 2010, 2012).

This chapter aims to identify the upstream and downstream controls on the stratigraphic architecture of the Mungaroo Formation and fluvio-deltaic successions more generally. This will be achieved by drawing on literature and observations made from the dataset used in this study, in order to determine what can be learned about the boundary conditions of fluvio-deltaic systems by studying their geomorphology (seismic stratal slices), sedimentology (wireline and core logs) and stratigraphy (stacking of preserved sequences).

Specific research objectives of this chapter are as follows: (i) to discuss the allogenic processes that are known to affect fluvial stratigraphy, and which may act as significant controls on the preserved stratigraphy of the Mungaroo Formation, including climate, source-area uplift, basin subsidence and base-level (buttress) rise (Shanley & McCabe, 1994; Holbrook et al., 2006; Miall, 2014); (ii) discuss the autogenic processes (including avulsion and localised floodplain effects) that may act to control stacking patterns seen in the studied intervals of the Mungaroo Formation; (iii) discuss how the interaction of allogenic and autogenic processes might express themselves in the preserved succession based on an understanding of the style of accommodation generation and sediment supply, and how an awareness of the action of such processes may be used to gain an understanding of how the depositional setting of a fluvio-deltaic system such as the Mungaroo Formation may evolve through time.

7.3 Allogenic controls

7.3.1 Introduction

The role of allogenic processes in controlling stratigraphy, and in particular alluvial architecture, has been extensively investigated (cf. Allen & Posamentier, 1993; Aitken & Flint, 1994; Leeder & Stewart, 1996; Ethridge et al., 1998; Blum & Törnqvist, 2000; Cohen et al., 2005; Ethridge et al., 2005; Ambrose et al., 2009; Abels et al., 2013), with much of the body of research focussing on fluvial response to changes in base-level (cf. Allen & Posamentier, 1993; Aitken & Flint, 1994; Leeder & Stewart, 1996; Ethridge et al., 2005; Hollbrook et al., 2006; Holbrook & Bhattacharya, 2012; Zaitlin et al., 2012). This section

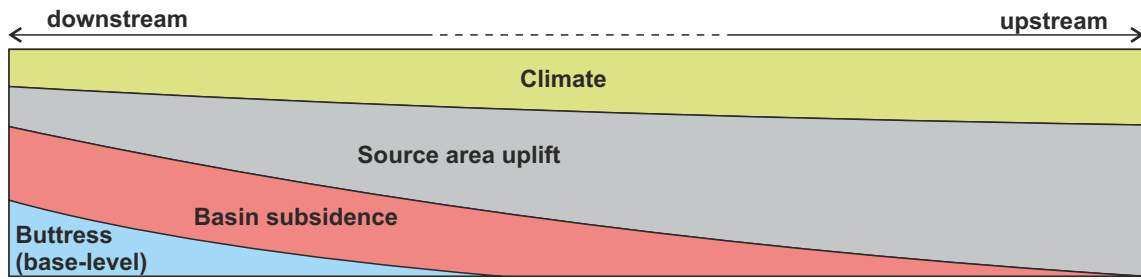


Figure 7.1: Upstream and downstream relative influence of allogenic controls on fluvial architecture (after Shanley & McCabe, 1994)

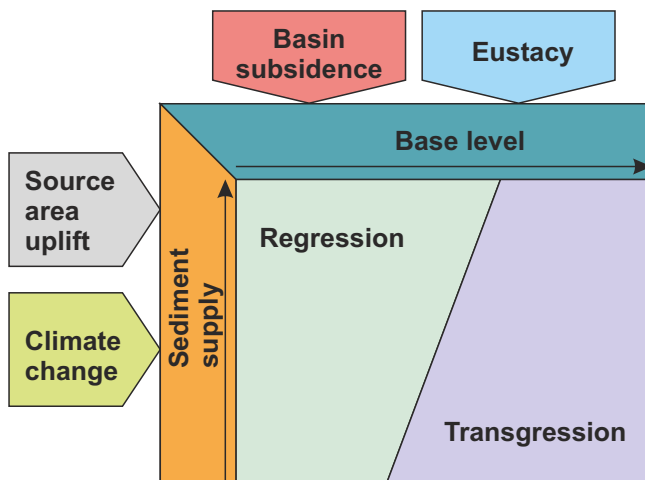


Figure 7.2: Allogenic controls (Source area uplift, climate change, basin subsidence, eustacy) on upstream (sediment supply) and downstream (base level) conditions (after Ethridge et al., 1998).

discusses the allogenic factors that may be considered as controlling factors during the deposition of the Mungaroo Formation. Figures 7.1 and 7.2 demonstrate the relative influence of upstream and downstream allogenic controls on fluvial deposition.

7.3.2 Climate

Climate is known to exert a primary control on deposition in upstream regions (Blum, 1993; Shanley & McCabe, 1994) and is seen to affect fluvial and fluvio-deltaic deposition by influencing sediment discharge (Cecil & Edgar, 2007). Many previous studies on the upstream climatic and downstream sea-level control on fluvial deposition have concentrated on case studies of the Texas Gulf Coastal Plain (Suter & Berryhill, 1985; Knox, 1987; Anderson et al., 1996; Aslan & Autin, 1999; Aslan & Blum, 1999; Blum & Törnqvist, 2000; Benedetti, 2003) and on the Rhine-Meuse Delta (Törnqvist, 1993, 1994; Van der Woude, 1984).

Climate controls discharge rate and sediment yield through precipitation, e.g. rainfall floods (Benedetti, 2003; Holbrook et al., 2006) and hence controls primary sediment supply from the source region that lies up-dip of the receiving basin. Climate also controls seasonal fluctuations in discharge and sediment supply, e.g. through snowmelt floods (Benedetti, 2003), which are expressed as variations in grain size within formations and thin silt drapes representing a decrease in flow strength (Jablonski & Dalrymple, 2014). Temperate, seasonal conditions tend to have the highest sediment yields (Miall, 2014). Allen et al., (2013) summarise the sedimentology of seasonally-influenced fluvial deposits, demonstrating that fluvial systems with a strong seasonal influence would have a more frequent occurrence of channel deposits with low-angle-inclined cross-bedding, parting laminations and silt drapes, climbing ripple cross-lamination and convolute bedding. Seasonally influenced floodplain deposits of wet systems tend to be preserved as successions with laterally discontinuous, thin

coals present in poorly-drained floodplain successions, and crevasse-splay deposits generated by flood events.

Evidence for seasonal sedimentation patterns is present in the Mungaroo Formation in the weakly-tidal S2-S3 interval (Figures 3.13; 4.10), including variations in grain size (taken to mean episodically increased and decreased discharge) where there are no salinity indicators. Other indications of seasonal influence on sedimentation patterns are present in the S1-S2 interval (Figure 6.8), which is characterised by thick (>50 m-thickness), multi-story, downstream accreting sand-bodies, which are more typical of perennial fluvial channels (Allen et al., 2013); however, the presence of fine-grained laminae on cross-bed surfaces, and regular changes in grain size from medium to fine-grained sandstone indicates some fluctuation in flow regime. Given the absence of evidence to support tidal influence interpreted from core at this interval, a seasonal variation in flow rates is inferred. The interpretation of the Mungaroo Formation as being influenced by varying sediment yields responding to seasonal variations in discharge is supported by Triassic climate research and previous studies of the Mungaroo Formation. The climate can be interpreted to have been temperate-warm, humid and monsoonal, with wet and dry episodes (Dickens, 1985; Bradshaw et al., 1994; Payenberg et al., 2013, Preto et al., 2010; Arche & López-Gómez, 2014), which would infer high rates of sedimentation in temperate-warm seasonal periods, and lower rates of sedimentation in more humid periods (Figure 7.3 (Cecil, 1990, 2003)).

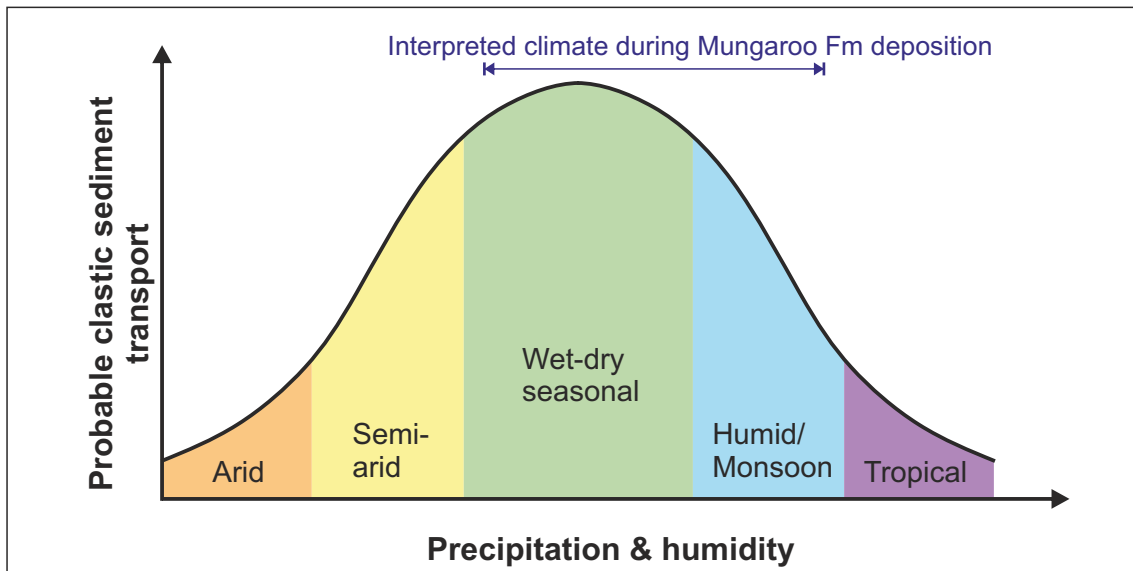


Figure 7.3: Response of sediment transport to climate change (after Cecil, 1990). Sediment transport rates are highest in wet-dry seasonal climates, such as the S1-S2 and S3-S4 intervals of the Mungaroo Formation, and are lower in humid climates (possible humid climate at the time of deposition of the S5-S6 interval).

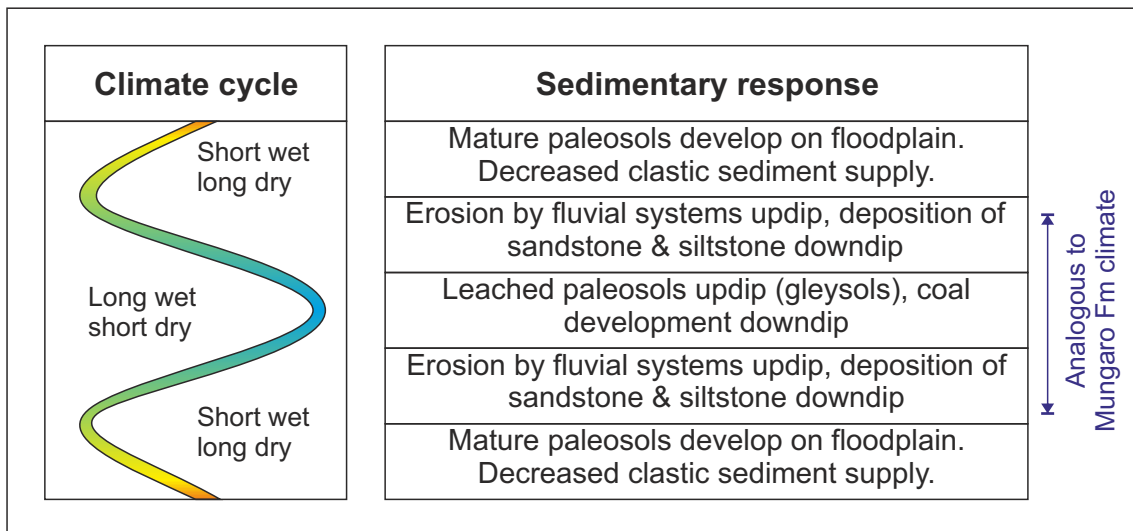


Figure 7.4: Sedimentary response to climate cycles (After Cecil, 1990). In climates with shorter wet seasons, mature paleosols develop on the floodplain, while decreased discharge leads to decreased rates of clastic sedimentation. In climates with long wet seasons, gleysols and coals (such as those seen in the S3-S4 and S5-S6 intervals of the Mungaroo Formation) form on the floodplain. Intermediate conditions favour updip incision by fluvial systems and downdip deposition of sandstones and siltstones. Intermediate climates will have the highest potential for sediment transport.

Climate changes between wetter and drier episodes has been shown to exert an influence on floodplain development (Fielding, 1986; Benedetti, 2003). One such climate indicator recorded in floodplain deposits is the development of palaeosols and related coals (Blum & Price, 1998; Abels et al., 2013), which may be used to discern the role of climate cycles in floodplain sedimentation. It has been proposed by Abels et al. (2013) that the development of cycles of mature, red palaeosols (an indicator of relatively dry, stable floodplain conditions) can be linked to climate cycles. Humid and very humid conditions are characteristically associated with increased vegetation and the development of coals (Miall, 2014). Figure 7.4 (after Cecil, 1990) demonstrates the sedimentary response of fluvial systems to wetter and drier climates. Cantuneanu (2006) also recognises the significance of gleysols as indicators of episodes of sediment aggradation, within sequences, whereas mature entisols and vertisols tend to be indicative of episodes of non-deposition at sequence boundaries. Cantuneanu (2006) states that where driven by allogenic forcing, alternations between the formation of gleysols and coals (e.g. S5-S6 floodplain deposits) are most likely the result of climate and fluvial discharge variations (subaerial exposure vs. flooding of overbank environments), rather than base-level changes.

No mature palaeosols are encountered in the Mungaroo Formation within the study area, although gleysols and thin coals develop in some intervals. Payenberg et al. (2013) postulate that the widespread development of gleysols and poorly developed coals represent 'wetter' episodes in the development of the Mungaroo Formation, whereas intervals with few gleysols or where such soil intervals are thin and of restricted lateral extent may represent 'drier' episodes.

This conjecture is supported by biostratigraphic analysis of the 'wet' and 'dry' intervals: Payenberg et al. (2013) also interpret a transgressive surface at TR22 (equivalent of S3 in this study), below which they interpret relatively dry conditions, and above which they interpret relatively wet conditions, with an abundance of freshwater algae and hydrophytic spores. This is in line with the transition from the S1-S2 fluvial deposits, to the S2-S3 upper delta plain deposits (with restricted gleysol development), to the 'wetter' S5-S6 delta plain deposits with widespread gleysols, muds and thin coals. The abundance of plant material ('tea-leaf structures') in the S6-S7 deposits (Figure 3.12c) is indicative of a humid climate with thick vegetation cover, likely a wetland environment with a high water table and surface water ponding (Hillier et al., 2007).

7.3.3 Tectonic controls

Tectonic style controls the magnitude, development and position of developing drainage basins (Leeder, 1993) through the creation of accommodation space as determined by complex spatio-temporal patterns of subsidence, commonly driven by fault movement. Such complex patterns of tectonic basin development influence sediment supply (uplift of the source area) and set up preferential pathways for drainage networks.

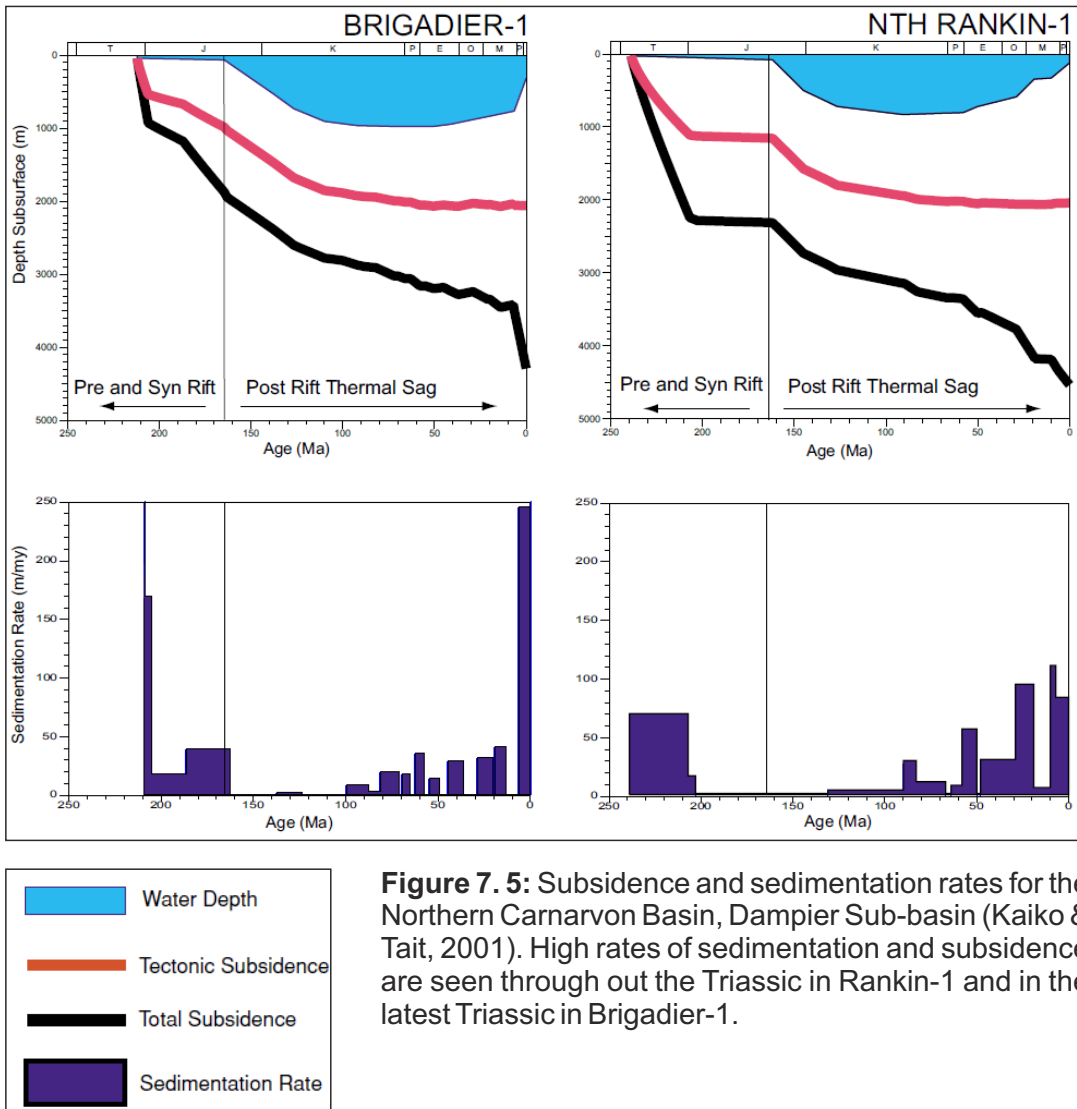
7.3.3.1 Tectonic uplift (of source area)

Clastic wedges form in response to the regional uplift of source areas (Sloss, 1962; Miall, 2014). The Mesozoic deposits of the Northern Carnarvon Basin form a clastic wedge (Exon, 1982; Boot & Kirk, 1989; Westphal & Aigner, 1997)

that prograded approximately westward from the Pilbarra High and Ross High (Jablonski et al., 1997; Westphal & Aigner, 1997). It can therefore be inferred that the source areas of the Ross High and Pilbarra High were uplifting throughout the Mesozoic.

7.3.3.2 Basin subsidence

The Mesozoic sedimentary wedge, to which the Triassic Mungaroo Formation contributes, formed in a continental sag basin (Boote & Kirk, 1989; Westphal & Aigner, 1997), in a relatively quiescent tectonic period, following Permian rifting (Boote & Kirke, 1989). Triassic movement of faults defining structural terraces is evidenced by thickening of the Locker Shale across the faults and deep lowstand-canyon erosion of the Locker Shale on some terraces (Gorter, 1994). Relatively slow, asymmetric subsidence can be inferred from this tectonic style (Mitchell & Reading, 1986). However, Kaiko & Tait (2001) demonstrate that at wells Brigadier-1 and North Rankin-1 in the Dampier Sub-basin (Figure 7.5 shows the location of the Dampier Sub-basin) record relatively high rates of subsidence and sediment supply in the late Triassic, which occurred concurrently with the accumulation of the Mungaroo Formation, although these rates may not be consistent with subsidence rates across the Exmouth Plateau overall. Indeed, low rates of subsidence are seen in the northern and eastern parts of the Northern Carnarvon Basin (Kaiko & Tait, 2001).



7.3.4 Base-level rise and fall

Base-level – the lower erosional limit of river profiles (Powell, 1875) – is commonly taken as sea level, or in the case of fluvio-lacustrine systems, lake level (Holbrook et al., 2006). There has been considerable debate over the impact that changes in base-level have on the accumulation and preservation of continental strata (e.g. Shanley & McCabe, 1994). Traditional models by Mackin, 1948, and built upon by Miall (1991), Schumm (1993), Leeder and Stewart (1996) Blum and Törnqvist (2000) among others, express the fluvial response to base-level change in terms of changing gradient of the fluvial profile in that streams will attempt to grade themselves to base-level (i.e. strive to attain an equilibrium profile). Depending on the rate of base-level fall or rise, rivers will adjust their profiles in an attempt to equilibrate with the new base-level by changing their channel pattern, discharge and sediment load, and in cases of significant base-level fall, undertaking valley incision (Shanley & McCabe, 1993; Westcott, 1993; Koss et al., 1994). However, care should be taken when applying such concepts generally because natural systems are inherently complicated. The effects of changes in base-level (e.g. valley incision or drowning, deposition of marine strata within valleys, changes in channel style in response to change in the gradient of the fluvial profile) tend to diminish up-dip (Saucier, 1996; Blum & Törnqvist, 2000).

7.3.4.1 Base-level fall as expressed in fluvial stratigraphy

Following a fall in base-level, fluvial systems initially tend to adjust rapidly toward a new base-level through down-cutting of fluvial valleys, although the

degree to which the fluvial system will be affected depends on the gradient of the graded shelf-slope profile, discharge rate, sediment load and the rate of base-level change (Miall, 1991; Westcott, 1993; Shumm & Ethridge, 1994). It is also possible for a fall in base-level to trigger accumulation: for example, in cases where the gradient of a recently exposed shallow marine shelf is less than the gradient of the alluvial profile (Emery and Myers, 1996). Given that tidal effects lessen up-dip and seasonal effects lessen down-dip within a system (Figures 6.17 (after Jablonski & Dalrymple, 2014) and Figure 7.1, (after Shanley & McCabe, 1994)), following a fall in base-level, the bayline will tend to shift further down-dip, and greater seasonal effects and decreased tidal effects will be expected to be seen in deposits overlying tidally influenced deposits.

7.3.4.2 Base-level rise expressed in fluvial stratigraphy

The response of the fluvial system to base-level rise will be affected by the rate of relative sea-level (or lake-level) rise and the contrast in gradient between the the shelf and the alluvial system (Posamentier & Vail, 1988).

Bristow et al. (1999) propose a link between crevasse-splay development, channel aggradation and base-level rise, such that an abundance of crevasse splays in braided systems may be used as an indicator of base-level rise and aggradation. This has relevance for the S2-S3 deposits, which have an abundance of crevasse-splay deposits (accounting for 25% of the S2-S3 deposits (36% of non-channelized deposits) by logged thickness (Figure 3.14), whilst having channel deposits formed by predominantly low-moderate sinuosity rivers (with downstream accreting barforms). This also has relevance for the B-

C seam deposits interpreted at the South Blackwater Mine (Figures 2.6, 2.13, 2.14), where an abundance of splay deposits interpreted within a succession whose primary channels record a low-sinuosity fluvial system (Fielding et al., 1993), indicates a high-accommodation setting.

The rate of base-level rise can influence channel morphology in fluvio-deltaic settings (Shanley & McCabe, 1994): a high rate of base-level rise, with accompanying high ground water levels (as seen in the Rhine-Meuse delta (Törnqvist, 1993; Törnqvist et al., 1993), may give rise to anastomosing stream patterns, whereas a lower rate of base-level rise may preferentially give rise to meandering streams. The anastomosing pattern of channels seen in the S5-S6 interval (Figure 4.10), together with the interpretation of the floodplain as being poorly-drained (as evidenced by gleysols and coal formation) is most obviously explained as a record of fluvial system development under the influence of a rapid rate of base-level rise. Flooding surfaces may be identified in seismic data within fluvial successions as continuous, laterally extensive reflections. Within core data, the flooding surfaces in the down-dip section of fluvial successions may be present as mudrocks (particularly where marine-influenced inchnofauna are present). In wireline logs, these may be identified as high GR peaks. In high-accommodation fluvial successions, coals may be present in as the up-dip equivalent of maximum flooding surfaces (e.g. Fanti & Cantuneanu, 2010). These are identifiable in cores and in wireline logs (as a low GR combined with low density (c.f. Figure 2.4). Both of these possible flooding surface types have been identified in the Mungaroo Formation.

7.3.4.3 Buffers and buttresses models

Holbrook et al. (2006) introduced the concept of “buffers and buttresses” to explain the varying influences of upstream and downstream allogenic controls on fluvial geometry and architecture, including channel-body stacking patterns through time and space, by illustrating the processes by which preservation space can be created along a depositional profile. Chapter 6.7.2 and Figure 6.14a explains the buffers and buttresses model as described by Holbrook et al.

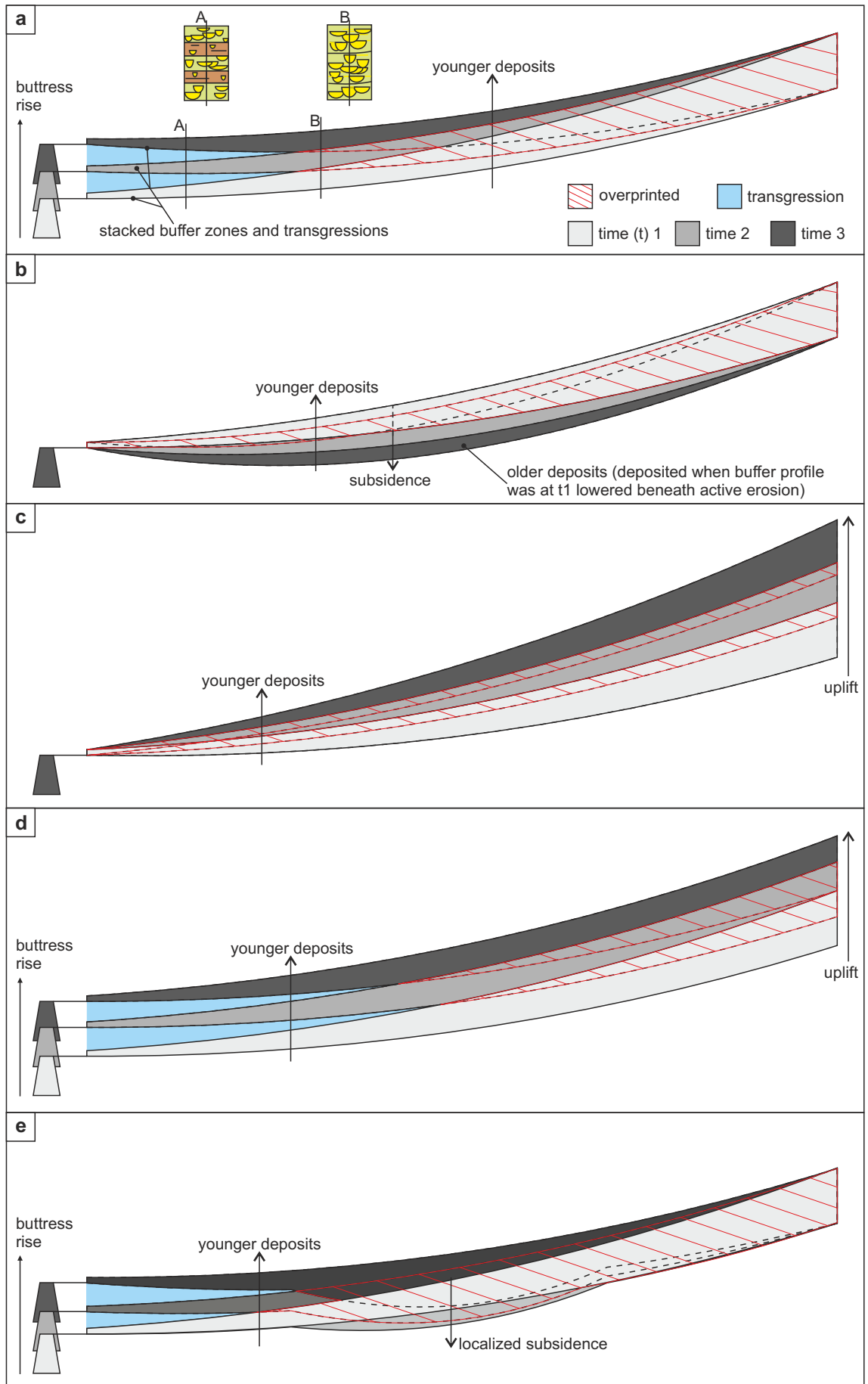


Figure 7.6: Methods of creation of preservation space demonstrated using the buffers and buttresses model. **a:** buttress rise. **b:** localized basin subsidence. **c:** up-dip uplift. **d:** Up-dip uplift and buttress rise. **e:** localized subsidence and buttress rise. Accommodation space created within buffer zones and transgressions are shown, as well as areas of deposits that are overprinted by deposits of successive buffer zones.

(2006) and Holbrook (2009). Figure 7.6 demonstrates the response of a fluvial profile to variations in upstream (uplift) and downstream (buffer level rise or fall, localized subsidence) parts of the system, illustrated as a series of dip-orientated profiles.

The buffers and buttresses model can be used to explain how allogenic factors control the overall generic configuration of a fluvio-deltaic succession as a stacked series of buffer zones and transgressions (Figure 7.7), which can then be tailored to specific settings. Figure 6.14d attempts to demonstrate the temporal evolution of the Mungaroo Formation in the study area, as a series of stacked buffer zones and transgressions, which is in line first-order base-level rise occurring throughout the TR20-TR20 Mungaroo Formation deposits interpreted by Marshall & Lang (2013).

7.3.4.4 Using buffers and buttresses model to distinguish between low- and high-accommodation settings

Low accommodation

When the buttress (e.g. sea level) falls, river profiles fall, typically causing incision (cf. Miall, 1991). In these circumstances the buffer profile will fall as well (Holbrook, 2006, 2009). Figure 7.8a demonstrates that up-dip, there will still be potential preservation space for the aggradation of deposits between the old and new buffer profiles, despite the overall incisional conditions. The same applies where a lowering of the base-level fall results in a down-profile shift in buttress and an extension of the buffer profile: there will be repeated incision

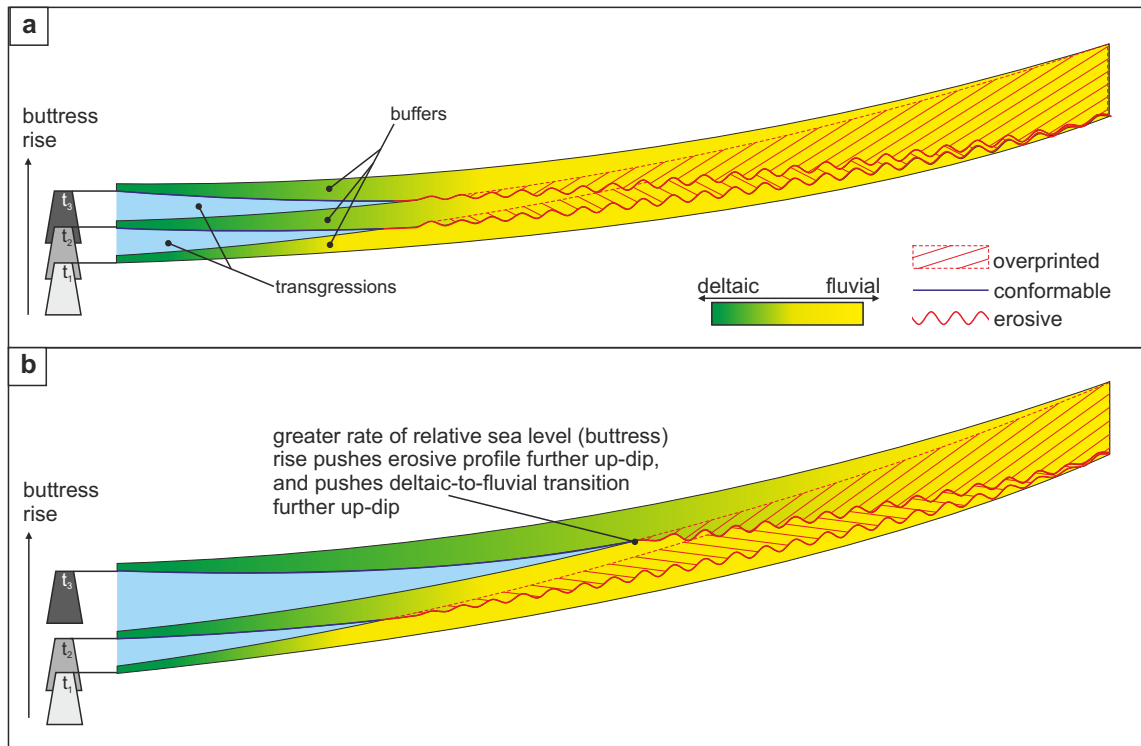


Figure 7.7: Buffers and buttresses models showing effect of butress rise on a fluvio-deltaic succession. **a:** Butress (relative sea level) rise results in stacked fluvio-deltaic buffer zones and marine-influenced transgression zones down-dip, and stacked buffer zones containing fluvial deposits that incise into and/or overprint underlying buffer zone deposits up-dip. **b:** butress rise with differing rates of relative sea level rise. The greater rate of butress rise between t_2 and t_3 results in a larger transgression that extends further up-dip, extending deltaic deposits further up-dip, explaining the successive stacking of more deltaic-influenced deposits within the stacked buffer zones of the Mungaroo Formation.

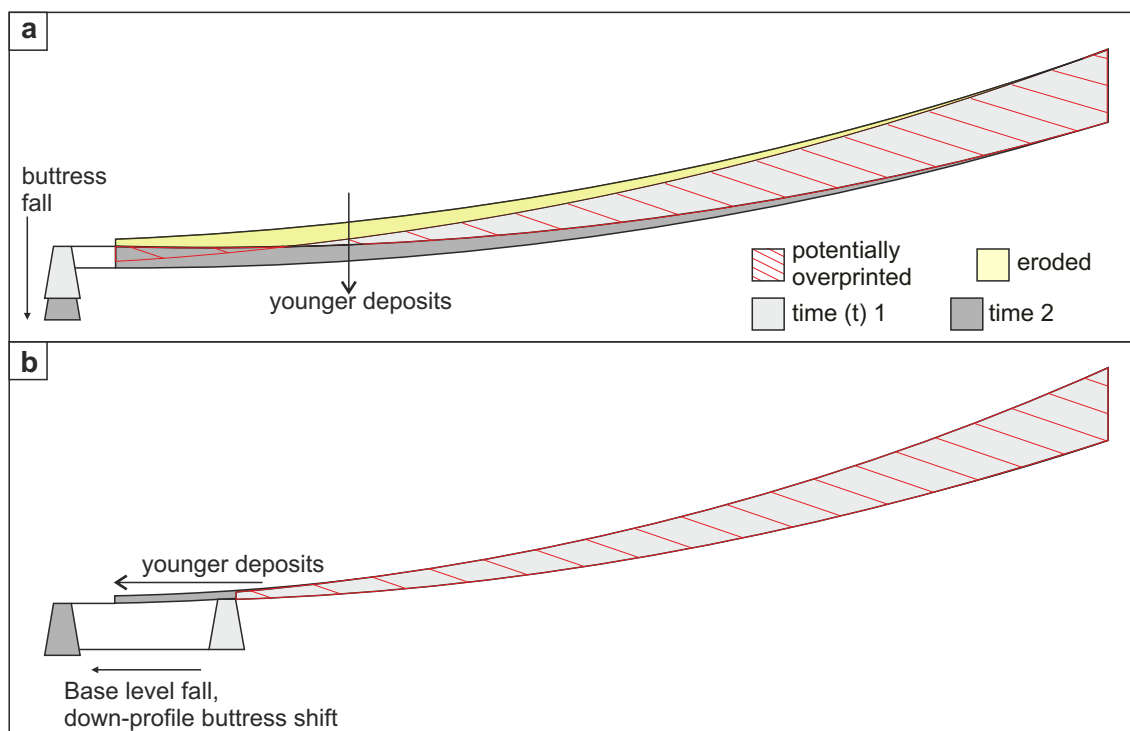


Figure 7.8: Buffers and buttresses models to explain how a drop in base level can still create preservation space for fluvial deposits (after Holbrook et al., 2006; Holbrook, 2009). **a:** base-level fall forces a drop in river profiles through valley incision. Buffer profiles drop, however preservation space is still added shortly up-dip of the buttrass. **b:** If base-level fall does not force a drop in river profiles, the buffer profile will be extended down-profile, and sediment will repeatedly incise and aggrade between buffer profiles.

and aggradation of deposits up-dip (Figure 7.8b). Buffer profiles may move laterally and vertically, such that even during low stand systems tracts, there will still be deposition and preservation of deposits up-dip through lateral and vertical migration of profiles. This in turn results in repeated stacking, incision and lateral migration of channel belts, underlain by a scour surface. This surface is reshaped by each successive incision and stacking event and is referred to as a 'composite surface' (Figure 7.9, after Holbrook, 2009); such surfaces are commonly interpreted as sequence boundaries.

This 'composite surface' as described by Holbrook (2009) differs from traditional interpretations of sequence boundaries as it does not represent a single point in time (c.f. Hunt & Tucker, 1992); rather, it is formed over the duration of the falling stage. The Buffers and Buttresses model allows for sediment accumulation above this surface throughout the falling stage (cf. Figure 7.8) and so the 'composite surface', although erosional in appearance, would not be a sub-aerial exposure surface. The surface may be formed not through downcutting valley incision but by lateral planation of a migrating channel belt or valley. Figure 7.9 shows this 'composite surface' as expressed by thin and thick preservation space. In zones of thicker preservation space, large-scale multi-valley complexes will tend to form with a composite surface or sequence boundary at the base. In zones of thinner preservation space, laterally migrating channel sheets will tend to form above the composite surface. Hence, following this model, the interpretation of an incised valley is not necessary for the interpretation of a sequence boundary.

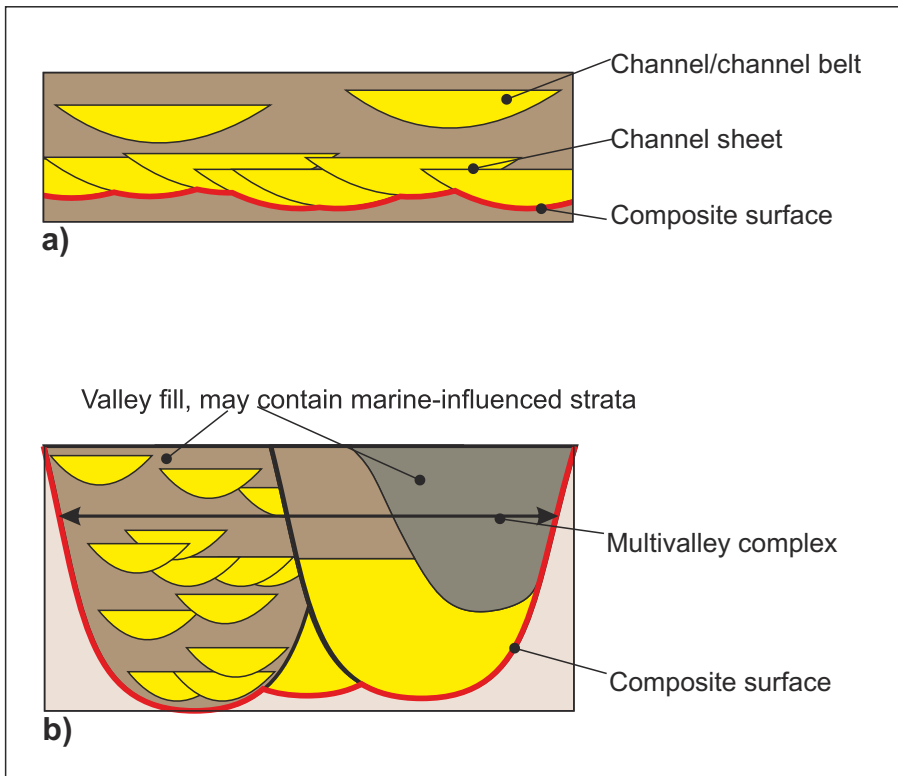


Figure 7.9: Composite surfaces: architectural sequence boundaries as formed in both **a)** thin preservation space, where they form by lateral planation of channel belt sheets, and **b)** in thicker preservation space, where they form following repeated phases of incision, infill and lateral migration of a multivalley complex. After Holbrook (2009).

In the Mungaroo Formation, sequence boundaries have been interpreted at the base of many of the interpreted valley and multi-valley fills (such as those seen in the S1-S2 interval (Figure 3.6)). With the relatively limited extent of core (limited to the upper S1-S2 interval, S2-S3 interval and S6-S7 interval), it has not always been possible to observe the nature of the surface at the base of many of the interpreted channel-belt and valley deposits, and many scour surfaces seen in core (within the S2-S3 interval) are predominantly interpreted as the scour surfaces of individual channel belts or valleys within stacked complexes. However, where large-scale multi-valley complexes are interpreted from seismic slices (Figure 4.9), a sequence boundary may be interpreted at its base. The varying expressions of the 'composite surface' sequence boundary has implications for the interpreted sequence stratigraphy of the Mungaroo Formation: by applying the Buffers and Buttresses model, it is not necessary to identify valley or multivalley deposits in order to interpret a sequence boundary; rather, all that is necessary is evidence for repeated overprinting, amalgamation and lateral planation of channel-belt deposits, as is seen in the S6-S7 deposits. This is of particular interest because upon detailed examination of the seismic geomorphology of the Mungaroo Formation, many of the channelized deposits previously identified as valley fill (cf. Adamson et al., 2013), have been re-interpreted as channel-belt deposits as a result of this thesis, as they are without evidence of regional erosion or incision events.

High accommodation

Applying the Buffers and Buttresses model to higher accommodation settings may explain the lack of composite surfaces encountered in the cored intervals of the Mungaroo Formation, despite the presence of channel-belt, amalgamated channel-belt and valley deposits. In high-accommodation settings, high rates of aggradation result in the preservation of both channel and overbank deposits (Wright & Marriott, 1993). Although rates of lateral migration of sinuous channels may be lower (Berenden & Stouthamer, 2001), avulsion rates tend to be high. The high rate of accommodation generation and aggradations means that buffer profiles tend not to be stable (Holbrook, 2009), regional erosion is rare, and composite surfaces may not form (Figure 7.10). In the S5-S6 interval of the Mungaroo Formation, the numerous, anabranching channels, together with interpreted lacustrine and mire deposits indicate a high accommodation setting. The amalgamated channel-belt deposits which form an approximately east-west aligned cluster indicate multiple avulsions during aggradation. One would not expect to see a 'composite surface' sequence boundary at the base of these deposits as they were unlikely to have been deposited under falling-stage conditions.

7.3.4.5 The buffers and buttresses model as it applies to selected intervals from the Mungaroo Formation

This section will apply the Buffers and Buttresses model to selected intervals of the Mungaroo Formation.

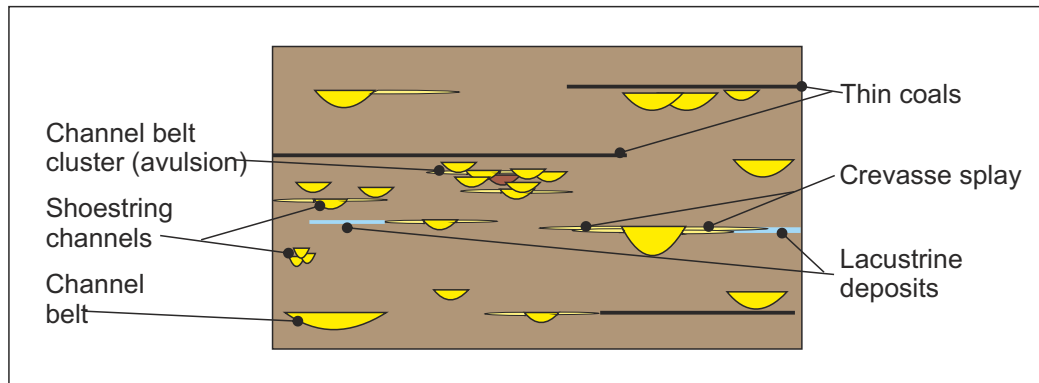


Figure 7.10: High accommodation scenario. Rapid aggradation leads to greater sediment storage, including fine-grained overbank deposits. Channels tend to be low sinuosity, however channel clusters form due to high rates of avulsion. Crevasse splay, coal and lacustrine deposits are more commonly preserved in high accommodation settings. Due to the high aggradation rate, incision may not occur, such that composite surfaces do not form. This has implications for identifying sequence boundaries in high accommodation settings.

S1-S2: Buttress fall

The S1-S2 interval shows evidence of a fall in base-level (buttress), with regional erosion and incision forming multivalley complexes in the lower S1-S2 interval (cf. Figure 4.9) and narrow, incised valleys in the upper S1-S2 interval (cf. Figure 6.6). The Buffers and Buttresses model relevant to this interval shows a lowering in buffer profile due to relative sea-level (buttress) fall, with a composite surface at its base (Figure 7.11).

S2-S3: Slow rate of buttress rise

The S2-S3 interval shows a landward shift in facies compared to the S1-S2 interval. The preservation of channel, splay and fine-grained overbank deposits indicates a relatively high-accommodation setting, although relatively narrow incised and stacked channel belt deposits indicate that there could still be a candidate composite surface at the base of this interval, either through the presence of a stable buttress level, or a slight lowering in buttress level (Figure 7.12).

S5-S6: Rapid buttress rise

In the S5-S6 interval, buttress rise leads to an increasing rate of accommodation generation and marine influence. Fine-grained overbank deposits are preserved, whereas channels form a distributary network prone to avulsion. The Buffers and Buttresses model relevant to this interval is the generic 'buffer rise' model presented as Figure 7.7, and shows a rise in buffer profile with an associated marine transgression, shifting marine influence further

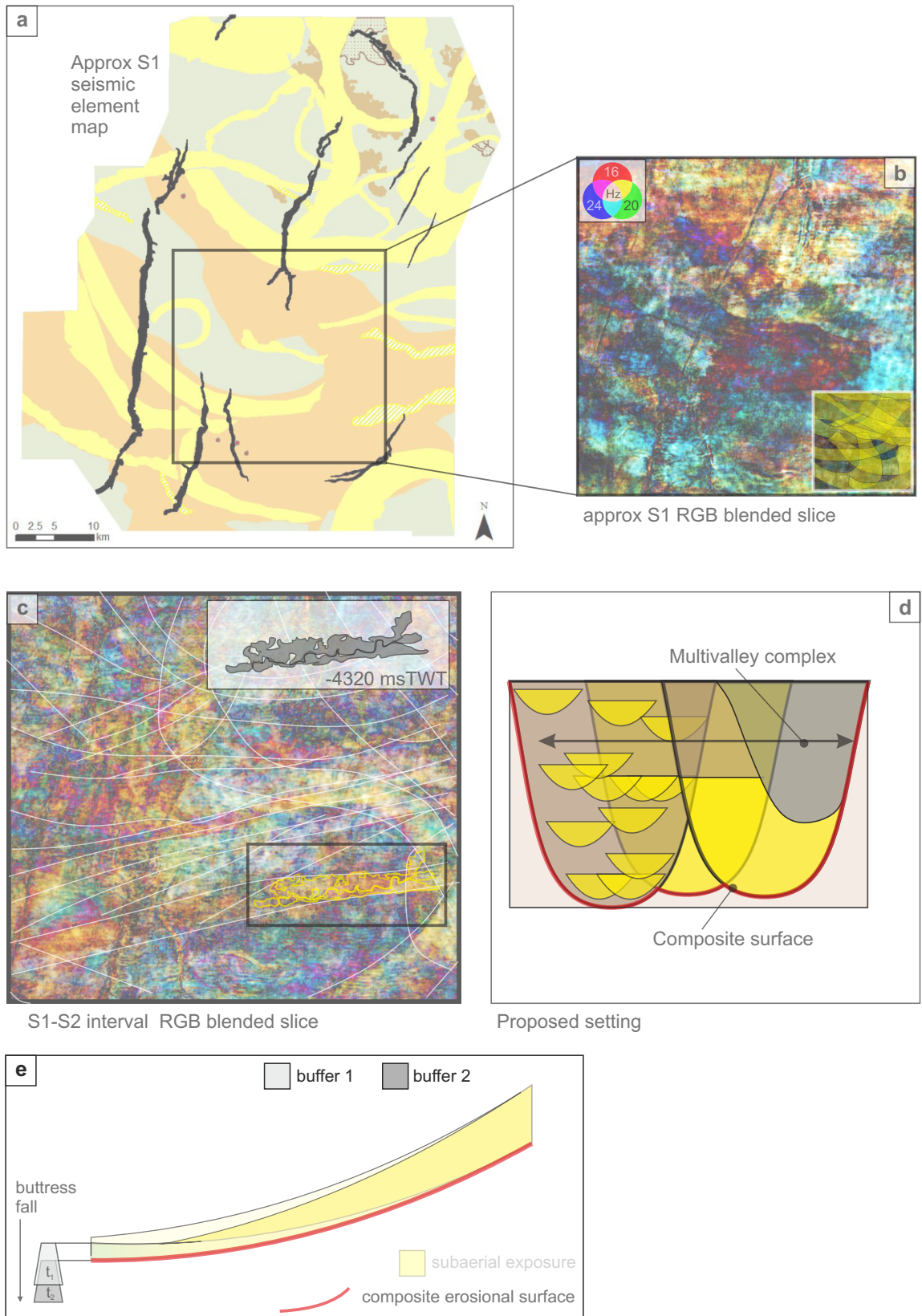


Figure 7.11: Buffers and buttresses model appropriate to the S1-S2 interval. **a:** seismic element map (approx S1) showing interpreted valley complexes. **b:** RGB blended slice from the same approximate location. **c:** RGB blended slice from within the S1-S2 interval, showing narrower valley deposits. **d:** Simple schematic depositional cross-section; multivalley complexes with composite surface (sequence boundary) at the base. **e:** Buffers and buttresses model: The extensive incised deposits indicate a response to drop in base level. This lowering of the buttress has caused a drop in the buffer profile, with a composite surface (sequence boundary) at the base.

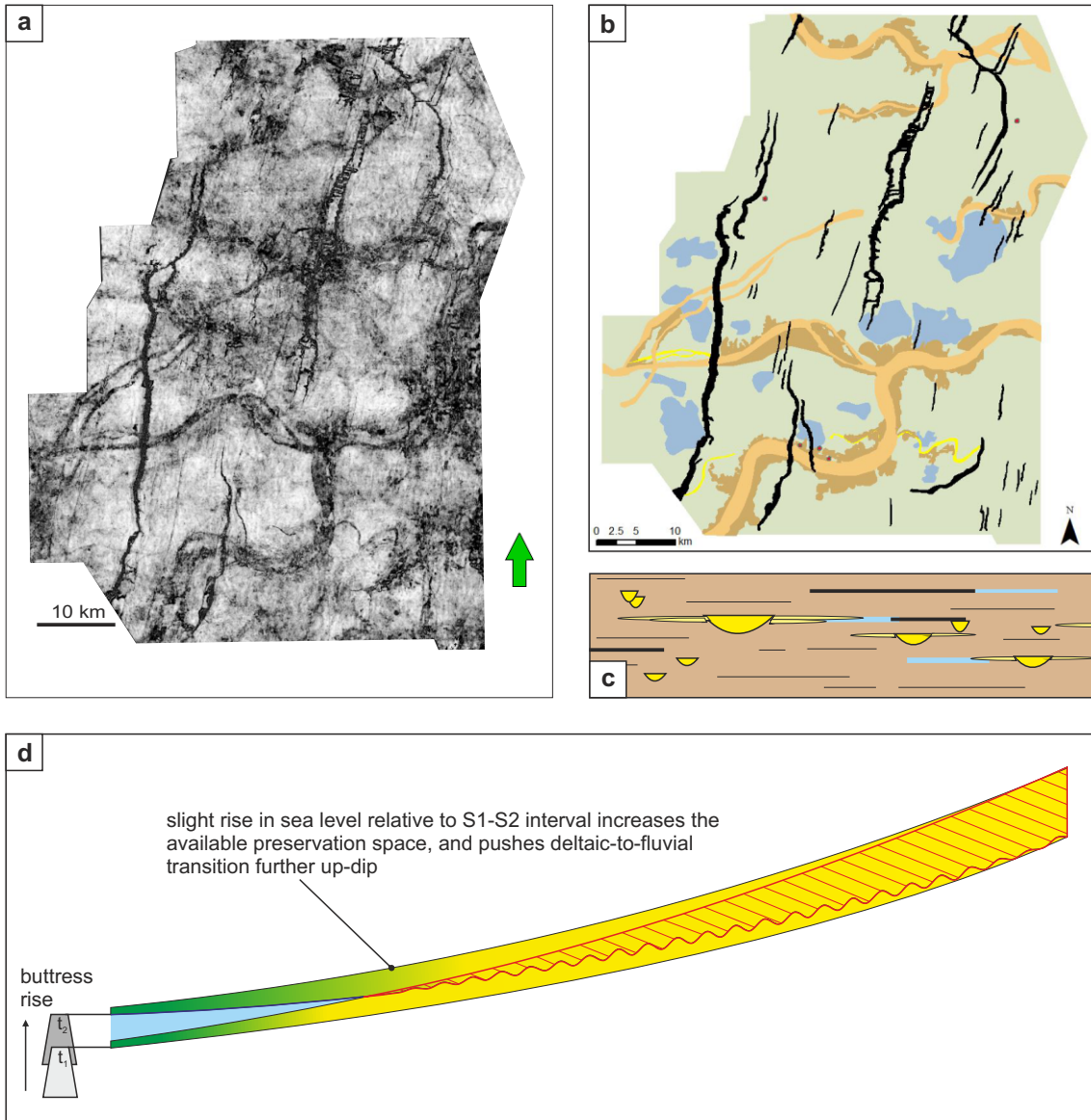


Figure 7.12: Buffers and buttresses model for the S2-S3 interval of the Mungaroo Formation. **a:** horizon slice from near S3, and **b:** interpreted seismic element map (refer to Chapter 4 for detailed description). **c:** schematic representation of S2-S3 deposits: channel belts, small, shoestring channels, crevasse splays and laterally restricted lacustrine and coal deposits. Due to relative base-level rise, accommodation space has increased, such that no composite surface is interpreted at the base of channel belt deposits. **d:** buffers and buttresses model appropriate to the S2-S3 interval: a slight rise base-level causes a rise in buffer profile, pushes the deltaic-to-fluvial transition further up dip.

up profile (Figure 7.13). There would not be a composite surface interpreted at the base of the channel deposits in this interval.

S6-S7: Base-level fall, down-profile buttress shift

The S6-S7 interval is a candidate for the ‘thin preservation space’ buffer described by Holbrook (2009) in a low-accommodation setting. The likely buffer & buttress model has been inferred from the low accommodation but laterally migrating and aggrading (rather than incising) tidal deposits. For this interval, base-level has fallen, but this has not resulted in a drop in buffer profile, rather it is interpreted as causing an elongation in the fluvial profile. Therefore valley incision does not occur; rather, repeated cross-cutting and aggradation of channel-belt deposits takes place (Figure 7.14).

7.4 Autogenic controls

7.4.1 Introduction

Autogenic processes, such as flood events, bar deposition and migration, and lateral accretion control the construction and potential reworking of floodplain deposits. Such autogenic controls on deposition can explain some of the stacking patterns and the configuration of channel bodies within the buffer zones described in the previous section. This section will discuss the effects of avulsion and localised floodplain effects as seen in the Mungaroo Formation.

7.4.2 Avulsion

Avulsion – the shifting of channels to new positions on the floodplain (Smith et al., 1989; Mohrig et al., 2000; Slingerland & Smith, 2004) – is arguably the most important floodplain process (Miall, 2014) and the main process by which coarse-grained channel deposits are introduced to the floodplain. As discussed

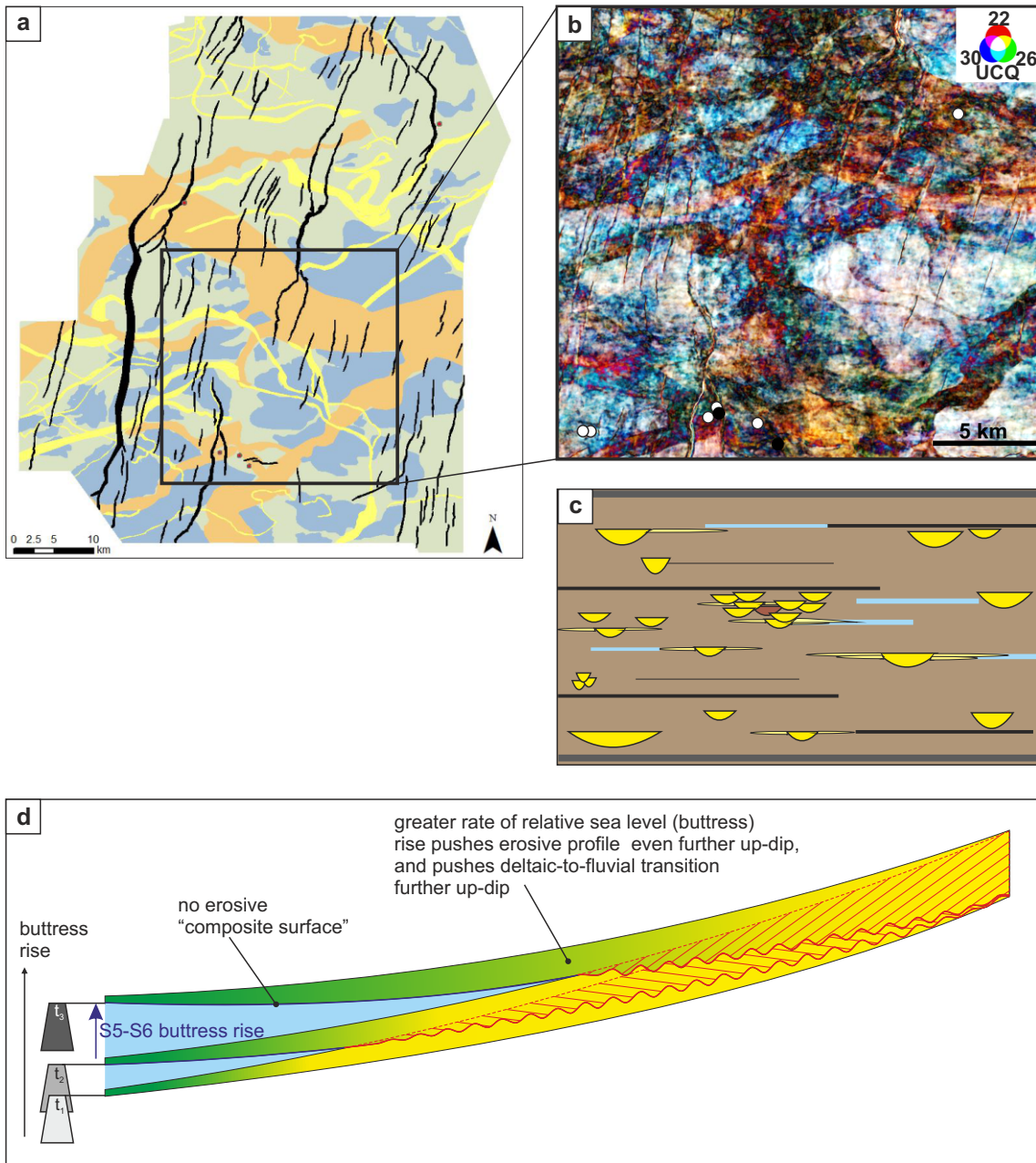


Figure 7.13: Buffers and buttresses model for the deltaic S5-S6 interval of the Mungaroo Formation. **a:** seismic element map from near S6 (c.f. Figure 4.11 for more detail), and **b:** RGB frequency blended horizon slice showing detail of overprinting channel belts in the central area of the dataset (refer to Chapter 6 for detailed description). **c:** schematic representation of S5-S6 deposits: clustered channel belts, channel deposits, crevasse splays and extensive lacustrine and coal deposits. Due to relative base-level rise, accommodation space has increased, such that no composite surface is interpreted at the base of channel belt deposits. **d:** buffers and buttresses model appropriate to the S5-S6 interval: The rate of relative base-level/buttress rise is greater than that of the S3-S4 interval, so the marine-influenced section is pushed further up the buffer profile.

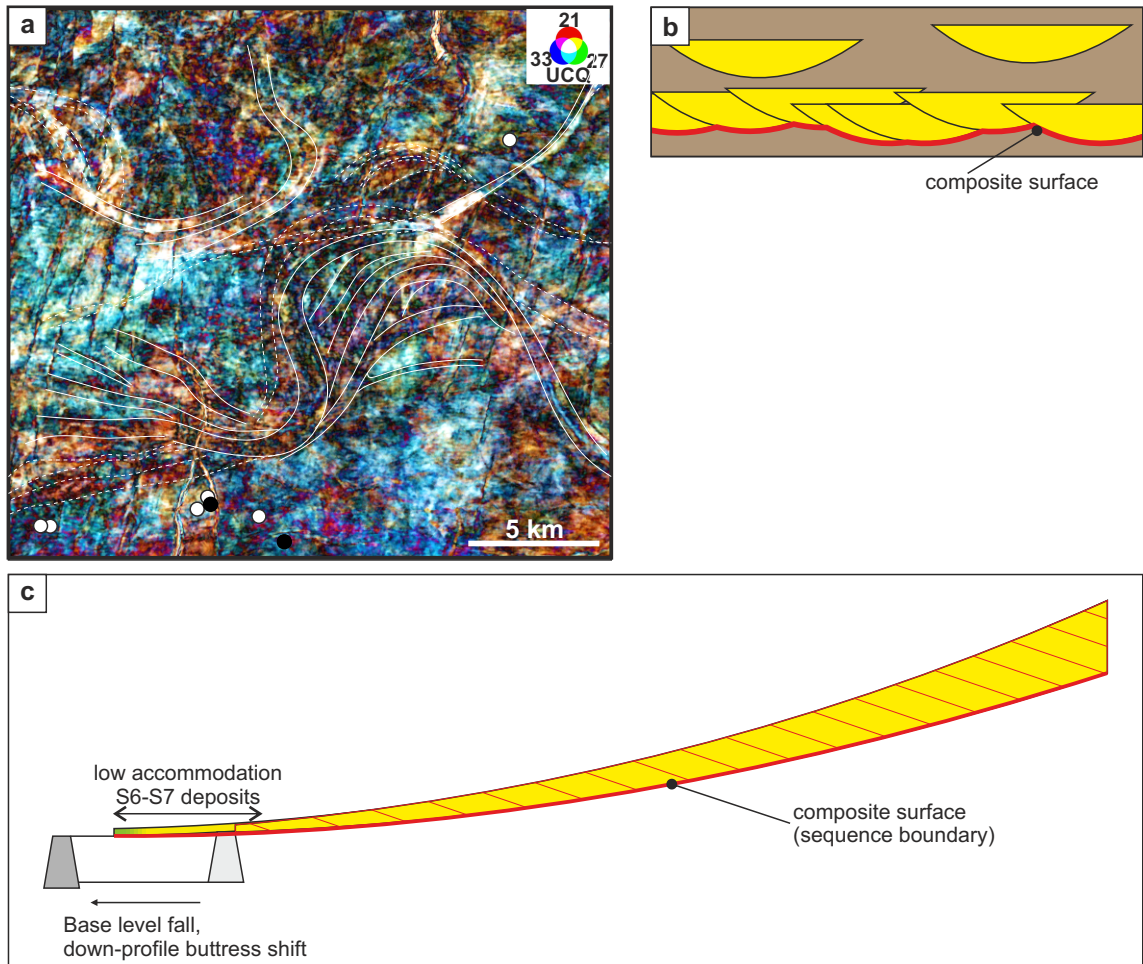


Figure 7.14: Buffers and buttresses model for the tidally-influenced, fluvial S6-S7 interval of the Mungaroo Formation. **a:** horizon slice from the S6-S7 interval (RGB blended volume) showing overprinting of deposits, indicating very low accommodation setting. **b:** schematic diagram showing low accommodation fluvial channel belt deposits with a basal composite surface, in a 'thin preservation space' setting. **c:** buffers and buttresses model appropriate to the S6-S7 interval: A slight lowering of base-level results in a down-dip translation in buttress and an extension of the buffer profile down-dip.

in Chapter 2, avulsion occurs primarily through the erosion of channel banks, forming a crevasse channel, which will either form a progradational crevasse splay delta, or an incisional crevasse channel (Smith et al., 1989; Mohrig et al., 2000; Hajek & Edmonds, 2014). The tendency for crevasse channels to prograde or incise depends in part on the floodplain composition: sandy floodplains tend to be prone to incision, whereas finer-grained, muddy floodplains tend to host avulsions by progradation (Hajek & Edmonds, 2014). Avulsion can also occur by annexation of previously fully or partially abandoned channels, such as is seen in the Saskatchewan River (Smith et al., 1998; Pérez-Arlucea & Smith, 1999).

Slingerland and Smith (2004), summarise six types of avulsion: partial, full, nodal, local, random and regional. The S2-S3 interval appears to have both local and regional avulsions (Figure 7.15 after Heller & Paola, 1996), but in fact shows evidence of a partial avulsion, and subsequent local avulsion.

The preservation space available and the channel aggradation rate act to determine the avulsion frequency (Bryant et al., 1995; Postma, 2014). This will be discussed in more detail in section 7.4.4.

7.4.3 Local floodplain effects

As the S5-S6 interval in particular of the Mungaroo Formation has preserved possible raised mire deposits as poor-quality coals, it is possible that a local control on channel location is given by compaction of peat (van Asselen, 2011), which created localised, small-scale basin subsidence (cf. Figure 7.6e for the effect of localised subsidence on the creation of preservation space for fluvial successions). This could account in part for the concentration (clustering) of

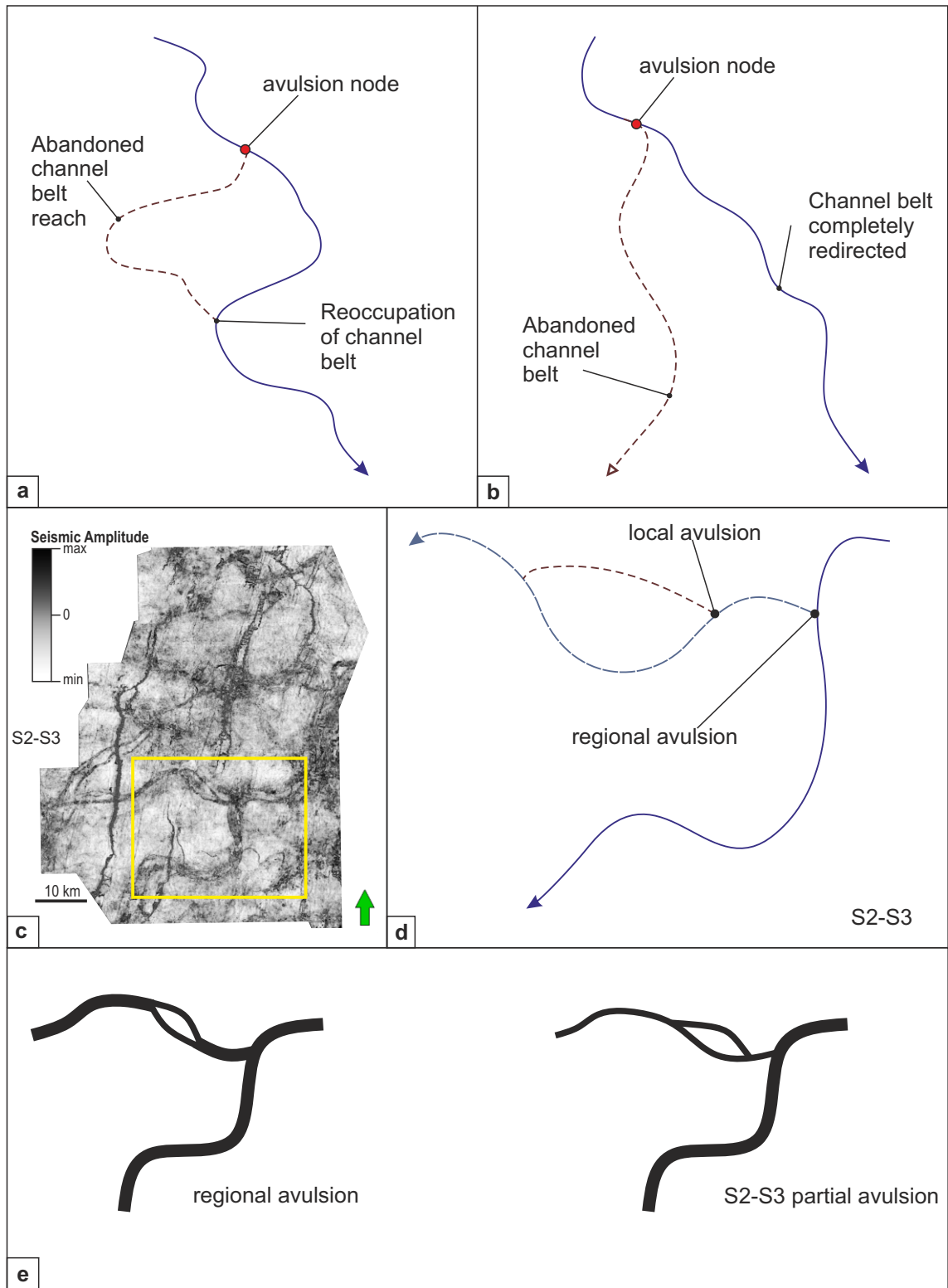


Figure 7.15: The effect of local (a) and regional (b) avulsion, after Heller & Paola (1996). The stratal slice from the S2-S3 interval c), shows evidence of both local and possible regional avulsion of channel belt deposits. Fig. 7.14d shows a simple cartoon illustration of the local and regional avulsions identified in the highlighted box in Fig. 7.14c. Closer investigation of the channel belts in planform shows a change in scale between the norther and southern channel belt, indicating that rather than a regional avulsion, it is a partial avulsion (Fig. 7.14e c.f. Slingerland & Smith, 2004).

channel-belt deposits in the S6-S7 interval seen in Figures 4.11 and 6.9. A similar response to differential compaction is proposed as one of the controls on local abundance of channel deposits in the B-C seam of the Rangal Coal Measures. The floodplain substrate of poorly-drained floodplains may locally control channel morphology (Bos et al., 2009), depending on whether channels incise into organic-rich lake deposits, or peat mire deposits: organic-rich, clastic lake deposits tend to develop lower stability banks, leading to higher-sinuosity channels, whereas peat deposits tend to be resistant to erosion, thereby leading to the development of relatively straight channels. The presence of mud-rich lake and gleysol deposits on the delta plain of the S5-S6 interval Mungaroo Formation may account for the moderate sinuosity (Table 4.2c) of some of these channels, despite their lower delta plain depositional setting.

7.4.4 Channel-body clustering (discussion of avulsion rate v floodplain aggradation)

Recent research by Hajek et al. (2010; 2012) indicates that autogenic processes will tend to obscure the sedimentary signals of allogenic processes, and that over basin-filling timescales, autogenic processes may produce similar sedimentary patterns to those caused by allogenic processes, i.e. changing boundary conditions (Jerolmack & Paola, 2007; Kim et al., 2006; Van de Weil, 2010). Although avulsion is generally assumed to be random or quasi-random, research by Hajek et al. (2012), focussing on the Late Cretaceous to Paleocene Ferris Formation (Wyoming, USA), suggests that channel-belt clustering may not be due to allogenic forcing (e.g. by differential subsidence) but may instead be the result of long-term self-organisation of channel belts through avulsion, formed under constant boundary conditions (Figure 7.16). It cannot therefore be

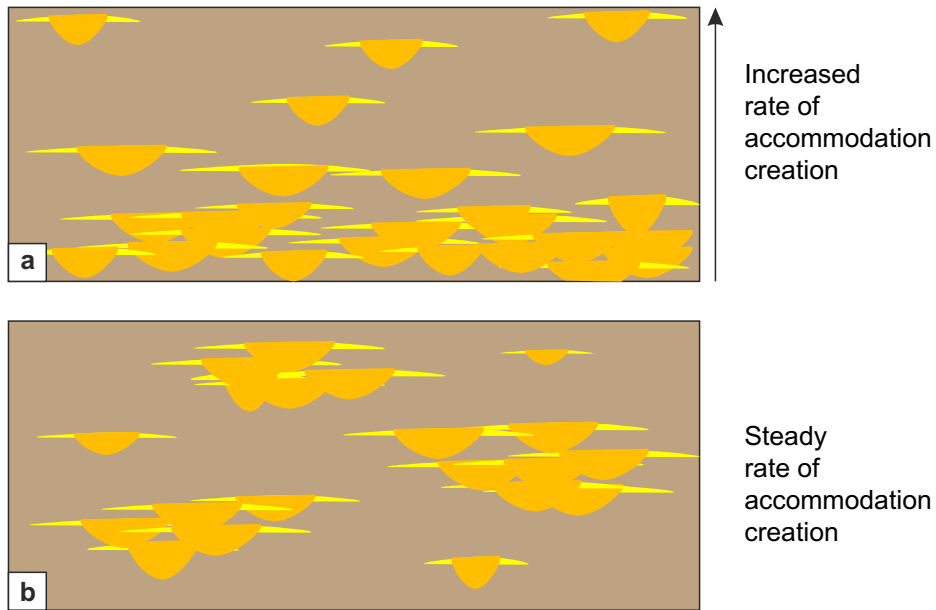


Figure 7.16: Alluvial stratigraphy produced by **a)** increased aggradation rates and **b)** non-random avulsive clustering. After Hajek et al. (2012).

assumed that avulsion deposits, and in particular clustering of channel-belt deposits (such as is seen in the S5-S6 interval), are necessarily indicative of a change in boundary conditions; instead autogenic avulsive clustering must be considered as a potential control on the style of aggrading fluvial architecture. The Ferris Formation floodplain morphodynamics are somewhat analogous to those interpreted in the S5-S6 interval of the Mungaroo Formation: fine-grained, dark, often carbonaceous floodplain muds, with rare thin coal seams, and immature palaeosols, indicating a high-accommodation, poorly drained floodplain, such as that of the S5-S6 interval. Of note, erosional surfaces in the Interval of the Ferris Formation studied by Hajek et al. (2012) are similar to those of the S5-S6 Mungaroo Formation interval, as they are restricted to basal channel scours, with no regional erosional 'composite' surfaces.

7.5 Discussion

7.5.1 Accommodation vs. Sediment supply

The interplay of accommodation rate and sediment supply rate can have distinct effects on alluvial architecture (Martinius et al., 2014). Assessing fluvial (and fluvio-deltaic) systems in terms of accommodation vs. sediment supply ratio may provide an alternative to sequence stratigraphic approaches (such as those of Allen & Posamentier, 1993; Shanley & McCabe, 1994; Plint et al., 2001; Weissmann et al., 2000; Holbrook, 2006), as no universal non-marine sequence stratigraphic model has yet been developed (Martinius et al., 2014) and it may not be possible or appropriate to apply 'traditional' (marine) sequence stratigraphic terms to alluvial stratigraphy (Ethridge et al., 1998). This has particular resonance with theories of 'self-organisation' of channel belts

(Hajek et al., 2010; 2012), which have shown experimentally and in ancient outcrops that the sedimentological signature of the changes in boundary conditions required to apply systems tracts to alluvial deposits may be partially or completely obscured by the product of autogenic processes.

The accommodation vs. sediment supply approach does not attempt to place deposits within systems tracts, but instead focuses on identifying parameters that indicate a change in the accommodation/sediment supply (A/S) ratio. Table 7.1 lists these parameters.

Table 7.1: Parameters indicating a change in A/S ratio (after Martinius et al., 2014)

Parameter indicating A/S change	Change indicated	Importance
Changes in degree of maturation and thickness of paleosol	Less mature paleosols indicate an increased accommodation rate	High
Variation in type and proportion of preserved fluvial sandstone a) lithofacies and b) facies associations	Change in channel style in response to upstream changes in discharge and/or sediment load	a) High b) Moderate
Variation in channel belt thickness and width compared to channel thickness and width	Changes in vertical and lateral connectivity off sandstone related to changes of accommodation generation with respect to sediment flux and stream discharge. High accommodation generation coupled with high sediment supply rate will give rise to frequent avulsions with highly connected sandstone deposits, as channel deposits erode finer floodplain deposits and the tops of channel deposits. High accommodation rate with a lower sediment supply rate will result in the preservation of more floodplain fines.	High

Parameter indicating A/S change	Change indicated	Importance
Variations in the amount of fine grained deposits preserved in the succession	Changes in rate of accommodation generation with respect to sediment delivery to the floodplain	High (in low-mod subsidence rate)
Frequency of occurrence and characteristics of erosion surfaces between facies associations	May indicate floodplain-wide degradation, or just local downcutting by channels and valleys	Moderate
Variations in long-term avulsion frequency and channel stability	Higher aggradations rates are expected to result in higher avulsion frequencies; lower avulsion frequencies indicate lower aggradation rates	Moderate

Application of the A/S variation indicators (Martinius et al., 2014) gives further insight into the conditions present at the time of deposition of the studied intervals of the Mungaroo Formation. The high proportion of preserved sandstone (interpreted from seismic section and wireline log) in the S1-S2 interval, coupled with interpreted regional incision events in the lower S1-S2 interval, indicates a low A/S ratio. The S2-S3 interval appears to have a moderate to relatively high A/S ratio, with more complete preservation of both channel and floodplain facies associations, but also some evidence of downcutting by higher-energy channel belt complexes. The S5-S6 interval appears to have both moderate- and low-sinuosity channel forms, possibly indicating a fluctuating rate of sediment supply. The high frequency of avulsions and preservation of floodplain facies indicates high accommodation rates, whereas stacking of channel belts with high connectivity may indicate concurrent high sediment supply rates. The deposits of the lower S6-S7 interval show preferentially high preservation of sandstone lithofacies coupled with amalgamation and overprinting of the channel deposits, which indicates a low

A/S ratio with high rate of sediment delivery. These channel deposits are overlain by lower net:gross tidal bay-fill deposits with greater preservation of floodplain fines, (Figure 6.12), probably indicating an increase in A/S ratio towards the top of this interval. Figure 7.17 attempts to describe conceptually the possible variations in A/S ratio throughout the Mungaroo Formation using a series of Barrell (Barrell, 1917) diagrams.

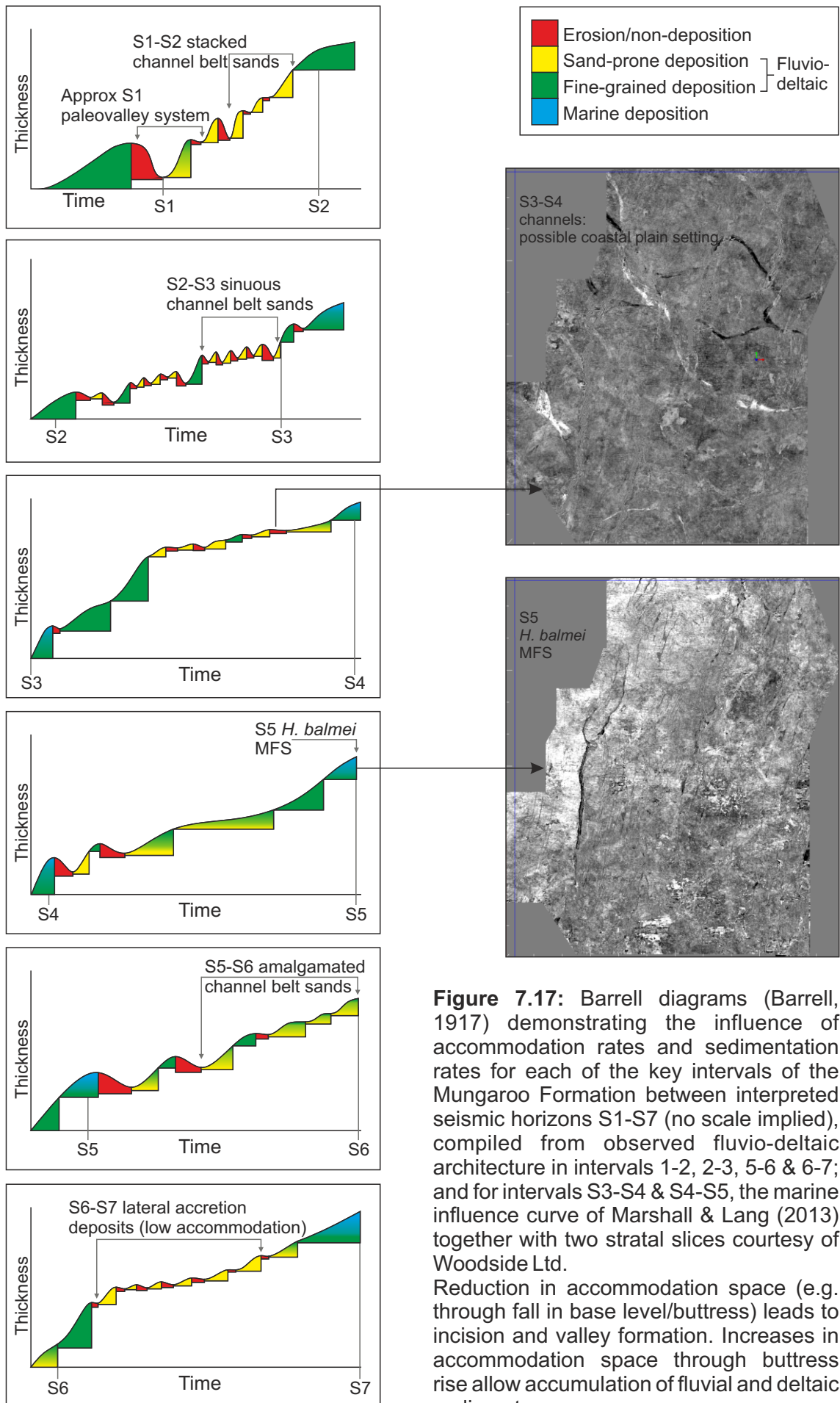


Figure 7.17: Barrell diagrams (Barrell, 1917) demonstrating the influence of accommodation rates and sedimentation rates for each of the key intervals of the Mungaroo Formation between interpreted seismic horizons S1-S7 (no scale implied), compiled from observed fluvio-deltaic architecture in intervals 1-2, 2-3, 5-6 & 6-7; and for intervals S3-S4 & S4-S5, the marine influence curve of Marshall & Lang (2013) together with two stratal slices courtesy of Woodside Ltd.

Reduction in accommodation space (e.g. through fall in base level/buttruss) leads to incision and valley formation. Increases in accommodation space through buttruss rise allow accumulation of fluvial and deltaic sediments.

7.6 Mungaroo Fm Depositional model

The Mungaroo Formation deposits encountered in this study show a range of localised depositional sub-environments: (i) incised multi-valley deposits; (ii) alluvial and upper delta plain deposits; (iii) lower delta plain distributary network and mires; (iv) tidal point bar deposits. Figure 7.18 shows a generalised fluvio-deltaic depositional setting, with possible locations of the studied intervals of the Mungaroo Formation annotated.

7.6.1 Modern analogues

For each of the studied intervals of the Mungaroo Formation, an attempt has been made to assign a suitable modern analogue.

7.6.1.1 *S1-S2: Incised valley system*

The S1-S2 interval deposits show high-energy channel fill, with mostly downstream migrating barforms, poor preservation of overbank deposits, and an erosive (candidate 'composite surface' sequence boundary) base. The lack of marine and tidal indicators implies a purely fluvial regime; variations in grain size indicate a possible seasonal influence on sedimentation. The geomorphology of the upper S1-S2 interval deposits (Figure 6.6), in particular, is interesting: straight valleys (possible bypass valleys), with moderate-high sinuosity channel belts, which is somewhat at odds with the dominantly downstream migrating barforms observed in core. A possible modern analogue for the S1-S2 deposits is found in one of the modern rivers of Madagascar,

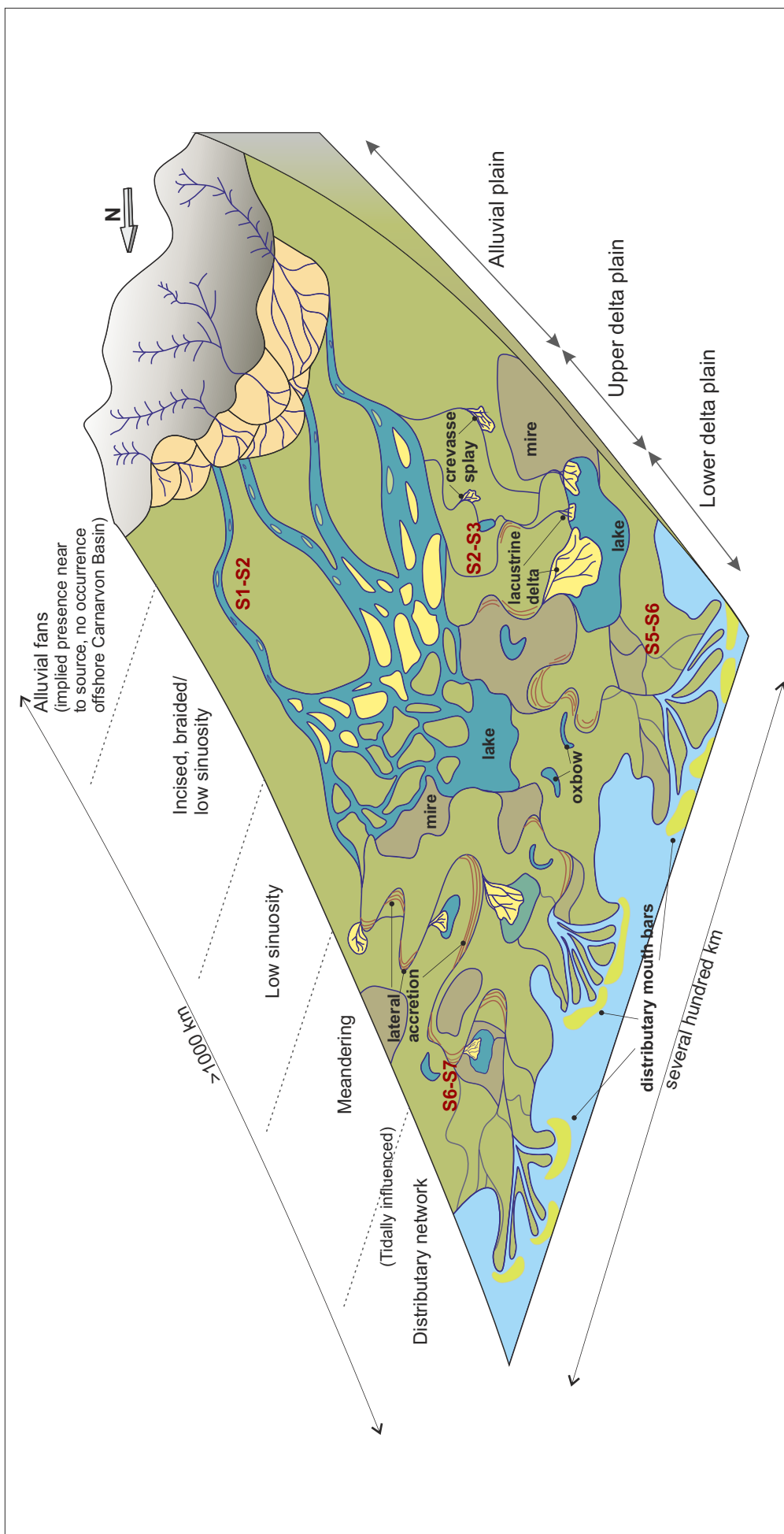


Figure 7.18: Generalised model of a fluvial-deltaic depositional environment, such as would have formed the Mungaroo Formation, passing from the source (uplands), through incised valley systems; braided fluvial system, meandering fluvial system, meandering upper delta plain, tidally-influenced lower delta plain, to distributary mouth bars. Lakes, crevasse splays, lacustrine deltas, lateral accretion deposits and mires are present. Prospective relative locations of the S1-S2, S2-S3, S5-S6 and S6-S7 intervals are marked.

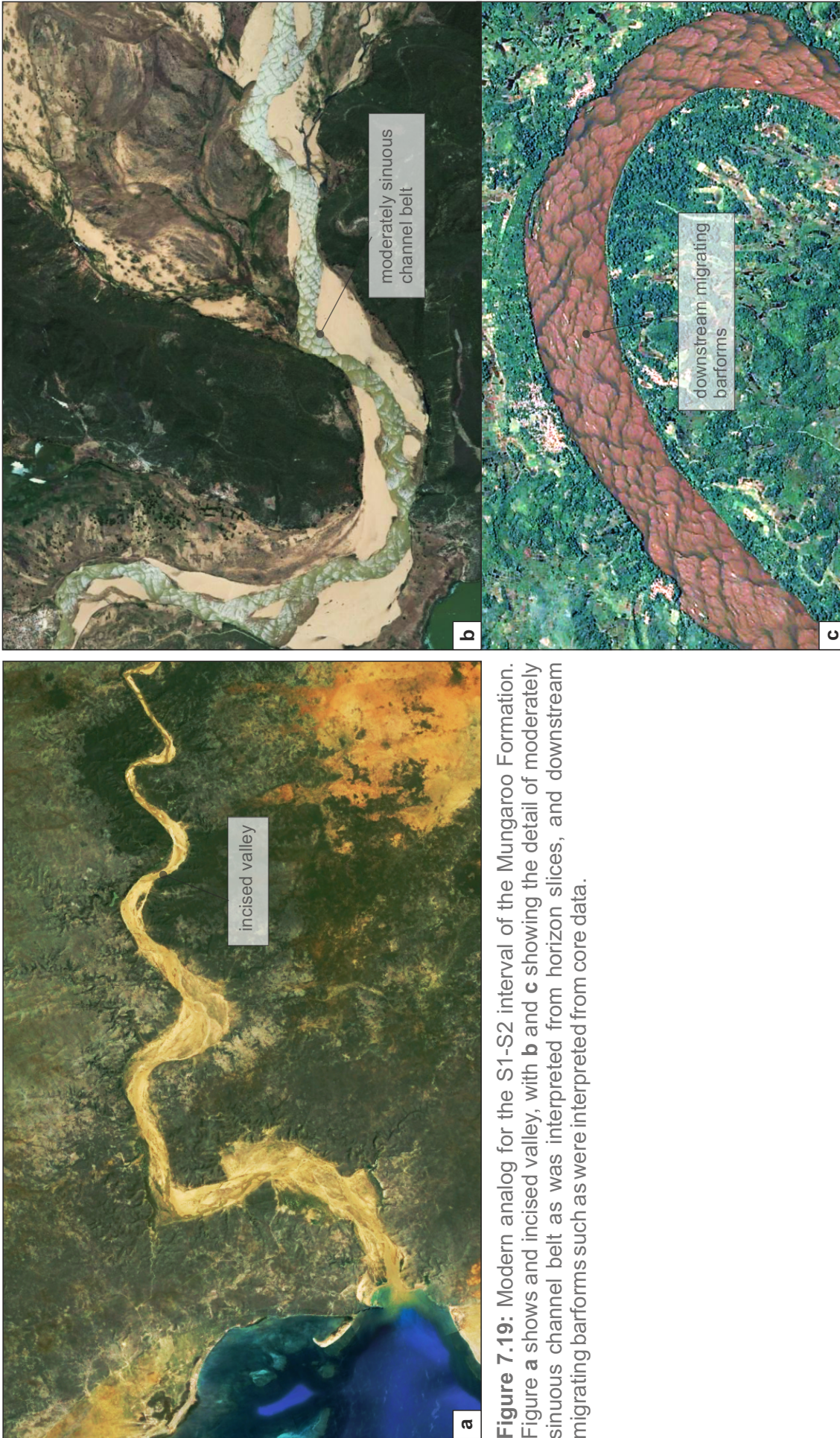


Figure 7.19: Modern analog for the S1-S2 interval of the Mungaroo Formation. Figure a shows an incised valley, with b and c showing the detail of moderately sinuous channel belt as was interpreted from horizon slices, and downstream migrating barforms such as were interpreted from core data.

where sinuous channel belts contain downstream-migrating, low-sinuosity channels (Figure 7.19).

7.6.1.2 S2-S3: Upper delta plain

The S2-S3 interval is characterised by a combination of low-sinuosity, high-energy channel bodies, and higher-sinuosity, low-energy channel bodies. The frequency of crevassing encountered in core and identified on seismic slices indicates a relatively high-accommodation setting, prone to local, partial and regional avulsion. The presence of gleysols, lacustrine deposits and thin, laterally restricted coals, as well as weak tidal indicators, indicates a poorly drained upper delta plain setting. The Cumberland Marshes (Saskatchewan, Canada) show this wide range of deposits (albeit in a lacustrine rather than marine delta setting) and are presented as a possible modern analogue for the S2-S3 interval (Figure 7.20).

7.6.1.3 S5-S6: Lower delta plain

Deposits interpreted from the S5-S6 interval represent a high-accommodation, poorly drained, high-water table setting, prone to avulsions in an anastomosing, distributary network. Autogenic clustering of channel belts (possibly driven in part by peat compaction) is noted. The depositional setting is interpreted as the lower delta plain of a river-dominated delta, with abundant lakes and mires (possibly raised mires). The Kobuk river is chosen as a modern analogue due to similarities in scale and the variety of deposits: however, a caveat must be attached to the use of this analogue as the Kobuk River is affected by permafrost and is therefore not analogous in terms of its climate setting,



Figure 7.20a: Modern analog for the S2-S3 interval of the Mungaroo Formation: Cumberland Marshes, Saskatchewan, Canada. The Cumberland Marshes show many of the features of the S2-S3 interval, including a poorly drained floodplain, channel belts, lakes and peat mires, (b) crevasse splay deltas and (c) minor distributary channels.

although the higher-sinuosity permafrost-influenced channels share morphologic similarities with those interpreted as being affected by incising into and through clastic lake fill in the Mungaroo Formation (Figure 7.21).

7.6.1.4 S6-S7: Tidally-influenced point bars

The dominant deposits of the S6-S7 interval are tidally influenced point-bar deposits, showing a high level of amalgamation and overprinting, in a highly vegetated floodplain. This setting is highly analogous to the ancient deposits of the McMurray Formation (cf. Hubbard et al., 2011). The modern system widely considered to be analogous to the McMurray Formation is the Peace River (Smith, 1988; Smith et al., 2009; Smith et al., 2011). Figure 7.22 shows modern point- and counterpoint-bar deposits from the Peace River (reproduced from Figure 6.11).

No single modern analogue describes the Mungaroo Formation as various boundary conditions and autogenic responses have changed during the temporal evolution of the formation.

7.6.2 Generic observations of response to allogenic and autogenic controls

The variations seen in the Mungaroo Formation deposits in response to changing allogenic and autogenic controls may be applied to make more generic predictions of the response of fluvio-deltaic systems to changing allogenic and autogenic controls.

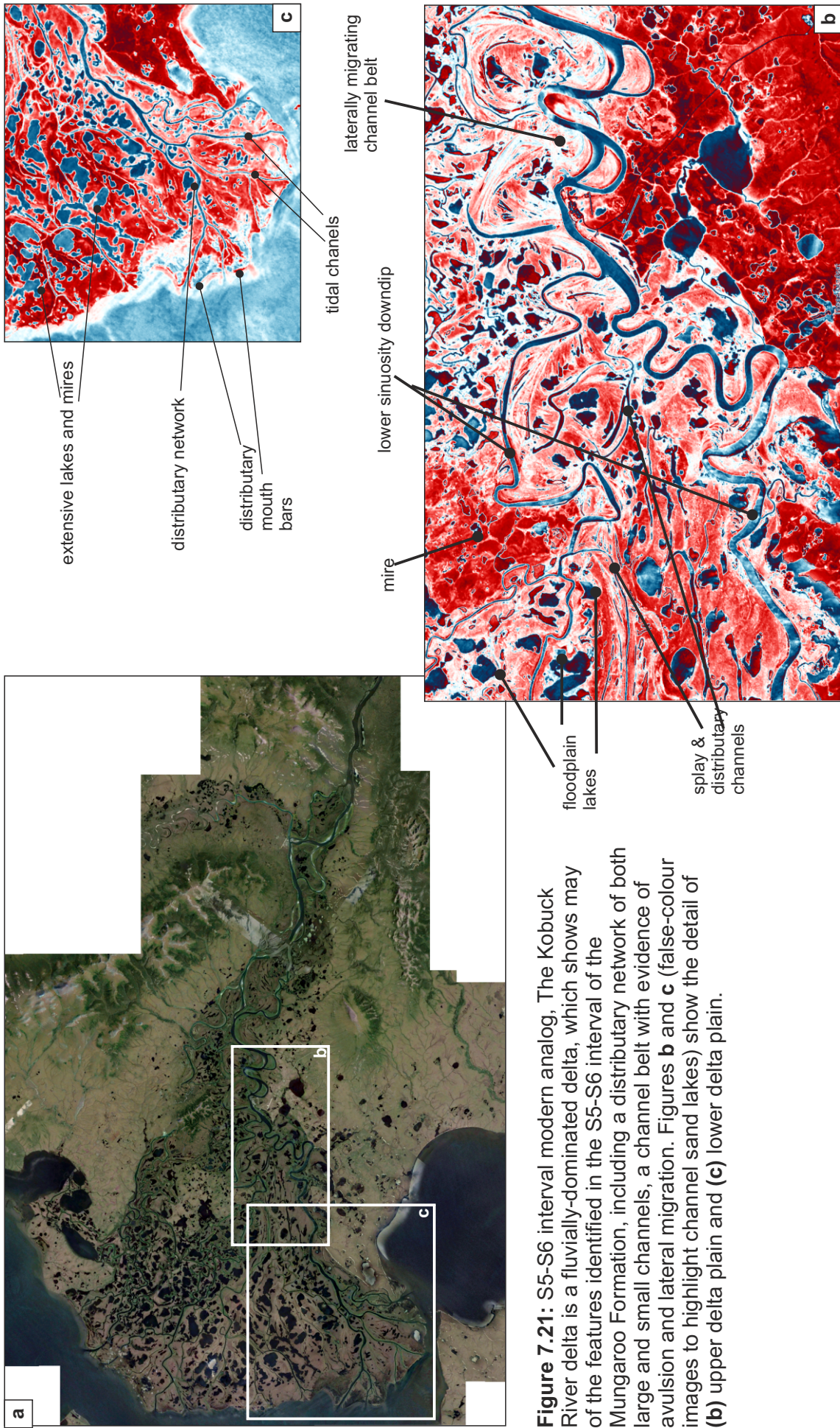


Figure 7.21: S5-S6 interval modern analog, The Kobuck River delta is a fluvially-dominated delta, which shows many of the features identified in the S5-S6 interval of the Mungaroo Formation, including a distributary network of both large and small channels, a channel belt with evidence of avulsion and lateral migration. Figures **b** and **c** (false-colour images to highlight channel sand lakes) show the detail of (b) upper delta plain and (c) lower delta plain.



Figure 7.22: Analogs for the S6-S7 interval of the Mungaroo Formation: **a:** Reproduced from Lebreque et al. (2011). The McMurray Formation, Alberta, as an ancient, tidally-influenced, low accommodation, fluvial setting, featuring overprinting of lateral accretion deposits, analogous to the S6-S7 interval of the Mungaroo Formation. **(b)** The Peace River is a frequently used modern analog of the McMurray Formation (c.f. Hubbard et al., 2011; Smith et al., 2009, 2011) and is therefore deemed by this study to be a suitable analog for the S6-S7 interval of the Mungaroo Formation.

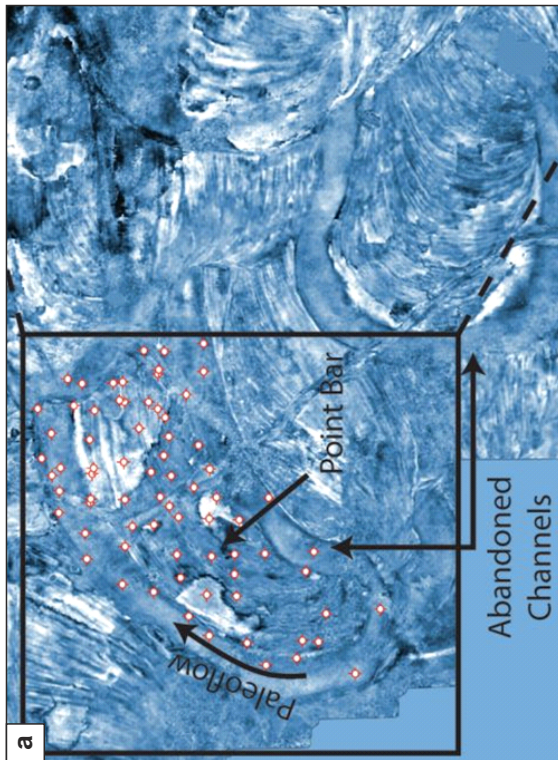


Table 7.2: Response of fluvio-deltaic systems to allogenic and autogenic controls, as observed in the Mungaroo Formation.

Type	Control	Response
Allogenic	Base-level fall	Incised valley deposits, or low accommodation, amalgamated channel deposits. Basinwards shift in facies.
Allogenic	Base-level rise	Increased marine influence e.g. salinity indicators, marine/brackish ichnofacies, tidal indicators. Higher rate of accommodation space creation. Poorly-drained floodplain (rise in water table).
Allogenic	Wetter climate	Floodplain response: gleysol and coal deposits, increased vegetation (leading to plant material in channel deposits), poorly-drained floodplain.
Allogenic	Sediment supply (function of climate & tectonic uplift of source area)	Changes in grain size distribution indicating intermittent or pulsed flow. Change in ratio of channel v overbank fines in preserved section.
Autogenic	Increased avulsion frequency	Increase in crevasse splay deposits in preserved overbank section, increased connectivity of channel deposits.
Autogenic	Local floodplain effects	Floodplain substrate may exert a local control on channel morphology and create localised accommodation space for channel deposition.
Autogenic	Channel belt clustering	Increased channel connectivity & clustering of channel belts does not necessarily require a change in boundary conditions.

7.7 Conclusions

The following allogenic controls have been identified as affecting the architecture of the Mungaroo Formation.

Base-level. There is a gradual evolution from purely fluvial, incised-valley deposits, through fluvial and upper delta plain deposits, to lower delta plain and tidally influenced point-bar deposits, largely forced by a regional rise in sea level (cf. Marshall & Lang (2003) Triassic sea-level curve).

Source uplift and subsequent erosion provided the sediment load deposited as the Mungaroo Formation.

Climate. In addition to the generally wetter and drier periods interpreted by Payenberg et al. (2013), evidence has been presented here to support episodes with higher seasonal variations in discharge (implying wet-dry seasonality and possible monsoonal events), as well as generally wetter periods with increased vegetation, as evidenced by 'tea-leaf' structures, coals, and gleysol development, for example.

Allogenic controls have been shown to control the overall regional stacking patterns of sequences within fluvio-deltaic successions, such as the Mungaroo Formation.

Autogenic controls, such as crevassing (leading to avulsion) and channel belt clustering, have been shown to have exerted a control on the local arrangement of channel and floodplain architecture through substrate compaction, erosion and autogenic clustering of channel belts in some intervals.

The various interpreted deposits of the Mungaroo Formation have been applied to a general depositional model of fluvio-deltaic deposits, and modern analogues have been assigned based on observed plan-form architecture, as well as interpreted climate, tidal, accommodation and vegetation conditions.

Chapter 8 Conclusions and future work

8.1 Chapter overview

This chapter aims to provide concise answers to each of the research questions proposed in Chapter 1. The findings and conclusions of each chapter within this study are drawn together to provide summaries and final conclusions for this work. This chapter considers possible future work that could build upon the outcomes of this body of research.

8.2 Research questions

The following sub-sections address each research question in turn to summarise this body of research.

8.2.1 To what extent do minor (secondary and tertiary crevasse splay and distributary) channels contribute to fluvial overbank successions, and how likely are they to form connected reservoir bodies?

This question was addressed by the investigation of the deposits of two interseams of the Rangal Coal Measures, at the South Blackwater Mine, Queensland. The interseam packages were investigated using high-resolution, closely-spaced wireline logs, and were found to be composed predominantly of overbank deposits. Small-scale (crevasse and distributary) channel deposits are a potentially significant repository for sandstone lithofacies in overbank successions, with 22% of the B-C interseam deposits of the Rangal Coal Measures at the South Blackwater Mine accounted for by secondary and tertiary channel-fill deposits. The proportion of infill composed of these deposits is both temporally and spatially variable, as deposits are interpreted to be intimately associated with avulsive deposits (e.g. crevasse splay deltas) and so

are influenced by local autogenic controlling factors such as bank stability, as well as regional allogenic controls such as changing rates of accommodation creation that are potentially attributed to factors such as rises in base level. The change in accommodation conditions is interpreted as responsible for the contrast in architectural element proportions in the two studied interseams: the low net:gross (3% channel infill) of the A-B interseam is interpreted to reflect deposition under higher accommodation conditions than the B-C interval (23% channel infill), with a wider spread of lacustrine deposits (constituting 70% of infill) attributed to base-level (lake-level) rise.

Stochastic modelling of both splay and distributary channel elements was undertaken to estimate the potential connectivity between sand-prone minor channel deposits in the Rangal Coal Measures, as well as to observe general trends applicable to crevasse and distributary channel sandstone-body connectivity. The connectivity of minor channel deposits is influenced not only by the infill proportion of the deposits, but by the channel type, i.e. likely planform geomorphology of the deposits. Where channel deposits form during progradational events (i.e. as part of a crevasse splay delta), relatively good connectivity is observed in proximal positions in the splays; however, connectivity decreases distally from the source as channel elements diverge. Connectivity between crevasse channels tends to be greater down the axis of splays, with more isolated channel bodies occurring at the margins. Connectivity tends to be greater and more uniform between distributary channels rather than splay channels. Modern analogues were used to demonstrate potential plan-form geomorphological arrangements of the channelized deposits, as well as the pattern of interconnectivity between channels.

8.2.2 What is the nature of the stratigraphy and sedimentology of the Triassic Mungaroo Formation in block WA-404-P, Exmouth Plateau, Australia?

The Late Triassic Mungaroo Formation represents a large fluvio-deltaic system that was constructed in the Northern Carnarvon Basin throughout the Norian. The temporal evolution of the Mungaroo Formation represents a stratigraphic response to a first-order transgression, with the depositional setting evolving from a purely fluvial regime to a tidally-influenced, fluvially-dominated deltaic setting. The deposits of the Mungaroo Formation studied herein can be split into six intervals (S1-S2, S2-S3, S3-S4, S4-S5, S5-S6, S6-S7), each separated by transgressive and flooding surfaces that are recognised and interpreted using a high-resolution 3D seismic survey.

Sixteen lithofacies and seven facies associations were interpreted from core, and related to wireline log expression. Owing to the limited stratigraphic extent of core available within the study area, observations regarding the lithology of the Mungaroo Formation are based primarily on the S2-S3 interval, which has a complete cored interval in one well, encompassing both channelized and overbank successions. Within the S2-S3 interval, lithofacies and facies associations indicate a fluvially-dominated, at times tidally-influenced, upper delta plain setting, with systematic and predictable transitions from more fluvial-dominated to more deltaic-dominated episodes of accumulation. Core samples from the uppermost interval (S6-S7) show a greater tidal influence, consisting of tidally influenced point-bar deposits, overlain by tidal and marine-influenced bay-fill deposits.

Several styles of channels were interpreted from their lithological expression and dip-log data. Certain trends in channel style were observable, most notably

that higher energy channel deposits tended to be low sinuosity, composed of downstream migrating barforms, whereas lower-energy channels (including splay channels) tended to be higher sinuosity. Within the studied interval, it remained difficult to distinguish from well data alone between incised valley and amalgamated channel-belt deposits.

8.2.3 What are the broad variations in depositional environment at key intervals of the Mungaroo Formation? Can seismic facies be used to distinguish between fluvial and fluvio-deltaic deposits?

Each of the three intervals (S1-S2, S2-S3, S5-S6) studied in Chapter 4 represent 'snapshots' at key stages in the accumulation of the Mungaroo Formation, and have, distinct depositional palaeoenvironmental settings: (i) S1-S2 represents dominantly incised valley deposits; (ii) S2-S3 represents an upper delta plain setting, with channel belts and associated splay belts. The floodplain shows evidence of being poorly drained at certain times during its evolution (with the development of spatially restricted mires, and gleysol deposits), though within the regional context of this relatively distal study of the Mungaroo Formation, this interval represents a relatively well-drained floodplain setting; (iii) S5-S6 represents a poorly drained upper delta-plain setting, with a distributary network of channel belts and minor distributary channels, as well as extensive organic-rich deposits including gleysols and coals. Considering the deposits interpreted in a vertical sense moving up through the succession, as they record a transition from valley fill, to relatively well-drained fluvial floodplain, to poorly drained delta plain: Although the Mungaroo Formation represents several small-scale fluctuations in base-level it overall records a general base-level rise.

Seismic facies has been linked to sedimentology through by integrating wireline log, core log and seismic data, developing a 'seismic element' scheme that can be used to identify key depositional elements of fluvial and deltaic environments. From careful analyses of plan-form geomorphology and assessment of relative proportions of seismic elements, it is possible to distinguish between purely fluvial, upper delta plain and lower delta plain depositional sub-environments. Key distinguishing observations included: (i) wet versus dry substrate conditions, as indicated by the presence or absence of gleysols indicative of a poorly drained floodplain, as is seen at the S5-S6 interval; (ii) the presence of incised valley systems, as identified around S1, an interval with large valley features, with negligible deposition away from the large features, indicating deposition is confined within them; (iii) aggradational delta plain, as indicated by fluvio-deltaic deposits accumulated across a broad floodplain area, as identified at S6. Reduced seismic resolution at greater depths remains a limiting control on data quality and granularity and this has implications for interpretations; in particular, it remains very difficult to distinguish definitively and routinely between valley-fill and channel-belts.

8.2.4 What techniques can be employed to identify channelized deposits at a range of scales, and also non-channelized floodplain deposits? Can any seismic interpretation techniques be used to bring out more detailed interpretations?

A range of seismic interpretation techniques were investigated and proven to be useful in the interpretation of both channelized and non-channelized fluvio-deltaic deposits. The need for such an investigation stems from the scale of fluvial deposits, which are often approaching or even below conventional seismic resolution. A robust stratigraphic framework aids in the identification of

horizons that represent key surfaces of stratigraphic significance. A major outcome of this study has been the recognition that flooding surfaces overlying fluvial and fluvio-deltaic sequences, which are more laterally continuous than the basal erosive surfaces underlying channel deposits, are more useful for seismic interpretation as they can be traced over a greater area. Due to the small scale of some of the fluvial deposits, noise cancellation and frequency enhancement provided a considerable uplift in the visible detail of deposits. Horizon or stratal slicing is an essential technique for viewing non-horizontal deposits, particularly where there has been post-depositional faulting, although the quality and reliability of the horizon and stratal slices depends on the fidelity of the interpreted seismic horizons. Frequency decomposition enabled the visualisation of deposits that are below normal seismic resolution by allowing the viewer to focus on specific frequency ranges revealing subtle features. Several seismic attributes including structural attributes, signal processing and stratigraphic attributes also demonstrated their utility in identifying the edge of channelized features, as well serving to distinguish between higher porosity sand-rich channel belt deposits, and lower porosity overbank fines.

8.2.5 How can a range of seismic interpretation techniques, including spectral decomposition, be used to resolve the internal architecture of channel belt deposits within the Mungaroo Formation? Can these techniques provide further insight into fluvial styles, distinguishing between entrenched valleys and amalgamated channel belts?

As previously discussed, horizon slicing through flattening of the 3D seismic cube enables the visualisation of large-scale fluvial deposits; however, this technique does not enable the visualisation of the detailed architecture of individual channel-belt deposits, as they are typically close to the limit of seismic

resolution. Spectral decomposition and colour blending of frequency volumes has proven effective for visualising the channelized deposits of the Mungaroo Formation, even at depths >3 km, representing a significant uplift in the resolution compared to seismic reflectivity data. Three intervals (S1-S2, S5-S6, S6-S7) of the Mungaroo Formation were studied. By analysing horizon slices from colour blended volumes, it was possible to distinguish between incised valleys and amalgamated channel belts, where previously interpretations had been ambiguous, i.e. S5-S6 interval deposits. In the deepest interval (S1-S2), it was possible to make some interpretations regarding the nature of the channel-belt fill within an incised valley, charting the lateral migration of the deposits through time, and estimating the relative sinuosity of the formative rivers from channel-belt rugosity. The shallowest interval (S6-S7) showed the most improvement in resolution: for this interval it was possible to trace out overprinting lateral accretion deposits, which, when related to core samples, were found to be tidal point-bar deposits, analogous to those of the Cretaceous McMurray Formation of Alberta, Canada.

8.2.6 What are the possible autogenic and allogenic controls on the variations in depositional style identified in the Mungaroo Formation? What can this tell us about fluvio-deltaic systems more generally?

Up-dip and down-dip allogenic and autogenic controls on fluvial deposition were discussed with reference to literature, and related to observations and interpretations of the Mungaroo Formation made in Chapters 3-6 of this thesis, in order to explain of the overall pattern of stacking of architectural elements present in the formation, as well as the detailed architectural expression of key stratigraphic intervals and surfaces.

Allogenic controls have been found to be the major control on the overall stacking of fluvio-deltaic sequences; notable allogenic controls include base-level change, source uplift, and climate. Allogenic controls were also deemed responsible for some smaller-scale depositional variations, for example climate-induced variations that promoted increased vegetation and which resulted in the accumulation of thick deposits of 'tea-leaf' structures in the tidally influenced S6-S7 interval.

The Buffers and Buttresses model (Holbrook, 2006) has proven useful in describing the temporal evolution of the Mungaroo Formation, as a series of stacked buffer zones and transgressions. The model has been used to explain the preservation of deposits even in the very low-accommodation S6-S7 interval. The four intervals of the Mungaroo Formation studied in this thesis (S1-S2, S2-S3, S5-S6, S6-S7) have been described in terms of their responses to rising and falling buttresses at the time of deposition: S1-S2, buttress fall; S2-S3, slow buttress rise; S5-S6, rapid buttress rise; S6-S7, base-level fall with a down-profile buttress shift.

Autogenic controls have been interpreted as having exerted a control on the local arrangement of channel and floodplain architecture through crevassing (leading to avulsion in the S2-S3 interval), substrate compaction (potential local accommodation space creation through peat compaction in the S5-S6 interval may have influenced the clustering of channel belts), erosion and avulsion-driven clustering of channel belts via compensational stacking in some intervals.

The Mungaroo Formation has been used to demonstrate how observations of interpreted deposits in specific intervals can be related to a more general

assessment of depositional environments in terms of their accommodation vs. sediment supply (A/S) ratio driven by allogenic and autogenic controls.

The depositional sub-environments at each of the four interpreted intervals of the Mungaroo Formation have been assessed and modern analogues have been assigned to each of the intervals. No single modern analogue fully matches the complexity present in the Mungaroo Formation because various boundary conditions and autogenic responses have changed during the temporal evolution of the formation. Observations of the response of the Mungaroo delta system to changing boundary and autogenic conditions have been summarised as potential generic trends that arose in response to the evolution of a fluvio-deltaic system governed by a complex set of allogenic and autogenic controls.

8.3 Concluding remarks

The preserved stratigraphy of the Rangal Coal Measures and the Mungaroo Formation demonstrate that fluvio-deltaic systems respond in terms of proportion of preserved depositional elements and connectivity of channel deposits to changes in both allogenic and autogenic controls, with different depositional intervals being classified in terms of their accommodation setting and their relative degree of marine influence.

Base-level rise drives an overall increase in marine influence during the temporal evolution of the Mungaroo Formation. However the interpretation of deposition is much more complex than a simple transgression, as multiple, small-scale fluctuations in base level, as well as climate changes and changes in autogenic controls have created several distinct depositional sub-environments within the Mungaroo Formation. The interplay of allogenic and

autogenic controls has resulted in large-scale (regional) stacking patterns, as well as more localised channel and overbank deposit architectures and related subtle sedimentological features. Tidal influence varies greatly within the formation, and is generally interpreted as increasing up-stratigraphy. A summary table of generic responses of fluvio-deltaic systems to allogenic and autogenic controls based on observations from the Mungaroo Formation has been compiled (Table 7.2).

Seismic or well data alone cannot provide detailed interpretations of fluvio-deltaic deposits; instead a more holistic approach, incorporating well data and advanced interpretation techniques such as spectral decomposition and frequency blending has been employed. A generic workflow for the optimised interpretation of fluvial and fluvio-deltaic deposits in the subsurface has been presented, whereby it is possible to make detailed interpretations of individual channel-belt deposits, providing greater confidence in interpretations of depositional sub-environment.

8.4 Recommendations for future work

The findings outlined above and the research carried out as part of this study could be continued and extended in several ways.

8.4.1 Three-dimensional modelling of the Mungaroo Formation

Three-dimensional modelling was beyond the scope of this project but could form the basis for a follow-up study. The seismic element maps, in particular, could be scaled up in order to populate reservoir models, following the methods outlined by Massey et al. (2014). Reservoir property data (e.g. porosity and permeability) could be interpreted from well data in order to provide a greater understanding as to which facies associations would act as effective net

reservoir and non-net reservoir, and also to quantify connectivity between the various channel deposits identified.

8.4.2 Seismic QI

Although this study has focussed on qualitative interpretation techniques, a quantitative interpretation (QI) study of the seismic and well data would enable quantitative assessment of the seismic response to different lithofacies, modelling AVO response, for example. This would allow greater constraint of the lithofacies present at each of the studies intervals, potentially removing some ambiguity; for example, coals and gleysols are seen (qualitatively) to have the same seismic response in this study.

8.4.3 Comparison with modern and ancient analogues

Comparison of the findings from this study with ancient tidally influenced, fluvially dominated delta settings would further augment the dataset and improve the quality of subsurface interpretations, particularly with respect to analysing three-dimensional, sub-seismic scale architectural elements, which were not fully constrained as part of this study.

Assessment of the detailed geomorphology of modern analogue systems in the vein of Smith et al. (2009) and Russell et al. (2014) would provide additional granularity to the interpretations of channel and channel-belt deposits (particularly point-bar deposits) that can be made from seismic and well data. The combined study of modern and ancient analogues could help to elucidate the interplay of different controlling factors, including the extent to which local and regional architecture is controlled by changing boundary conditions or through self-organisation, for example.

This work could benefit from extension through comparison with analogous systems characterised in relational databases describing fluvial and fluvio-deltaic sedimentary architecture that are currently being developed. One such example is the Fluvial Architecture Knowledge Transfer System (FAKTS) database (cf. Colmbera et al., 2012, 2013).

References

- Abels, H.A., Kraus, M.J., Gingerich, P.D., 2013. Precession-scale cyclicity in the fluvial lower Eocene Willwood Formation of the Bighorn Basin, Wyoming (USA). *Sedimentology* 60 (1467-1483).
- Adamson, K.R., Lang, S.C., Marshall, N.M., Seggie, R.J., Adamson, N.J., Bann, K.L., 2013. Understanding the Late Triassic Mungaroo and Brigadier Deltas of the Northern Carnarvon Basin, North West Shelf, Australia, in: Keep, M., Moss, S.J. (Eds.), *The Sedimentary Basins of Western Australia IV: Proceedings of the Petroleum Exploration Society of Australia Symposium Perth*.
- Ainsworth, R.B., Walker, R.G., 1994. Controls of estuarine valley-fill deposition by fluctuations of relative sea-level, Cretaceous Bearpaw-Horseshoe Canyon transition, Drumheller, Alberta, Canada., in: Dalrymple, R.W., Boyd, R., Zaitlin, B.A. (Eds.), *Incised valley systems: Origin and sedimentary sequences*. SEPM, Tulsa, USA, pp. 159-174.
- Aitken, J.F., Flint, S.S., 1994. High Frequency Sequences And The Nature Of Incised-Valley Fills In Fluvial Systems Of The Breathitt Group (Pennsylvanian), Appalachian Foreland Basin, Eastern Kentucky. *SEPM Special Publication* 51, 353-367.
- Alexander, J., 1993. A discussion on the use of analogues for reservoir geology. *Geological Society Special Publications* 69, 175-194.
- Allen, G.P., 1991. Sedimentary processes and facies in the Gironde estuary: a Recent model for macrotidal estuarine systems, in: Smith, D.G., Reinson, G.E., Zaitlin, B.A., Rhamani, R.A. (Eds.), *Clastic tidal sedimentology*. Canadian Society of Petroleum Geologists Memoir, pp. 29-40.
- Allen, G.P., Posamentier, H.W., 1993. Sequence stratigraphy and facies model of an incised valley fill: the Gironde estuary, France. *Journal of Sedimentary Petrology* 63, 378-391.
- Allen, J.P., Fielding, C.R., 2007. Sequence architecture within a low-accommodation setting: An example from the Permian of the Galilee and Bowen basins, Queensland, Australia. *AAPG Bulletin* 91 (11), 1503-1539.
- Allen, J.P., Fielding, C.R., Gibling, M.R., Rygel, M.C., 2014. Recognizing products of palaeoclimate fluctuation in the fluvial stratigraphic record: An example from the Pennsylvanian to Lower Permian of Cape Breton Island, Nova Scotia. *Sedimentology* 61 (5), 1332-1381.
- Allen, J.P., Fielding, C.R., Rygel, M.C., Gibling, M.R., 2013. Deconvolving Signals of Tectonic and Climatic Controls From Continental Basins: An Example From the Late Paleozoic Cumberland Basin, Atlantic Canada. *Journal of Sedimentary Research* 83 (10), 847-872.
- Allen, J.R.L., 1982. *Sedimentary Structures: Their Character and Physical Basis*. Elsevier, Amsterdam. 593 p.
- Ambrose, W.A., Hentz, T.F., Bonnaffe, F., Loucks, R.G., Brown, L.F., Wang, F.P., Potter, E.C., 2009. Sequence-stratigraphic controls on complex reservoir architecture of highstand fluvial-dominated deltaic and lowstand valley-fill deposits in the Upper Cretaceous (Cenomanian) Woodbine Group, East Texas field: Regional and local perspectives. *AAPG Bulletin* 93 (2), 231-269.
- Ambrose, W.A., Lakshminarasimhan, S., Holtz, M.H., Núñez-López, V., Hovorka, S.D., Duncan, I., 2008. Geologic factors controlling CO₂ storage capacity and permanence: case studies based on experience with heterogeneity in oil and gas reservoirs applied to CO₂ storage. *Environmental Geology* 54 (8), 1619-1633.
- Anderson, J.B., Abdulah, K., Sarzalejo, S., Siringin, F., Thomas, M.A., 1996. Late Quaternary sedimentation and high resolution sequence stratigraphy of the East Texas Shelf. *Geological Society Special Publications* 117, 95-124.
- Arche, A., López-Gómez, J., 1999. Subsidence Rates and Fluvial Architecture of Rift-Related Permian and Triassic Alluvial Sediments of the Southeast Iberian Range, Eastern Spain. *Special Publications of the International Association of Sedimentologists* 28, 283-304.
- Arche, A., López-Gómez, J., 2014. The Carnian Pluvial Event in Western Europe: New data from

- Iberia and correlation with the Western Neotethys and Eastern North America – NW Africa Regions. *Earth Science Reviews* 128, 196-231.
- Aslan, A., Autin, W.J., 1999. Evolution of the Holocene Mississippi River Floodplain, Ferriday, Louisiana: Insights on the Origin of Fine-Grained Floodplains. *Journal of Sedimentary Research* 69 (4), 800-815.
- Aslan, A., Blum, M.D., 1999. Contrasting Styles of Holocene Avulsion, Texas Gulf Coastal Plain, USA. *Special Publications of the International Association of Sedimentologists* 28, 193-209.
- Avenell, L.C., 1998. The South Blackwater Reservoir Analogue Project, School of Natural Resource Sciences. Queensland University of Technology, Brisbane, p. 70.
- Bal, A.A., Prosser, J.D., Magee, T.J., 2002. Sedimentology of the Mungaroo Formation in the Echo-Yodel Field: a borehole image perspective, in: Keep, M., Moss, S.J. (Eds.), *The sedimentary Basins of West Australia 3: Proceedings of the Petroleum Society of Australia Symposium*, Perth, pp. 662-685.
- Barrell, J., 1917. Rhythms and the measurements of geologic time. *GSA Bulletin* 28, 43-46.
- Benedetti, M.M., 2003. Controls on overbank deposition in the Upper Mississippi River. *Geomorphology* 56 (3-4), 271-290.
- Berendsen, H.J.A., Stouthamer, E., 2001. Paleogeographic development of the Rhine-Meuse delta. Koninklijke Van Gorcum B.V., Assen, The Netherlands. 268 p.
- Beynon, B.M., Pemberton, S.G., 1992. Ichnological signature of a brackish water deposit: An example from the Lower Cretaceous Grand Rapids Formation, Cold Lake oil sands area, Alberta. *SEPM Special Publication CW17*, 199-221.
- Blakey, R., 2013. Late Triassic Mollwiede Globe Paleogeographic Map. Available online: <http://cpgeosystems.com/220moll.jpg> [Accessed 10/06/2013].
- Blum, M.D., Price, D.M., 1998. Quaternary alluvial plain construction in response to glacio-eustatic and climatic controls, Texas Gulf coastal plain. *Special Publication-SEPM* 59 (31-48).
- Blum, M.D., Törnqvist, T.E., 2000. Fluvial responses to climate and sea-level change: a review and look forward. *Sedimentology* 47, 2-48.
- Boote, D.R.D., Kirk, R.B., 1989. Depositional wedge cycles on evolving plate margin, western and northwestern Australia. *AAPG Bulletin* 73 (2), 216-243.
- Bos, I.J., H., F., Bunnik, F., Schokker, J., 2009. Influence of organics and clastic lake fills on distributary channel processes in the distal Rhine-Meuse delta (The Netherlands). *Palaeogeography, Palaeoclimatology, Palaeoecology* 284, 355-374.
- Bourquin, S., Peron, S., Durand, M., 2006. Lower Triassic sequence stratigraphy of the western part of the Germanic Basin (west of Black Forest): Fluvial system evolution through time and space. *Sedimentary Geology* 186 (3-4), 187-211.
- Bradshaw, M.T., Bradshaw, J., Murray, A.P., Needham, D.J., Spencer, L., Summons, R.E., Wilmot, J., Winn, S., 1994. Petroleum systems in West Australian basins, in: Purcell, P.G. (Ed.), *The Sedimentary Basins of Western Australia: Proceedings of the PESA Symposium*, Perth, pp. 93-118.
- Bridge, J.S., Tye, R.S., 2000. Interpreting the Dimensions of Ancient Fluvial Channel Bars, Channels, and Channel Belts from Wireline-Logs and Cores. *AAPG Bulletin* 84 (8), 1205-1228.
- Brierley, G.J., Ferguson, R.J., Woolfe, K.J., 1997. What is a fluvial levee? *Sedimentary Geology* 114 (1-4), 1-9.
- Bristow, Skelly, Ethridge, 1999. Crevasse splays from the rapidly aggrading, sand-bed, braided Niobrara River, Nebraska: effect of base-level rise. *Sedimentology* 46 (6), 1029-1047.

- Bristow, C.S., Best, J.L., 1993. Braided rivers: perspectives and problems. *Geological Society Special Publications* 75, 1-11.
- Bryant, M., Falk, P., Paola, C., 1995. Experimental-study of avulsion frequency and rate of deposition. *Geology* 23, 365-368.
- Burst, J.F., 1965. Subaqueously formed shrinkage cracks in clay. *Journal of Sedimentary Petrology* 35 (2), 348-353.
- Catuneanu, O., 2006. *Principles of Sequence Stratigraphy*. Elsevier, Amsterdam. 375 p.
- Cazanacli, D., Smith, N.D., 1998. A study of morphology and texture of natural levees - Cumberland Marshes, Saskatchewan, Canada. *Geomorphology* 25 (1-2), 43-55.
- Cecil, C.B., 1990. Paleoclimate controls on stratigraphic repetition of chemical and siliciclastic rocks. *Geology* 18, 533-536.
- Cecil, C.B., 2003. The concept of autocyclic and allocyclic controls on sedimentation and stratigraphy, emphasizing the climatic variable, in: Blaine Cecil, C., Terence Edgar, N. (Eds.), *Cimate controls on stratigraphy*. SEPM Special Publication 77, Tulsa, pp. 13-20.
- Cheadle, B., McCrimmon, G., 1997. High frequency sequence stratigraphy of compound tidal-fluvial incised valley fills in the Clearwater Formation, Cold Lake, Alberta. *CSPG Special Publications Sedimentary Events, Hydrocarbon Systems*.
- Choi, K.S., 2010. Rythmic climbing-ripple cross-lamination in inclined heterolithic stratification (IHS) of a macrotidal estuarine channel, Gosmo Bay, west coast of Korea. *Journal of Sedimentary Research* 80, 550-561.
- Choi, K.S., Dalrymple, R.W., Chun, S.S., Kim, S.-P., 2004. Sedimentology of Modern, Inclined Heterolithic Stratification in the Macrotidal Han River Delta, Korea. *Journal of Sedimentary Research* 74, 677-689.
- Chopra, S., Marfurt, K.J., 2005. Seismic attributes - A historical perspective. *Geophysics* 70 (5), 3SO-28SO.
- Chopra, S., Marfurt, K.J., 2007. Curvature attribute applications to 3D surface seismic data. *The Leading Edge* 26 (4), 404-414.
- Chopra, S., Marfurt, K.J., 2008. Emerging and future trends in seismic attributes. *The Leading Edge* 27 (3), 298-318.
- Cohen, K.M., Gouw, M.J.P., Holten, J.P., 2005. Fluvio-deltaic floodbasin deposits recording differential subsistence within a coastal prism (central Rhine-Meuse delta, The Netherlands). *Special Publications of the International Association of Sedimentologists* 35, 295-320.
- Coleman, J.M., Gagliano, S.M., 1960. Sedimentary structures: Mississippi River deltaic plain. *SEPM Special Publication* 12, 133-148.
- Coleman, J.M., Gagliano, S.M., Wenn, J.E., 1964. Minor sedimentary structures in a prograding distributary. *Marine Geology* 1 (3), 240-258.
- Collinson, J., Preater, J., 2009. Reckconnect: Connectivity modelling software. <http://www.reckconnect-software.com/>.
- Collinson, J.D., Mountney, N.P., Thompson, D.B., 2006. *Sedimentary Structures*, 3 ed. Terra, Hertfordshire, UK. 292 p.
- Colombera, L., Felletti, F., Mountney, N.P., McCaffrey, W.D., 2012. A database approach for constraining stochastic simulations of the sedimentary heterogeneity of fluvial reservoirs. *AAPG Bulletin* 96 (11), 2143-2166.
- Colombera, L., Mountney, N.P., McCaffrey, W.D., 2012. A Relational Database for the Digitization of Fluvial Architecture: Concepts and Example Applications. *Petroleum Geoscience* 18, 129-140.

- Colombera, L., Mountney, N.P., McCaffrey, W.D., 2013. A quantitative approach to fluvial facies models: methods and example results. *Sedimentology* 60, 1526-1558.
- Cuba, P.H., Miskimins, J.L., Anderson, D.S., Carr, M., 2013. Impacts of Diverse Fluvial Depositional Environments on Hydraulic Fracture Growth in Tight Gas Reservoirs. *SPE Production & Operations* 28, 8-25.
- Dalrymple, R.W., Choi, K.S., 2007. Morphologic and facies trends through the fluvial-marine transition in tide-dominated depositional systems: A schematic framework for environmental and sequence-stratigraphic interpretation. *Earth Science Reviews* 81, 135-174.
- Davies, D.K., Ethridge, F.G., 1975. Sandstone composition and depositional environment. *AAPG Bulletin* 59 (2), 239-264.
- De Boer, P., Oost, A.P., Visser, M.J., 1989. The diurnal inequality of the tide as a parameter for recognizing tidal influences. *Journal of Sedimentary Petrology* 59, 912-921.
- de Groot, P., Huck, A., de Bruin, G., Hemstra, N., Bedford, J., 2010. The horizon cube: A step change in seismic interpretation! *The Leading Edge* 29 (9), 1048-1055.
- Dickens, J.M., 1985. Climate of the Triassic. *Hornibrook Symposium, Extended Abstracts, New Zealand Geological Survey* 9, 34-36.
- Donselaar, M.E., Cuevas Gozalo, M., Moyano, S., 2011. Abstract: Thin-Bedded Fluvial Sheet Sandstone as Secondary Reservoir Target: Outcrop Analogue Study of a Quaternary Semi-arid Fluvial System, Altiplano Basin, Bolivia. *AAPG Search and Discovery Article* (90135).
- Donselaar, M.E., Schmidt, J.M., 2010. The application of borehole image logs to fluvial facies interpretation, in: Pöppelreiter, M., García-Carballido, C., Kraaijveld, M. (Eds.), *Dipmeter and borehole image log technology: AAPG Memoir 92*. AAPG, Tulsa, Oklahoma, pp. 145-166.
- Dorn, G.A., 2011. Implications of 3-D domain transform for structural and stratigraphic interpretation, *AAPG Annual Convention and Exhibition*. AAPG Search and Discovery, Houston, Texas, p. 29.
- Dorn, G.A., 2013. Domain transform: A tool for imaging and interpreting geomorphology and stratigraphy in seismic volumes. *The Leading Edge* February 2013, 146-153.
- Dzulynski, S., Smith, A.J., 1963. Convolute lamination, its origin, preservation and directional significance. *Journal of Sedimentary Research* 33, 616-627.
- Emery, D., Myers, K.J., (eds.), 1996. *Sequence Stratigraphy*. Blackwell Science, London. 297 p.
- Ethridge, F.G., Germanoski, D., Schumm, S.A., Wood, L.J., 2005. The morphological and stratigraphical effects of base-level change: a review of experimental studies. *Special Publications of the International Association of Sedimentologists* 35 (Fluvial Sedimentology VII), 213-241.
- Ethridge, F.G., Jackson, T.J., Youngeberg, A.D., 1981. Floodbasin Sequence of a Fine-grained Meander Belt Subsystem: The Coal-bearing Lower Wasatch and Upper Fort Union Formations, Southern Powder River Basin, Wyoming. *SEPM Special Publication* 31, 191-209.
- Ethridge, F.G., Schumm, S.A., 2007. *Fluvial seismic geomorphology: a view from the surface*. Geological Society, London, *Special Publications* 277 (1), 205-222.
- Ethridge, F.G., Wood, L.J., Schumm, S.A., 1998. Cyclic variables controlling fluvial sequence development: Problems and Perspectives. *SEPM Special Publication* 59, 17-29.
- Exon, N.F., von Rad, U., von Stackelberg, U., 1982. The Geological Development of the Passive Margins of the Exmouth Plateau off Northwest Australia. *Marine Geology* 47, 131-152.
- Falvey, D.A., Veevers, J.J., 1974. Physiography of the Exmouth and Scott Plateaus, Western Australia, and adjacent Northeast Wharton Basin. *Marine Geology* 17, 21-59.
- Fanti, F., Catuneanu, O., 2010. *Fluvial Sequence Stratigraphy: The Wapiti Formation*,

- West-Central Alberta, Canada. *Journal of Sedimentary Research* 80 (4), 320-338.
- Farrell, K.M., 2001. Geomorphology, facies architecture, and high-resolution, non-marine sequence stratigraphy in avulsion deposits, Cumberland Marshes, Saskatchewan. *Sedimentary Geology* 139 (2), 93-150.
- ffa, 2013. Geoteric 2013.3 Training Manual. ffa, Aberdeen. 359 p.
- Fielding, C.R., 1984. Upper delta plain lacustrine and fluviolacustrine facies from the Westphalian of the Durham coalfield, NE England. *Sedimentology* 31 (4), 547-567.
- Fielding, C.R., 1985. Coal depositional models and the distinction between alluvial and delta plain environments. *Sedimentary Geology* 42 (1-2), 41-48.
- Fielding, C.R., 1986. Fluvial channel and overbank deposits from the Westphalian of the Durham coalfield, NE England. *Sedimentology* 33 (1), 119-140.
- Fielding, C.R., Falkner, A.J., Scott, S.G., 1993. Fluvial response to foreland basin overfilling; the Late Permian Rangal Coal Measures in the Bowen Basin, Queensland, Australia. *Sedimentary Geology* 85 (1-4), 475-497.
- Fisher, W.L., McGowen, J.H., 1963. Depositional Systems in Wilcox Group (Eocene) of Texas and Their Relation to Occurrence of Oil and Gas. *AAPG Bulletin* 53 (1), 30-54.
- Flood, P.G., Brady, S.A., 1985. Origin of large-scale crossbeds in the late permian coal measures of the Sydney and Bowen basins, eastern Australia. *International Journal of Coal Geology* 5 (3), 231-245.
- Fustic, M., Hubbard, S.M., Spencer, R., Smith, D.G., Leckie, D.A., Bennett, B., Larter, S., 2012. Recognition of down-valley translation in tidally-influenced meandering fluvial deposits, Athabasca Oil Sands (Cretaceous), Alberta, Canada. *Marine and Petroleum Geology* 29, 219-232.
- Galloway, W.E., 1989. Genetic Stratigraphic Sequences in Basin Analysis I: Architecture and Genesis of Flooding-Surface Bounded Depositional Units. *AAPG Bulletin* 73 (2), 125-142.
- Galloway, W.E., 1989. Genetic stratigraphic sequences in basin analysis II: Application to Northwest Gulf of Mexico Cenozoic Basin. *AAPG Bulletin* 73 (2), 143-154.
- Gibling, M.R., 2006. Width and Thickness of Fluvial Channel Bodies and Valley Fills in the Geological Record: A Literature Compilation and Classification. *Journal of Sedimentary Research* 76 (5), 731-770.
- Gundesø, R., O., E., 1990. SESIMIRA—A New Geological Tool for 3D Modelling of Heterogeneous Reservoirs, in: Buller, A.T. (Ed.), *North Sea Oil and Gas Reservoirs—II*. Springer Netherlands, Amsterdam, pp. 363-371.
- Hagstrom, C.A., Leckie, D.A., Hubbard, S.M., 2014. Seismically constrained sediment distribution in immense point bars of the Lower Cretaceous McMurray Formation, Alberta, Canada, in: Geologists, C.S.o.P. (Ed.), *Oil Sands & Heavy Oil Symposium: A Local to Global Multidisciplinary Collaboration*, Calgary, Alberta.
- Hajek, E.A., Edmonds, D.A., 2014. Is river avulsion style controlled by floodplain morphodynamics? *Geology* 42 (3), 199-202.
- Hajek, E.A., Heller, P.L., Schur, E.L., 2012. Field test of autogenic control on alluvial stratigraphy (Ferris Formation, Upper Cretaceous-Paleogene, Wyoming). *GSA Bulletin* 124 (11/12), 1898-1912.
- Hajek, E.A., Heller, P.L., Sheets, B.A., 2010. Significance of channel-belt clustering in alluvial basins. *Geology* 38 (6), 535-538.
- Hampson, G.J., Davies, S.J., Elliott, T., Flint, S.S., Stollhofen, H., 1999. Incised valley fill sandstone bodies in Upper Carboniferous fluvio-deltaic strata: recognition and reservoir characterization of Southern North Sea analogues. *Geological Society, London, Petroleum*

Geology Conference Series 5, 771-788.

Hampson, G.J., Davies, W., Davies, S.J., Howell, J.A., Adamson, K.R., 2005. Use of spectral gamma-ray data to refine subsurface fluvial stratigraphy: late Cretaceous strata in the Book Cliffs, Utah, USA. *Journal of the Geological Society* 162 (4), 603-621.

Hardage, B.A., Levey, R.A., Pendleton, V., Simmons, J., Edson, R., 1994. A 3-D seismic case history evaluating fluviially deposited thin-bed reservoirs in a gas-producing property. *Geophysics* 59 (11), 1650-1665.

Hardage, B.A., Remington, R.L., 1999. 3-D seismic stratal-surface concepts applied to the interpretation of a fluvial channel system deposited in a high-accommodation environment. *Geophysics* 64 (2), 609-620.

Heldreich, G., Redfern, J., Gerdes, K., Legler, B., Taylor, S., Hodgetts, D., Williams, B., 2013. Analysis of Geobody Geometries within the Fluvio-Deltaic Mungaroo Formation, NW Australia, in: Keep, M., Moss, S.J. (Eds.), *The Sedimentary Basins of Western Australia IV: Proceedings of the Petroleum Exploration Society of Australia Symposium*, Perth.

Heller, P.L., Paola, C., 1996. Downstream Changes In Alluvial Architecture: An Exploration of Controls on Channel-stacking Patterns. *Journal of Sedimentary Research* 66 (2), 297-306.

Henderson, J., Purves, S.J., Fisher, G., Leppard, C., 2008. Delineation of geological elements from RGB colour blending of seismic attribute volumes. *The Leading Edge* 27, 342-350.

Hillier, R.D., Marriott, S.B., Williams, B.P.J., Wright, V.P., 2007. Possible climate variability in the Lower Old Red Sandstone Conigar Pit Sandstone Member (early Devonian), South Wales, UK. *Sedimentary Geology* 202, 35-57.

Hocking, R.M., Moors, H.T., Van De Graaff, W.J.E., 1987. *Geology of the Carnarvon Basin Western Australia*. Geological Survey Western Australia Bulletin 133.

Holbrook, J.M., 2001. Origin, genetic, interrelationships, and stratigraphy over the continuum of fluvial channel-form bounding surfaces: an illustration from middle Cretaceous strata, southeastern Colorado. *Sedimentary Geology* 144, 179-222.

Holbrook, J.M., 2009. Generating sequence boundaries, architecture and sediment storage in high vs. low accommodation phases of coastal tropical rivers, AAPG Hedberg Conference. AAPG Search and Discovery, Jakarta, Indonesia.

Holbrook, J.M., Bhattacharya, J.P., 2012. What happened to my fluvial reservoir? Implications of falling stage and lowstand fluvial sediment storage during "sequence boundary" scour for sand starvation of coastal marine reservoirs, AAPG Annual Convention. AAPG Search and Discovery, Long Beach, California.

Holbrook, J.M., Scott, R.W., Oboh-Ikuenobe, F.E., 2006. Base-level buffers and buttresses: A model for upstream versus downstream control on fluvial geometry and architecture within sequences. *Journal of Sedimentary Research* 76, 162-174.

Horne, J.C., Ferm, J.C., Caruccio, F.T., Baganz, B.P., 1978. *Depositional Models in Coal Exploration and Mine Planning in Appalachian Region*. AAPG Bulletin 62 (12), 2379-2411.

Hubbard, S.M., Smith, D.G., Nielsen, H., Leckie, D.A., Fustic, M., Spencer, R.J., Bloom, L., 2011. Seismic geomorphology and sedimentology of a tidally influenced river deposit, Lower Cretaceous Athabasca oil sands, Alberta, Canada. *AAPG Bulletin* 95 (7), 1123-1145.

Hunt, D., Tucker, M.E., 1992. Stranded parasequences and the forced regressive wedge systems tract: deposition during base level fall. *Sedimentary Geology* 81 (1-9).

Hyne, N.J., Cooper, W.A., Dickey, P.A., 1979. Stratigraphy of Intermontane, Lacustrine Delta, Catatumbo River, Lake Maracaibo, Venezuela. *AAPG Bulletin* 63 (11), 2042-2057.

Jablonski, B.V.J., Dalrymple, R., 2014. Fluvial Seasonality: A Predictive Tool for Deciphering the Sedimentological Complexity of Inclined Heterolithic Stratification Deposited on Large-Scale Tidal-Fluvial Point Bars, CSPG/CSEG/CWLS GeoConvention 2013. Search and Discovery,

Calgary.

Jablonski, D., 1997. Recent advances in the sequence stratigraphy of the Triassic to Lower Cretaceous succession in the Northern Carnarvon Basin, Australia. *The Australian Petroleum Production and Exploration Journal* 34, 429-454.

Jerolmack, D.J., Paola, C., 2010. Shredding of environmental signals by sediment transport. *Geophysical Research Letters* 37 (19), L19401.

Johnson, S.M., Dashtgard, S.E., 2014. Inclined heterolithic stratification in a mixed tidal-fluvial channel: Differential tidal versus fluvial controls on sedimentation. *Sedimentary Geology* 301, 41-53.

Jorgensen, P.J., Fielding, C.R., 1996. Facies architecture of alluvial floodbasin deposits: three-dimensional data from the Upper Triassic Callide Coal Measures of east-central Queensland, Australia. *Sedimentology* 43 (3), 479-495.

Kaiko, A.R., Tait, A.M., 2001. Post-rift tectonic subsidence and paleo-water depths in the Northern Carnarvon Basin, Western Australia. *APPEA Journal* 2001, 367-379.

Kallweit, R.S., Wood, L.C., 1982. The limits of resolution of a zero-phase wavelet. *Geophysics* 47 (7), 1034-1046.

Karamitopoulos, P., Dalman, A.F., 2014. Allogenic controls on autogenic variability in fluvio-deltaic systems: inferences from analysis of synthetic stratigraphy. *Basin Research* 26, 767-799.

Kidd, G., 1999. Fundamentals of 3-D seismic volume visualization. *The Leading Edge* 18 (6), 702-709.

Kim, W., Petter, A., Straub, K., Mohrig, D., 2014. Investigating the autogenic process response to allogenic forcing: experimental geomorphology and stratigraphy. *International Association of Sedimentologists Special Publications* 46, 127-138.

Klausen, T.G., Ryseth, A.E., Helland-Hansen, W., Gawthorpe, R., Laursen, I., 2014. Spatial and temporal changes in geometries of fluvial channel bodies from the Triassic Snadd Formation of offshore Norway. *Journal of Sedimentary Research* 84, 567-585.

Klein, J., 1996. Method for locating thin bed hydrocarbon reserves utilizing electrical anisotropy. United States Patent Office, Patent No. 5,550,473.

Knox, J.C., 1987. Climatic influences on Upper Mississippi Valley Floods, in: Baker, V.R., Kochel, R.C., Patton, P.C. (Eds.), *Flood Geomorphology*. Wiley, New York, pp. 279-300.

Koss, J.E., Ethridge, F.G., Schumm, S.A., 1994. An experimental study of the effects of base-level change on fluvial coastal plain and shelf systems. *Journal of Sedimentary Research* B64 (2), 90-98.

Kraus, M.J., 1998. Development of potential acid sulfate paleosols in Paleocene floodplains, Bighorn Basin, Wyoming, USA. *Palaeogeography, Palaeoclimatology, Palaeoecology* 144, 203-224.

Kraus, M.J., Hasiotis, S.T., 2006. Significance of Different Modes of Rhizolith Preservation to Interpreting Paleoenvironmental and Paleohydrologic Settings: Examples from Paleogene Paleosols, Bighorn Basin, Wyoming, U.S.A. *Journal of Sedimentary Research* 76 (4), 633-646.

Labrecque, P.A., Hubbard, S.M., Jensen, J.L., Nielsen, H., 2011. Sedimentology and stratigraphic architecture of a point bar deposit, Lower Cretaceous McMurray Formation, Alberta, Canada. *Bulletin of Canadian Petroleum Geology* 59 (2), 147-171.

Lang, S.C., Kassan, J., Benson, J., Grasso, C., Hicks, T., Hall, N., Avenell, C., 2002. Reservoir Characterisation of Fluvial, Lacustrine and Deltaic Successions - Applications of Modern and Ancient Geological Analogues. *Proceedings, Indonesian Petroleum Association* 1, 557-578.

Larue, D.K., Hovadik, J., 2006. Connectivity of channelized reservoirs: a modelling approach.

Petroleum Geoscience 12, 291-308.

Leeder, M.R., 1993. Tectonic controls upon drainage basin development, river channel migration and alluvial architecture: implications for hydrocarbon reservoir development and characterization. Geological Society, London, Special Publications 73 (1), 7-22.

Leeder, M.R., Stewart, M.D., 1996. Fluvial incision and sequence stratigraphy: alluvial responses to relative sea-level fall and their detection in the geological record. Geological Society, London, Special Publications 103, 25-39.

Lewis, C.J., Sircombe, K.N., 2013. Use of U-Pb geochronology to delineate provenance of North West Shelf sediments, Australia, in: Keep, M., Moss, S.J. (Eds.), The Sedimentary Basins of Western Australia IV: Proceedings of the Petroleum Exploration Society of Australia Symposium, Perth.

Longley, I.M., Buessenschuett, C., Clydsdale, L., Cubitt, C.J., Davis, R.C., Johnson, M.K., Marshall, N.M., Murray, A.P., Somerville, R., Spry, T.B., Thompson, N.B., 2002. The North West Shelf of Australia - a Woodside perspective, in: Keep, M., Moss, S.J. (Eds.), The Sedimentary Basins of Western Australia 3: Proceedings of the Petroleum Exploration Society of Australia Symposium, Perth, pp. 22-88.

Lowell, J., Eckersley, A., Kristensen, T., Szafian, P., McArdle, N.J., 2014. Improvements to Frequency Decomposition Methodologies for Use with Broad Bandwidth Seismic Datasets, 76th EAGE Conference & Exhibition. EAGE, Amsterdam, The Netherlands.

Mackin, J.H., 1948. Concept of the graded river. GSA Bulletin 59 (5), 463-512.

Marenessi, S.A., Limarino, C.O., Tripaldi, A., Net, L.I., 2005. Fluvial systems variations in the Rio Leona Formation: Tectonic and eustatic controls on the Oligocene evolution of the Austral (Magallanes) Basin, southernmost Argentina. Journal of South American Earth Sciences 19 (3), 359-372.

Marshall, N.G., Lang, S.C., 2013. A new sequence stratigraphic framework for the North West Shelf, Australia, in: Keep, M., Moss, S.J. (Eds.), The Sedimentary Basins of Western Australia IV: Proceedings of the Petroleum Exploration Society of Australia Symposium, Perth.

Martinius, A.W., Elfenbein, C., Keogh, K.J., 2014. Applying accommodation versus sediment supply ratio concepts to stratigraphic analysis and zonation of a fluvial reservoir. International Association of Sedimentologists Special Publications 46, 101-126.

Martinius, A.W., Gowland, S., 2011. Tide-influenced fluvial bedforms and tidal bore deposits (Late Jurassic Lourinhã Formation, Lusitanian Basin, Western Portugal). Sedimentology 58, 285-324.

McArdle, N.J., Ackers, M.A., 2012. Understanding seismic thin-bed responses using frequency decomposition and RGB blending. First Break 30, 57-65.

McArdle, N.J., Iacopini, D., KunleDare, M.A., Paton, G.S., 2014. The use of geologic expression workflows for basin scale reconnaissance: A case study from the Exmouth Subbasin, North Carnarvon Basin, northwestern Australia. Interpretation 2 (1), SA163-SA177.

McCabe, P.J., 1984. Depositional environments of coal and coal-bearing strata. Special Publications of the International Association of Sedimentologists 7, 13-42.

Miall, A.D., 1978. Lithofacies types and vertical profile models in braided river deposits: a summary. In: Miall, A. D. (Ed) Fluvial sedimentology. Canadian Society of Petroleum Geology Memoirs 5, 597-604.

Miall, A.D., 1983. Basin Analysis of Fluvial Sediments. Special Publications of the International Association of Sedimentologists 6, 279-286.

Miall, A.D., 1985. Architectural-Element Analysis: A New Method of Facies Analysis Applied to Fluvial Deposits. Earth-Science Reviews 22, 261-308.

Miall, A.D., 1988. Architectural elements and bounding surfaces in fluvial deposits: Anatomy of the Kayenta Formation (Lower Jurassic), Southwest Colorado. Sedimentary Geology 55 (3-4),

233-262.

Miall, A.D., 1991. Stratigraphic sequences and their chronostratigraphic correlation. *Journal of Sedimentary Petrology* 61, 497-505.

Miall, A.D., 1994. Reconstructing fluvial macroform architecture from two-dimensional outcrops: examples from the Castlegate Sandstone, Book Cliffs, Utah. *Journal of Sedimentary Research* B64 (2), 146-158.

Miall, A.D., 2000. *Principles of Sedimentary Basin Analysis*, 3rd ed. Springer-Verlag, Berlin. 616 p.

Miall, A.D., 2002. Architecture and sequence stratigraphy of Pleistocene fluvial systems in the Malay Basin, based on seismic time-slice analysis. *Aapg Bulletin* 86 (7), 1201-1216.

Miall, A.D., 2006. *The Geology of Fluvial Deposits: Sedimentary Facies, Basin Analysis, and Petroleum Geology*, 4th ed. Springer, Berlin. 582 p.

Miall, A.D., 2014. *Fluvial Depositional Systems*. Springer, Heidelberg. 316 p.

Michaelsen, P., Henderson, R.A., 2000. Facies relationships and cyclicity of high-latitude, Late Permian coal measures, Bowen Basin, Australia. *International Journal of Coal Geology* 44 (1), 19-48.

Mitchell, A.H.G., Reading, H.G., 1986. Sedimentation and tectonics, in: Reading, H.G. (Ed.), *Sedimentary environments and facies* 2 ed. Blackwell Science, Oxford, pp. 471-519.

Mitchum, R.M.J., Vail, P.R., Thompson, S., 1977. Seismic stratigraphy and global changes of sea level, Part Two: The depositional sequence as a basic unit for stratigraphic analysis, in: Payton, C.E. (Ed.), *AAPG Memoir 26: Seismic Stratigraphy - applications to hydrocarbons exploration*. AAPG, Tulsa, pp. 53-62.

Mjøs, R., Walderhaug, O., Prestholm, E., 1993. Crevasse splay sandstone geometries in the Middle Jurassic Ravenscar Group of Yorkshire, UK, in: Marzo, M., Puigdefábregas, C. (Eds.), *Alluvial Sedimentation*. International Association of Sedimentologists, Special Publication 17, pp. 167-174.

Mohrig, D., Heller, P.L., Paola, C., Lyons, W.J., 2000. Interpreting avulsion process from ancient alluvial sequences: Guadaloupe-Matarranya system (northern Spain) and Wasatch Formation (western Colorado). *GSA Bulletin* 112 (12), 1787-1803.

Morozova, G.S., Smith, N.D., 2000. Holocene avulsion styles and sedimentation patterns of the Saskatchewan River, Cumberland Marshes, Canada. *Sedimentary Geology* 130 (1-2), 81-105.

Musial, G., Reynaud, J.-Y., Gingras, M.K., Féliès, H., Labourdette, R., Parize, O., 2012. Subsurface outcrop characterization of large tidally influenced point bars of the Cretaceous McMurray Formation (Alberta, Canada). *Sedimentary Geology* 279, 156-172.

Muto, T., Steel, R.J., 2001. Autostepping during the transgressive growth of deltas: Results from flume experiments. *Geology* 29 (9), 771-774.

Mutton, A.J., 2003. *Queensland Coals* 14th Edition. Queensland Department of Natural Resources and Mines.

O'Brien, P.E., Wells, A.T., 1986. A small, alluvial crevasse splay. *Journal of Sedimentary Research* 56 (6), 876-879.

Orton, G.J., Reading, H.G., 1993. Variability of deltaic processes in terms of sediment supply, with particular emphasis on grain size. *Sedimentology* 40, 475-512.

Partyka, G., Gridley, J., Lopez, J., 1999. Interpretational applications of spectral decomposition in reservoir characterisation. *The Leading Edge* 18 (3), 353-360.

Payenberg, T., Willis, B., Pusca, V., Sixsmith, P., Bracken, B., Posamentier, H., Pycrz, M.J., Sech, R., Connell, S., Milliken, K., Sullivan, M., 2014. Channel Belt Rugosity in Reservoir

Characterization (Poster), AAPG ACE. AAPG Search and Discovery, Houston.

Payenberg, T.H.D., Howe, H., Marsh, T., Sixsmith, P., Kowalik, W.S., Powell, A., Ratcliffe, K., Iasky, V., Allgoewe, A., Howe, R.W., Montgomery, P., Vonk, A., Croft, M., 2013. An Integrated Regional Triassic Stratigraphic Framework for the Carnarvon Basin, NWS, Australia, in: Keep, M., Moss, S.J. (Eds.), *The Sedimentary Basins of Western Australia IV: Proceedings of the Petroleum Exploration Society of Australia Symposium*, Perth.

Pemberton, S.G., Wightman, D.M., 1992. Ichnological characteristics of brackish water deposits. *SEPM Special Publication CW17*, 141-167.

Pérez-Arlucea, M., Smith, N.D., 1999. Depositional patterns following the 1870s avulsion of the Saskatchewan River (Cumberland Marshes, Saskatchewan, Canada). *Journal of Sedimentary Research* 69, 62-73.

Plint, A., 1986. Slump blocks, intraformational conglomerates and associated erosional structures in Pennsylvanian fluvial strata of eastern Canada. *Sedimentology* 33 (3), 387-399.

Plint, A.G., McCarthy, P.J., Faccini, U.F., 2001. Nonmarine sequence stratigraphy: Updip expression of sequence boundaries and systems tracts in a high-resolution framework, Cenomanian Dunvegan Formation, Alberta foreland basin, Canada. *AAPG Bulletin* 85 (11), 1967-2001.

Posamentier, H.W., 2005. Application of 3D seismic visualization techniques for seismic stratigraphy, seismic geomorphology and depositional systems analysis: examples from fluvial to deep-marine depositional environments. Geological Society, London, *Petroleum Geology Conference Series* 6, 1565-1576.

Posamentier, H.W., 2013. Integration of Seismic Stratigraphy and Seismic Geomorphology for Prediction of Lithology; Applications and Workflows, in: Keep, M., Moss, S.J. (Eds.), *The Sedimentary Basins of Western Australia IV: Proceedings of the Petroleum Exploration Society of Australia Symposium*, Perth.

Posamentier, H.W., Vail, P.R., 1988. Eustatic controls on clastic deposition - sequence and systems tract models. *SEPM Special Publication* 42, 126-154.

Postma, G., 2014. Generic autogenic behaviour in fluvial systems: lessons from experimental studies. *International Association of Sedimentologists Special Publications* 46, 1-18.

Postma, G., van den, A.P., van Saparoea, B., 2008. Impact of discharge, sediment flux and sea-level change on stratigraphic architecture of river–delta–shelf systems, *Special Publications of the International Association of Sedimentologists* (40) *Analogue and Numerical Modelling of Sedimentary Systems: From Understanding to Prediction*, *Special Publications of the International Association of Sedimentologists* 40. Wiley-Blackwell, pp. 191-205.

Powell, J.W., 1875. Exploration of the Colorado River of the West and its tributaries: Explored in 1869, 1870, 1871, and 1872, under the direction of the Secretary of the Smithsonian Institution. Government Printing Office, Washington, D.C. 368 p.

Pranter, M.J., Ellison, A.I., Cole, R.D., Patterson, P.E., 2007. Analysis and modeling of intermediate-scale reservoir heterogeneity based on a fluvial point-bar outcrop analog, Williams Fork Formation, Piceance Basin, Colorado. *AAPG Bulletin* 91 (7), 1025-1051.

Preto, N., Kutatscher, E., Wignall, P.B., 2010. Triassic Climates – State of the art and perspectives. *Paleogeography, Palaeoclimatology, Palaeoecology* 290, 1-10.

Qayyum, F., de Groot, P., Hemstra, N., Catuneanu, O., 2014. 4D Wheeler diagrams: concept and applications, in: Smith, D.G., Bailey, R.J., Burgess, P., M., Fraser, A.J. (Eds.), *Strata and Time: Probing the Gaps in Our Understanding*. Geological Society, London, *Special Publications*.

Rabelo, I.R., Luthi, S.M., Van Vliet, L.J., 2007. Parameterization of meander-belt elements in high-resolution three-dimensional seismic data using the GeoTime cube and modern analogues. Geological Society, London, *Special Publications* 277 (1), 121-137.

Reijnenstein, H.M., Posamentier, H.W., Bhattacharya, J.P., 2011. Seismic geomorphology and

high-resolution seismic stratigraphy of inner-shelf fluvial, estuarine, deltaic, and marine sequences, Gulf of Thailand. AAPG Bulletin 95 (11), 1959-1990.

Roksandic, M.M., 1965. Discussion on: "A 3-D seismic case history evaluating fluvially deposited thin-bed reservoirs in a gas-producing property," by B. A. Hardage, R. A. Levey, V. Pendleton, J. Simmons, and R. Edsen (November 1994 Geophysics, 59, p. 1650-1665). Geophysics 60 (5), 1585-1592.

Russell, C., Mountney, N.P., Hodgson, D.M., 2014. Internal sedimentary architecture and heterogeneity within fluvial point-bar successions: A talk presented at the 2014 British Sedimentological Research Group (BSRG) Annual Meeting, BSRG AGM, Nottingham, UK.

Sarkar, S., Marfurt, K.J., Slatt, R.M., 2010. Generation of sea-level curves from depositional pattern as seen through seismic attributes-seismic geomorphology analysis of an MTC-rich shallow sediment column, northern Gulf of Mexico. The Leading Edge 29 (9), 1084.

Saucier, R.T., 1996. A contemporary appraisal of some key Fiskian concepts with emphasis on Holocene meander belt formation and morphology. Engineering Geology 45, 67-86.

Schumm, S.A., 1993. River response to base level change: implications for sequence stratigraphy. The Journal of Geology 101, 279-294.

Schumm, S.A., Ethridge, F.G., 1994. Origin, evolution and morphology of fluvial valleys. SEPM Special Publication 51, 13-26.

Seggie, R.J., Lang, S.C., Marshall, N.M., Cubitt, C.J., Alsop, D., Kirk, R., Twartz, S., 2007. Integrated Multi-Disciplinary Analysis of the Rankin Trend Gas Reservoirs Northwest Shelf, Australia. APPEA Journal 2007, 53-67.

Shanley, K.W., McCabe, P.J., 1993. Alluvial architecture in a sequence stratigraphic framework: a case history from the Upper Cretaceous of southern Utah, USA, in: Flint, S.S., Bryant, I.D. (Eds.), The geological modelling of hydrocarbon reservoirs and outcrop analogues. International Association of Sedimentologists, Special Publication 15, pp. 21-56.

Shanley, K.W., McCabe, P.J., 1994. Perspectives on the Sequence Stratigraphy of Continental Strata. AAPG Bulletin 78 (4), 544-568.

Shiers, M.N., Mountney, N.P., Hodgson, D.M., Cobain, S.L., 2014. Depositional controls on tidally influenced fluvial successions. Sedimentology 311, 1-16.

Sisulak, C.F., Dashtgard, S.E., 2012. Seasonal controls on the development and character of inclined heterolithic stratification in a tide-influenced, fluvially-dominated channel: Fraser River, Canada. Journal of Sedimentary Research 82 (244-257).

Slingerland, R., Smith, N.D., 2004. River avulsions and their deposits. Annual Review of Earth and Planetary Science 32, 257-285.

Sloss, I.L., 1962. Stratigraphic models in exploration. AAPG Bulletin 46, 1050-1057.

Smith, D.G., 1987. Meandering river point bar lithofacies: modern and ancient examples compared, in: Ethridge, F.G., Flores, R.M., Harvey, M. (Eds.), Recent developments in fluvial sedimentology. SEPM Special Publication 39, Tulsa, Oklahoma, pp. 83-91.

Smith, D.G., 1988. Modern point bar deposits analogous to the Athabasca oil sands, in: de Boer, P.L., Van Gelder, A., Nio, S.D. (Eds.), Tide-Influenced Sedimentary Environments and Facies. Springer, Dordrecht, pp. 417-432.

Smith, D.G., Hubbard, S.M., Lavigne, J.R., Leckie, D.A., Fustic, M., 2011. Stratigraphy of counter point bars and eddy accretion deposits in low energy meander belts of the Peace-Athabasca Delta, Northeast Alberta, Canada, in: Davidson, S.K., Leleu, S., North, C.P. (Eds.), From river to rock record: The preservation of fluvial sediments and their subsequent interpretation. SEPM Special Publication 97, Tulsa, Oklahoma, pp. 143-152.

Smith, D.G., Hubbard, S.M., Leckie, D.A., Fustic, M., 2009. Counter point bar deposits: lithofacies and reservoir significance in the meandering modern Peace River and ancient McMurray

- Formation, Alberta, Canada. *Sedimentology* 56, 1655-1669.
- Smith, N.D., Cross, T.A., Dufficy, J.P., Clough, S.R., 1989. Anatomy of an avulsion. *Sedimentology* 36 (1), 1-23.
- Smith, N.D., Pérez-Arlucea, M., 1994. Fine-Grained Splay Deposition in the Avulsion Belt of the Lower Saskatchewan River, Canada. *Journal of Sedimentary Research* 64B (2), 159-168.
- Stear, W.M., 1983. Morphological Characteristics of Ephemeral Stream Channel and Overbank Splay Sandstone Bodies in the Permian Lower Beaufort Group, Karoo Basin, South Africa. *Special Publications of the International Association of Sedimentologists* 6, 405-420.
- Stoner, S.B., 2010. Fluvial architecture and geometry of the Mungaroo Formation on the Rankin Trend of the Northwest Shelf of Australia. MSc Thesis, The University of Texas at Arlington, p. 143.
- Stouthamer, E., Berendsen, H.J.A., 2007. Avulsion: the relative roles of autogenic and allogenic processes. *Sedimentary Geology* 198, 309-325.
- Stouthamer, E., Cohen, K.M., Gouw, M.J.P., 2011. Avulsion And Its Implications For Fluvial-Deltaic Architecture: Insights From The Holocene Rhine–Meuse Delta. *SEPM Special Publication* 97, 215-231.
- Straub, K.M., Wang, Y., 2013. Influence of water and sediment supply on the long-term evolution of alluvial fans and deltas: Statistical characterization of basin-filling sedimentation patterns. *Journal of Geophysical Research: Earth Surface* 118 (3), 1602-1616.
- Stuart, J.Y., Mountney, N.P., McCaffrey, W.D., Lang, S.C., Collinson, J.D., 2014. Prediction of channel connectivity and fluvial style in the flood-basin successions of the Upper Permian Rangal coal measures (Queensland). *AAPG Bulletin* 98 (2), 191-212.
- Taylor, A.M., Goldring, R., 1993. Description and analysis of bioturbation and ichnofabric. *Journal of the Geological Society* 150 (1), 141-148.
- Thomas, R.G., Smith, D.G., Wood, J.M., Visser, J., Calverley-Range, E.A., Koster, E.H., 1987. Inclined heterolithic stratification—Terminology, description, interpretation and significance. *Sedimentary Geology* 53 (1–2), 123-179.
- Törnqvist, T.E., 1993. Holocene alteration of meandering and anastomosing of meandering fluvial systems in the Rhine-Meuse Delta (central Netherlands) controlled by sea level rise and sub-soil erodibility. *Journal of Sedimentary Petrology* 63, 683-693.
- Törnqvist, T.E., 1994. Middle and late Holocene avulsion history of the River Rhine (Rhine-Meuse Delta, Netherlands). *Geology* 22, 711-714.
- Törnqvist, T.E., van Ree, M.H.M., Faessen, E.L.J.H., 1993. Longitudinal facies architectural changes of a middle Holocene anastomosing distributary system (Rhine-Meuse delta, central Netherlands). *Sedimentary Geology* 85, 203-219.
- Tye, R.S., Hickey, J.J., 2001. Permeability characterization of distributary mouth bar sandstones in Prudhoe Bay field, Alaska: How horizontal cores reduce risk in developing deltaic reservoirs. *AAPG Bulletin* 85 (3), 459-475.
- Vail, P.R., Mitchum, R.M., Jr., 1977. Seismic stratigraphy and global changes of sea level, Part One, Overview, in: Payton, C.E. (Ed.), *AAPG Memoir 26: Seismic Stratigraphy - applications to hydrocarbons exploration*. AAPG, Tulsa, pp. 51-52.
- van Asselen, S., Stouthamer, E., Smith, N.D., 2010. Factors Controlling Peat Compaction in Alluvial Floodplains: A Case Study in the Cold-Temperate Cumberland Marshes, Canada. *Journal of Sedimentary Research* 80, 155-166.
- Van De Wiel, M.J., 2010. Self-organized criticality in river basins: Challenging sedimentary records of environmental change. *Geology* 38 (1), 87-90.
- van den Berg, J.H., Boersma, J.R., van Gelder, A., 2007. Diagnostic sedimentary structures of the

- fluvial-tidal transition zone – Evidence from deposits of the Rhine and Meuse. *Netherlands Journal of Geosciences* 86 (3), 287-306.
- Van der Woude, J.D., 1984. The fluviolagoonal palaeoenvironment in the Rhine/Meuse deltaic plain. *Sedimentology* 31 (395-400).
- van Dijk, M., Postma, G., Kleinhans, M.G., 2009. Autocyclic behaviour of fan deltas: An analogue experimental study. *Sedimentology* 56, 1569-1589.
- Van Dyke, S.K., 2010. *Spectral Decomposition: A Powerful Tool for the Seismic Interpreter*. Nexen Petroleum U.S.A. Inc., Dallas, p. 3.
- Van Wagoner, J.C., Mitchum, R.M., Campion, K.M., Rahmanian, V.D., 1990. Siliciclastic Sequence Stratigraphy in Well Logs, Cores, and Outcrops: Concepts for High-Resolution Correlation of Time and Facies. *AAPG Special Volumes A174*, III-55.
- Walker, R.G., James, N.P., 1992. Facies models. Response to sea level change. *Geological Association of Canada*. 409 p.
- Weissmann, G.S., Mount, J.F., Fogg, G.E., 2002. Glacially driven cycles in accumulation space and sequence stratigraphy of a stream-dominated alluvial fan, San Joaquin Valley, California, USA. *Journal of Sedimentary Research* 72 (2), 240-251.
- Wescott, W.A., 1993. Geomorphic thresholds and complex response of fluvial systems -- Some implications for sequence stratigraphy. *AAPG Bulletin* 77, 1208-1218.
- Westphal, H., Aigner, T., 1997. Seismic stratigraphy and subsidence analysis in the Barrow–Dampier Subbasin, Northwest Australia. *AAPG Bulletin* 81, 1721-1749.
- White, R., Subekti, A., Rizal, Y., Prasetya, A., Reader, J., 2012. Stratal Slicing Uncovers Complex Depositional Architectures in the Northern Kutei Basin. *Search and Discovery Article* 41094.
- Widess, M.B., 1973. How thin is a thin bed. *Geophysics* 38 (6), 1176-1180.
- Willcox, J.B., 1981. Petroleum Prospectivity of Australian Marginal Plateaus, SG12: Energy Resources of the Pacific Region, *Studies in Geology* 12. American Association of Petroleum Geologists, Tulsa, pp. 245-272.
- Willis, B.J., 2005. Deposits of tide-influenced river deltas. *SEPM Special Publication* 83, 87–129.
- Wood, L.J., 2007. Quantitative seismic geomorphology of Pliocene and Miocene fluvial systems in the Northern Gulf of Mexico, U.S.A. *Journal of Sedimentary Research* 77, 713-730.
- Wood, L.J., Peuch, D., Schulein, B., Helton, M., 2000. Seismic attribute and sequence stratigraphic integration methods for resolving reservoir geometry in San Jorge Basin, Argentina. *The Leading Edge* 19 (9), 952-962.
- Wright, V.P., Marriott, S.B., 1993. The sequence stratigraphy of fluvial depositional systems: the role of floodplain sediment storage. *Sedimentary Geology* 86, 203-210.
- Yeates, A.N., Bradshaw, M.T., Dickens, J.M., Brakel, A.T., Exon, N.F., Langford, R.P., Mulholland, S.M., Totterdel, J.M., Yeung, M., 1986. The Westralian Superbasin, an Australian link with Tethys, in: McKenzie, K.G. (Ed.), *Proceedings of the International Symposium on Shallow Tethys 2: Wagga Wagga, Australia*. A.A. Balkema, Rotterdam, pp. 199–213.
- Zaitlin, B.A., Dalrymple, R.W., Boyd, R., 1994. The stratigraphic organization of incised valley systems associated with relative sea-level change, in: Dalrymple, R.W., Boyd, R., Zaitlin, B.A. (Eds.), *Incised valley systems: origin and sedimentary sequences*. *SEPM Special Publications*, pp. 45-60.
- Zeng, H., 2001. From Seismic Stratigraphy to Seismic Sedimentology: A Sensible Transition. *Gulf Coast Association of Geological Societies Transactions* 51, 412-420.
- Zeng, H., 2004. Seismic geomorphology-based facies classification. *The Leading Edge* 23 (7), 644-688.

- Zeng, H., 2010. Stratal slicing: Benefits and challenges. *The Leading Edge* 29 (9), 1040-1047.
- Zeng, H., 2013. Stratal slice: The next generation. *The Leading Edge* February 2013, 140-144.
- Zeng, H., Backus, M.M., Barrow, K.T., Tyler, N., 1998. Stratal slicing, Part I: Realistic 3-D seismic Model. *Geophysics* 63 (2), 502-513.
- Zeng, H., Henry, S.C., Riola, J.P., 1998. Stratal slicing, Part II: Real 3-D seismic data. *Geophysics* 63 (2), 514-522.
- Zeng, H., Hentz, T.F., 2004. High-frequency sequence stratigraphy from seismic sedimentology: Applied to Miocene, Vermilion Block 50, Tiger Shoal area, offshore Louisiana. *AAPG Bulletin* 88 (2), 153-174.
- Zhu, F., Goosens, P., Najwani, H., Harris, J., Scholten-Vissinga., M., Ma'mary, T., 2014. Tuning is not necessarily bad—Channel sand delineation from seismic data of the Upper Gharif in Oman. *The Leading Edge* 33 (1), 50-60.

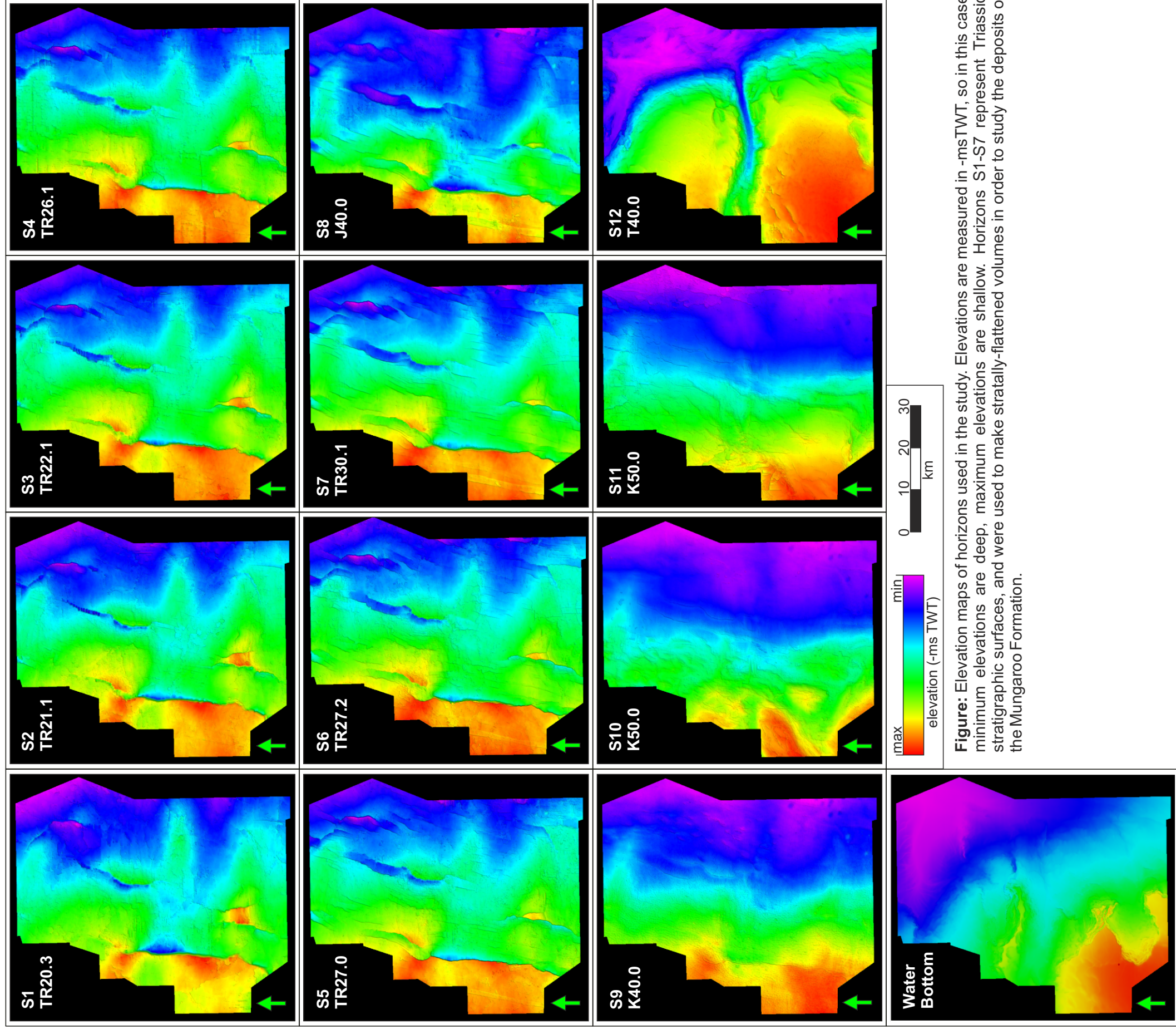


Table: Nomenclature, stratigraphic and elevation information for seismic horizons used in the study

Seismic horizon	Stratigraphic surface	Bounding surface type	Stage	Z Mean (-ms TWT)	Z Max (-ms TWT)	Z Min (-ms TWT)
Water Bottom	-	-	-	1876	1477	2156
S12	T40.0	Sequence boundary	Messinian	2191	1843	2690
S11	K60.0	Sequence boundary	Campanian	2842	2239	3284
S10	K50.0	Sequence boundary	Cenomanian	2934	2380	3309
S9	K40.0	Sequence boundary	Aptian	3041	2691	3373
S8	J40.0	Sequence boundary	Oxfordian	3244	2923	3466
S7	TR30.1	Transgressive surface	Norian	3335	2941	3840
S6	TR27.2	Maximum flooding surface	Norian	3517	3128	3944
S5	TR26.5	Maximum flooding surface	Norian	3592	3195	4017
S4	TR26.1	Transgressive surface	Norian	3713	3328	4256
S3	TR22.1	Transgressive surface	Norian	3955	3580	4485
S2	TR21.1	Transgressive surface	Norian	4175	3817	4642
S1	TR20.3	Sequence boundary	Norian	4510	4124	4961

Appendix 2

Noblige-2 / Well-11 core photographs with interpreted lithofacies associations.








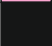
Core depths:

Core 01: 3866.50m - 3902.84m

Core 02: 3918.00m - 3974.80m

Core 03: 3975.00m - 4073.97m

Core 04: 4074.00m - 4147.71m

Lithofacies association key			
	High-energy channel		Gleysol
	Low-energy channel		Lake
	Proximal splay		Bay-fill
	Distal splay		Coal

Noblige-2
Core Photos

3867m

3868m

3869m

328

3870m

3871m

3872m

3873m

Top Core 1
3866.50m

1m scale

1m scale

3874m

3875m

3876m

3877m

3878m

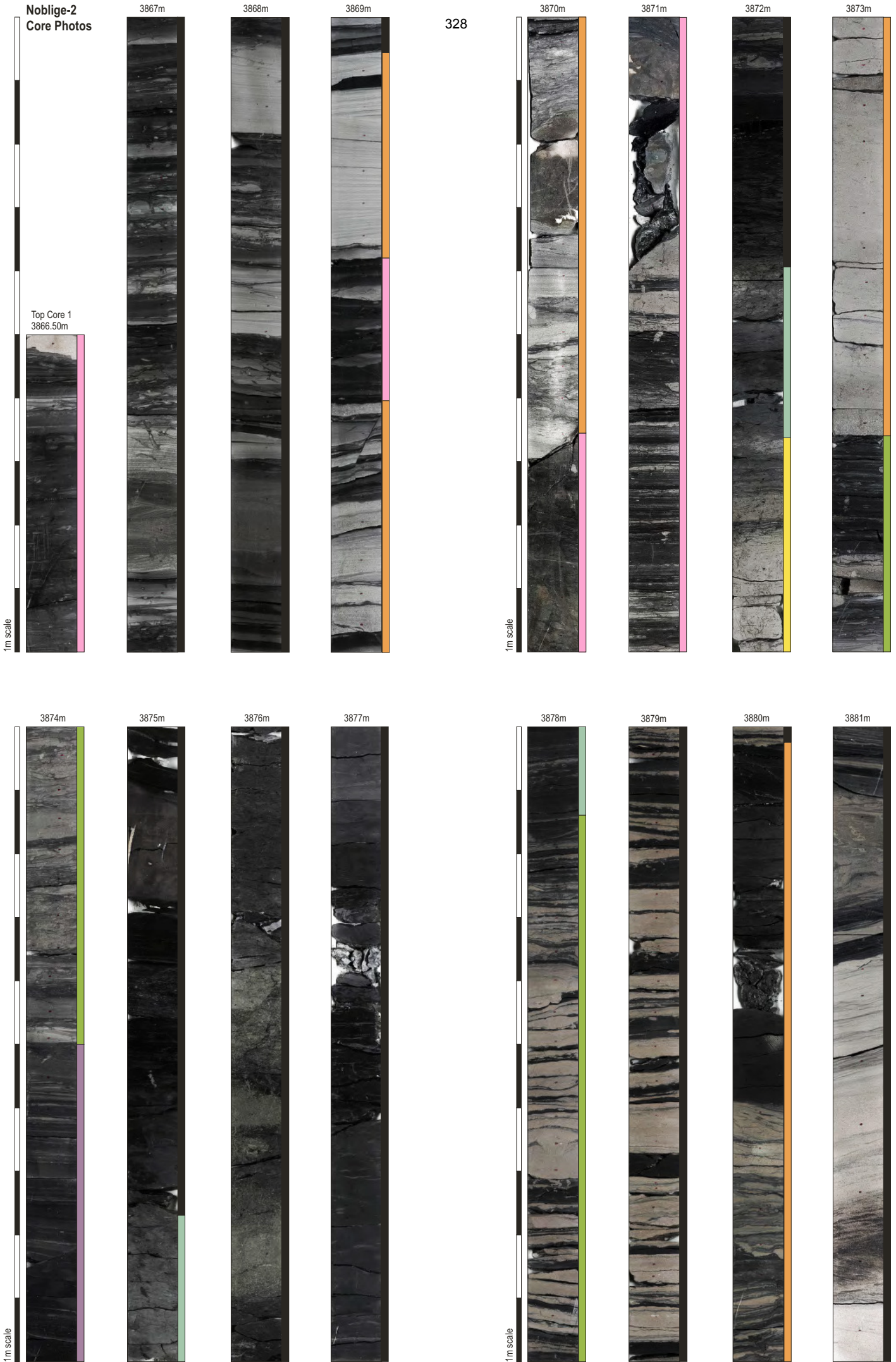
3879m

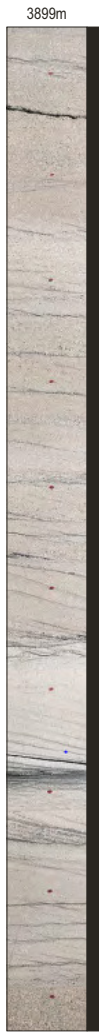
3880m

3881m

1m scale

1m scale





330



